VU VRIJE UNIVERSITEIT AMSTERDAM

VU Research Portal

Hydrological processes in a humid tropical rain forest: a combined experimental and modelling approach

Schellekens, J.

2000

document version
Publisher's PDF, also known as Version of record

Link to publication in VU Research Portal

citation for published version (APA)
Schellekens, J. (2000). *Hydrological processes in a humid tropical rain forest: a combined experimental and modelling approach*. [PhD-Thesis - Research and graduation internal, Vrije Universiteit Amsterdam]. VU.

General rights
Copyright and moral rights for the publications made accessible in the public portal are retained by the authors and/or other copyright owners and it is a condition of accessing publications that users recognise and abide by the legal requirements associated with these rights.

- Users may download and print one copy of any publication from the public portal for the purpose of private study or research.
- You may not further distribute the material or use it for any profit-making activity or commercial gain
- You may freely distribute the URL identifying the publication in the public portal

Take down policy
If you believe that this document breaches copyright please contact us providing details, and we will remove access to the work immediately and investigate your claim.

E-mail address:
vuresearchportal.ub@vu.nl

Download date: 22. May. 2025

HYDROLOGICAL PROCESSES IN A HUMID TROPICAL RAIN FOREST: A COMBINED EXPERIMENTAL AND MODELLING APPROACH

JAAP SCHELLEKENS

Cover: View on the Bisley catchment (taken from the meteorological tower) just after a storm.

Schellekens, Jaap

Hydrological processes in a humid tropical rain forest: a combined experimental and modelling approach. Jaap Schellekens, Doctoral Thesis Vrije Universiteit amsterdam. – With index, ref. – With summary in Dutch.

Subject headings: Tropical forest / Hydrology / Puerto Rico / Modelling

This thesis was typeset using LaTeX2e. Figures were made with Octave/Gnuplot and Idraw

VRIJE UNIVERSITEIT

Hydrological processes in a humid tropical rain forest: a combined experimental and modelling approach

ACADEMISCH PROEFSCHRIFT

ter verkrijging van de graad van doctor aan
de Vrije Universiteit te Amsterdam,
op gezag van de rector magnificus
prof.dr. T. Sminia,
in het openbaar te verdedigen
ten overstaan van de promotiecommissie
van de faculteit der Aardwetenschappen
op donderdag 7 september 2000 om 15.45 uur
in het hoofdgebouw van de universiteit,
De Boelelaan 1105

door

JAAP SCHELLEKENS

geboren te 's-Gravenhage

Promotor	:	prof.dr. I. Simmers
Copromotoren	:	dr. L.A. Bruijnzeel
		dr. F.N. Scatena

CONTENTS

LIST OF FIGURES

LIST OF TABLES

ACKNOWLEDGEMENTS

The research on which this thesis is based was funded by the Vrije Universiteit Amsterdam and as part of the Luquillo Long-Term Ecological Research Program by the the International Institute for Tropical Forestry, Rio Piedras, Puerto Rico.

Many people have contributed to this thesis in one way or another, here I will try and mention most of them.

Prof.dr. Ian Simmers acted as my promotor. In addition, he managed the project's finances... with a smile.

Two people made the big difference in this thesis: my co-promotors Sampurno Bruijnzeel and Fred Scatena. Not only did they come up with the research plan, so I could get started, but they also remained heavily involved throughout the entire process. Sampurno not only kept me going with remarks like 'we've got a classic paper here...' and his unreproducible humour, but really made a difference with his extensive edits of the manuscripts and his never relenting input of new ideas and information. Fred not only promptly answered my Saturday morning e-mails but his enormous support during my stays in Sabana was the key to the success of the field campaigns. In addition, his comments, edits and substantial input to the various chapters in this thesis improved the quality considerably.

In 1996 I was accompanied by three MSc students from our university: Friso Holwerda, Rutger Hogezand and Bart Wickel. Together we conquered stinging plants, rain, defect floppy disks and mud mud mud... In addition their reports proved to be good starting points when writing this thesis, good work, boys!

The 1997 fieldwork was a relative short one. However, in that period our three people team (Michel Groen, Albert van Dijk and myself) managed to carry a truckload of stuff through the forest. Back-breaking geophysical equipment (powered by car batteries) was carried around with a smile and a constant supply of (mostly rude) jokes. In addition, Michel's expertise in geophysics and Albert's writing talent allowed for rapid and good interpretation of the data. I hope we can do something like this again.

Many people helped to make my stay at Sabana a 'good one'. Bruce's remarks at the start of a day always cheered me up ;-). All 'Sabana bunker' (and later Villa) inhabitants have made a mark on me in some way. Thanks Paul, Demon, Mayda and all the others. In addition, Carlos, Carlos and Angel were always willing to help me getting stuff done and did not mind answering

my questions, thanks!

Rob Vertessy and the CRC's staff and students made my stay in Canberra a very enjoyable time. Having a meal with Rob and Debbie, accompanied with some fine Australian wine, is a wonderful experience. I will not easily forget the company of Johan Rockstrom during my stay: two weird Europeans upside down, forgetting their bicycle helmets wherever they went.

The advisory role of prof.dr. H. F. Vugts in the fields of micrometeorology, datalogger programming, running and drinking beer is gratefully acknowledged. Nienk Jan Bink provided help when I struggled comparing micrometeorology with my throughfall measurements. The help from Antoon Meesters in helping me understand complex equations is gratefully acknowledged.

My colleagues, fellow AOI's and Post-Doc's here at the University provided a great atmosphere to work in and a good platform for discussing science as well as life in general over a coffee or beer. The yearly trips for some sports and beer with Arnoud Frumau, Ben Gouweleeuw, Raymond Hafkenscheid, Michiel van der Molen, Paul Smeets, Raymond Venneker and Joost Vermeulen were very good for renewing energy and keeping things into perspective. Aljosja Hooyer and Jan van der Lee are responsible for my shift from musicology to hydrology back in 1986: no regrets! Raymond Hafkenscheid has been my roommate for the last four years at the VU allowing us to share the pain and fun of completing our theses.

Fieldwork equipment plus support and expertise was supplied by M. M. A. Groen and the VUA workshop. Notwithstanding, the fact that I requested for an enormous variety of stuff, they were able to supply it. Thanks! The VUA electronics department, notably J. de Lange and R. Lootens, constructed great equipment that lasted in the wet tropical conditions of the LEF. It proved to be of vital importance for this thesis.

I also wish to thank the VUA IT department, notably Fred Cannemijer, Arie Bikker, Gerard Kok and Frans Stevens for keeping up with me when I asked (again) for more CPU cycles, storage capacity etc.

It must be in the minds of most people who start such an undertaking: 'will there be any friends left when I'm finished?'. Although some have warned me (Aljosja, Sacha, thanks..) not to start, i did it anyway. At the end I think I am blessed with the patience of my friends and family. I can assure all of you this has been a one-time thing. If you are still around, let's go out dancing or drink some wine/beer…I'm back.

Of course non of this would have been possible without the support of my parents, thanks for making all of this possible!

Clarice is by far the one that has suffered most from all this; but she never gave up on me. Instead, she made it a fun time! Especially now that Amina has entered our life…danki dushi!!

1

INTRODUCTION

1.1 BACKGROUND

With populations growing explosively in the tropical parts of the world, and the per capita water demands increasing where living standards improve, optimisation of water resources is becoming increasingly important [*Bonell et al.*, 1993]. Similarly, the strong demands for industrial wood (pulpwood, saw and veneer logs), fuelwood and charcoal, require the establishment of large areas of fast-growing plantation forests, often on land that is currently not forested [*Evans*, 1992; *Brown et al.*, 1997]. Coupled with *(i)* the continued indiscriminate clearing of the world's tropical forests [*Jepma*, 1995; *Nepstad et al.*, 1999] which in many areas serve as the traditional supplier of high quality water; *(ii)* the associated deterioration of soil and water quality due to erosion and pollution [*Oldeman*, 1994], plus *(iii)* the possibility of gradually less dependable precipitation inputs and (in certain 'maritime' tropical areas away from the equator) an increasing frequency of devastating hurricanes due to 'global change' [*Wasser and Harger*, 1992], a sound understanding of the hydrological functioning of tropical forests is arguably even more important nowadays than ever before [*cf. Bruijnzeel*, 1990, 2000a].

Bruijnzeel and Abdul Rahim [1992] suggested that in a time of dwindling resources, additional forest hydrological research in the humid tropics could best be carried out at a limited number of carefully selected data-rich key locations that could be loosely joined together in a network that captures the environmental variability encountered in the humid tropics. Furthermore, *Bruijnzeel* [1993] and *Bonell and Balek* [1993] considered a catchment-based approach to offer the best framework for such research as this allows for the integration of hydrological, geomorphological, pedological and ecological observations in a spatial context, particularly if supplemented by process studies and physically-based distributed modelling.

1.2 THE HYDROLOGICAL CYCLE IN A TROPICAL RAIN FOREST

To avoid confusion about the terms used in this thesis, this section will first describe respective hydrological processes operating in a forest suggesting typical values for the respective variables for lowland tropical forest. A simplified picture of the hydrological cycle of a forested ecosystem is presented in Fig. 1.1.

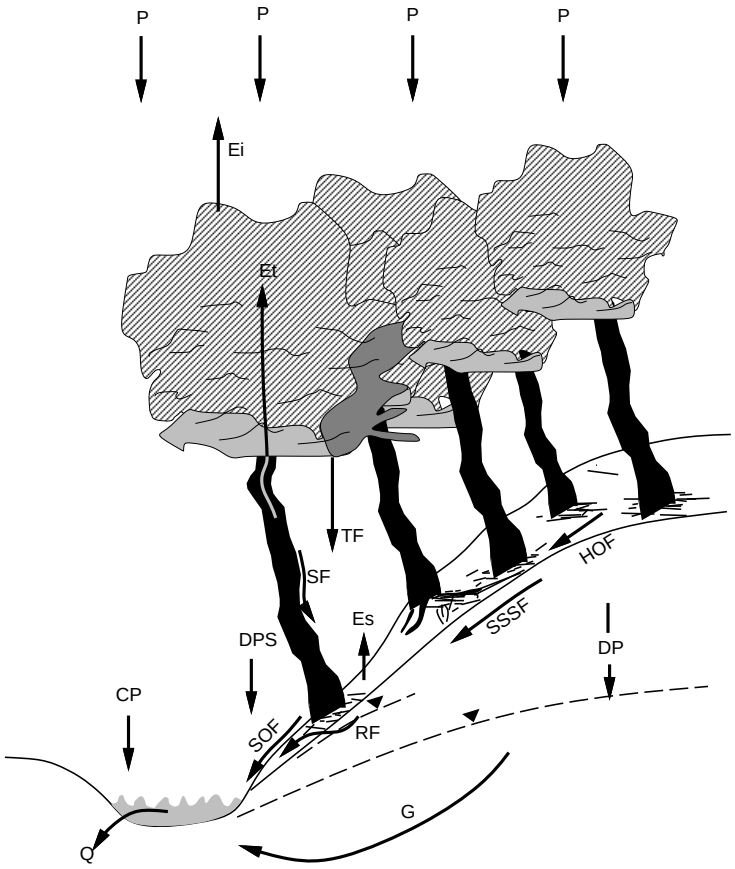

Figure 1.1: Schematic representation of the major water fluxes in a lowland tropical rain forest setting. P: Precipitation, TF: Throughfall, SF: Stemflow, E_i: Rainfall Interception, E_t: Transpiration, E_s: Soil Evaporation, CP: Channel precipitation, DPS: Direct precipitation onto saturated areas, HOF: Hortonian Overland Flow, $SSSF$: Sub Surface Storm Flow, RF: Return Flow, SOF: Saturation Overland Flow, DP: Deep percolation, G: Groundwater flow, Q: Discharge.

With the exception of specific coastal situations where fog may be an important form of precipitation [*Bruijnzeel*, 2000a], the sole precipitation into tropical forests is in the form of rainfall (P). Three pathways can be distinguished by which incident precipitation arrives at the forest floor: *(i)* A small fraction of the water reaches the forest floor without touching the leaves or stems – this is known as direct throughfall. *(ii)* Another – also generally small – fraction of the water flows down the tree trunks as stemflow (SF), of which some will evaporate back into the atmosphere. *(iii)* The rest of the water hits the canopy and continues as crown drip or leaves the canopy as evaporation during and shortly after the rain. The latter process is usually referred to as rainfall interception (E_i). In general, it is not possible to distinguish crown drip and direct throughfall in the field. Hence, the two are usually combined and simply referred to as throughfall (TF). Using the above we can construct the following equation describing the water balance for a wet canopy:

$$P = TF + SF + E_i \tag{1.1}$$

Of the water that reaches the forest floor a small fraction will be evaporated back into the atmosphere as litter and soil evaporation (E_s). In humid tropical forest, however, E_s is usually negligible. If the infiltration capacity of the soil is less than the throughfall and stemflow intensity, excess water runs off as 'Hortonian overland flow' (HOF). Within most undisturbed tropical forest this occurs relatively infrequent due to the high conductivity of the topsoil. a considerable part of the infiltrated water is taken up by the vegetation and returned to the atmosphere as transpiration (E_t). The sum of E_t, E_s and E_i is called evapotranspiration (ET). Water that infiltrates in the soil profile can flow through the profile to the stream in several ways. During storms it can flow laterally as saturated or unsaturated stormflow ($SSSF$). When the soil profile — or the top part of it — becomes saturated, rainfall that hits these areas (typically located in hillside hollows, concave footslopes or areas with an impeding layer close to the surface [*Bonell and Gilmour*, 1978]) will run off as saturation overland flow (SOF). The contributions of $SSSF$, SOF and SOF represent the fast flowpaths of water to the stream network, supplemented by the (usually small) contribution of direct channel precipitation (CP). The remaining soil moisture drains into the stream network by slow moving throughflow, accounting for a considerable part of the baseflow of streams [*Ward and Robinson*, 1990].

The components of the forest hydrological cycle [a detailed description can be found in *Bruijnzeel*, 1989a] are partitioned according to a number of factors related to forest and soil structure, climate and topography. The amount of rainfall interception depends on canopy storage (S) capacity and gap fraction (p) and the shape, size and kinetic energy of the droplets, the evaporative demand of the atmosphere and (usually to a lesser extent) the properties of branches, stems and the bark. Reliable estimates of the relative magnitude of the pathways of water to the forest floor in tropical rain forest have been relatively few notwithstanding the broad attention that has been given to this subject. *Bruijnzeel* [1990] observed considerable variation in both estimated

amounts and the reliability of such studies in the humid tropics which he attributed to the complexity of the rain forest canopy and the rigorous sampling procedures that are required to get an adequate estimate of TF [*cf. Lloyd and Marques-Filho*, 1988]. The most reliable estimates suggest that about 85 % (77–93 %) of incident precipitation reaches the forest floor as TF while stemflow (SF) usually accounts for 1–2 % [*Bruijnzeel*, 1990; *Anderson and Spencer*, 1991]. However, there is a growing number of studies that suggest (much) higher interception losses [30–50 %, *Clements and Colon*, 1975; *Gilmour*, 1975; *Read*, 1977; *Scatena*, 1990b] are possible under wet maritime tropical conditions. The estimation of stemflow (SF) is notoriously labour intensive. This, combined with the general perception that SF is negligible small in most cases, explains why so little is known about the dynamics of stemflow [*cf. Herwitz*, 1985]. Tree diameter is considered an important factor with small trunks generating more stemflow than large trunks [*Weaver*, 1972; *Lloyd and Marques-Filho*, 1988; *Bruijnzeel*, 1989b]. *Scatena* [1990b] showed that 50 % of the stemflow in the Bisley II area in eastern Puerto Rico was generated by only 15 % of the trees. Evapotranspiration losses (ET) from a humid tropical forest comprise the combined losses by rainfall interception, forest transpiration and soil evaporation. The latter term is usually negligible small [$< 70\ mm\ yr^{-1}$; *Roche*, 1982; *Tabón Marin*, 1999]. Transpiration, on the other hand often reaches values of c. 1000 $mm\ yr^{-1}$ [*Bruijnzeel*, 1990]. Total ET varies widely between sites because of differences in rainfall interception and other factors (see Section 1.3) but often approaches a value of 1300–1500 $mm\ yr^{-1}$ [*Bruijnzeel*, 1990]. Evapotranspiration therefore represents an important component of the water balance of tropical lowland rain forest, and therefore constitutes a major determinant of the amounts of water draining from such environments [*Anderson and Spencer*, 1991].

The subdivision of water at the soil surface into the various possible flow types (portrayed in Fig. 1.1) is determined by initial soil water conditions, soil hydraulic properties and (micro-)topography. As the pathways via which the water reaches the stream channel not only control the water yield of a catchment but also the water quality, its identification is of great interest in watershed research. Infiltration-excess (Hortonian) overland flow is rarely observed on undisturbed forest soils but may occur on especially clayey soils [*Bell*, 1973; *Elsenbeer and Cassel*, 1990] or where large volumes of stemflow are concentrated [*Herwitz*, 1986]. Overland flow due to saturation of the soil is more common, but this is usually restricted to valley bottoms, depressions and slope transitions [*Dunne*, 1978; *Bonell*, 1993] although exceptions are possible, *e.g.* where an impermeable horizon is found close to the surface [*Bonell and Gilmour*, 1978; *Elsenbeer et al.*, 1994b]. Saturation can occur throughout the profile but is more often observed above a specific layer with reduced hydraulic conductivity, resulting in a perched water table. Where steep, straight slopes are present, with abundant macropores or an otherwise conductive topsoil, subsurface storm flow ($SSSF$) is likely to account for most of the storm flow [*Dunne*, 1978] whereas SOF tends to dominate the stormflow hydrograph where slopes are concave, valley bottoms wide, and soils are shallow [*Dunne*, 1978]. Typical quickflow percentages (of incident rainfall) in the former case

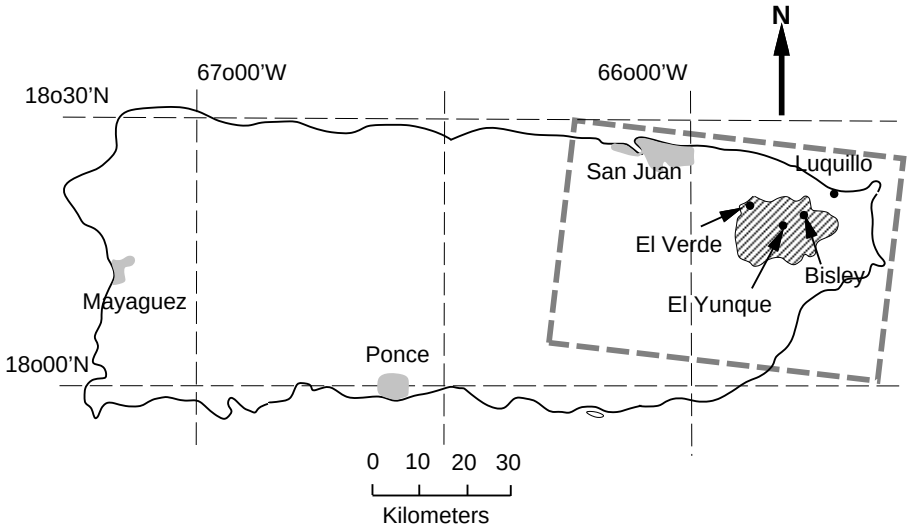

Figure 1.2: Map of Puerto Rico showing the location of the Bisley site within the Luquillo Experimental Forest (indicated by the hatched area). The area that is covered by the image in Fig. 1.3 is indicated by the dashed-gray rectangle.

are 5–10 % but this may increase to $>$ 30 % in cases with widespread SOF [*Dunne*, 1978; *Bonell and Gilmour*, 1978; *Bruijnzeel*, 1990].

1.3 EVAPOTRANSPIRATION IN HUMID TROPICAL FORESTS

Under the warm and wet conditions prevailing in the humid tropics, evapotranspiration (ET) tends to be high and thus strongly influences the total amount of water available as streamflow (catchment water yield) for a given rainfall regime. [*Bruijnzeel*, 1990]. *Calder* [1998] showed how the principal controls of evaporation from forests (notably radiation, temperature, atmospheric humidity deficit and soil water status) differ markedly between temperate and tropical regions, and between wet and dry zones in these regions. The maximum value of forest ET under wet temperate conditions is generally thought to be limited by the amount of advected energy available to evaporate intercepted rainfall from the wetted, aerodynamically rough forest canopy [*Shuttleworth and Calder*, 1979; *Calder*, 1998]. Conversely, *Calder* [1998] considered forest ET under humid tropical conditions to be limited primarily by radiation totals. With very few exceptions however [*Calder et al.*, 1986; *Shuttleworth*, 1988], the available estimates of tropical forest ET are based on the catchment water budget technique [*Bruijnzeel*, 1990; *Malmer*, 1993; *Lesack*, 1993; *Jetten*, 1994; *Abdul Rahim et al.*, 1995]. This method is notoriously prone to errors associated with ungauged subterranean transfers of water into or out of the catchment and may therefore produce relatively unreliable estimates of ET, unless the catchment

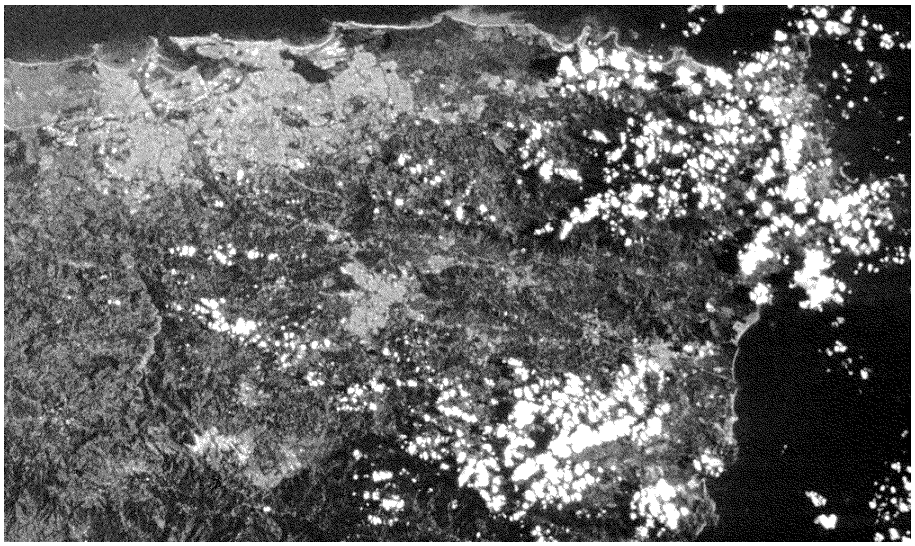

Figure 1.3: Image of eastern Puerto Rico taken from the Space Shuttle on 21 October 1989 at 12:51 GMT. The white spots are clouds. As humid air, brought in from the Atlantic Ocean by the north-easterly tradewinds, is forced upwards against the Luquillo Mountains, clouds are formed predominantly at the windward side of the mountains.

is demonstrably watertight [*Ward and Robinson*, 1990]. Such methodological problems prevented *Bruijnzeel* [1990] in his review of tropical rain forest water use from finding distinct differences in ET for the three major rain forest blocks of West Africa, Amazonia and South-east Asia. In addition, *Bruijnzeel* [1990] ascribed reported ET totals that were well above 1400–1500 $mm\,yr^{-1}$ to problems with catchment leakage rather than to specific climatic conditions favouring high evaporation [*cf. Richardson*, 1982]. *Shuttleworth* [1989] advanced the idea that, compared to mid-continental sites, tropical deforestation was likely to have the greatest effect on river flow (though not necessarily on climate) at continental edge and island locations. He based this contention on a comparison of the micrometeorology of a rain forest in central Amazonia [*Shuttleworth*, 1988] and a spruce plantation in Wales, U.K. [*Shuttleworth and Calder*, 1979] as well as on the reported contrast in rainfall interception (E_i) by lowland rain forests in central Amazonia [*Lloyd and Marques-Filho*, 1988] and West Java, Indonesia [*Calder et al.*, 1986]. Unfortunately, the latter comparison was limited by the use of markedly different methodologies for the estimation of E_i, which rendered the argument inconclusive at the time.

Since the late 1980's a number of rainfall interception studies conducted in tropical forests located at continental edges and islands receiving high rainfall totals (>3000 $mm\,yr^{-1}$) have confirmed the possibility of very high interception losses under such 'maritime' tropical conditions [*Bruijnzeel*, 1988; *Scatena*, 1990b; *Dykes*, 1997; *Cavelier et al.*, 1997; *Clark et al.*, 1998], although the

actual mechanism causing such high evaporation rates was not identified. Support for the importance of advected energy under maritime tropical conditions also comes from Hawaii. Depending on location (elevation, exposure to the tradewinds), the evaporation equivalents of advected energy were observed to range between -0.71 and 2.8 $mm\,d^{-1}$ [*Nullet*, 1987]. Such findings not only confirm the possibility of large non-radiant energy inputs but also illustrate their very local character. Also in Hawaii, *Giambelluca and Nullet* [1992] recorded very high (atmometer) evaporation rates (up to 6.5 $mm\,d^{-1}$) above a thermal inversion layer, which were increasing with elevation. Interestingly, the increases in evaporation were paralleled by a similar increase in night-time interception losses, again suggesting considerable advective influence. However, none of the studies that reported inferred contributions of advected energy to explain high interception losses in the humid tropics used above-canopy climatic observations and continuously recording throughfall equipment. Therefore the actual mechanism was not identified. Neither has the dry-canopy evaporation component of ET (transpiration, E_t) been studied at these locations and so the limits of forest ET under wet maritime tropical conditions remain to be explored.

1.4 DEVELOPMENT OF HYDROLOGICAL MODELS

Upon forest disturbance or conversion to other land uses, not only forest evapotranspiration — and thus catchment water yield — changes profoundly, but the flow regime is also affected [*Bruijnzeel*, 1989a, 1990, 1992; *Bonell*, 1993]. Traditionally, forest hydrologists have relied on time-consuming paired catchment experiments to evaluate such effects [*Gilmour*, 1977; *Pearce and Griffiths*, 1980; *Swindel et al.*, 1983; *Hewlett et al.*, 1984; *Hsia*, 1987; *Malmer*, 1992; *Fritsch*, 1992]. However, because of its 'black-box' character the paired catchment approach is unable to evaluate the relative importance of various factors that might underly differences in results between different sites, and this severely limits the possibilities for extrapolation of such results to other areas or periods. Arguably, for a proper understanding of changes in runoff response to rainfall associated with forest disturbance or conversion, insight is required into the underlying runoff generation processes [*Douglas and Spencer*, 1985; *Bonell*, 1993].

Physically-based distributed hydrological models represent an alternative way of predicting how catchments might respond to different forms of disturbance or management. The current movement towards increased development and application of physically-based distributed models is partly fed by a growing recognition that only such models are capable of representing the full spectrum of hydrological situations. Also, because many practical catchment/forest management questions have a spatial dimension attached, and because most landscapes consist of a complex mosaic of different land uses and covers, physically based models should preferably be of a distributed nature, *i.e.* capable of taking into account spatial variations in topography, soils, vegetation and climate [*Vertessy et al.*, 1993; *Vertessy and Elsenbeer*, 1999]. During the last 10–15

years, considerable progress has been made in the modelling of (forest) hydrological processes over a range of spatial and temporal scales [*e.g. Abbott et al.*, 1986a; *O'Loughlin*, 1986; *Running and Coughlan*, 1988; *Beven*, 1991; *Hatton et al.*, 1992; *Sivapalan et al.*, 1996; *Vertessy et al.*, 1996; *Watson et al.*, 1999]. A key feature of all these models is their ability to distribute parameters and relations over the catchment area. In general the area is represented as a rectangular grid but other systems (*e.g.* contour based ones) are used as well. As the models become more complex and better describe the underlying physical processes, they also demand more parameters [*Abbott et al.*, 1986b], notwithstanding the fact that it has been noted that only a few key parameters are generally needed to provide reasonable results [*Beven*, 1989]. To adequately model the hydrological behaviour of a catchment per se, is not the final goal of modelling but rather to apply some sort of land-use change scenario in which the model is used to predict the hydrological effects that particular treatment. If we take into account the questions raised by *Beven* [1989] with respect to the principles underlying the current generation of distributed physically based models, our state-of-the-art models are still an extreme simplification of reality. Therefore, the predictive value of these models is related to the amount of knowledge we have about the underlying system. This calls for a-priori knowledge of the major processes within catchment before a modelling exercise is started. This will allow for a better interpretation and validation of the model results [*Quinn et al.*, 1991; *Vertessy and Elsenbeer*, 1999].

Arguably, one of the most comprehensive process-based models is the TOPOG model [*O'Loughlin*, 1986; *Vertessy et al.*, 1993; *Dawes et al.*, 1997]. TOPOG integrates the water, carbon, solute and sediment balances at the small catchment scale (typically $\ll 10\ km^2$) and is particularly suited to explore complex feedback mechanisms between system properties. Examples of within-catchment applications of TOPOG include: the prediction of steady-state soil moisture distributions and saturated zones in the landscape during wet and dry periods [*O'Loughlin*, 1986; *Moore et al.*, 1988], the spatial distributions of surface erosion, gully initiation and landslide hazards [*Vertessy et al.*, 1990; *Constantini et al.*, 1993; *Dietrich et al.*, 1992], and the evaluation of the water balance and growth performance of different tree planting configurations under sub-humid conditions [*Silberstein et al.*, 1999]. Off-site applications of TOPOG include the successful simulations of changes in tree growth and water yield for a small catchment after clearfelling during 20 years of regeneration [*Vertessy et al.*, 1996].

Models like TOPOG thus constitute a powerful tool on whose predictions rational land use decisions may be based. However, while distributed models represent the only class of simulation modes capable of capturing the complex feedbacks occurring in natural and disturbed landscapes, they are also data-demanding. TOPOG model outputs are particularly sensitive to variations in vegetation leaf area index, soil hydraulic conductivity, the rainfall interception coefficient, and canopy conductance [*Vertessy et al.*, 1993; *Vertessy and Elsenbeer*, 1999]. Thus far, applications of TOPOG under humid tropical conditions have been few. Recently *Vertessy and Elsenbeer* [1999] applied an adaptation of the TOPOG modelling system (TOPOG_SBM) to a small fast-responding lowland

rain forested catchment in the Amazonian part of Peru. TOPOG_SBM is essentially a hybrid between the spatially, fully dynamic model TOPOG_DYNAMIC [*Vertessy et al.*, 1996; *Dawes et al.*, 1997] and the quasi-dynamic model TOPMODEL [*Beven and Kirkby*, 1979; *Beven*, 1997]. The TOPOG_SBM model consists of a simple bucket model for soil water accounting, a one-dimensional kinematic wave overland flow scheme, and a contour-based element network for routing surface and subsurface flows.

1.5 SCOPE AND OBJECTIVES OF THIS STUDY

The objective of this study is twofold. Firstly, to describe and quantify the chief hydrological processes (rainfall interception, transpiration, runoff generation) operating in the small rain forested Bisley II catchment under the wet maritime tropical conditions prevailing in eastern Puerto Rico. This is done with the aim of shedding more light on the evaporation process and to explore the limits to evaporation as well as to get a detailed picture of the relative importance of the different components of the hydrological cycle under such conditions. To aid in the interpretation of the results and to prepare for the second stage of modelling, a one-dimensional Soil Vegetation Atmosphere model (named VAMPS) was developed. The second objective is to test the performance of the TOPOG modelling system in this area of frequent, low intensity rainfall and steep topography. As the present application marks the first published attempt to use TOPOG for the prediction of both seasonal water yield and stormflow response in a wet maritime tropical steepland setting, the results may be considered a good test of the robustness of the TOPOG package. Also, the detailed process studies referred to above may be used to draw up an overall conceptual representation of the various processes operating in the catchment, and so reduce the changes of getting the 'right answers' for the 'wrong reasons' [*Beven*, 1989; *Grayson et al.*, 1992].

The investigation was carried out in the Bisley II catchment (18^o 18′ N, 65^o 50′ W at an elevation of 265–456 m a.s.l.) in the Luquillo Experimental Forest (LEF), eastern Puerto Rico (Fig. 1.2). The area is steep and dissected. Slopes in excess of 45 % (24^o) cover more than 50 % of the catchment. The 0.8–1.0 m deep clayey soils that have developed in the underlying thick-bedded tuffaceous sandstones and indurated siltstones are strongly leached Ultisols [*Scatena*, 1989]. Non-weathered bedrock is found at depths greater than 15 m below the level of the stream channel [*Van Dijk et al.*, 1997]. A more elaborate description of the soils and the geological structure of the catchment is presented in Chapter 4. The forest of the catchment is of the so-called Tabonuco type [*Odum and Pidgeon*, 1970] has an irregularly shaped, 20–25 m high upper canopy, an understory of palms and woody vegetation, and ground level herbs and shrubs. Both the structure and composition of the vegetation vary with topography and aspect relative to the trade winds [*Lugo and Scatena*, 1995]. The average leaf area index (LAI) of mature Tabonuco forest is between 6 and 7 [*Odum et al.*, 1970a]. In September 1989 the Bisley area was severely

impacted and nearly completely defoliated by Hurricane Hugo [*Scatena et al.*, 1993]. However, by 1996 when the present study was initiated the LAI, canopy interception, and forest biomass were again similar to pre-hurricane conditions [*Scatena et al.*, 1996; *Holwerda*, 1997].

The climate at Bisley is maritime tropical (type A2m according to the Köppen classification), with the north-easterly trade winds bringing about 70 % of the annual rainfall of 3530 mm $\pm$ 22.6 % C.V. (as measured at the nearby long-term rainfall station at El Verde, 450 m a.s.l.; see Fig. 1.2 for location) in association with tropical waves, depressions and cyclones. Rainfall is distributed fairly evenly throughout the year, with May and November being relative wet, and January – March relatively 'dry'. As shown in Figures 1.2 and 1.3, the Luquillo mountains constitute the first sizeable object encountered by the north-easterly tradewinds that prevail in the area, leading to extensive cloud formation at $\sim$800 m a.s.l. [*Malkus*, 1955]. There is a strong orographic effect on amounts of rainfall received in the LEF. At the base of the mountains about 2500 $mm\,yr^{-1}$ is received, while the highest peaks (1050 m a.s.l.) receive up to 4500 $mm\,yr^{-1}$ [*Odum et al.*, 1970b; *Brown et al.*, 1983; *García-Martinó et al.*, 1996]. The seasonal variation in mean monthly temperatures in the Bisley area is about 3.5^oC, ranging from $\sim$24^oC in December – February to about 27.5^oC in July–August. Seasonal variation in average daily relative humidity levels is small (84 – 90 %). Average monthly wind speeds in the lower reaches of the LEF are $<$2 $m\,s^{-1}$ but vary between 2 and 5 $m\,s^{-1}$ around exposed summits at higher elevations. Average incoming solar radiation in the lowlands adjacent to the LEF (Cape San Juan) ranges from 13.8 $MJ\,m^{-2}\,d^{-1}$ in December to 26.0 $MJ\,m^{-2}\,d^{-1}$ in the summer months. At 1000 m elevation these amounts are roughly halved [*Brown et al.*, 1983]. Pan evaporation was determined at El Verde by *Odum et al.* [1970b] at 670 $mm\,yr^{-1}$ while reference open-water evaporation [*Penman*, 1956] in the Bisley area is estimated at $\sim$1100 $mm\,yr^{-1}$ [*Holwerda*, 1997].

Early studies of rainfall interception (E_i) in the Tabonuco forest (200–500 m a.s.l) in the LEF by *Clegg* [1963], *Clements and Colon* [1975] and *Scatena* [1990b] all reported very high interception losses (up to 45 % of annual rainfall) whereas simple water balance computations for intermediate-sized catchments in the area [*Lugo*, 1986; *Larsen and Concepción*, 1998] suggested ET totals that far exceeded the average of 1400$\pm$100 $mm\,yr^{-1}$ derived in a pan-tropical survey by *Bruijnzeel* [1990]. However, these high E_i and ET values were not addressed in terms of underlying processes. Other important related studies in the Bisley area include the soil chemical and aeration work of *Silver et al.* [1994, 1999], the role of subsurface soil creep and extreme rainfall in determining mechanisms and occurrence of slope failure [*Simon et al.*, 1990; *Scatena and Larsen*, 1991; *Larsen and Simon*, 1993], and the riparian nitrogen dynamics in relation to subsurface solute transport patterns [*McDowell et al.*, 1992]. Extensive descriptions of the physiognomy, floristics and soils of the Tabonuco rain forest at nearby El Verde (450 m a.s.l.; *cf.* Fig. 1.2) as well as a host of ecological processes, have been given by *Odum and Pidgeon* [1970], whereas more recent ecological information has been compiled by *Lugo and Scatena* [1995]. The initial effects

of hurricane Hugo in September 1989 on the (Tabonuco) forest and the gradual recovery over the years are described by *Walker et al.* [1991], *Scatena et al.* [1993], *Scatena and Lugo* [1995], and *Lugo and Scatena* [1995].

The present project was started in 1995 with funding granted by the International Institute of Tropical Forestry (IITF), Rio Piedras, Puerto Rico and the Faculty of Earth Sciences, Vrije Universiteit, Amsterdam (FES-VUA) for a period of four years. After a short exploratory visit in the spring of 1995 the author stayed in Puerto Rico for a period of three months in 1996, complemented by a month in 1997 for additional geophysical work. During 1996 the author also spent one month at the Cooperative Research Centre for Catchment Hydrology (CRCCH), Canberra to learn the basics of the TOPOG model from its developers. The rest of the time was spent processing the gathered data and writing this thesis.

A companion collaborative project between IITF and FES-VUA addressing the water and energy budgets of lowland coastal forest and pasture (Ir. M. K. van der Molen) was initiated in late 1996.

1.6 OUTLINE OF THIS THESIS

The thesis consists of a series of closely related papers. Chapter 2 presents a water budget of the Bisley II catchment using a water-budged based approach in combination with above-canopy climatic measurements and detailed throughfall data. The chapter focuses on the water use of the forest, notably on the high interception loss. Chapter 3 deals with the interception process in more detail and compares the simulation results obtained using an analytical and a numerical interception model. In particular, the outcome of the model applications is used to further investigate the probable causes of the observed high interception losses at Bisley. Chapter 4 describes the runoff generation processes in the catchment using a combination of geophysics, hydrometrical measurements and natural chemical tracers. In addition, a newly developed one-dimensional model of soil-vegetation-atmosphere water flow [VAMPS: *Schellekens*, 1997, Appendix A] is used to model soil water tensions and relate these to the runoff generating processes operating within the catchment. In Chapter 5 the TOPOG model is applied to simulate water yield, as well as storm flow amount for the catchment, marking the first application of the model in a wet maritime tropical environment. In doing so, special attention is paid to an assessment of how well the respective processes studied and quantified in the previous chapters are represented by the model. Finally, a summary of all preceding chapters is presented in Chapter 6 which also contains various recommendations for future research in the area.

2

EVAPORATION FROM A TROPICAL RAIN FOREST, LUQUILLO EXPERIMENTAL FOREST, EASTERN PUERTO RICO*

ABSTRACT

Evaporation losses from a watertight 6.34 ha rain forest catchment under wet maritime tropical conditions in the Luquillo Experimental Forest, Puerto Rico, were determined using complementary hydrological and micrometeorological techniques during 1996 and 1997. At 6.6 $mm\,d^{-1}$ for 1996 and 6.0 $mm\,d^{-1}$ for 1997, the average evapotranspiration (ET) of the forest is exceptionally high. Rainfall interception (E_i), as evaluated from weekly throughfall measurements and an average stemflow fraction of 2.3 %, accounted for much (62–74 %) of the ET at 4.9 $mm\,d^{-1}$ in 1996 and 3.7 $mm\,d^{-1}$ in 1997. Average transpiration rates (E_t) according to a combination of the temperature fluctuation method and the Penman-Monteith equation were modest at 2.2 $mm\,d^{-1}$ and 2.4 $mm\,d^{-1}$ in 1996 and 1997, respectively. Both estimates compared reasonably well with the water-budget based estimates (ET - E_i) of 1.7 $mm\,d^{-1}$ and 2.2 $mm\,d^{-1}$. Inferred rates of wet canopy evaporation were roughly four to five times those predicted by the Penman-Monteith equation, with nighttime rates very similar to daytime rates, suggesting radiant energy is not the dominant controlling factor. A combination of advected energy from the nearby Atlantic Ocean, low aerodynamic resistance, plus frequent low-intensity rain is thought to be the most likely explanation of the observed discrepancy between measured and estimated E_i.

*With: L.A. Bruijnzeel, F.N. Scatena, N.J. Bink and F. Holwerda, Accepted for publication in *Water Resources Research*

2.1 INTRODUCTION

The recognition that tropical rain forest destruction can have serious hydrological and climatic implications [reviewed by *Bruijnzeel*, 1990; *Gash et al.*, 1996] has prompted a number of investigations into tropical forest evapotranspiration. Evapotranspiration (ET) represents an important component of the water balance of tropical lowland rain forest, and therefore constitutes a major determinant of the amounts of water draining from such environments. With very few exceptions however [*Calder et al.*, 1986; *Shuttleworth*, 1988], the available estimates of tropical forest ET are based on the catchment water budget technique [*Bruijnzeel*, 1990; *Malmer*, 1993; *Lesack*, 1993; *Jetten*, 1994; *Abdul Rahim et al.*, 1995]. This method is notoriously prone to errors associated with ungauged subterranean transfers of water into or out of the catchment and may therefore produce relatively unreliable estimates of ET, unless the catchment is demonstrably watertight [*Ward and Robinson*, 1990]. The problem is illustrated by the contrasting results obtained for various small forested catchments in central Amazonia whose reported apparent annual ET ranges from 1120 mm [*Lesack*, 1993] to 1675 mm [*Leopoldo et al.*, 1982] despite similar climatic and geological conditions. Similarly, annual water-budget based estimates of ET for lowland and hill dipterocarp rain forests on granitic substrates in Peninsular Malaysia — receiving over 2000 mm of rain annually without a pronounced dry season — vary from about 1000 mm [*Low and Goh*, 1972] to almost 1800 mm [*Abdul Rahim and Baharuddin*, 1986].

Such methodological problems prevented *Bruijnzeel* [1990] in his review of tropical rain forest water use from finding distinct differences in ET for the three major rain forest blocks of West Africa, Amazonia and South-east Asia. In addition, *Bruijnzeel* [1990] ascribed ET totals that were well above 1400–1500 $mm\ yr^{-1}$ to problems with catchment leakage rather than to specific climatic conditions favouring high evaporation [*cf. Richardson*, 1982].

Shuttleworth [1989] advanced the idea that, compared to mid-continental sites, tropical deforestation was likely to have greatest effect on river flow (though not necessarily climate) at continental edge and island locations. He based this contention on a comparison of the micrometeorology of a rain forest in central Amazonia [*Shuttleworth*, 1988] and a spruce plantation in Wales, U.K. [*Shuttleworth and Calder*, 1979] as well as on the reported contrast in rainfall interception (E_i) by lowland rain forests in central Amazonia [*Lloyd and Marques-Filho*, 1988] and West Java, Indonesia [*Calder et al.*, 1986]. Unfortunately, the latter comparison was limited by markedly different methodologies for the estimation of E_i which rendered the argument inconclusive.

However, since the late 1980's a number of rainfall interception studies conducted in tropical forests located at continental edges and islands receiving high rainfall totals (>3000 $mm\ yr^{-1}$) have confirmed the possibility of very high E_i under such 'maritime' tropical conditions [*Bruijnzeel*, 1988; *Scatena*, 1990b; *Dykes*, 1997; *Cavelier et al.*, 1997; *Clark et al.*, 1998]. None of these studies used above-canopy climatic observations and continuously recording throughfall equipment which could have helped to explain the inferred high rates

of interception. Therefore the actual mechanisms and their relative importance were not identified. Neither has the dry-canopy evaporation component of ET (transpiration, E_t) been studied at these locations, and so the limits of forest ET under wet maritime tropical conditions remain to be explored [*Richardson*, 1982; *Malmer*, 1993; *Waterloo et al.*, 1999].

Arguably, a good way to resolve some of the methodological problems referred to above, is to combine hydrological and micrometeorological process studies. The present study aimed to evaluate the magnitude of ET and its components under the wet maritime tropical conditions prevailing in the Luquillo Experimental Forest (LEF), eastern Puerto Rico, through a combination of catchment hydrological, geophysical, throughfall and micrometeorological measurements. Earlier work in the LEF [*Scatena*, 1990b] had already suggested very high interception losses (up to 40 % of incident rainfall on an annual basis), adding further interest to the determination of a potentially extreme value for total ET. This paper reports results for ET and its main components as obtained during two years of observations in the 6.43 ha Bisley II catchment in the Tabonuco forest zone of the LEF. [*Schellekens et al.*, 1999, Chapter 3] present the results of a comparative application of various rainfall interception models.

2.2 STUDY AREA

The Bisley II catchment is situated at 18^o 18' N, 65^o 50' W at an elevation of 265–456 m above sea level (asl) (Fig. 2.1). The area is steep and dissected, with sharp divides, steep stream gradients and bowl-shaped valleys. Slopes in excess of 45 % (24^o) cover more than 50 % of the catchment. The 0.8 to 1.0 m deep clayey soils that have developed in the underlying thick-bedded tuffaceous sandstones and indurated siltstones are strongly leached Ultisols [*Scatena*, 1989]. Nonweathered bedrock is found at depths greater than 15 m below the level of the stream channel, regardless of position within the catchment [*Van Dijk et al.*, 1997]. Overlying the fresh bedrock is a zone of weathered rock of very low permeability ($< 2\ mm\, d^{-1}$).

The climate is maritime tropical (type A2m according to the Köppen classification), with the north-easterly trade winds bringing about 70 % of the annual rainfall of 3530 $mm \pm 22.6$ % (as measured at the nearby long-term rainfall station at El Verde, 450 m asl; see Fig. 2.1 for location) in association with tropical waves, depressions and cyclones. Rainfall is distributed fairly evenly throughout the year, with May and November being relative wet, January – March relatively 'dry' (Fig. 2.2). Rainfall at El Verde is delivered as numerous (267 rain days per year), relatively small (median daily rainfall 3.0 mm) storms of low intensity [$<5\ mm\, hr^{-1}$; *Brown et al.*, 1983; *García-Martinó et al.*, 1996]. Further information on rainfall characteristics will be given in Section 2.4.1.

The seasonal variation in mean monthly temperatures in the Bisley area is about 3.5^oC, ranging from $\sim 24^oC$ in December – February to about 27.5^oC in July–August. Seasonal variation in average daily relative humidity levels is

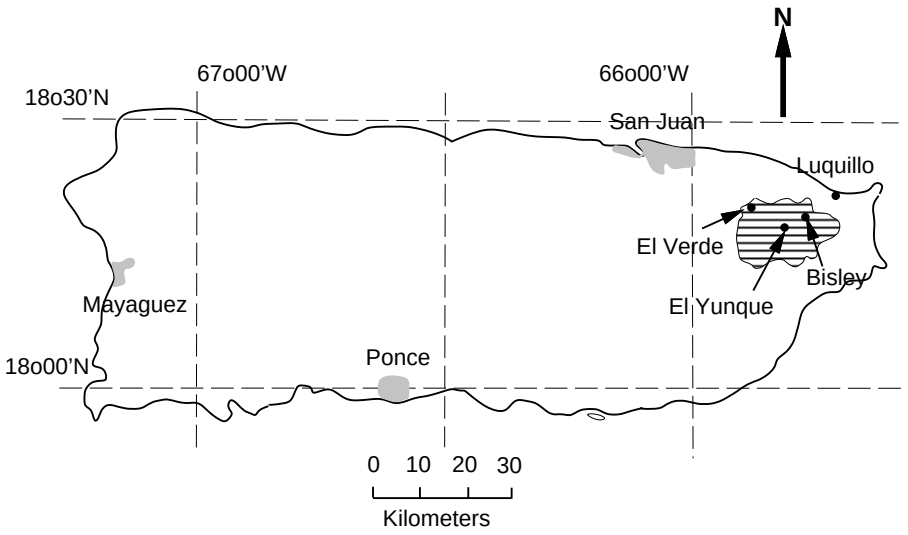

Figure 2.1: Map of Puerto Rico showing the location of the study site within the Luquillo Experimental Forest (indicated by the hatched area).

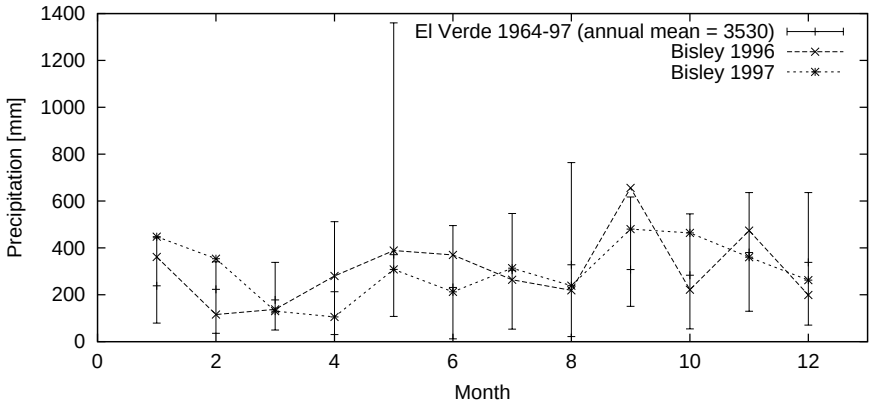

Figure 2.2: Monthly rainfall at Bisley in 1996 and 1997 compared with long-term means at El Verde (450 m above sea level; 1964–1997). The bars represent recorded minimum and maximum values for the respective months.

small (84 – 90 %). Average monthly wind speeds in the lower reaches of the LEF are $<$2 $m\,s^{-1}$ but vary between 2 and 5 $m\,s^{-1}$ around exposed summits at higher elevations. Average incoming solar radiation in the lowlands adjacent to the LEF (Cape San Juan) ranges from 13.8 $MJ\,m^{-2}\,d^{-1}$ in December to 26.0 $MJ\,m^{-2}\,d^{-1}$ in the summer months. At 1000 m elevation these amounts are roughly halved [*Brown et al.*, 1983]. Reference open-water evaporation [*Penman*, 1956] in the Bisley area is estimated at $\sim$1100 $mm\,yr^{-1}$ [*Holwerda*, 1997].

The Tabonuco forest is one of the four chief vegetation types found in the Luquillo Mountains, the others being colorado, palm and dwarf forests [*Wadsworth and Bonnet*, 1951; *Brown et al.*, 1983]. The Tabonuco forest has an irregularly shaped, 20–25 m upper canopy, an understory of palms and woody vegetation, and ground level herbs and shrubs. It occupies the lower reaches of the Luquillo Mountains (below 600 m). Both the structure and composition of the vegetation vary with topography and aspect relative to the trade winds [*Lugo and Scatena*, 1995]. The average leaf area index (LAI) of mature Tabonuco forest is between 6 and 7 but may range between 12.1 on ridges and 1.95 in dark ravines and riparian valleys [*Odum et al.*, 1970a]. In September 1989 the Bisley area was severely impacted and nearly completely defoliated by Hurricane Hugo [*Scatena et al.*, 1993]. However, by 1996 when the present study was initiated the LAI, canopy interception, and forest biomass were again similar to pre-hurricane conditions [*Scatena et al.*, 1996; *Holwerda*, 1997].

2.3 Methods and Instrumentation

2.3.1 Methods

The catchment water balance equation for the evaluation of ET [*Ward and Robinson*, 1990] reads as follows:

$$P = Q + ET + \Delta S + \Delta G + L \tag{2.1}$$

where P is the precipitation input, Q the amount of stream flow leaving the catchment, ΔS and ΔG the changes in soil moisture and ground water storages over the period of measurement, respectively and L the leakage into or out of the catchment (all expressed as mm of water). The results of a geophysical survey [*Van Dijk et al.*, 1997] strongly suggested that the catchment is watertight, that is, no significant amounts of water leave the catchment by some ungauged pathway. Consequently L in Eq. 2.1 was assumed negligible. A stage-discharge relationship developed for the culvert at the outlet of the catchment [*Scatena*, 1990a] was used to obtain discharge after converting the logger readings to water levels at the culvert entrance. Water level records were corrected for changes in stream bed geometry when necessary.

An estimate of ΔS was made by comparing the precipitation totals of the two weeks preceding the beginning and end of the water balance period. To estimate ΔG, discharge levels at the start and end of the water balance period were inserted into a master recession curve consisting of two superimposed

linear reservoirs [*Hall*, 1968] for which the coefficients were determined via non-linear regression [*Marquardt*, 1963]:

$$Q_t = Q_1 \cdot K_1^t + Q_2 \cdot K_2^t \tag{2.2}$$

where:

Q_t	discharge at time t	$[mm\,5min^{-1}]$
Q_1	initial discharge of reservoir 1	$[mm\,5min^{-1}]$
Q_2	initial discharge of reservoir 2	$[mm\,5min^{-1}]$
K_1	recession constant of reservoir 1	[-]
K_2	recession constant of reservoir 2	[-]
t	time	$[days]$

Furthermore, the change in groundwater storage between two points on the recession curve (Q_0 and Q_t) can be calculated according to:

$$\Delta G = \frac{\partial Q}{\partial t} = \frac{Q_t - Q_0}{lnK_1} + \frac{Q_t - Q_0}{lnK_2} \tag{2.3}$$

Total ET is made up of rainfall interception (E_i, evaporation from a wet canopy), transpiration (E_t, evaporation from a dry canopy) and evaporation from the soil/litter layer (E_s). The latter term proved very small for the El Verde forest [*Odum et al.*, 1970b] with only 3.5 % of the radiation reaching the forest floor [*Odum et al.*, 1970a]. In the present study, however, E_s is included in the estimate of E_t (see below). Amounts of E_i were derived by subtracting throughfall (TF) and stemflow (SF) from incident rainfall (P). Stemflow was not measured during the present study. Instead, an average value of 2.3 % of P, as obtained by *Scatena* [1990b] before the forest was disturbed by Hurricane Hugo, was adopted.

The magnitude of E_t was evaluated using the temperature variance (TVAR) method [*Tillman*, 1972; *De Bruin*, 1982] during dry canopy conditions, in combination with the simplified energy balance equation [*Brutsaert*, 1982]. Assuming that all available energy (A) is used either to warm up the air (sensible heat flux, H) or for evaporation (latent heat flux, $\lambda E = \lambda E_t$), while neglecting various small storage terms [*Brutsaert*, 1982] and equating A to net radiation (R_n), E_t can be derived from:

$$\lambda E_t = \lambda E = R_n - H \tag{2.4}$$

where:

λE	latent heat flux	$[W\,m^{-2}]$
R_n	net radiation	$[W\,m^{-2}]$
H	sensible heat flux	$[W\,m^{-2}]$

Net radiation (R_n) was estimated using a regression equation that was modified from that of *Shuttleworth et al.* [1984] for a lowland rain forest in central

Amazonia. To represent the difference in albedo between the forest at Bisley and the Amazonian forest, measurements of incoming and reflected solar radiation ($R_s\downarrow$ and $R_s\uparrow$) at Bisley were used to estimate the coefficient of the equation. The offset (representing the net long-wave component) was left unaltered:

$$R_n = 0.88R_s\downarrow -35 \tag{2.5}$$

where R_n and $R_s\downarrow$ are again expressed in $W\,m^{-2}$.

The TVAR method evaluates the magnitude of H under dry unstable atmospheric conditions from the standard deviation of rapid temperature fluctuations [*Tillman*, 1972; *De Bruin*, 1982] using the following equation:

$$H = \rho c_p \left[(\frac{\sigma_T}{C_1})^3 (kg\frac{z}{T}) \frac{(1 - C_2\frac{z}{L})}{-\frac{z}{L}} \right]^{\frac{1}{2}} \tag{2.6}$$

where:

ρ	density of dry air	$[kg\,m^{-3}]$
c_p	specific heat of air at constant temperature T	$[J\,kg^{-1}\,K^{-1}]$
σ_T	standard deviation of temperature fluctuations	$[K]$
g	acceleration due to gravity	$[m\,s^{-2}]$
z	height above the surface	$[\,m]$
T	air temperature	$[K]$
z/L	stability parameter	[-]
k	von Kármán's constant, 0.41	[-]
C_1, C_2	empirical constants [2.9 and 28.4 respectively, *De Bruin et al.*, 1993]	[-]

Under unstable atmospheric conditions, z/L equals the Richardson number (Ri). In the case of free convection ($Ri < -1$), Eq. 2.6 can be simplified to [*Vugts et al.*, 1993]:

$$H = 1.075\rho c_p \sigma_T^{\frac{3}{2}} \left(\frac{kgz}{T} \right)^{\frac{1}{2}} \tag{2.7}$$

Combining Eq. 2.7 and Eq. 2.4 enables the determination of λE and thus E_t from rapid dry-bulb temperature fluctuations measured at a single level. When measuring above a forest, however, it is necessary to replace z by $(z - d)$ in Eq. 2.7, where d is the zero plane displacement [*Thom*, 1975]. A value of d of 17.2 m ($0.86h_v$ where h_v is vegetation height in m [*Shuttleworth*, 1989]) was used throughout the calculations. When both wet- (σ_q) and dry-bulb temperature fluctuations are known, a Bowen ratio (β) approach can be applied [*Vugts et al.*, 1993]:

$$\beta = \frac{C_p \sigma_T}{\lambda \sigma_q} \tag{2.8}$$

Assuming that the spectra for temperature and humidity are the same, the use of the Bowen ratio approach should not produce an underestimation of H as a

result of the frequency losses associated with the use of thermocouples [*Moore*, 1986; *Van Asselt et al.*, 1991].

For those periods for which no thermocouple data were available, E_t was computed with the Penman-Monteith equation [*Monteith*, 1965]:

$$\lambda E = \frac{\Delta A + \rho C_p \, VPD / r_a}{\Delta + \gamma (1 + r_s / r_a)} \tag{2.9}$$

For wet canopy conditions Eq. 2.9 reduces to Eq. 2.10:

$$\lambda E = \frac{\Delta A + \rho C_p \, VPD / r_a}{\Delta + \gamma} \tag{2.10}$$

where:

λE	latent heat flux	$[W\,m^{-2}]$
A	Available energy	$[W\,m^{-2}]$
Δ	slope of the temperature-vapour pressure relationship at temp. T	$[Pa\,K^{-1}]$
γ	psychrometric constant	$[Pa\,K^{-1}]$
VPD	vapour pressure deficit	$[Pa]$
r_a	aerodynamic resistance	$[s\,m^{-1}]$
r_s	surface resistance	$[s\,m^{-1}]$

Values for the surface resistance parameter (r_s, in $s\,m^{-1}$) during selected hourly periods were derived using the corresponding TVAR-based estimates of E_t in an inverse application of the Penman-Monteith equation [*Shuttleworth*, 1988]:

$$r_s = \frac{\rho c_p}{\gamma} \frac{VPD}{\lambda E} + r_a \left(\frac{\Delta A}{\gamma \lambda E} - \frac{\Delta}{\gamma} - 1 \right) \tag{2.11}$$

The aerodynamic resistance (r_a) is normally obtained by Eq. 2.12 [*Thom*, 1975]:

$$r_a = \frac{(ln \frac{z-d}{z_0})^2}{k^2 u_{(z)}} \tag{2.12}$$

where:

z	measurement height above the ground surface	$[m]$
d	zero plane displacement height	$[m]$
z_0	roughness length	$[m]$
$u_{(z)}$	wind speed at height z	$[m\,s^{-1}]$

The ratio $0.06 h_v$ for the roughness length (z_0) of the forest in central Amazonia [*Shuttleworth*, 1989] was also applied in the present case.

2.3.2 INSTRUMENTATION

A 25.3 m scaffolding tower situated at 335 m asl on the eastern water divide of the catchment was instrumented to monitor above-canopy climatic conditions at 26 m. Incoming shortwave radiation (350–1100 nm) was measured by a Li-Cor LI-200X pyranometer. Air temperature and humidity were determined using a Vaisala HMP35C probe which was protected against direct sunlight and precipitation by a Model 41002 radiation shield. The accuracy of the humidity sensor was typically better that 2 % whereas a long-term stable precision of less than 1 % per year was stated by the manufacturer. Both the temperature and humidity were regularly calibrated against readings with an Assmann psychrometer. Two fast-response dry-bulb thermocouples and one wet-bulb thermocouple [chromel – constantane wire type, 0.127 mm diameter; *Tillman*, 1972] were used to measure rapid fluctuations in air temperature between 5 May and 9 July 1996 (66 days) for use in the TVAR method to derive sensible heat fluxes. Wind speed and direction were measured with a Met-One 014A Wind Set. A Texas Instruments tipping bucket rain gauge (TE525LL-L; 0.254 mm per tip) recorded precipitation. An adjacent totalizing rain gauge serving as a backup was emptied every week. All climatic data were stored in a Campbell Scientific Ltd. 21X data logger and retrieved weekly for further processing. The thermocouples were sampled every 2-sec whereas the other instruments were sampled every 5-sec. Precipitation data were stored at 5-min intervals. Averages of wet- and dry-bulb temperatures, their standard deviations and correlation coefficients were calculated every 5-min to avoid trends in the standard deviations. These were in turn averaged over 30-min periods and stored in the data logger. All other climatic data were stored at hourly intervals. Above-canopy climatic data (hourly measurements) were available for the whole of 1996 and 1997. Additional measurements of incoming and reflected shortwave radiation were made between 11 June 1997 and 16 June 1998 using a Kipp & Zonen model CM-7 type albedometer.

Throughfall (TF) was recorded continuously between 5 May and 9 July 1996 (66 days) using three flat-bottomed, sharp-rimmed steel gutters (6 x 300 cm) placed at a steep angle to minimize splash-out. Each gutter was equipped with a 180-litre capacity tipping bucket with logger system. To minimize wetting and drying losses the gutters were cleaned and sprayed with a silicone solution every week. In addition, TF was measured with 20 randomly placed but non-roving collectors (143 cm^2 surface area) which were emptied every week throughout 1996 and 1997. These fixed gauges have been in operation since June 1987 [*Scatena*, 1990b]. A roving gauge technique [*Lloyd and Marques-Filho*, 1988] had been adopted in the beginning but when an initial comparison of the performance of the fixed and roving gauges did not reveal significant differences, only the fixed network was maintained [*cf. Brouwer*, 1996]. The gutters and gauges were distributed throughout the catchment. The 5-min TF records obtained with the gutters were converted to areal averages every time the manual gauges were emptied, using a weighting procedure based on the relative magnitude of the surface areas of the respective gauge types.

Stream water levels were recorded at 5-min intervals by a Druck Ltd. PDCR-830 pressure transducer (1.5 mm accuracy) connected to a CTL data logger. Manual measurements using a staff gauge were made daily to check for instrumental drift. A nearly complete record of daily discharge totals was available for 1996 and 1997 [*IITF, unpublished data, 1998*].

2.4 RESULTS

2.4.1 RAINFALL CHARACTERISTICS

Total amounts of rainfall recorded at Bisley in 1996 and 1997 were 3687 and 3480 mm, *i.e.* slightly above (1996) and similar to (1997) the long-term mean of 3530 $mm\,yr^{-1}$ for El Verde. During the 66-day period of detailed micrometeorological observations in 1996 a total of 852 mm of rain was received, distributed over 80 events. Events were separated by a dry period of at least 3 hr which was the time over which the canopy was considered to dry completely. The average intensity of these events was 3.0 $mm\,hr^{-1}$, and the average storm size 10.7 mm, with an average duration of $3hr43min$ (Table 2.1). However, the results were influenced considerably by an extreme event (estimated return period > 5 yr) occurring on 13 May, 1996 during which 227.7 mm was delivered over a period of almost 21 hr (Table 2.1) of which more than 120 mm fell in three hr. Because of their rather skewed frequency distributions (Fig. 2.3A and Fig. 2.3B), the median values of storm size and duration — and (with them) rainfall intensity — were markedly lower than the average values (Table 2.1). Some 65 % of the storms were ≤ 5 mm (Fig. 2.3A) but owing to their small size their overall contribution to the total was much smaller ($\sim$12 %, Fig. 2.3C). On average, small storms also had a lower intensity compared to larger storms (compare Figures 2.3A and 2.3B). The diurnal distribution of rainfall occurrence and amount is shown in Fig. 2.4. Although more rain falls during the day, rainfall occurrence is higher during the night and early morning. This indicates the prevalence of small, low-intensity storms during the latter periods as opposed to the larger events that tend to occur mainly during the day.

2.4.2 THROUGHFALL CHARACTERISTICS

Throughfall totals for 1996 and 1997 amounted to 1814 and 2036 mm, corresponding to 49 and 59 % of gross precipitation respectively. At 45 % of P the relative amount of TF determined between 5 May 1996 and 9 July 1996 (period of continuous recording) represents one of the lowest values measured between March 1996 and March 1998 (Fig. 2.5).

The May–July 1996 TF dataset was subdivided into daytime and nighttime events. Table 2.2 lists the properties of the 54 storms that could be used in a day/night comparison (*i.e.* , a subset of those shown in Table 2.1). Storms that crossed the day/night boundary were excluded, as were storms larger than 15 mm so as to make the two sub-sets more comparable. As shown in Fig. 2.6, there was no significant difference in the relationship between TF and

Table 2.1: Statistical parameters for 80 rainfall (P) and throughfall (TF) events at Bisley during the period 5 May–9 July 1996.

	Size		**Duration**		**Intensity**	
	$P[mm]$	$TF[mm]$	$P[day{:}hr{:}min]$	$TF[day{:}hr{:}min]$	$P[mm\ hr^{-1}]$	$TF[mm\ hr^{-1}]$
Mean	10.7	4.8	00:03:34	00:04:41	3.0	1.0
Range	0.2–227.7	0.0–91.0	00:00:10–00:20:25	00:00:05–00:20:55	0.2–13.8	0.0–4.5
Median	3.3	1.4	00:02:25	00:03:16	1.9	0.4
Total	852.3	387.3	11:22:15	15:15:37		

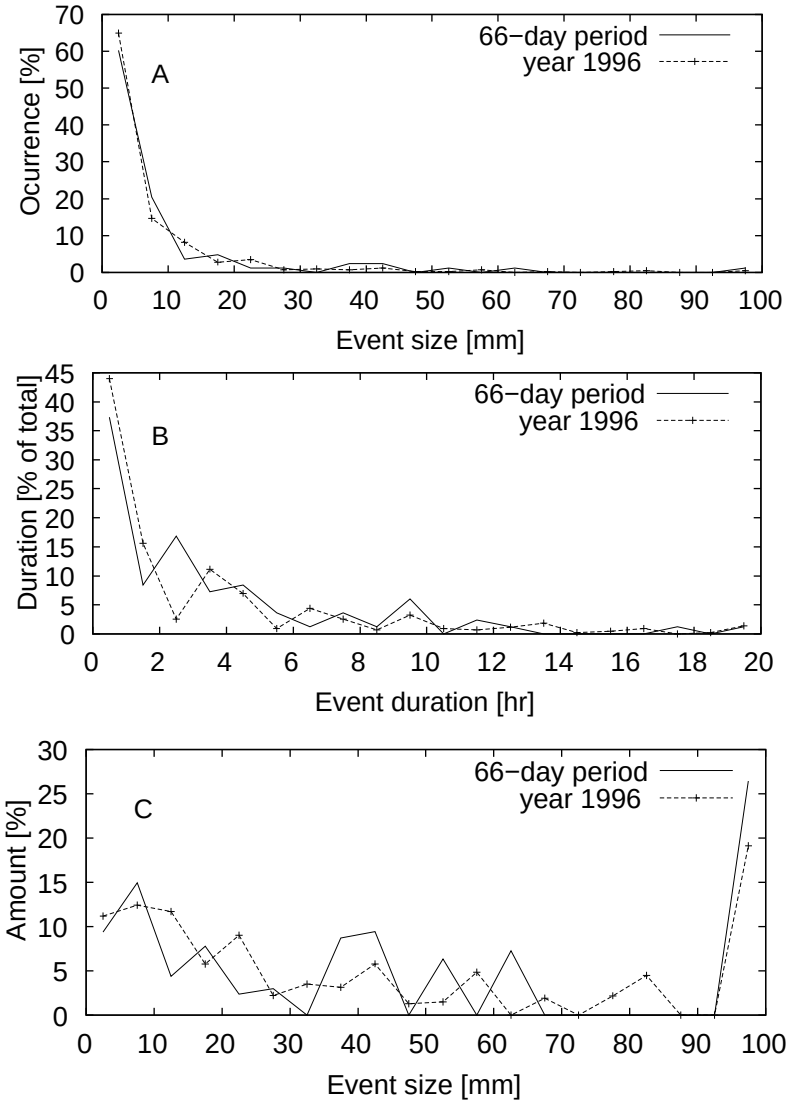

Figure 2.3: Frequency distributions of (A) rainfall; (B) event duration and (C) the relative contribution to total rainfall by differently sized events at Bisley during the whole of 1996 and during the 66-day period of intensive measurements in May–July 1996.

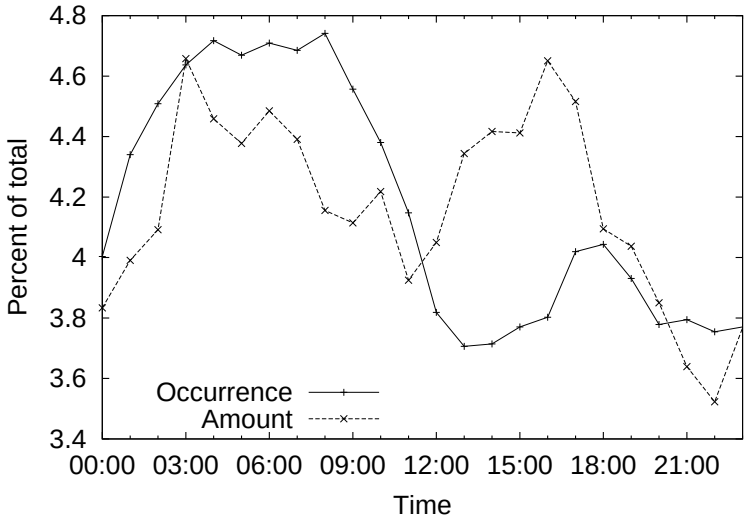

Figure 2.4: Diurnal distribution of relative amounts and occurrence of rainfall at Bisley in 1996 and 1997.

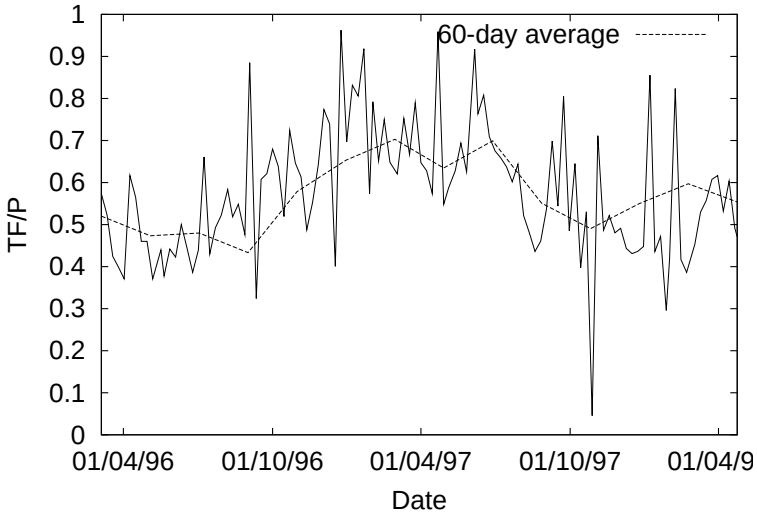

Figure 2.5: Seasonal variation in relative amounts of weekly throughfall at Bisley between March 1996 and April 1998.

Table 2.2: Statistical parameters of rainfall events during the period 5 May–9 July 1996 (all values in mm), separated by daytime or nighttime occurrence.

	Night		**Day**	
Number of storms	32		22	
	P	TF	P	TF
Mean	3.4	1.2	5.6	1.7
Median	2.9	0.8	5.3	1.5

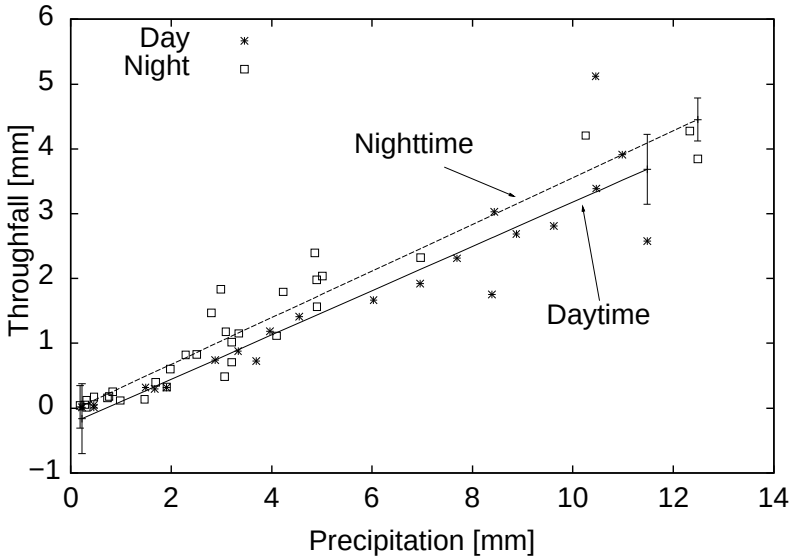

Figure 2.6: Relationships between incident rainfall and throughfall for daytime and nighttime conditions at Bisley between 5 May and 9 July, 1996.

P for daytime and nighttime conditions. Also, at least for storms ≤ 15 mm, the TF/P ratio was remarkably constant and apparently independent of storm size (Fig. 2.6). However, on a longer time scale, the TF/P ratio does vary (Fig. 2.5). The implications of these observations will be discussed in Section 2.5.3.

2.4.3 CATCHMENT WATER BALANCE

The amounts of water leaving the catchment as streamflow during the 66-day period of detailed TF and micrometeorological measurements, and 1996 and 1997 as a whole were 278, 1267 and 1301 mm, respectively, corresponding to 32, 34 and 37 % of P for the respective periods (Table 2.3). The changes in groundwater storage (ΔG in Eq. 2.1) for the observation periods were evaluated by determining the values of the constants in Eq. 2.3 using streamflow data for the May–July 1996 period. Application of Eq. 2.3 yielded negligibly

small values for ΔG in all cases, that is, 0.06 mm for the 66-day period in 1996, -0.04 mm for 1996 and 0.03 mm for 1997. Changes in soil water storage (ΔS in Eq. 2.1) were estimated by comparing precipitation totals during the two weeks preceding the start and end of the respective periods. Because the amounts of rainfall were found to be comparable in all cases (namely, 128 and 115 mm for the May–July 1996 period; 146 and 113 mm for 1996; 129 mm and 122 mm for 1997), ΔS was also assumed negligible. In addition, runs with a soil moisture model [*Schellekens*, 2000a] confirmed this contention. Because deep leakage (L in Eq. 2.1) had been proven to be negligible as well [*Van Dijk et al.*, 1997], Eq. 2.1 simplifies to:

$$ET = P - Q \tag{2.13}$$

Application of Eq. 2.13 yields a value for ET of 574 mm (8.70 $mm\,d^{-1}$) for the 66-day period in 1996 whereas ET totals for 1996 and 1997 were estimated at 2420 mm (6.61 $mm\,d^{-1}$) and 2179 mm (5.97 $mm\,d^{-1}$), respectively (Table 2.3).

2.4.4 EVAPORATION COMPONENTS

Water-budget based estimates of rainfall interception and transpiration

Rainfall interception losses (E_i) were derived from:

$$E_i = P - (TF + SF) \tag{2.14}$$

Applying a constant stemflow fraction of 2.3 % [*Scatena*, 1990b] yielded the following values of E_i for the 66-day period in 1996, the whole of 1996, and 1997 respectively: 444 mm (52.1 % of P), 1788 mm (48.5 %) and 1364 mm (39.2 %). By further subtracting the values of E_i from the corresponding ET totals, an estimate of transpiration (E_t) was obtained. This resulted in values of 130 mm (2.0 $mm\,d^{-1}$) for the May–July 1996 period, 632 $mm\,yr^{-1}$ (1.7 $mm\,d^{-1}$) for 1996 and 815 $mm\,yr^{-1}$ (2.2 $mm\,d^{-1}$) for 1997 (Table 2.3).

Transpiration according to the TVAR method

A total of 509 hours of thermocouple data was selected from the climatic record during which the canopy was dry and net radiation (R_n) intensity was ≥ 50 $W\,m^{-2}$, for use in the temperature variance (TVAR) method (Eq. 2.7). The selection criterion of 50 $W\,m^{-2}$ as representing intervals with free convection is somewhat on the low side considering the roughness of the forest. However, because an increase in the threshold value to 150 $W\,m^{-2}$ influenced the results only marginally (giving an increase in total E_t of 2 %) the criterion was maintained at 50 $W\,m^{-2}$. A comparison of H derived from Eq. 2.7 and Eq. 2.8 indicated an underestimation of H when using Eq. 2.7 of 32 %, close to the theoretical estimate of 30 % for frequency losses expected under the conditions prevailing at Bisley [*cf. Moore*, 1986]. A correction factor for frequency losses of 1.32 was therefore applied to H as estimated from the dry-bulb temperature fluctuations. Combining the resulting values for hourly sensible heat fluxes with corresponding amounts of R_n, E_t including evaporation from the soil was

Table 2.3: Total evapotranspiration (ET), transpiration (E_t), and rainfall interception (E_i) for the Bisley forest as determined with different methods during a 66-day period in May–July 1996, and the years 1996 and 1997. Amounts of rainfall (P), streamflow (Q), throughfall (TF) and stemflow (SF) have been added for comparison.

Water balance component	**Period**								
	May–July 1996			1996			1997		
	$[mm]$	$[mm/d]$	% of P	$[mm]$	$[mm/d]$	% of P	$[mm]$	$[mm/d]$	% of P
Rainfall	852	12.9	100	3687	10.1	100	3480	9.50	100
Throughfall	388	5.90	44.9	1814	4.96	49.2	2036	5.59	58.5
Stemflow	20	0.30	2.30	85	0.25	2.30	80	0.20	2.30
Streamflow	278	4.21	32.1	1267	3.46	34.4	1301	3.56	37.4
Evapotranspiration-$_{WB}{}^{*}$	574	8.70	67.4	2420	6.61	65.6	2179	5.97	62.6
Evapotranspiration-$_{PM}{}^{**}$	192	2.91	22.5	1039	2.84	28.2	1146	3.14	32.9
Transpiration-$_{WB}{}^{+}$	130	1.97	15.3	632	1.73	17.1	815	2.23	23.4
Transpiration-$_{PM}{}^{++}$	151	2.28	17.7	817	2.29	22.2	858	2.35	24.6
Interception-$_{WB}{}^{o}$	444	6.73	52.1	1788	4.88	48.5	1364	3.74	39.2
Interception-$_{PM}{}^{oo}$	41	0.62	4.81	221	0.60	5.99	287	0.79	8.25
Interception-$_{WBPM}{}^{x}$	403	6.11	47.3	1532	4.19	41.6	1218	3.34	35.0

*Catchment water budget method (Eq. 2.13); value for 1997 extrapolated from 359 days of runoff observations, annual value for 1996 extrapolated from 275 days

**Penman-Monteith method (Eq. 2.9 and Eq. 2.10); extrapolated from 324 days of climatic records in 1996 and 300 days in 1997

$^{+}$Water budget method ($E_{tWB} = P - Q - (P - TF - SF)$)

$^{++}$Penman-Monteith method (Eq. 2.9)

^{o}Water budget method ($E_{iWB} = P - TF - SF$)

^{oo}Penman-Monteith method (Eq. 2.10)

^{x} $E_{iWBPM} = P - Q - E_{tPM}$

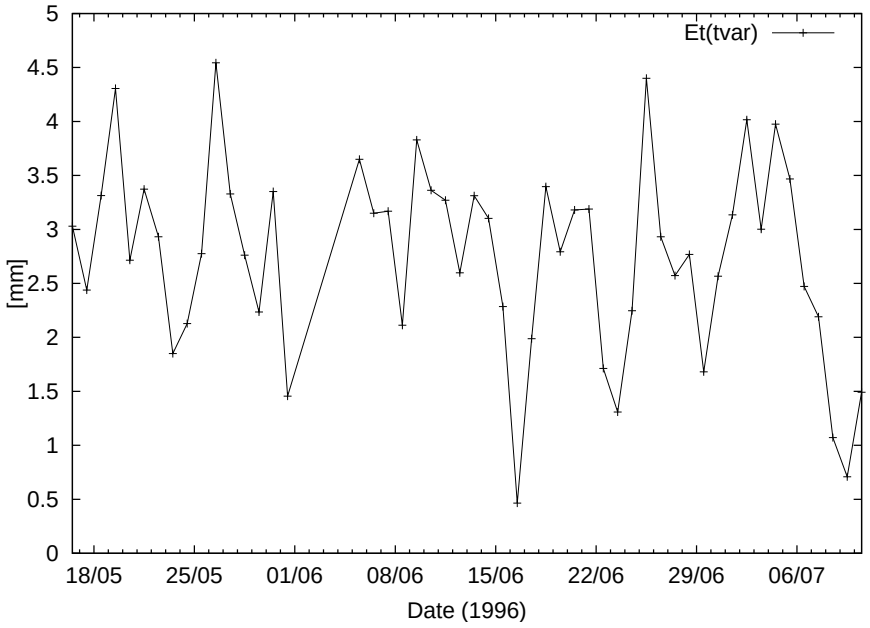

Figure 2.7: Daytime transpiration totals at Bisley as determined using the TVAR method between May and July, 1996.

estimated using Eq. 2.4. The application of Eq. 2.4 assumes that heat storage in trees as well as the soil heat flux are negligible. The small fraction of incoming radiation that reaches the forest floor in Tabonuco forest [3.5 %; *Odum et al.*, 1970a] indicates that the soil heat flux must be negligible. To evaluate the heat storage in the vegetation the approach of *Meesters and Vugts* [1996] was followed which uses daily average wind speeds in combination with biomass and hourly temperature data to estimate heat storage in stems. Maximum hourly heat storage was 12.1 $W\,m^{-2}$ while the minimum was -8.6 $W\,m^{-2}$. Incorporating changes in heat storage in the determination of E_t using the TVAR method resulted in a 2.4 % reduction, indicating that heat storage in trees can indeed be neglected at Bisley. The average value of E_t derived in this way for the selected hours amounted to 2.75 $mm\,d^{-1}$ (range 0.5–4.5 $mm\,d^{-1}$; Fig. 2.7), corresponding to a total dry canopy evaporation over a 52-day period of 143 mm.

Evaporation according to the Penman-Monteith equation

Before the Penman-Monteith equation (Eq. 2.9) could be applied to compute E_t for those days for which no thermocouple data were available, aerodynamic and surface resistances to evaporation (r_a, r_s) needed to be evaluated. Values of r_a were initially derived with Eq. 2.12 during periods of approximately neutral stability [*Thom*, 1975]. The resulting average diurnal pattern of r_a is shown

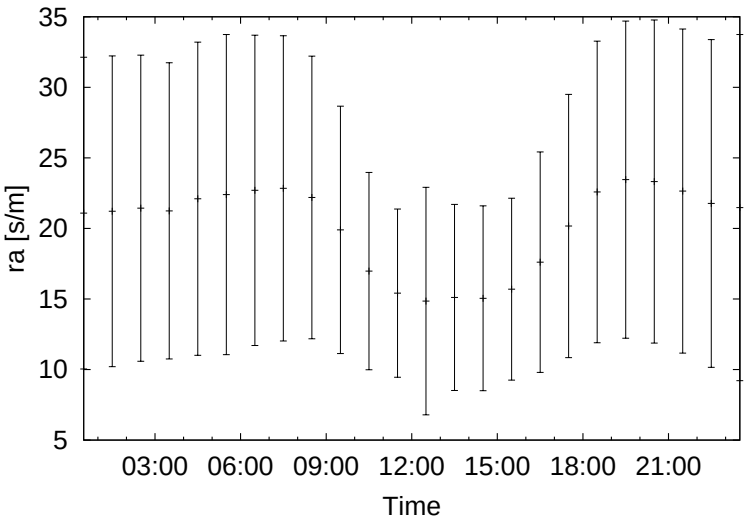

Figure 2.8: Average diurnal course of the aerodynamic resistance (r_a) of the Bisley forest in 1996 and 1997. Vertical bars represent corresponding standard deviation around the mean.

in Fig. 2.8. An average value of $\sim$20 $s\,m^{-1}$ was estimated. Inserting the values of E_t obtained for 52 days with the TVAR method into Eq. 2.11 produced the average diurnal pattern of r_s shown in Fig. 2.9. The average daytime value of r_s was determined at 58 $s\,m^{-1}$. To extend our estimates of r_s to other days as well, hourly values of r_s were regressed against corresponding hourly ambient climatic variables, notably $R_s\downarrow$, VPD, air temperature (T) and wind speed (u) as follows ($r^2 = 0.52, n = 509$):

$$r_s = e^{(0.6251 - 0.0019 R_s\downarrow + 0.1550\, VPD + 0.2247 T - 0.5699 u)} \tag{2.15}$$

This equation Eq. 2.15 is valid for daytime ($R_n > 50 W/m^2$) periods with dry canopy conditions.

Daytime totals of dry canopy evaporation (E_t) were computed by inserting the appropriate values for r_s and r_a into the Penman-Monteith equation (Eq. 2.9). The resulting E_t totals for the 66-day period in May–July 1996 ('calibration period'), and the years 1996 and 1997 amounted to 171 mm (2.6 $mm\,d^{-1}$), 888 $mm\,yr^{-1}$ (2.4 $mm\,d^{-1}$) and 961 $mm\,yr^{-1}$ (2.6 $mm\,d^{-1}$), respectively. As such, the Penman-Monteith based estimates of E_t were 16 % (May–July 1996), 29 % (year 1996) and 5 % (1997) higher than the corresponding catchment water budget-based estimates (Table 2.3). Expressed as a percentage of corresponding rainfall totals the difference between the two estimates of E_t amounted to 5 %, 7 % and 4 %, respectively (Table 2.3). Hourly rates of wet canopy evaporation [$r_s = 0$; *Monteith*, 1965] were computed with Eq. 2.10 and summed to total values for the three periods. Adding the resulting totals of 41 mm, 221 mm

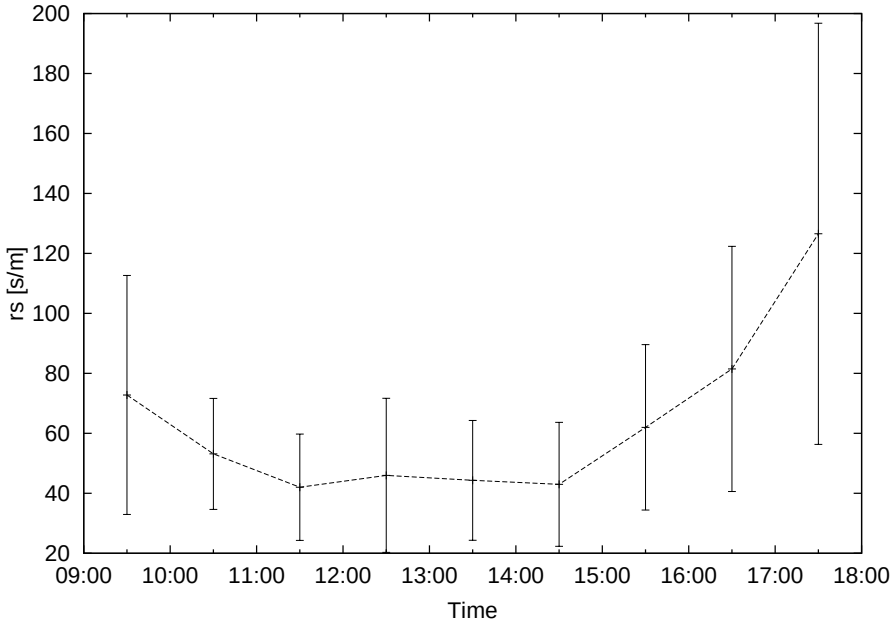

Figure 2.9: Average diurnal course of the surface resistance (r_s) of the Bisley forest based on an inverted application of the Penman-Monteith equation for 52 days between 17 May and 10 July 1996. Vertical bars represent standard deviation around the mean.

and 287 mm to the corresponding totals of E_t derived earlier, yielded Penman-Monteith-based estimates of total ET of 192 mm (2.9 $mm\,d^{-1}$), 1039 mm (2.8 $mm\,d^{-1}$) and 1146 mm (3.1 $mm\,d^{-1}$) for the 66-day period in May–July 1996 and the years 1996 and 1997, respectively (Table 2.3). As such, the estimates of ET obtained with the Penman-Monteith equation are much lower than those derived from the catchment water balance, mainly because of the contrast in the respective values estimated for wet canopy evaporation/rainfall interception (Table 2.3).

2.5 DISCUSSION

2.5.1 RAINFALL AND THROUGHFALL CHARACTERISTICS

At 3.0 $mm\,hr^{-1}$ the average rainfall intensity at Bisley is lower than the values reported for a number of lowland equatorial sites [5–10 $mm\,hr^{-1}$; *Bruijnzeel and Wiersum*, 1987; *Lloyd et al.*, 1988; *Noguchi et al.*, 1996] and only a little higher than the values characteristic of the maritime climates of more temperate latitudes [1.75–2.1 $mm\,hr^{-1}$; *Gash et al.*, 1980; *Pearce et al.*, 1980].

Relative amounts of throughfall (TF) in the Bisley forest rank as some of the lowest recorded for tropical lowland rain forest [typically 70–90 % of inci-

dent rainfall *Bruijnzeel*, 1990]. *Read* [1977] observed a similarly low TF value (50 %) in a lowland forest near the Caribbean coast of eastern Panama whereas values of 55–62 % have recently been reported for a number of montane forests in Central and South America [*Cavelier et al.*, 1997; *Clark et al.*, 1998; *Ataroff*, 1998]. However, the latter are likely to be caused primarily by the presence of abundant mosses and other epiphytes on branches and trunks which increases the canopy's capacity to intercept and store precipitation [*Veneklaas and Van Ek*, 1990] whereas the estimate for the lowland Panamanian forest was based on measurements made with only one throughfall trough. *Jackson* [1971] already noted that TF is notoriously difficult to estimate accurately, mostly due to the large spatial variability. *Lloyd and Marques-Filho* [1988] suggested that this is even more true for lowland tropical rain forest with its high species diversity and proposed a roving technique to reduce the sampling error. The forest at Bisley differs from the Amazonian forest, however, in that the trees are smaller and species diversity is considerably lower [*Scatena*, 1989]. In addition to being distributed throughout the catchment (instead of being concentrated in a small plot), the total area of the gauges and gutters employed in the present study was considerably larger than the area in the study by *Lloyd and Marques-Filho* [1988] in central Amazonia. Consequently, we would expect the present error in estimated TF to be smaller than the 11 % predicted for a non-roving setup with 20 gauges by *Lloyd and Marques-Filho* [1988].

As shown in Fig. 2.5, the seasonal variation in the TF/P ratio at the study site is considerable, with relatively low values in the 'summer' months (down to $\sim$0.45) and higher values during the 'winter' and 'spring' period (up to $\sim$0.70). Seasonal changes in rainfall, radiation and temperature are thought to be the main contributors to this variation.

Interestingly, a separate analysis of daytime and nighttime events did not reveal a significant difference in the TF/P ratio for daytime and nighttime conditions (Fig. 2.6). *Asdak et al.* [1998] observed a similar phenomenon for a lowland rain forest in central Kalimantan, Indonesia. Working in more temperate environments both *Pearce et al.* [1980] and *Dunin et al.* [1988] reported significant wet canopy evaporation during nocturnal events for *Nothofagus* and *Eucalyptus* forests in Southern New Zealand and South-east Australia, respectively. At the New Zealand site, where rainfall was both high (annual total 2610 mm) and often of long duration, nighttime evaporation even made up 50 % of the total wet canopy evaporation loss [*Pearce et al.*, 1980]. As will be discussed in more detail later, such observations strongly suggest that radiant energy alone is not sufficient to maintain such high wet canopy evaporation [*cf. Shuttleworth and Calder*, 1979]. Although the simple linear regression shown in Fig. 2.6 does not do justice to the complexity of the interception process the figure suggests that the same applies to the Bisley situation.

2.5.2 Catchment water balance and evaporation components

At 2420 and 2179 $mm\ yr^{-1}$ the evapotranspiration (ET) totals for the Bisley forest for 1996 and 1997 derived with the catchment water budget technique (Ta-

ble 2.3) represent some of the highest values ever obtained for lowland tropical rain forest [*Bruijnzeel*, 1990, his Table 1]. It is also higher than the 1707 $mm\ yr^{-1}$ derived for the entire elevational range in the LEF by *García-Martinó et al.* [1996] but compares well with the 1860–2154 $mm\ yr^{-1}$ found by *Odum et al.* [1970b] for the Tabonuco forest at El Verde and recent water budget based estimates for the entire Rio Mameyes watershed (17 km^2, of which the Bisley II catchment is part) for 1996 (2337 $mm\ yr^{-1}$) and 1997 (2134 $mm\ yr^{-1}$) by *Larsen and Concepción* [1998]. Although water budget estimates of ET can have wide error margins because of the accumulation of errors in the individual components of the water balance equation (Eq. 2.1) [*Lee*, 1970], these are likely to be limited in the present case. Not only must the catchment be considered watertight [*Van Dijk et al.*, 1997] but also the changes in groundwater and soil moisture storages (ΔG and ΔS in Eq. 2.1, respectively) were shown to be negligible. The errors in the remaining terms, precipitation (P) and streamflow (Q), are estimated at 5 and 10 % at the most respectively, suggesting the overall error in ET to be about 12 %, *i.e.* 70 mm, 290 mm and 260 mm for the May–July 1996 period and the years 1996 and 1997, respectively.

Part of the high value derived for E_i, and thus for total ET, may be attributed to our simple estimate of SF as a constant fraction of P [*Scatena*, 1990b]. This assumption might not be valid for large high-intensity storms [*Waterloo*, 1994]. Assuming the error in rainfall and throughfall measurements to be about 5 % [*Gash et al.*, 1980] the error in measured interception loss (at 45 % of gross rainfall) would be 16 %. A second argument for the validity of the high ET totals obtained for the Bisley forest concerns the reasonable agreement between the water-budget based values of ET and the sum of the micrometeorological (Penman-Monteith) estimates of E_t plus measured E_i ($\sim$7 %, Table 2.3). Accepting therefore, the high values for ET at Bisley, further inspection of Table 2.3 shows that the bulk of the total evaporation consists of wet canopy evaporation (E_i), namely, 57 % for 1997 and 65 % in 1996. As shown in Table 2.4, the magnitude of the dry canopy component of ET (E_t) at Bisley is quite comparable with results obtained for other lowland rain forests, confirming once more the importance of E_i at the study site.

Several possible sources of error can be identified for the present application of the temperature variance method. First, the Monin-Obhukov similarity theory requires measurements to be made high enough above the vegetation, preferably outside the roughness layer. However, it is equally important that the terrain should be as homogeneous and level as possible to avoid advection. Frequency losses caused by the use of relative slow-sampling thermocouples and the employed sampling procedures represent another source of error. Such losses depend on the diameter of the thermocouple wire, wind speed and measurement height [*Moore*, 1986; *Van Asselt et al.*, 1991]. Taking into account the prevailing wind speeds at Bisley, an underestimation of the sensible heat flux as much as 30 % may be obtained in this way [*cf. Moore*, 1986]. In a study above a palm forest in the LEF (at 700 m) and at a lowland forest site about 45 km to the west, M.K. van der Molen (personal communication, 1999) found no significant differences between sensible heat flux estimates above these forests

Table 2.4: Evaporation components for selected tropical and warm temperate forests. Evaporation values ($mm\ yr^{-1}$) rounded off to the nearest 5. Type codes: 1: Coastal and island sites, outer tropics; 2: Continental edge, equatorial; 3: Continental, equatorial; 4: Coastal sites, temperate latitude.

Location	Type	P	ET	E_i	E_t	E_i/E_t
Queensland, Australia[1]	1	4035	1420	1010	420	2.40
Puerto Rico[2]	1	3685	2420	1790	630	2.84
Puerto Rico[3]	1	3480	2180	1365	815	1.67
Fiji[4]	1	2015	1740	365	1375	0.27
Fiji[5]	1	2015	1540	355	1185	0.30
Sipitang, East Malaysia[6]	2	3945	1835	870	965	0.90
Jamaica[7]	2	3745	2000	710	1290	0.55
French Guyana[8]	2	3725	1440	560	880	0.64
West Java, Indonesia[9]	2	2850	1480	595	885	0.67
Peninsular Malaysia[10]	2	2775	1555	640	915	0.70
Eastern Brazil[11]	2	1819	1365	220	1145	0.19
Western Amazonia, Peru[12]	3	3065	1535	470	1065	0.44
Guyana[13]	3	2480	1485	345	1135	0.30
Central Amazonia, Brazil[14]	3	2390	1225	245	980	0.25
Sapulut, East Malaysia[15]	3	2370	1440	290	1150	0.25
Tai, Ivory Coast[16]	3	1995	1415	265	1150	0.23
South Island, New Zealand[17]	4	2610	1100	650	350	1.86
Plynlimon, Wales, U.K.[18]	4	2035	865	530	335	1.58

[1]*Gilmour* [1975] – [2]This study, 1996 – [3]This study, 1997 – [4]*Waterloo et al.* [1999], 6-year-old pines – [5]*Waterloo et al.* [1999], 15- year-old pines – [6]*Malmer* [1993] – [7]*Richardson* [1982] – [8]*Roche* [1982] – [9]*Calder et al.* [1986] – [10]*Abdul Rahim et al.* [1995] – [11]*Hölscher et al.* [1997] – [12]*Elsenbeer et al.* [1994a];*R. A. Vertessy, personal communication* – [13]*Jetten* [1994] – [14]*Shuttleworth* [1988]; *Lloyd and Marques-Filho* [1988] – [15]*Kuraji and Paul* [1994] – [16]*Collinet et al.* [1984]; *Hutjes et al.* [1990] – [17]*Pearce and Rowe* [1979]; *Rowe* [1979]; – [18]*Calder* [1990]

made at several heights (with $z - d$ ranging from 4.7 to 15.7) and concluded that the performance of the temperature variance method does not depend on the position in the roughness sublayer in these locations. Similar findings were obtained by *Vugts et al.* [1993] above a pine forest in Fiji. When comparing the TVAR based results with simultaneous eddy correlation measurements (using a sonic anemometer) at the lowland site an underestimation of the sensible heat flux by the TVAR method of up to 35 % was found (M.K. van der Molen, personal communication, 1999). These findings are in line with our Bowen ratio-based estimate (using both wet and dry-bulb thermocouples), which yielded a correction factor of 1.32 for the sensible heat flux (H), as derived with dry-bulb thermocouple temperature fluctuation measurements only.

In his review of evaporation from tropical rain forests, *Bruijnzeel* [1990] suggested an average value of about 1400 $mm\ yr^{-1}$ for forests not subjected to significant water stress, ascribing the occasionally reported outlier [*e.g.* 2000 $mm\ yr^{-1}$ for a sub-montane forest on the leeward site of Jamaica; *Richardson*, 1982] to catchment leakage [something which was not entirely ruled out by Richardson herself; *J. H. Richardson, personal communication, 1988*]. However, since 1990 there have been several studies that have also obtained high evap-

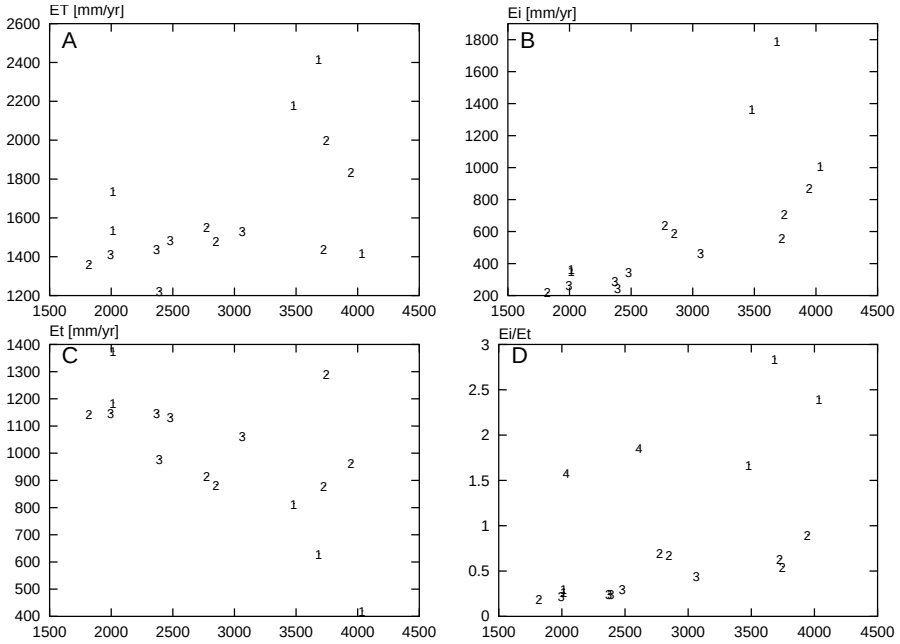

Figure 2.10: Annual precipitation *vs.* annual evapotranspiration (ET, A), transpiration (E_t, B), interception (E_i, C) and the E_i/E_t ratio (D) for the forests listed in Table 2.4 ('type 4' locations not included in A, B and C).

oration totals ($> 1700\ mm\ yr^{-1}$, Table 2.4), both in equatorial areas with high rainfall [*e.g.* Sipitang, East Malaysia; *Malmer*, 1993] and in the more seasonal outer tropics [leeward Viti Levu, Fiji; *Waterloo et al.*, 1999, *cf.* Table 4]. To these can be added the recent estimates for the entire Rio Mameyes catchment [*Larsen and Concepción*, 1998] and the present study. Such results seem to confirm the original finding of *Richardson* [1982], although her explanation ('high rainfall and breezy conditions') is not necessarily valid for the other high evaporation sites as well. As shown in Fig. 2.10A, annual totals of ET for lowland tropical forests increase with rainfall, although the scatter is considerable, particularly for rainfall exceeding 3500 $mm\ yr^{-1}$.

Interestingly, for a given rainfall, values of ET observed for forests located on islands in the outer tropics (*e.g.* Fiji, Jamaica, Puerto Rico; 18^o N or S, 'type 1') tend to be higher than those for forests situated closer to the equator (0–10^o N or S). The latter group may be subdivided into 'continental edge' ('type 2') and 'mid-continental' locations ('type 3'). The scatter in ET values is primarily due to the very large variation in intercepted rainfall (range: 220–1790 $mm\ yr^{-1}$; Table 2.4 and Fig. 2.10B) whereas the variability in dry canopy evaporation is generally less pronounced (range: 630–1375 $mm\ yr^{-1}$; Table 2.4 and Fig. 2.10C; leaving the exceptionally low value derived for NE Queensland [*Gilmour*, 1975]

aside for the moment which may be related to an overestimation of the stemflow component; *Bruijnzeel* [2000b]. It should be noted however, that with a few exceptions (Fiji, Brazil, Java) most of the estimates of E_t listed in Table 2.4 were derived by subtracting interception losses from overall ET. As such, they should be treated with caution. Nevertheless, an interesting pattern emerges when plotting the ratio E_i/E_t against rainfall (Fig. 2.10D). At the low end of the rainfall spectrum ($P<$ 2000 $mm\ yr^{-1}$), rainfall interception typically makes up 20–25 % of the total evaporation, regardless of site location in term of proximity to the ocean or the equator (*i.e.* types 1, 2 or 3). However, rainfall interception becomes gradually more important when annual rainfall exceeds a value of *ca.* 2500–2700 $mm\ yr^{-1}$, both in the absolute sense (Fig. 2.10B) and relative to E_t (Fig. 2.10D). Also, for similar amounts of rainfall above this 'threshold' of 2500 – 2700 $mm\ yr^{-1}$, both absolute and relative values of E_i tend to be somewhat higher for 'type 2' locations (equatorial continental edge sites) than for 'type 3' locations (mid-continental sites). In turn, values for 'type 1' locations (maritime outer tropical sites) exceed those for 'type 2' locations (Fig. 2.10B and Fig. 2.10D). Interestingly, two temperate maritime sites with high rainfall but lower absolute values of ET and E_t (Plynlimon, Wales, U.K.; NW tip of the South Island of New Zealand; Table 2.4) exhibit very similar values for E_i/E_t (Fig. 2.10D), confirming the importance of intercepted rainfall in both humid tropical and temperate maritime settings [*e.g. Pearce et al.*, 1980; *Calder*, 1990]. Such findings lend further credibility to the presently found high values for E_i and ET in Puerto Rico.

2.5.3 Wet canopy evaporation: inferred rates and possible explanations

The evaporation data for the Bisley forest presented in the preceding sections represent some of the highest values reported for lowland tropical rain forest (Table 2.4). Averaged over the two years 1996 and 1997, the total ET loss was approximately 42 % higher than the evaporation equivalent of the total net radiant energy input (R_n). The contrast becomes even larger when considering evaporation from a wet canopy. The observed annual rainfall interception totals of 1788 and 1364 mm for 1996 and 1997, respectively, correspond to average evaporation rates from a wet canopy (E_w) of 0.93 and 1.13 $mm\ hr^{-1}$. The latter far exceed the evaporation equivalents of the corresponding net radiant energy inputs, namely, 0.10 and 0.11 $mm\ hr^{-1}$, suggesting that at Bisley for wet canopy conditions typically only about 10 % of the required energy is supplied in the form of radiant energy. A similar, though less extreme, case has been documented by *Shuttleworth and Calder* [1979]. Here, the canopy of a spruce plantation at Plynlimon, Wales, U.K., was shown to receive typically only 20 % of its total energy input during wet canopy conditions in the form of radiant energy, whereas the average annual ET loss from the forest exceeded the total radiant energy input by about 12 % [*Shuttleworth and Calder*, 1979]. The maximum value of forest ET under wet temperate conditions is generally though to be limited by the amount of advected energy available to evaporate inter-

cepted rainfall from the wetted, aerodynamically rough forest canopy [*Shuttleworth and Calder*, 1979; *Calder*, 1998]. Conversely, under humid tropical conditions *Calder* [1998] considered forest ET to be limited primarily by radiation totals. Present findings suggest that this is most probably not the case at Bisley. High values of E_w [0.5–0.8 $mm\,hr^{-1}$; *Bruijnzeel and Wiersum*, 1987; *Dykes*, 1997; *Waterloo et al.*, 1999] have also been inferred from rainfall and throughfall measurements at other maritime tropical locations but much lower values [typically about 0.2 $mm\,hr^{-1}$or less; *Lloyd and Marques-Filho*, 1988; *Hutjes et al.*, 1990; *Asdak et al.*, 1998; *Waterloo et al.*, 1999] are usually calculated from above-canopy climatic measurements using Eq. 2.10. Similarly, *Gash et al.* [1980] derived an average value of 0.13 $mm\,hr^{-1}$ for E_w in the case of the Plynlimon spruce forest referred to earlier when using the climate data whereas a value of 0.24 $mm\,hr^{-1}$ was inferred from measured interception.

The origin of the energy needed in surplus of the radiant energy is still largely a matter of speculation. Advected warm air from the nearby Atlantic ocean is a likely source [*cf. Shuttleworth and Calder*, 1979], although, unlike the situation in Wales, wind speeds in the study area are rather low [typically 1.1–2.3 $m\,s^{-1}$; *Holwerda*, 1997; *Schellekens et al.*, 1998]. Another possible energy source is heat released upon condensation of water vapour in the air above the forest. The latter possibility seems to find support from the observation that larger rainfall events are accompanied by higher E_i (*i.e.*, the TF/P ratio is independent of storm size: Fig. 2.6) suggesting a positive feedback of rainfall amount (and thereby condensation) on the magnitude of E_i.

Accepting that the presently measured E_w requires the total available energy A in Eq. 2.10 to be much higher than measured R_n also has consequences for the magnitude of r_a. Typical daytime values of r_a at Bisley as computed with Eq. 2.12 were about 18 $s\,m^{-1}$ *vs.* about 22 $s\,m^{-1}$ at night when wind speeds are slightly lower [Fig. 2.8; *Holwerda*, 1997; *Schellekens et al.*, 1998]. The values for r_a can be compared with the r_a that would be required to match the measured and predicted rainfall interception (*i.e.*, E_i calculated from Eq. 2.14 and Eq. 2.10). Assuming that $A = \lambda E_w$ Eq. 2.10 can be rearranged to give:

$$r_a = \frac{\rho C_p\, VPD}{\gamma \lambda E_w} \tag{2.16}$$

The resulting average value for r_a was 2.1 $s\,m^{-1}$, a very low value. *Asdak et al.* [1998] obtained an average value of 3.2 $s\,m^{-1}$ for a forest in central Kalimantan, Indonesia (where similarly low wind speeds prevail), using a similar method. *Calder* [1977] derived an optimum value of 3.5 $s\,m^{-1}$ for the Plynlimon forest referred to earlier [*vs.* a theoretical value of 5.4 $s\,m^{-1}$ using Eq. 2.12 at an average wind speed of 3.75 $m\,s^{-1}$, *Calder*, 1990]. Even when taking into account the sensitivity of r_a (and thus E_w) as determined with Eq. 2.12 to variations in the magnitude of z_0 [*Gash et al.*, 1980] — particularly at high values of d/h_v — the latter parameters would have to be reduced to unrealistically low values to bring the outcome of Eq. 2.12 in agreement with Eq. 2.16. However, the outcome of Eq. 2.16 is sensitive to errors in VPD, especially under highly humid conditions [*Gash et al.*, 1980]. Lowering the relative humidity at Bisley

during rainfall by 2 % to an average value of 97.2 % (VPD is 79 Pa) raised the inversely determined r_a to 3.2 $s\,m^{-1}$, which is very similar to the values suggested by *Asdak et al.* [1998] and *Calder* [1990]. However, given the very low wind speeds at Bisley, this is not nearly enough a change to make the results from Eq. 2.12 and Eq. 2.16 comparable; to do so, unrealistically low values for the relative humidity during precipitation would be needed.

Thus, the question remains how the r_a at Bisley can be so low compared to values predicted by Eq. 2.12. *Calder* [1990] drew attention to the possibility of enhanced upward transport of evaporated moisture by gusts and eddies, even during neutral or stable conditions, although he added that the 'extent to which these gusts are associated with thermal- or humidity driven plumes, local topography or other factors is still unknown'. More recently, *McNaughton and Laubach* [1998] showed that such enhanced upward moisture transport increases with a relative increase of the standard deviation of wind speed compared to the mean wind speed. This confirms the contention of *Calder* [1990] that gusts may indeed be important, and although further study of the instantaneous wind data is needed it is probable that gusts are relatively important because of the low mean wind speed. In addition, the aerodynamic roughness of the Bisley forest may be increased further by its very irregularly shaped canopy as a result of hurricane damage in the past [*Scatena et al.*, 1993]. Further work is necessary to improve our understanding of the transport mechanism of evaporated moisture under conditions of low wind speed during rain events. Clearly, such transport at Bisley is much more efficient than suggested by Eq. 2.12.

An alternative approach to match measured and predicted rainfall interception totals was followed by *Calder et al.* [1986] when an application of the Rutter model of rainfall interception [*Rutter et al.*, 1971] underestimated measured E_i by more that 50 % in a secondary lowland rain forest in West Java, Indonesia. Apart from optimizing the value for r_a to 5 $s\,m^{-1}$ and modifying the wetting and drainage functions of the Rutter model, *Calder et al.* [1986] proposed the use of much larger values for the canopy storage capacity (S, up to 4–5 mm) than the 0.75–1.3 mm that have usually been obtained for tropical forests using more traditional techniques [*e.g. Jackson*, 1975; *Lloyd et al.*, 1988; *Asdak et al.*, 1998]. However, to match measured E_i totals at Bisley with those predicted by the analytical model of rainfall interception [*Gash*, 1979; *Gash et al.*, 1995] using above-canopy climatic parameters and Eq. 2.10 would require an optimized canopy storage capacity of $\pm$ 20 mm. In addition, the application of such an unrealistically high value for S produced a pattern of E_i that differed markedly from the measured one. Conversely, optimizing for E_w gave a near-perfect fit with observed daily totals. A further discussion of the performance of various interception models using the Bisley dataset was given in a companion paper [*Schellekens et al.*, 1999].

2.6 CONCLUSIONS

Although values of transpiration (evaporation from a dry canopy, E_t) for the Bisley forest in eastern Puerto Rico are within the 'low to normal' range for lowland tropical rain forests, those for intercepted rainfall (evaporation from a wet canopy, E_i) are exceptionally high (up to 50 % of incident precipitation, P). As a result, annual values of total evapotranspiration (ET) in eastern Puerto Rico are also very high (2180–2420 mm).

Several factors are believed to be responsible for these observations, including: *(i)* the frequent occurrence of rainstorms of low intensity associated with frontal activity; *(ii)* a highly effective net upward transport of evaporated moisture from the wetted canopy driven by the release of heat upon condensation; probably aided by: *(iii)* the proximity of the site to the warm waters of the Atlantic Ocean which may act as a source of advected energy brought in by the trade-winds; and *(iv)* a comparatively low aerodynamic resistance due to the broken-up character of the forest as a result of hurricane damage and its location in highly dissected terrain.

Comparison of the present results with those obtained for other tropical island and continental locations suggests that high ET losses may well be a distinct feature of near-coastal locations. The Penman-Monteith evaporation model failed to predict the observed high values for E_i unless the value of r_a was reduced to 2.1 $s\,m^{-1}$, a very low value. Further research is needed (and intended), especially on: *(i)* the proper quantification of the aerodynamic characteristics of lowland rain forest subject to hurricane disturbance and *(ii)* the elucidation of the nature of the large amounts of additional non-radiant energy required for sustaining the observed high evaporation rates.

2.7 ACKNOWLEDGEMENTS

The authors gratefully acknowledge the support of M.M.A. Groen and J. de Lange for the supply and construction of equipment. M.K. van der Molen is thanked for providing additional radiation data and his support during the evaluation of the TVAR results. The authors also wish to thank A.J. Wickel and R.J.P. van Hogezand for their assistance in the field.

3

MODELLING RAINFALL INTERCEPTION BY A LOWLAND TROPICAL RAIN FOREST IN NORTHEASTERN PUERTO RICO*

ABSTRACT

Recent surveys of tropical forest water use suggest that rainfall interception by the canopy is largest in wet maritime locations. To investigate the underlying processes at one such location — the Luquillo Experimental Forest in eastern Puerto Rico — 66 days of detailed throughfall and above-canopy climatic data were collected in 1996 and analyzed using the Rutter and Gash models of rainfall interception. Throughfall occurred on 80 % of the days distributed over 80 rainfall events. Measured interception loss was 50 % of gross precipitation. When Penman-Monteith based estimates for the wet canopy evaporation rate (0.11 $mm\ hr^{-1}$ on average) and a canopy storage of 1.15 mm were used, both models severely underestimated measured interception loss. A detailed analysis of four storms using the Rutter model showed that optimizing the model for the wet canopy evaporation component yielded much better results than increasing the canopy storage capacity. However, the Rutter model failed to properly estimate throughfall amounts during an exceptionally large event. The analytical model, on the other hand, was capable of properly representing interception during the extreme event, but once again optimizing wet canopy evaporation rates produced a much better fit than optimizing the canopy storage capacity. As such, the present results support the idea that it is primarily a high rate of evaporation from a wet canopy that is responsible for the observed high interception losses.

*This chapter also appeared as: Schellekens, J., F. N. Scatena, L. A. Bruijnzeel and A. J. Wickel, Modelling rainfall interception by a lowland tropical rain forest in northeastern Puerto Rico, *J. of Hydrol. 225*, pp 168–184, 1999.

3.1 INTRODUCTION

A survey of tropical forest water use (evapotranspiration, ET) reveals that the highest values (2000–2400 $mm\ yr^{-1}$) are observed at continental edge and island locations of high rainfall [*Bruijnzeel*, 2000a]. Much lower values (∼1200–1450 $mm\ yr^{-1}$) occur at mid-continental equatorial sites. Closer scrutiny of the data reveals that at wet 'maritime' sites, rainfall interception (evaporation from a wet canopy, E_i) may constitute a very large portion — up to 70 % — of ET compared to only 20–25 % at more 'continental' sites [*Schellekens et al.*, 2000, Chapter 2]. Similar contrasts have been reported for coastal and inland locations at temperate latitudes [*Calder*, 1977; *Gash and Stewart*, 1977; *Pearce et al.*, 1976]. Such findings reinforce the contention that deforestation at continental edge and island locations is likely to have a greater effect on river flow than in the case of mid-continental sites [*Shuttleworth*, 1989].

Although evidence for high to very high values of E_i ($\geq$ 30 % of incident rainfall) in tropical maritime conditions is increasing steadily [*Clements and Colon*, 1975; *Gilmour*, 1975; *Scatena*, 1990b; *Cavelier et al.*, 1997; *Clark et al.*, 1998; *Hafkenscheid et al.*, 1998], very few of these studies have used high resolution recording throughfall gauges in combination with above-canopy climatic observations to explain these high values. In the three studies for which detailed observations are available [*Calder et al.*, 1986; *Hafkenscheid et al.*, 1998; *Schellekens et al.*, 2000] the average wet canopy evaporation rate (E_w) inferred from measurements of incident rainfall (P), throughfall (TF) and stemflow (SF) greatly exceeded the rates predicted by the Penman-Monteith equation [*Monteith*, 1965]. Interestingly, no such discrepancies were observed in similar studies in more continental tropical lowland rain forests [*Lloyd et al.*, 1988; *Hutjes et al.*, 1990].

Various solutions have been proposed to bridge the gap between measured and predicted E_i. For example, in West Java *Calder et al.* [1986] not only used a reduced (optimized) value for the aerodynamic resistance to evaporation r_a (5 $s\,m^{-1}$), but they also proposed a much larger value for the canopy saturation value (S, 4–5 mm) than the 0.75–1.3 mm range that is usually obtained for tropical rain forests using more traditional techniques [*e.g. Jackson*, 1975; *Murdiyarso*, 1985; *Lloyd et al.*, 1988; *Scatena*, 1990b; *Elsenbeer et al.*, 1994a; *Jetten*, 1996]. *Calder et al.* [1986] based their choice of a high value of S on laboratory experiments by *Herwitz* [1985]. *Lloyd et al.* [1988], on the other hand, considered such high values artefacts and reverted to traditionally derived values of S for their forest in central Amazonia.

Several studies have documented exceedingly high annual rainfall interception totals — up to 50 % of gross precipitation — in a lowland rain forest in maritime northeastern Puerto Rico [*Scatena*, 1990b; *Schellekens et al.*, 2000]. To gain more insight in the underlying causes and mechanisms, the present paper examines the performance of two widely used rainfall interception models — the Rutter model [*Rutter et al.*, 1971, 1975] and the analytical model [*Gash*, 1979; *Gash et al.*, 1995] — using detailed measurements of rainfall, throughfall and above-canopy weather conditions for the 66-day period between 5 May and 9

July 1996. Particular attention is paid to the effect of variations in the magnitude of S and r_a on predicted E_i with a view to examine the suitability of the solutions proposed by *Calder et al.* [1986] under the extreme climatic conditions prevailing at the study site.

3.2 THE STUDY SITE

The 6.34 ha Bisley II catchment — in which the present study was conducted — is located on the northeastern slopes of the Luquillo Experimental Forest (LEF), northeastern Puerto Rico. The catchment is situated at 18^o 18'N, 65^o 50' W, between 265 and 456 m above mean sea level and is covered with Tabonuco (*Dacryodes excelsa*) type forest. The Atlantic Ocean is located at less than 10 km from the outlet of the catchment. The forest was hit by Hurricane Hugo in September 1989 [*Scatena and Larsen*, 1991]. As a result the Bisley forest has an irregular upper canopy, with the highest Tabonuco trees located on ridge tops; an understory of palms and woody vegetation, and ground level herbs and scrubs [*Lugo and Scatena*, 1995]. However, long-term observations of throughfall, litterfall and canopy biomass development [*Scatena et al.*, 1993, Scatena, unpublished data] as well as recent leaf area index (LAI) estimates [estimated at 5.9 around the TF gutters on the basis of light attenuation measurements; *Holwerda*, 1997] indicated that conditions in May–July 1996 were comparable to those prevailing before the hurricane disturbance. The average LAI of a similar forest nearby was estimated at 6.4 although it ranged from 1.95 in ravines to 12.1 on ridge tops and slopes carrying tall emergents [*Odum et al.*, 1970a].

The climate at the site is maritime tropical, type A2m according to the Köppen classification. The annual rainfall is about 3500 mm of which about 70 % is brought by the north-easterly trade-winds [*García-Martinó et al.*, 1996]. Rainfall is distributed fairly evenly within the year. Usually, May and November are the wettest months with about 385 mm each while the January–March period is relatively 'dry' with 200 mm per month on average. Rainfall events at nearby El Verde (450 m a.s.l.) are generally small (median of daily rainfall 3 mm) but numerous (267 rain days per year) and of relatively low intensity [<5 $mm\,hr^{-1}$; *Brown et al.*, 1983]. Mean monthly temperatures in the Bisley area vary little during the year (24^{o}C in December–February, 27.5^{o}C in July–August). Average humidity is high at 84–90 %. Average monthly wind speeds are $< 2\ m\,s^{-1}$ with, again, little seasonal variation [*Brown et al.*, 1983].

3.3 INSTRUMENTS

The period under investigation lasted from 5 May until 9 July 1996. Precipitation (P) was measured every 5 min above the canopy at 26 m on a scaffolding tower using a Texas Instruments tipping bucket rain gauge (TE525LL-L; 0.254 mm per tip). Back-up was provided by an adjacent totalizing rain gauge that was emptied once a week. Throughfall (TF) was measured throughout the catchment with 20 randomly positioned but non-roving collectors (143 cm^2

surface area) which were emptied weekly. These fixed gauges have been in operation since June 1987 [*Scatena*, 1990b]. A roving gauge technique [*Lloyd and Marques-Filho*, 1988] had been adopted in the beginning but after initial comparison of the performance of the fixed and roving gauges did not show significant differences, only the fixed network was maintained [*cf. Brouwer*, 1996]. In addition TF was recorded continuously using three flat-bottomed, sharp-rimmed steel gutters (6 x 300 cm) placed at a steep angle to minimize losses via splash. Each gutter was equipped with a tipping bucket with logger system manufactured at the Vrije Universiteit, Amsterdam. To minimize wetting losses and prevent clogging by debris the gutters were cleaned and sprayed with a silicone solution every week. The TF records obtained with the gutters were converted to areal averages every time the manual gauges were emptied, using a weighting procedure based on the relative magnitude of the surface areas of the respective gauge types. This correction also included any changes in the calibration of the tipping buckets [*Marsalek*, 1981]. Stemflow was not measured in this study. An average value of 2.3 % of P as derived in earlier study [*Scatena*, 1990b] was used throughout.

Wind speed and direction were measured at 26 m using a Met-One 014A Wind Set. Incoming short-wave radiation (350–1100 nm) was measured by a Li-Cor LI-200X pyranometer. Air temperature and humidity at 26 m were determined using a Vaisala HMP35C probe which was protected against direct sunlight and precipitation by a Model 41002 radiation shield. All climatic data other than rainfall were stored at hourly intervals in a Campbell Scientific Ltd. 21X data logger and retrieved weekly for further processing.

3.4 METHODS

3.4.1 DERIVATION OF CANOPY PARAMETERS

Both the Rutter and the analytical (Gash) model of interception require knowledge of the canopy structure as described by the following parameters:

S	canopy storage capacity: the amount of water left on the canopy when rainfall and TF have ceased	[mm]
p	free throughfall coefficient: the proportion of the rain which falls to the ground without striking the canopy	[-]
S_t	trunk water capacity	[mm]
p_t	proportion of rain that is diverted to stemflow	[-]

Earlier work on stemflow in the Tabonuco forest at El Verde by *Clements and Colon* [1975] suggested a trunk water capacity value of 0.01 mm. Given the much higher tree biomass at El Verde compared to Bisley [*Odum et al.*, 1970a; *Scatena et al.*, 1993], S_t at Bisley will be negligibly small. Therefore evaporation from the trunks was not considered further and a value for p_t equal to the

average stemflow fraction of 0.023 was used [*Scatena*, 1990b].

The canopy storage capacity (S) of the forest was determined using the methods of *Jackson* [1975], *Gash and Morton* [1978] and *Rowe* [1983]. The *Jackson* [1975] approach also allows the derivation of the free throughfall coefficient (p) as the slope of the regression between P and TF for storms that are too small to fill the canopy storage. It is assumed that evaporation losses during these small storms are negligible. The TF *vs.* P graph steepens beyond the inflexion point where canopy saturation is reached. In the Jackson approach S is determined as:

$$S = P_{inflection} - TF_{inflection} \tag{3.1}$$

where the inflection point is defined as the intersection of the two regressions between TF and P for storms that do and those that do not fill the canopy storage [*Jackson*, 1975].

Gash and Morton [1978] drew a straight line of near-unit slope ($1 - p_t = 0.0977$ in this case) through the upper points of the TF *vs.* P graph for storms $\geq 1.5\ mm$, assuming the highest points to represent conditions with minimal evaporation losses. S is then obtained as the negative intercept of the line with the TF axis.

Rowe [1983] proposed a simple event-based canopy water balance approach to estimate S. Assuming that the canopy storage will be filled by storms $\geq 2\ mm$ and that evaporation losses will be negligible for storms $\leq 4\ mm$, S can be estimated from:

$$S = P - TF - SF \tag{3.2}$$

3.4.2 THE RUTTER MODEL

Rutter et al. [1971, 1975] developed a numerical model of rainfall interception based on a running water balance of the canopy (and trunks, if required). Originally developed for a Corsican pine forest in Great Britain it has been applied to numerous forest types around the world, including tropical forests [*Calder et al.*, 1986; *Lloyd et al.*, 1988; *Hutjes et al.*, 1990]. A brief description of the model is given below.

The change in amounts of water stored on the canopy is determined by the proportion of the rain that hits the canopy, the drainage from the canopy, and evaporation of intercepted water:

$$\begin{array}{lll} dC/dt = (1 - p - p_t)R - E_w - D & when & C \geq S \\ dC/dt = (1 - p - p_t)R - (C/S)E_w - D & when & C < S \end{array} \tag{3.3}$$

where:

C	amount of water on the canopy	$[mm]$
R	rainfall intensity	$[mm\ min^{-1}]$
E_w	evaporation rate from the wet canopy	$[mm\ min^{-1}]$
D	drainage rate of water stored on the canopy	$[mm\ min^{-1}]$

with S, p, and p_t defined as before. E_w is usually estimated using the Penman-Monteith equation with the canopy resistance parameter (r_s) set to zero [*Monteith*, 1965]:

$$\lambda E_w = \frac{\Delta A + \rho C_p VPD/r_a}{\Delta + \gamma} \tag{3.4}$$

where:

λE_w	latent heat flux from the wet canopy	$[W\,m^{-2}]$
A	available energy	$[W\,m^{-2}]$
Δ	slope of the temperature-vapour pressure relationship at temperature T	$[Pa\,K^{-1}]$
γ	psychrometric constant	$[Pa\,K^{-1}]$
VPD	vapour pressure deficit	$[Pa]$
r_a	aerodynamic resistance	$[s\,m^{-1}]$
ρ	density of dry air	$[kg\,m^{-3}]$
C_p	specific heat of air at constant temperature T	$[Jkg^{-1}K^{-1}\,]$

The aerodynamic resistance (r_a) is generally calculated from the wind speed and the surface roughness, using a relationship which assumes that effects of atmospheric stability and bluff body forces are either compensating or negligible [*Thom*, 1975]:

$$r_a = \frac{(ln\frac{z-d}{z_0})^2}{k^2 u_{(z)}} \tag{3.5}$$

where:

k	von Kármán's constant, 0.41	[-]
z	measurement height above the ground surface	$[m]$
d	zero plane displacement height	$[m]$
z_0	roughness length	$[m]$
$u_{(z)}$	wind speed at heigth z	$[m\,s^{-1}]$

The displacement length d was taken as $0.86h_v$ (h_v, being the vegetation height in m) and the roughness length z_0 as $0.06h_v$ [h_v was 20 m, see *Schellekens et al.*, 2000, for details (Chapter 2)].

When the canopy is calculated as being only partially wet ($C < S$) the estimated evaporation rate is reduced such that (see Eq. 3.3):

$$E_{reduced} = (C/S)E_w \tag{3.6}$$

An exponential function is used to calculate drainage from the canopy:

$$D = D_0 e^{b(C-S)} \tag{3.7}$$

where:

D	drainage rate	$[mm\ min^{-1}]$
D_0	drainage rate when $C = S$ (saturated canopy)	$[mm\ min^{-1}]$
b	empirical parameter	[-]

To be consistent with the definition of S given earlier, D is set to zero when $C < S$. This also avoids the problem of a small but finite drainage when $C = 0$ [*Calder*, 1977]. The Corsican pine stand to which the Rutter model was applied originally, had a value for D_0 of 0.0019 $mm\ min^{-1}$. For other canopies with a different LAI, this would be expected to be $0.0019LAI/LAI_c$, where LAI_c is the leaf area index of Rutter's Corsican pine forest. Assuming S is directly proportional to LAI, the saturated drainage rate for other canopies can be obtained from the value of S (1.05) for the Corsican pine stand of *Rutter et al.* [1975] [*Rutter and Morton*, 1977; *Lloyd et al.*, 1988; *Jetten*, 1996]. A similar procedure can be followed to adjust the value of b. Thus when recalculating to a 'standard' S of 1 mm we obtain:

$$D_0 = 0.0019/1.05 \cdot S = 0.0018 \cdot S \tag{3.8}$$

$$b = 3.7 \cdot 1.05/S = 3.86 \cdot S \tag{3.9}$$

In the present study the set of equations for the Rutter model was solved using an explicit finite difference approximation of dC/dt.

3.4.3 THE ANALYTICAL (GASH) MODEL

The analytical model of rainfall interception is based on Rutter's numerical model [see *Gash*, 1979; *Gash et al.*, 1995, for a full description]. The simplifications that *Gash* [1979] introduced allow the model to be applied on a daily basis, although a storm-based approach will yield better results in situations with more than one storm per day [*Pearce and Rowe*, 1981]. The amount of water needed to completely saturate the canopy [P', *Gash*, 1979] is defined as:

$$P' = \frac{-\overline{R}S}{\overline{E}_w} ln \left[1 - \frac{\overline{E}_w}{\overline{R}} (1 - p - p_t)^{-1} \right] \tag{3.10}$$

where:

$\overline{R}$	average precipitation intensity on a saturated canopy	$[mm\ hr^{-1}]$
$\overline{E}_w$	average evaporation from the wet canopy	$[mm\ hr^{-1}]$

and with the vegetation parameters S, p and p_t as defined previously. The model uses a series of expressions to calculate the interception loss during different phases of a storm (Table 3.1). An analytical integration of the total evaporation and rainfall under saturated canopy conditions is then done for each storm to determine average values of $\overline{E}_w$ and $\overline{R}$. The total evaporation from

Table 3.1: Formulation of the components of interception loss according to *Gash* [1979]

Component of interception loss	Formulation
For m small storms ($P_g < P'_g$)	$(1-p-p_t)\sum_{j=1}^{m} P_{g,j}$
Wetting up the canopy in n large storms ($P_g \geq P'_g$)	$n(1-p-p_t)P'_g - nS$
Evaporation from saturated canopy during rainfall	$\overline{E}/\overline{R}\sum_{j=1}^{n}(P_{g,j} - P'_g)$
Evaporation after rainfall ceases for n large storms	nS
Evaporation from trunks in q storms that fill the trunk storage	qS_t
Evaporation from trunks in $(m+n-q)$ storms that do not fill the trunk storage	$p_t \sum_{j=1}^{m+n-q} P_{g,j}$

the canopy (*i.e.* the total interception loss E_i) is calculated as the sum of the components listed in Table 3.1. Interception losses from the stems are calculated for days with $P \geq S_t/p_t$ [*Gash*, 1979]. Because p_t and S_t are small in the present case (see Section 3.4.1), evaporation from the stems was neglected.

In applying the analytical model, saturated conditions are assumed to occur when the hourly rainfall exceeds a certain threshold. Often a threshold of 0.5 $mm\,hr^{-1}$ is used [*Gash*, 1979; *Gash et al.*, 1980; *Lloyd et al.*, 1988]. $\overline{R}$ is calculated for all hours when the rainfall exceeds the threshold to give an estimate of the mean rainfall rate onto a saturated canopy. $\overline{E}_w$ is then calculated using Eq. 3.4 and Eq. 3.5 (as in the Rutter model) using the same hours.

Gash [1979] has shown that in a regression of interception loss on rainfall (on a storm basis) the regression coefficient should equal $\overline{E}_w/\overline{R}$. Assuming that neither $\overline{E}_w$ nor $\overline{R}$ vary considerably in time, $\overline{E}_w$ can be estimated in this way from $\overline{R}$ in the absence of above-canopy climatic observations [*Rowe*, 1983; *Bruijnzeel and Wiersum*, 1987; *Dykes*, 1997]. Values of $\overline{E}_w$ derived thusly generally tend to be (much) higher than those calculated with Eq. 3.4 and Eq. 3.5 [*Gash et al.*, 1980; *Bruijnzeel and Wiersum*, 1987; *Waterloo et al.*, 1999].

3.5 RESULTS

3.5.1 MEASURED RAINFALL, THROUGHFALL AND INTERCEPTION

Between 5 May and 9 July 1996 a total of 852 mm of rain was received, of which 227 mm occurred in an extreme event on 13 May. During this period 53 days had rain, of which 33 % fell at night. The average amount of rainfall per event was 10.7 mm and the average duration was $3hr34min$, resulting in an average rainfall intensity of 3.0 $mm\,hr^{-1}$. However, the distribution of the 80 events was strongly skewed [*Schellekens et al.*, 2000] and therefore the use of median rather than average values is more appropriate. Events were separated by 3 hr without rain to allow for the complete drying up of the canopy. Me-

dian rainfall, duration and intensity — based on event analysis — were 3.3 mm, $2hr25min$ and 1.85 $mm\,hr^{-1}$, respectively. However, the choice of the temporal resolution of the precipitation data used for the determination of the intensity greatly influenced the results. For example, the average rainfall intensity derived from the 5-min records — using only intervals with recorded precipitation — was 7.2 $mm\,hr^{-1}$ (median 2.5 $mm\,hr^{-1}$) while the average rainfall intensity derived from hourly values using the same method was only 2.8 $mm\,hr^{-1}$ (median 1.0 $mm\,hr^{-1}$) *i.e.* closer to the event-based estimate of 3.0 $mm\,hr^{-1}$ (median 1.85 $mm\,hr^{-1}$). *Wadsworth* [1949] estimated the number of storms per year in the LEF at about 1600 with an average storm duration of 19 min. These figures were also derived from high temporal resolution data. The implications of such differences are discussed later.

A total amount of 388 mm of throughfall (TF) was recorded, implying a total interception loss (E_i) of 444 mm (52 % of P) when assuming an average stemflow fraction of 2.3 %. There was no significant difference in the TF *vs.* P relationships for day-time and night-time events [*Schellekens et al.*, 2000].

3.5.2 FOREST STRUCTURAL PARAMETERS

The results obtained with the various methods for determining the canopy capacity S and the free throughfall coefficient p are summarized in Fig. 3.1. Values of S derived with the methods of *Jackson* [1975] and *Gash and Morton* [1978] were very similar at 1.12 mm and 1.15 mm respectively. The less refined approach of *Rowe* [1983] gave a value of 1.68 mm which may well have been influenced by evaporation during the storms. A value for S of 1.15 mm was adopted for further use in the models. The value established for p (0.23) seems rather high in view of the dense forest of the study plot but was used throughout the calculations.

3.5.3 APPLICATION OF THE RUTTER MODEL

Fig. 3.2 shows the cumulative TF pattern predicted by the Rutter model for the 66-day study period. Various runs were made. In the first run (model A, top) a value of S of 1.15 mm was used in combination with a value for E_w according to Eq. 3.4 and Eq. 3.5 (0.11 $mm\,hr^{-1}$). It is immediately apparent from these graphs that TF is seriously overestimated (*i.e.* E_i is underestimated), particularly during the extreme event of 13 May. Total TF predicted by model A was 752 mm, an overestimation of 94 %. Excluding the extreme event and repeating the exercise still produced an overestimation of 79 %(TF total of 532 mm, Fig. 3.2a). In model B the value of S was retained at 1.15 mm but E_w was optimized — using a trial and error procedure — to the (very high) value of 2.80 $mm\,hr^{-1}$ (Fig. 3.2b). The effect of a five-fold increase of S to 5.75 mm [*cf. Calder et al.*, 1986] but retaining the value of E_w as estimated via Eq. 3.4 and Eq. 3.5 (model C) was examined next. As shown in Fig. 3.2c the prediction by model C is somewhat better than in the case of model A but total TF is still overestimated considerably (estimated total TF 496 mm, an overestimation of

(a)

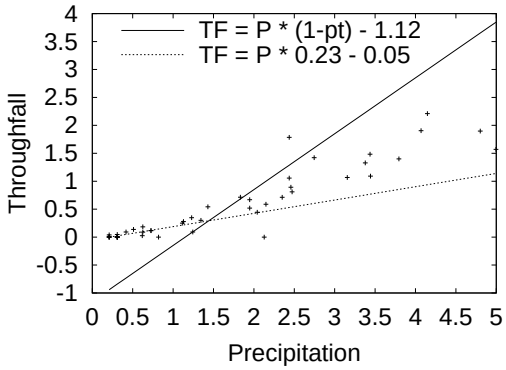

(b)

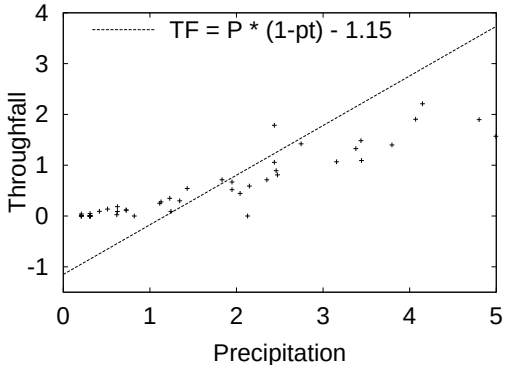

(c)

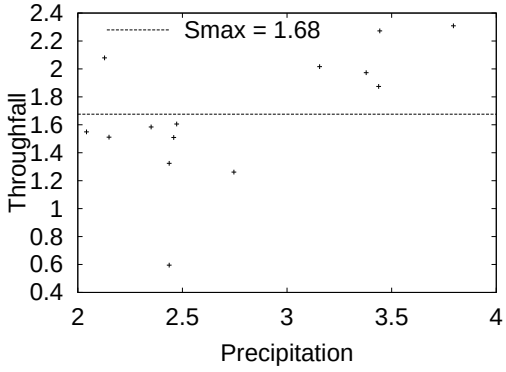

Figure 3.1: Estimation of the canopy parameters S and p using the methods of: (a) *Jackson* [1975] S = 1.12, p = 0.23, (b) *Gash and Morton* [1978] S = 1.15, and (c) *Rowe* [1983] S = 1.68. Y-axes show throughfall (TF, in mm) and X-axes show rainfall (P, in mm).

(a)

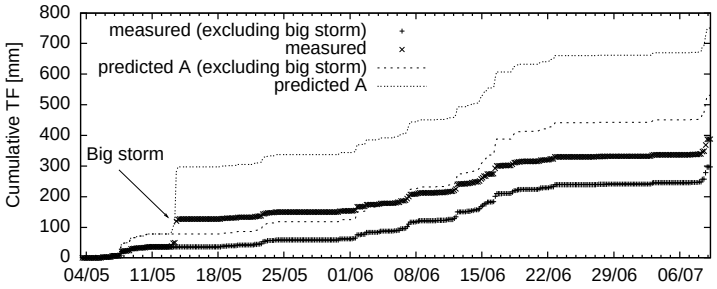

(b)

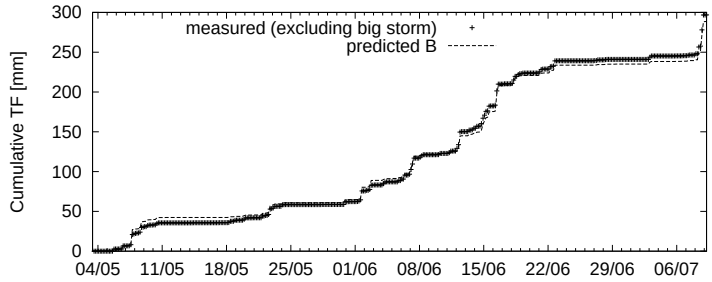

(c)

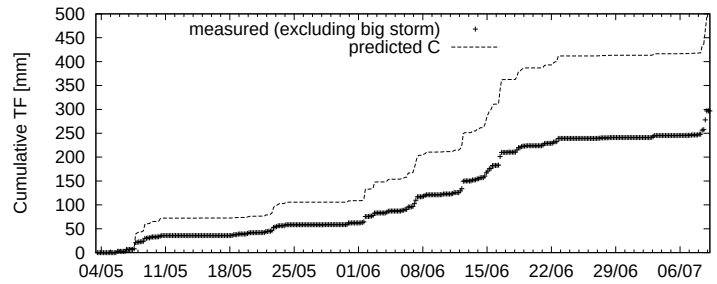

(d)

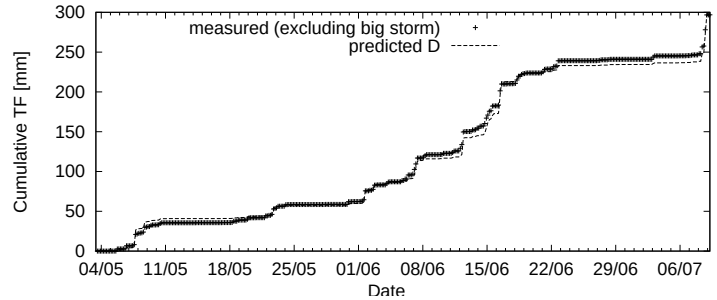

Figure 3.2: Measured and modelled cumulative throughfall for the Rutter model using four scenarios: (a) Model A, $S = 1.15\ mm$, $E_w = 0.11\ mm\,hr^{-1}$; (b) Model B, $S = 1.15\ mm$, $E_w = 2.80\ mm\,hr^{-1}$; (c) Model C, $S = 5.75\ mm$, $E_w = 0.11\ mm\,hr^{-1}$; (d) Model D, $S = 5.75\ mm$, $E_w = 1.10\ mm\,hr^{-1}$.

Table 3.2: Sensitivity analysis of the Rutter model to changes in the main parameters (model scenario B, 'optimum fit', excluding the big storm of 13 May 1996) showing the changes in predicted TF after increasing or decreasing a parameter by 10%.

Parameter	Resulting TF				
(initial value)	Measured	+ 10%	-10%	% change+	% change-
E_w (2.8 $mm\,hr^{-1}$)	296.3	287.6	305.9	-2.9	3.3
S (1.15 mm)	296.3	292.2	300.8	-1.4	1.5
p (0.23)	296.3	301.9	290.9	1.9	-1.8
p_t (0.023)	296.3	295.4	297.2	-0.3	0.3

30 %). An optimized value for E_w of 1.1 $mm\,hr^{-1}$ was required to fit measured and predicted TF totals when using the increased value for the storage capacity (5.75 mm, model D). The sensitivity of the present application of the Rutter model to changes in the magnitudes of E_w, S, p and p_t is explored in Table 3.2. The sensitivity of the model to changes in E_w in particular is clearly borne out by these simulations.

A more detailed look at the performance of the Rutter model during four individual storms is presented in Figures 3.3 and 3.4. The first storm (no. 29, 8.55 mm of precipitation, 3hr duration) occurred on 30 May 1996 (Fig. 3.3-a,b), the second one (no. 56, 54.8 mm of precipitation in 10hr30min) on June 16 1996 (Fig. 3.3-c,d). The third and fourth storms occurred on 18 June 1996 (no. 58, 17.3 mm of precipitation in 6hr, Fig. 3.4-a,b) and on 8 July 1996 (no. 78, 62.7 mm in 10hr Fig. 3.4-c,d) respectively. The parts (a) and (c) of each Figure depict the actually measured patterns of P and TF plus predicted TF according to models B (S = 1.15 mm; optimized E_w = 2.80 mm) and D (S = 5.75 mm; optimized E_w = 1.1 mm) given earlier. Although neither of the two scenarios gives a perfect fit to the measured data it is clear that model B (original S) conforms better to reality than model D (increased S). As shown in parts (a) and (c) of Fig. 3.3 and Fig. 3.4, the throughfall predicted by model D reacts too slowly to changes in rainfall intensity, which leads to serious overestimation of TF after rainfall has ceased. Furthermore, as illustrated in parts (b) and (d) of Fig. 3.3 and Fig. 3.4, the amount of water stored on the canopy (C) predicted by model D sometimes attains unrealistically high values (up to 10 mm). Modelling efficiencies as calculated with the method developed by *Nash and Sutcliffe* [1970] (a value of 1 indicates a perfect fit) for model B were determined as 0.56 (storm 26), 0.50 (storm 56), 0,67 (storm 58) and 0.74 (storm 78) while those for model D were determined at 0.65 (storm 26), 0.45 (storm 56), 0.63 (storm 58) and 0.73 (storm 78).

3.5.4 APPLICATION OF THE ANALYTICAL MODEL

Measured and predicted totals of TF as determined by the analytical model are presented in Fig. 3.5. Initially the model was run both on a daily and on an event basis. Because the difference between the two respective predictions was

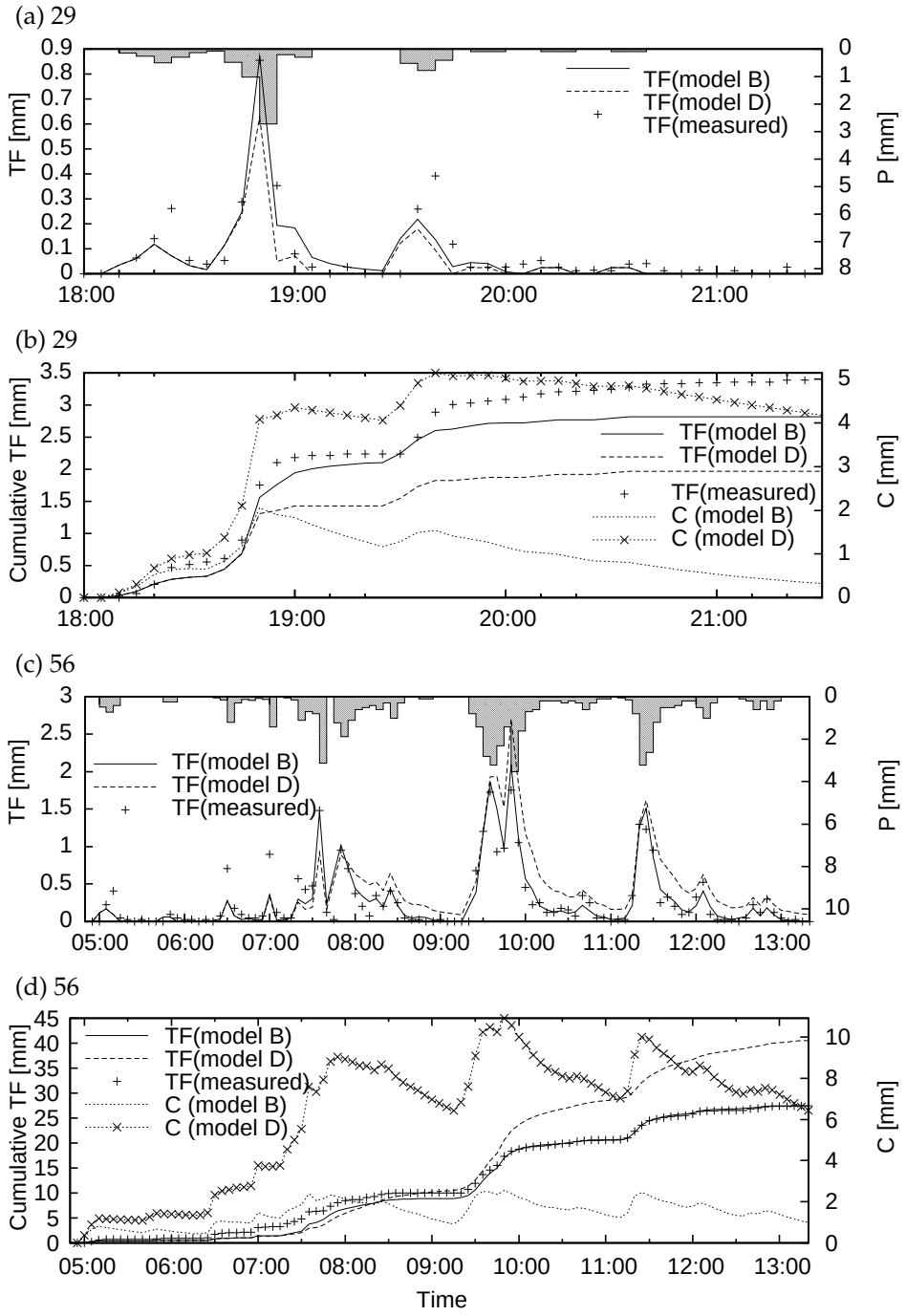

Figure 3.3: Measured and modelled throughfall patterns predicted by the Rutter model for: (a, b) storm no. 29 (8.5 mm) and (c, d) storm no. 56 (54.8 mm). Also indicated in (b) and (d) are the predicted amounts of water stored on the canopy.

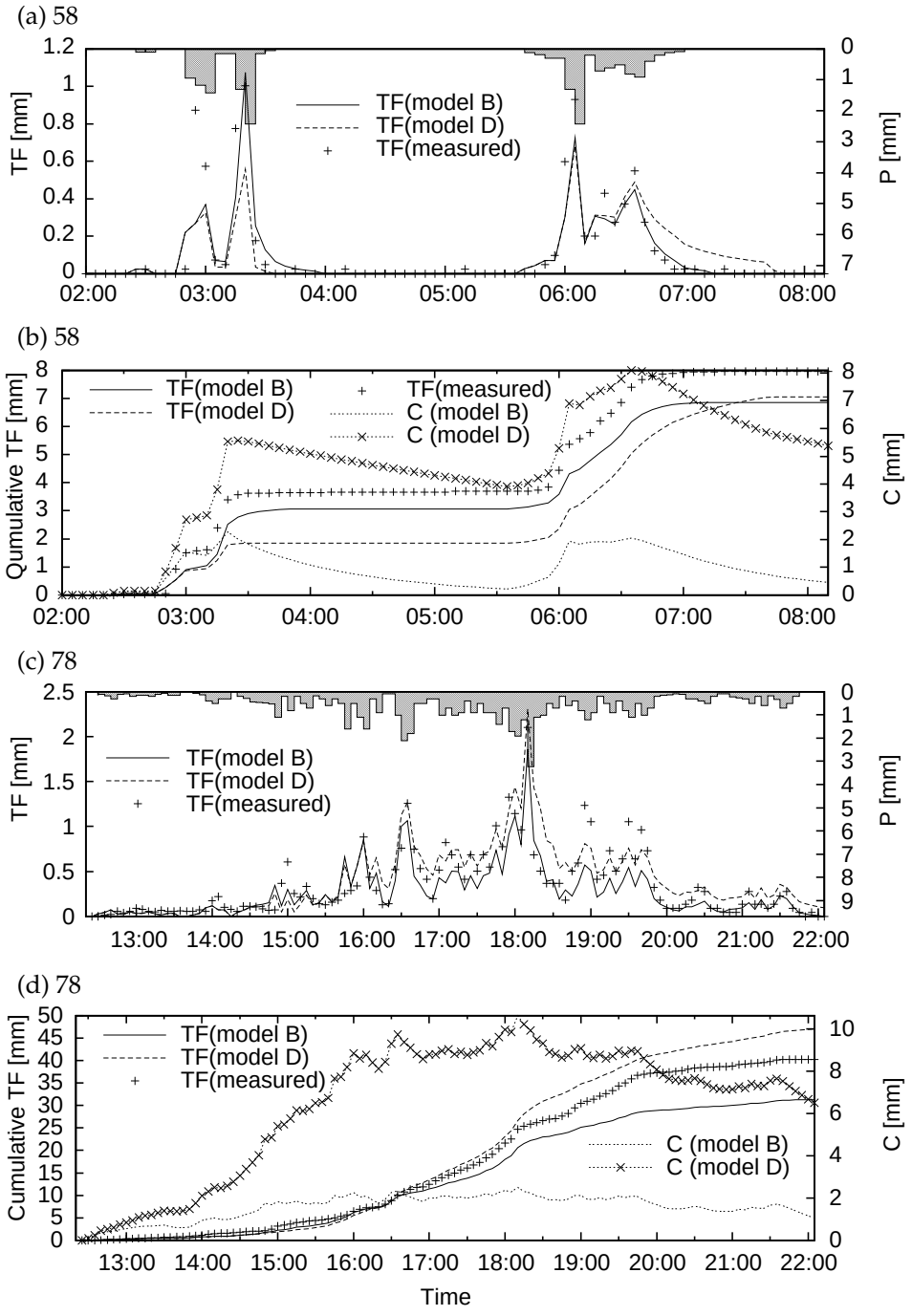

Figure 3.4: Measured and modelled throughfall patterns predicted by the Rutter model for: (a, b) storm no. 58 (17.3 mm) and (c, d) storm no. 78 (62.7 mm). Also indicated in (b) and (d) are the predicted amounts of water stored on the canopy.

Table 3.3: Amounts of throughfall and components of interception loss for four scenarios used in an application of the Gash model. A: S = 1.15, $\overline{E}_w/\overline{R}$ = 0.06; B: S = 1.15, $\overline{E}_w/\overline{R}$ = 0.51; C: S = 5.75, $\overline{E}_w/\overline{R}$ = 0.06, D: S = 5.75, $\overline{E}_w/\overline{R}$ = 0.395. Model efficiency values according to the method of *Nash and Sutcliffe* [1970].

Component of interception loss	Model			
	A [mm]	B [mm]	C [mm]	D [mm]
total gross rainfall	850	850	850	850
wetting-up of the canopy	4.7	38.6	56.5	162.3
evaporation from a saturated canopy	46.8	378.2	34.0	198.3
evaporation from canopy after rainfall ceases	47.2	42.6	155.3	97.8
total calculated interception loss	99	459	246	458
total calculated throughfall	732	371	585	372
total measured throughfall	386	386	386	386
model efficiency	0.11	0.96	0.12	0.91

Table 3.4: Sensitivity analysis of various parameters in the 'model B' scenario of the analytical model showing the change in predicted TF after increasing or decreasing a parameter by 10%.

Parameter	Resulting TF				
(initial value)	Original	+ 10%	-10%	% change+	% change-
$\overline{E}_w/\overline{R}$ (0.51)	371.3	331.7	411.3	-10.7	10.8
S (1.15 mm)	371.3	369.0	373.6	-0.6	0.6
p (0.23)	371.3	372.5	370.1	0.3	-0.3
p_t (0.023)	371.3	369.5	373.1	-0.5	0.5

very small, daily rainfall was used in the various simulations discussed below.

Model A employed a value of S of 1.15 mm and an $\overline{E}_w/\overline{R}$ of 0.06 as based on the estimated evaporation using Eq. 3.4 and Eq. 3.5 and recorded rainfall intensity (1.85 $mm\,hr^{-1}$). As shown in Fig. 3.5, model A severely underestimated the measured interception loss (*cf.* Table 3.3). An optimum fit (model B, including the 13 May event) was obtained when using the original estimate of S and an optimized value for $\overline{E}_w/\overline{R}$ of 0.51 as derived from the regression of interception loss *vs.* gross precipitation [*Gash*, 1979, *cf.* Table 3.3]. Increasing S to 5.75 mm (model C) produced a somewhat better result than model A but to establish an optimum fit $\overline{E}_w/\overline{R}$ still had to be increased to 0.395 (model D).

The importance of $\overline{E}_w/\overline{R}$ to the outcome of the analytical model is further highlighted by the sensitivity analysis given in Table 3.4. A 10 % change in the magnitude of $\overline{E}_w/\overline{R}$ produced an equally large change in predicted TF. As shown in Table 3.3, evaporation from a saturated canopy contributed the bulk (82 %) of the total predicted interception loss in model B ($S = 1.15$, optimized $\overline{E}_w/\overline{R}$), with near-equal contributions by evaporation during the wetting up and drying of the canopy (8 and 9 % respectively) and only minor contribu-

(a)

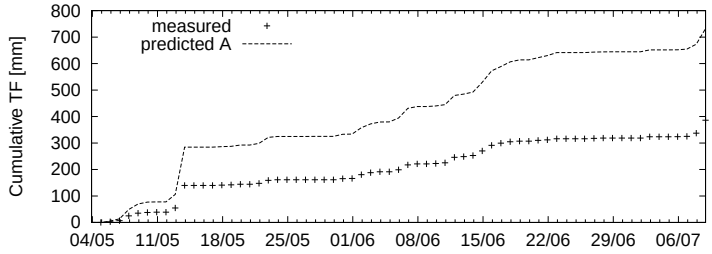

(b)

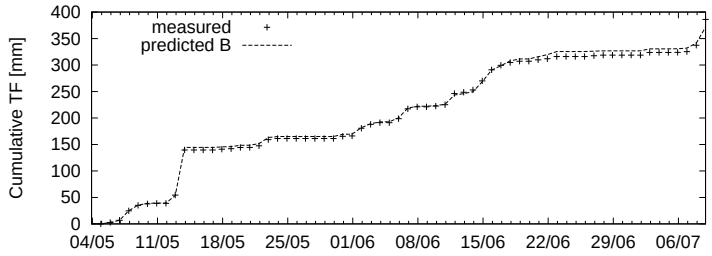

(c)

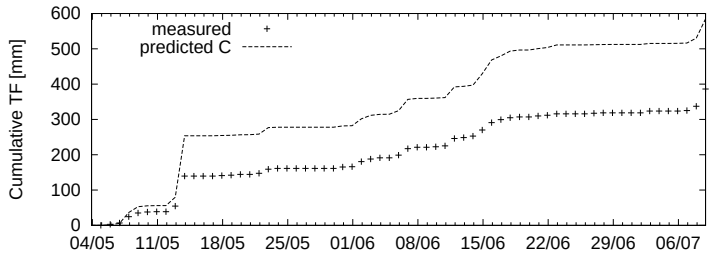

(d)

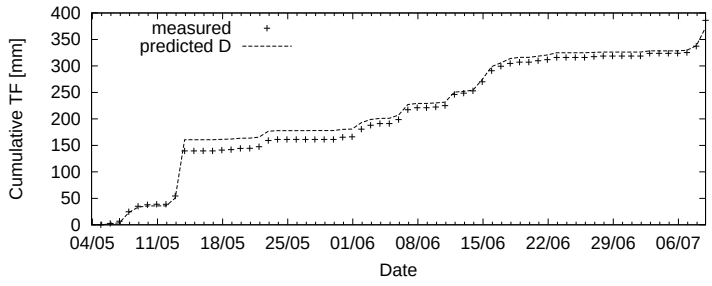

Figure 3.5: Observed and predicted cumulative throughfall according to the analytical model for four scenarios: (a) model A, $S = 1.15\ mm$, $\overline{E}_w/\overline{R}= 0.06$; (b) Model B, $S = 1.15\ mm$, $\overline{E}_w/\overline{R}= 0.51$; (c) Model C, $S = 5.75\ mm$, $\overline{E}_w/\overline{R}= 0.06$; (d) Model D, $S = 5.75\ mm$, $\overline{E}_w/\overline{R}= 0.395$.

tions associated with small storms. Naturally, raising the value of S to 5.75 mm greatly increased the predicted importance of the wetting and drying components (models C and D; Table 3.3). Table 3.3 also lists the respective model efficiencies as calculated using the *Nash and Sutcliffe* [1970] method indicating a slightly better performance for model B compared to model D.

Based on the $\overline{E}_w/\overline{R}$ value derived from the regression of E_i on P (0.51), an apparent average wet canopy evaporation rate of 0.94 $mm\,hr^{-1}$ is obtained when inserting the median rainfall intensity of 1.85 $mm\,hr^{-1}$ in the case of $S = 1.15$; the corresponding value of E_w for S = 5.75 mm is 0.73 $mm\,hr^{-1}$. As indicated earlier, $\overline{E}_w$ based on Eq. 3.4 and Eq. 3.5 was only 0.11 $mm\,hr^{-1}$.

3.6 DISCUSSION

3.6.1 FOREST STRUCTURAL PARAMETERS

The presently adopted value for the canopy capacity (S, 1.15 mm) compares favourably with earlier (pre-hurricane Hugo) estimates for the Bisley forest by *Scatena* [1990b]. His estimates ranged from 0.08 mm for open canopy, palm-filled ravine sites to 1.3 mm for well-stocked ridges. *Clements and Colon* [1975] reported values between 0.76 and 1.27 mm for a similar forest at a slightly higher elevation (450 m) at nearby El Verde. Otherwise, the present value is somewhat higher than reported for a number of forests in Amazonia [0.74 mm–1.03 mm; *Lloyd and Marques-Filho*, 1988; *Elsenbeer et al.*, 1994a; *Jetten*, 1996; *Ubarana*, 1996], East Africa [0.89 mm; *Jackson*, 1975], or South-east Asia [$\sim$0.9 mm; *Murdiyarso*, 1985; *Dykes*, 1997] which is in line with the higher interception loss at the study site [*cf. Schellekens et al.*, 2000].

On the other hand, the value for the free throughfall coefficient (p, 0.23) is unexpectedly high considering the nature of the forest and the high E_i. *Lloyd et al.* [1988] and *Ubarana* [1996] reported p-values of 0.03–0.08 for Amazonian forest based on anascope readings. *Elsenbeer et al.* [1994a] obtained a value of 0.32 for a forest in western Peru, whereas *Jackson* [1975] found a p of 0.24 for a tall montane forest of exceptional biomass in Tanzania [*Lundgren*, 1978]. The latter two interception studies based their estimates of p on an analysis of small storms. It is possible, therefore, that these estimates do not represent 'true' free throughfall but rather 'indirect' throughfall occurring before the canopy is fully saturated. The foliar structure of the Tabonuco forest which features pointed leaves with a waxy surface that are pointed downwards [*cf. Ubarana*, 1996] would certainly facilitate this. Such characteristics would also tend to speed up drainage from the canopy and so limit canopy water retention. This is also confirmed by our application of the Rutter model which clearly showed that the use of a large value of S seriously overestimates TF after rainfall has ceased (*cf.* Fig. 3.3-(a,c) and Fig. 3.4-(a,c)). As such, the claims of very large storage capacities for tropical rain forests [*Herwitz*, 1985; *Calder et al.*, 1986] are not supported by the present analysis. However, extra storage on and subsequent evaporation from trunks and branches during high intensity rain cannot

be ruled out entirely and further work on the stemflow dynamics at Bisley is required.

3.6.2 Performance of the Rutter and analytical models

Despite the fact that the Rutter model is more sophisticated than the analytical model, its performance on our data was not better (*cf.* Figures 3.5 and 3.2). In order to match measured and predicted TF totals the (average) value of E_w had to be increased to 2.8 $mm\,hr^{-1}$. Nevertheless, a comparison of the detailed TF records with the model predictions for individual storms (Fig. 3.3 and Fig. 3.4) indicates that high evaporation is more likely than an increased storage capacity. In addition, when using a value of S of 5.75 mm the tendency of the Rutter model to overestimate TF for large storms and to underestimate TF for small storms remains. Also, the model failed completely to predict the TF total associated with the major event occurring on 13 May (Fig. 3.2). The main reason for this (and why the simpler analytical model does not have this problem; Fig. 3.5) lies in the variable character of the rainfall at Bisley. As shown in Fig. 3.3-(a,c) and Fig. 3.4-(a,c), several intervals of relatively high rainfall and throughfall intensity may occur within a storm. In particular, the relation between 5-min TF and P totals at Bisley is almost linear. This is where the Rutter model breaks down (because E_w in the model does not keep up with rainfall intensity). This is less of a problem with the analytical model where variations in rainfall intensity are evened out by the use of $\overline{R}$ for entire storms. A similar problem was encountered by *Jetten* [1996] for a forest in Guyana. He therefore proposed a multi-layer version of the Rutter model (Cascade) whose main advantage is its ability to store larger quantities of water during large, high intensity events. The Cascade model was also applied to the present data. However, although it solved the problem of overestimation of TF for large events to some extent, the results were not satisfactory on a 5-min time scale. In particular, the TF pattern predicted by Cascade after rainfall had ceased, resembled that produced by the Rutter model with increased S (*cf.* Fig. 3.3-(a,c), Fig. 3.4-(a,c)). An alternative, stochastic, approach was advanced by *Calder* [1986] in which rainfall interception is described in terms of the stochastic manner in which individual elements of a canopy are struck and wetted by individual raindrops. An application of the stochastic model using the present data is in preparation.

The drainage function (Eq. 3.7) is an important component of the Rutter model. As indicated in the previous section, it seems plausible that drainage at Bisley also occurs before $C = S$. A potential improvement of the Rutter model for application at the study site and possibly other rain forests with similar characteristics, therefore, would be to adjust the drainage function accordingly and to reduce the value of p to the average gap fraction as estimated, for example, using an anascope [*Gash and Morton*, 1978; *Ubarana*, 1996]. However, the difficulties associated with the proper quantification of E_w at Bisley (see below) tend to overshadow such refinements.

The analytical model performed very well on our data as long as the value

of $\overline{E}_w/\overline{R}$ was derived from the regression of E_i on P. By contrast, the use of the much smaller) value of $\overline{E}_w/\overline{R}$ based on Eq. 3.4 and Eq. 3.5 resulted in a hugely overestimated amount of TF (Fig. 3.5 and Table 3.3). Good results with 'measured' $\overline{E}_w/\overline{R}$ were obtained by *Lloyd et al.* [1988] for a forest in Central Amazonia and by *Ubarana* [1996] using measured E_w in the Rutter model in Western Amazonia, *i.e.* at mid-continental equatorial locations with low wind speeds. Under more maritime tropical conditions, regression-based estimates of $\overline{E}_w/\overline{R}$ tend to be (much) higher than those based on the Penman-Monteith equation [*cf. Bruijnzeel and Wiersum*, 1987; *Dykes*, 1997; *Waterloo et al.*, 1999]. However, caution is needed when comparing regression-based values of $\overline{E}_w/\overline{R}$ and Penman-Monteith based values of $\overline{E}_w$. The cited maritime tropical studies all used mean rather than median rainfall intensities to represent $\overline{R}$. In the present case, the use of an average rainfall intensity would yield an apparent $\overline{E}_w$ of 1.52 $mm\,hr^{-1}$ *vs.* 0.94 $mm\,hr^{-1}$ for the median rainfall intensity. Just as important is the temporal resolution of the rainfall data used to estimate $\overline{R}$. For Bisley, rainfall intensity estimated from 5-min, hourly and event-based data amounted to: 7.2 $mm\,hr^{-1}$ (median 2.5 $mm\,hr^{-1}$), 2.8 $mm\,hr^{-1}$ (median 1.0 $mm\,hr^{-1}$) and 3.0 $mm\,hr^{-1}$ (median 1.9 $mm\,hr^{-1}$) respectively. Consequently, the variation in $\overline{E}_w$ derived from inserting of the respective values of $\overline{R}$ in $\overline{E}_w/\overline{R}$ would be just as large.

3.6.3 WET CANOPY EVAPORATION

Both the Rutter and the analytical model could be adjusted in such a way as to predict observed TF totals at Bisley satisfactorily under most circumstances (Fig. 3.2 and Fig. 3.5 respectively). However, this required adjusting the rate of evaporation from the wet canopy E_w as predicted by Eq. 3.4 and Eq. 3.5 by at least one order of magnitude. Interestingly, the optimized value for E_w was markedly different for the two models, with the larger value needed for the Rutter model. This is due to the problem of variable rainfall intensities within storms referred to already.

Schellekens et al. [2000] reported a total evapotranspiration (ET) for the forest at Bisley over the two years 1996 and 1997 that was approximately 42 % higher than the evaporation equivalent of the total net radiant energy input (R_n). The contrast becomes even larger when considering evaporation from a wet canopy. The corresponding radiant input only amounts to 0.11 $mm\,hr^{-1}$ (*vs.* optimized E_w values of 1.1 – 2.8 $mm\,hr^{-1}$), suggesting that during wet canopy conditions typically < 10 % of the required energy at Bisley is supplied in the form of radiant energy. A similar, though less extreme, case has been documented by *Shuttleworth and Calder* [1979]. Here, the canopy of a spruce plantation at Plynlimon, Wales, U.K., was shown to receive typically 20 % of its total energy input during wet canopy conditions in the form of radiant energy, whereas the average annual ET from the forest exceeded the total radiant energy input by about 12 % [*Shuttleworth and Calder*, 1979]. High values of E_w [0.5–0.8 $mm\,hr^{-1}$; *Bruijnzeel and Wiersum*, 1987; *Dykes*, 1997; *Waterloo et al.*, 1999] have also been inferred from rainfall and throughfall measurements

at other maritime tropical locations but much lower values [typically about 0.2 $mm\,hr^{-1}$or less, *Lloyd et al.*, 1988; *Hutjes et al.*, 1990; *Asdak et al.*, 1998; *Waterloo et al.*, 1999] are usually calculated from above-canopy climatic measurements using Eq. 3.4. Similarly, *Gash et al.* [1980] derived an average value of 0.13 $mm\,hr^{-1}$ for E_w in the case of the Plynlimon spruce forest referred to earlier when using the climate data whereas a value of 0.24 $mm\,hr^{-1}$ was inferred from measured interception. Another strong argument for the importance of non-radiant energy for evaporation at Bisley is the observation of *Schellekens et al.* [2000] that TF/P ratios did not differ significantly for daytime and nighttime events.

However, the origin of the energy needed in surplus of radiant energy is still largely a matter of speculation. Large-scale advection of warm air from the nearby Atlantic ocean is a likely source [*cf. Shuttleworth and Calder*, 1979], although, unlike the situation in Wales, wind speeds in the study area are rather low [typically 1.1–2.3 $m\,s^{-1}$; *Holwerda*, 1997; *Schellekens et al.*, 1998]. Another possible energy source is heat released upon condensation of water vapour in the air above the forest. The latter possibility seems to find support from the observation that larger rainfall events at Bisley are accompanied by higher E_i [*i.e.* the TF/P ratio is independent of storm size; *Schellekens et al.*, 2000] suggesting a positive feedback of rainfall amount (and thereby condensation) on the magnitude of E_i.

Accepting that the presently measured E_w requires the total available energy A to be much higher than measured R_n also has consequences for the magnitude of r_a. Typical values of r_a at Bisley as computed with Eq. 3.5 are about 20 $s\,m^{-1}$ [*Holwerda*, 1997; *Schellekens et al.*, 1998]. *Schellekens et al.* [2000] used an inverse application of Eq. 3.4 to estimate r_a from measured interception losses (equating A with λE_w), and obtained an average value of 2.1 $s\,m^{-1}$ (a very low value). Using a similar approach, *Asdak et al.* [1998] obtained an average value of 3.2 $s\,m^{-1}$ for a forest in central Kalimantan, Indonesia whereas *Calder* [1977] derived an optimum value of 3.5 $s\,m^{-1}$ for the Plynlimon forest *vs.* a theoretical value of 5.4 $s\,m^{-1}$ when using Eq. 3.5. However, when taking into account the sensitivity of r_a (and thus E_w) as determined with Eq. 3.5 to variations in the magnitude of z_0 — particularly at high values of d/h_v [*Gash et al.*, 1980] — the latter parameters would have to be reduced to unrealistically low values to bring the outcome of Eq. 3.5 in agreement with r_a as estimated from measured interception losses. Thus, the question remains how the r_a at Bisley can be so low compared to values predicted by Eq. 3.5. *Calder* [1990] drew attention to the possibility of enhanced upward transport of evaporated moisture by gusts and eddies, even during neutral or stable conditions, although he added that the 'extent to which these gusts are associated with thermal- or humidity driven plumes, local topography or other factors is still unknown'. More recently, *McNaughton and Laubach* [1998] showed that such enhanced upward moisture transport increases with a relative increase of the standard deviation of the wind speed compared to the mean wind speed. This confirms the contention of *Calder* [1990] that gusts may indeed be important, and although further study of the instantaneous wind data at Bisley is

needed, it is probable that gusts are relatively important because of the prevailing low mean wind speed. In addition, the aerodynamic roughness of the Bisley forest may be increased further by its very irregularly shaped canopy as a result of hurricane damage in the past [*Scatena et al.*, 1993]. Further work is necessary to improve our understanding of the transport mechanism of evaporated moisture under conditions of low wind speed during rain events. Clearly, at Bisley such transport is much more efficient than suggested by Eq. 3.5.

3.7 CONCLUSIONS

The use of a wet canopy evaporation rate based on the Penman-Monteith equation can result in severely underestimated interception losses as predicted by the Rutter and the analytical models. A detailed analysis of the results obtained with the Rutter model for four storms of variable magnitude showed that the results were improved more by increasing the wet canopy evaporation component than by increasing the canopy storage capacity to fit measured throughfall. Using an optimized value for the wet canopy evaporation component, both models were able to predict measured throughfall amounts satisfactorily. However, the Rutter model encountered severe problems for a large event with variable rainfall intensity. The analytical model experienced no such problems because it uses an averaged rainfall rate. Our results support the idea that it is primarily a high rate of evaporation from a wet canopy that is responsible for the high interception losses observed under wet maritime tropical conditions.

4

STORMFLOW GENERATION IN A SMALL RAIN FOREST CATCHMENT IN THE LUQUILLO EXPERIMENTAL FOREST, PUERTO RICO*

ABSTRACT

Various complementary techniques were used to investigate the stormflow generating processes in a small headwater catchment in north-eastern Puerto Rico. A total of 102 samples was taken of soil matrix water, macropore flow, streamflow and precipitation during two storms of contrasting magnitude for the analysis of Ca, Mg, Si, K, Na and Cl. These were combined with hydrometric information on streamflow, return flow, precipitation, throughfall and soil moisture to distinguish water following different flow paths. Geoelectric sounding was used to survey the subsurface structure of the catchment revealing a weathering front that coincides with the elevation of the stream channel rather than run parallel to surface topography. The hydrometric data were used in combination with soil physical data, a one-dimensional hydrological model (VAMPS) and a three component chemical mass balance mixing model to describe the stormflow response of the catchment. It is shown that most stormflow traveled through macropores in the top 20 cm of the soil profile. During large events saturation overland flow also accounted for a considerable portion of the stormflow although it was not possible to fully quantify the associated volumes. No evidence was found for Hortonian overland flow. Although the mass balance mixing model approach gave valuable information about the various flow paths within the catchment it was not possible to distill the full picture from the model alone; additional hydrometric and soil physical evidence was needed to aid in the interpretation of the model results.

*With: F. N. Scatena, L. A. Bruijnzeel, A. I. J. M. van Dijk, M. M. A. Groen and R. J. P. van Hogezand, submitted to: *Hydrological Processes*

4.1 INTRODUCTION

A fundamental concept used in all studies of stormflow generation is the separation between fast and slow flow paths. Often the fast flow paths are referred to as stormflow (or quickflow) and the slower flow paths as delayed flow (or baseflow). These two fundamental components of streamflow are apparent in rivers of all sizes [*Ward*, 1984]. The concept of how this is linked to hillslope processes has changed considerably since *Horton* [1933] first presented his infiltration based model of runoff generation. Developed by *Hewlett and Hibbert* [1967] the 'variable source concept' [so named by *Dunne*, 1978] also includes soil depth, slope position and morphology in the runoff generating process as well as most superficial and subsurface flow types that have been observed in catchments throughout the world. However, later research [*McDonnell*, 1990; *McDonnell et al.*, 1996] has shown how the incorporation of new techniques (such as the use of stable isotopes) can change these conceptual views at the hillslope scale. Indeed, it is more or less accepted now that a combination of hydrometric and hydrochemical techniques is probably required to obtain a complete picture [*Bonell and Fritsch*, 1997]. Macropores have been suggested to play a key role in the hydrological response of headwater catchments in general, and forested ones in particular [*Beven and Germann*, 1982; *Bonell*, 1993]. Macropores are formed by the activities of soil fauna, root dynamics (growth, decay), the shrinking of clay, the erosive action of subsurface flow, or combinations of the above [*Jones*, 1971; *Beven and Germann*, 1982; *Lal*, 1987]. Macropores (especially 'pipes', *i.e.* macropores with a diameter exceeding 50 mm; [*Beven and Germann*, 1982]) may offer a fast flow path for water to the stream channel, depending on their size, frequency and the connectivity of the pores [*Whipkey*, 1965; *Jones*, 1971; *Mosley*, 1979, 1982; *Beven and Germann*, 1982; *Elsenbeer and Cassel*, 1990].

The spatial variability in occurrence of macropores (including pipes) and thus hillslope hydraulic conductivity is notorious [*Jones*, 1971; *Elsenbeer and Lack*, 1996; *Brammer and McDonnell*, 1996] and constitutes one of the main impediments to the successful application of physically-based runoff generation models to predict stormflow characteristics [*Smith and Hebbert*, 1979; *Merz and Plate*, 1997; *Loague and Kyriakidis*, 1997; *Vertessy and Elsenbeer*, 1999]. Despite the fact that the interest in, and imperatives for, the use of such models to forecast the hydrologic impacts of land use change in the humid tropics has never been greater [*Bruijnzeel*, 1990, 1993; *Jepma*, 1995; *Nepstad et al.*, 1999], only a handful of in-depth studies of runoff generation have been conducted under such conditions [reviewed by *Bonell*, 1993; *Bonell and Fritsch*, 1997]. Even fewer studies have attempted to model the runoff generation processes taking place on tropical hillsides, either before forest clearing [*Molicova et al.*, 1997; *Chappell*, 1998; *Vertessy and Elsenbeer*, 1999] or long after [*Rose and Yu*, 1998]. More importantly, all of the cited modelling studies conducted under tropical rain forest conditions pertained for lowland areas of low to moderate relief. Given the importance of soil depth, slope length and morphology on the runoff generation process [*Dunne*, 1978], major contrasts can be expected between the

response of headwater catchments situated in tropical steeplands and those on stable continents with low relief.

This paper offers a preliminary characterization of the hydrological response of one such tropical steepland catchment, the Bisley II catchment in the Luquillo Experimental Forest (LEF) in north-eastern Puerto Rico, using a combination of hydrometric and hydrochemical (mass-balance mixing model) techniques. In addition, attention is paid to unraveling the subsurface structure of the catchment, notably the thickness of the saprolite and the depth to bedrock, as well as the identification of isolated micro-topographic depressions in the soil-bedrock interface which store old water that may become re-mobilized as the depressions spill over during particularly wet spells [*Brammer and McDonnell*, 1996]. The present results will be used in a companion paper [*Schellekens*, 2000b, Chapter 5] to test the predictive capacity of the physically-based distributed catchment hydrological TOPOG model [*Vertessy and Elsenbeer*, 1999].

4.2 STUDY CATCHMENT

The Bisley II catchment is situated at 18^o 18′ N, 65^o 50′ W at an elevation of 265–456 m a.s.l. (*cf.* Fig. 4.1). The 6.4 ha catchment drains a dissected mountainous terrain [*Scatena*, 1989]. Stream gradients in and around the catchment are steep and hillslopes generally convex-concave in form. The upper slope segments are convex whereas their middle sections are typically straight. The lower slope segments are usually concave when they pass into first-order valleys and straight where they join the main channel. More than half of the catchment has slopes greater than 45 % (24^o) [*Scatena*, 1989]. Shallow earth movement, soil creep and tree fall are important geomorphic processes in the area [*Lewis*, 1974, 1976; *Simon et al.*, 1990; *Scatena and Larsen*, 1991]. The 0.8–1.0 m deep clayey soils that have developed in the underlying thick-bedded tuffaceous sandstones and indurated siltstones are strongly leached Ultisols. *Silver et al.* [1994] reported average soil bulk densities in the Bisley catchment area of 0.60 (0–10 cm), 0.98 (10–35 cm) and 1.30 $g\ cm^{-3}$ (35–60 cm). Similar values were obtained by *Edmisten* [1970] at nearby El Verde. Saturated hydraulic conductivity (K_{sat}) in riparian zones in the Bisley area was estimated by *McDowell et al.* [1992] to range between 1 and 20 $m\,d^{-1}$ using an infiltrometer and between 0.009 and 0.09 $m\,d^{-1}$ using recovery tests in piezometer tubes. Additional soil physical data and the results of a geophysical survey to define subsurface bedrock topography will be presented later in the paper.

The Tabonuco-type rain forest has an irregularly shaped, 20–25 m high upper canopy, an understory of palms and woody vegetation, and ground level herbs and shrubs. Both the structure and composition of the vegetation vary with topography and aspect relative to the trade winds [*Lugo and Scatena*, 1995]. The average leaf area index (LAI) of mature Tabonuco forest is between 6 and 7 but has been reported to range between 12.1 on ridges and 1.95 in dark ravines and riparian valleys [*Odum et al.*, 1970a]. In September 1989 the Bisley area was severely impacted and nearly completely defoliated by Hurricane Hugo

[*Scatena et al.*, 1993]. However, by 1996, when the present study was initiated, LAI and forest biomass were again similar to pre-hurricane conditions [*Scatena et al.*, 1996; *Holwerda*, 1997].

The climate is maritime tropical (type A2m according to the Köppen classification), with an annual rainfall of 3530 mm (as measured at the nearby long-term rainfall station at El Verde, 450 m a.s.l.). About 70 % of the annual rainfall is associated with tropical waves, depressions and cyclones and is brought in with the north-easterly tradewinds. Rainfall is distributed fairly evenly throughout the year, with May and November being relatively wet ($>$ 300 $mm\ month^{-1}$) and January – March relatively 'dry' ($<$ 200 $mm\ month^{-1}$). Rainfall at El Verde is delivered as numerous (267 rain days per year), relatively small (median daily rainfall 3.0 mm) storms of low intensity [$<$5 $mm\ hr^{-1}$; *Brown et al.*, 1983; *García-Martinó et al.*, 1996]. *Schellekens et al.* [1999] (Chapter 3) reported rainfall intensity for the 66-day study period in 1996 to have a mean value of 3.0 $mm\ hr^{-1}$ and a median value of 1.9 $mm\ hr^{-1}$. Average rainfall interception is exceptionally high at c. 50 %, regardless of storm size [*Schellekens et al.*, 1999].

The seasonal variation in mean monthly temperatures in the Bisley area is about 3.5 ^oC, ranging from 24 ^oC in December – February to about 27.5 ^oC in July–August. Seasonal variation in average daily relative humidity levels is small (84 – 90 %). Average monthly wind speeds in the lower reaches of the LEF are $<$2 $m\,s^{-1}$ but vary between 2 and 5 $m\,s^{-1}$ around exposed summits at higher elevations [*Brown et al.*, 1983]. Reference evaporation at Bisley was estimated at c. 1100 $mm\ yr^{-1}$ [*Holwerda*, 1997].

4.3 Methods and Instruments

Stormflow generation at Bisley was investigated using various techniques. At first, a detailed water budget evaluation of the catchment was performed [*Schellekens et al.*, 2000, Chapter 2], supplemented by chemical analysis of different water types during periods of baseflow and stormflow. Also, a geophysical survey was conducted to establish the subsurface properties of the catchment. The hydrometric data were used in combination with the soil and geophysical data and a one-dimensional hydrological model simulating soil water content with time, to quantitatively describe the stormflow response of the catchment. Finally, the chemical tracer data were used in an application of a mass balance flow separation model to complete the picture. The remainder of this section describes the methods and associated instrumentation in more detail (*cf.* Fig. 4.1 for locations).

A Texas Instruments tipping bucket rain gauge (TE525LL-L; 0.254 mm per tip) recorded above-canopy precipitation at 26 m. An adjacent totalizing rain gauge serving as a backup was emptied every week. All data were stored in a Campbell Scientific Ltd. 21X data logger and retrieved weekly for further processing. Precipitation data were stored at 5-min intervals.

Throughfall (TF) was recorded continuously between 5 May and 9 July

1996 (66 days) using three flat-bottomed, sharp-rimmed steel gutters (6 x 300 cm) placed at a steep angle to minimize splash-out. Each gutter was equipped with a 180-litre capacity tipping bucket with logger system. To minimize wetting and drying losses the gutters were cleaned and sprayed with a silicone solution every week. In addition, TF was measured with 20 randomly placed but non-roving collectors (143 cm^2 surface area) which were emptied every week. A roving gauge technique [*Lloyd and Marques-Filho*, 1988] had been adopted in the beginning but after initial comparison of the performance of the fixed and roving gauges did not show significant differences, only the fixed network was maintained [*cf. Brouwer*, 1996]. The 5-min TF records obtained with the gutters were converted to areal averages every time the manual gauges were emptied, using a weighting procedure based on the relative magnitude of the surface areas of the respective gauge types. Stemflow was estimated as 2.3 % of gross precipitation [*Scatena*, 1990b].

Streamwater levels at the catchment outlet were measured at 5 min intervals using a Druck Ltd. PDCR-830 pressure transducer (1.5 mm accuracy) connected to a CTL data logger. Daily water level measurements using a staff gauge were made to check for instrumental drift. Water level data were converted to discharge using a stage-discharge relation that was developed by *Scatena* [1990a]. Piezometers were installed in the areas that might contain floodplain groundwater and two of these were equipped with waterlevel recording equipment (Druck Ltd. PDCR-830 pressure transducer connected to a VUA data logger). In a small tributary gully fed by return-flow water during storms, a V-notch with a pressure transducer with logging system was placed on 18 June 1996. Finally, volumes of quickflow and delayed flow at the catchment outlet were estimated using a simple straight-line separation method [*Hewlett and Hibbert*, 1967]. A fixed slope of 0.025 $mmhr^{-1}d^{-1}$ was used in the separations rather than the 0.0472 $mmhr^{-1}d^{-1}$ proposed by *Hewlett and Hibbert* [1967] for catchments in the south-eastern United States with much deeper soils.

Soil water retention characteristics, *i.e.* pairs of soil water content (θ) *vs.* soil water tension (ψ) values, were obtained on undisturbed core samples (100 cm^3) using the porous medium with pressure-membrane technique [*Stakman*, 1973]. A total of 52 cores was used, distributed among three soil horizons (23 samples for the 0–20 cm interval, 18 between 20 and 50 cm and 11 between 50 and 140 cm). In addition, the cores were used to determine porosity, bulk density, and saturated hydraulic conductivity (K_{sat}), using a falling-head permeameter [*Wit*, 1962]. Furthermore, a total of 13 reversed auger-hole method measurements of K_{sat} [*Van Beers*, 1979] was also performed.

Soil moisture tension (ψ) was monitored using a six tensiometers nest at a ridgetop (7, 19, 49, 67 and 84 cm below fieldlevel) and three pairs of tensiometers (8 and 30 cm below fieldlevel) along one hillslope section. The instruments were read every 1–4 days using a needle plus transducer system accurate to the nearest cm. The maximum soil water tension that could be recorded with such a system was about 0.9 MPa ($pF = 2.9$). Values of ψ were converted to soil water content (θ) using so-called Van Genuchten curves describing the

ψ–θ pairs determined on the small cores [*Mualem*, 1976; *Van Genuchten*, 1980]. Both soil water content and suction head were simulated in detail (using 5-min time steps) with the aid of a one-dimensional soil water balance model (VAMPS: *Schellekens* [1997], Appendix A). Model predictions were calibrated against tensiometer readings made at several depths.

During the geophysical survey a total of 10 Schlumberger geo-electrical soundings [*Telford et al.*, 1976] were performed throughout the catchment using a Terrameter (SAS 4000). The Gosh filter technique [*Gosh*, 1971; *Koefoed*, 1979] and non-linear regression [*Marquardt*, 1963] were used to derive an interpretation of sub-surface structures according to a layered model [*Telford et al.*, 1976]. In addition, three boreholes (6.75, 8.0 and 8.7 m in depth) were done by hand using a Dutch auger. Laboratory determinations of the electric resistance and gravimetric water content of soil samples taken every 50 cm from these holes were done to validate the interpretation of the field soundings. For the same purpose, borehole logging using long- and short-normal electrodes [*Telford et al.*, 1976] was performed in two of the holes using the terrameter. Amounts of extractable Ca, Mg, Na, Fe, Mn, K, and P were determined for soil samples from one of the boreholes. The analyses were carried out at the International Institute of Tropical Forestry (IITF), Rio Piedras, Puerto Rico. After extraction by 1N *KCl* (for Ca) or the modified Olsen method [for P and K; *Hunter*, 1982] a Beckman plasma emission spectrometer was used for analysis of the respective extracts. A more detailed description of the analytical techniques can be found in *Silver et al.* [1994].

Samples for chemical analysis were also taken of the following water types: *(1)* precipitation (P), *(2)* floodplain groundwater (G), *(3)* streamflow (both during storms (STF) and during baseflow conditions (BF)), *(4)* return flow/gully flow (RF) and *(5)* soil water (SW). A total of 102 samples was taken and analyzed at the Vrije Universiteit Amsterdam for Ca, Mg, Si, K, Na and Cl using ICP photometric (Ca, Mg, Si) flamephotometric (K, Na) and auto-analyzer (Cl) techniques. Electrical conductivity (EC), Cl and Mg were determined in the field as well as in the laboratory.

Selected pairs of the analyzed constituents were used in a three-component flow separation model [*DeWalle et al.*, 1988]. Although temporal and spatial variations in concentrations of the chemical constituents in incident precipitation during a storm event exist [*Kendall and McDonnell*, 1993], these were neglected in the present research. The basic version of the technique [*Pinder and Jones*, 1969] uses a mass-balance based hydrograph separation determining two components: pre-event-water and event-water. If the discharge of one of the components is known, or if two tracers are used, a three-component model can be used [*DeWalle et al.*, 1988; *Genereux et al.*, 1993]. For a three-component mixing model the relative contribution (fraction) of each source to total streamflow can be obtained by solving the following set of equations:

$$\begin{aligned} f_1 + f_2 + f_3 &= 1 \\ [A]_1 f_1 + [A]_2 f_2 + [A]_3 f_3 &= [A]_s \\ [B]_1 f_1 + [B]_2 f_2 + [B]_3 f_3 &= [B]_s \end{aligned} \tag{4.1}$$

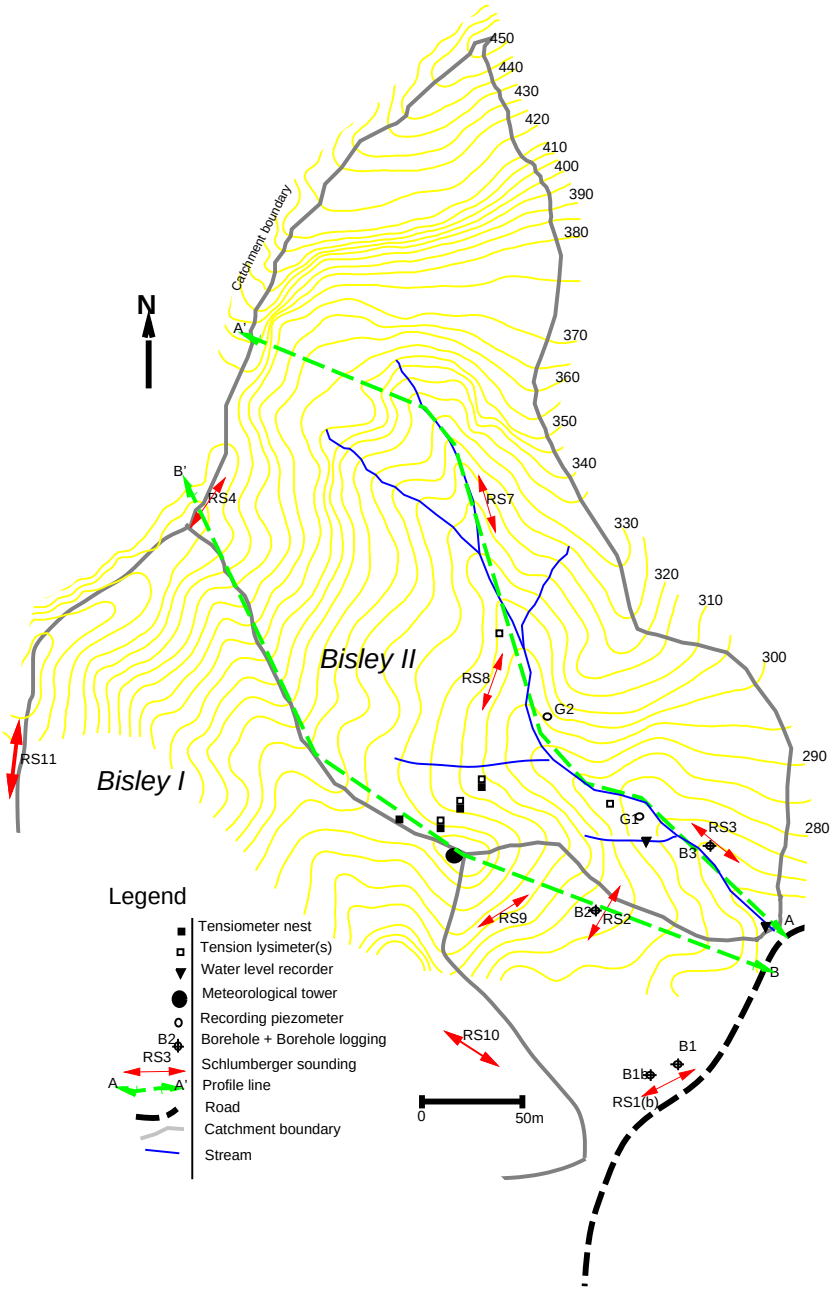

Figure 4.1: Map of the Bisley II catchment showing the location of the Schlumberger soundings, the instruments and profiles A–A′ and B–B′ depicted in Fig. 4.4.

where:

f	fraction that each component contributes to total streamflow	[-]
$[A]$	concentration of constituent A	[μeql^{-1}]
$[B]$	concentration of constituent B	[μeql^{-1}]

The subscript s denotes streamflow while the subscripts 1, 2 and 3 denote the different flow components (sources). The above set of equations was solved using an inverse matrix multiplication technique as available within the Octave software package [*Eaton*, 1997].

4.4 RESULTS

4.4.1 GEOPHYSICS

Although the combination of steep slopes and dense vegetation rendered laying out the Schlumberger arrays a difficult affair the resulting resistivity curves allowed unambiguous interpretation (Fig. 4.2). In some cases, lateral changes in the subsurface structure caused some shift in the upper part of the curves (for values of $L/2 < 4m$) but this did not affect the interpretation. As shown in Fig. 4.2, in which four soundings within the main valley are shown, a layer of high resistivity occurs below depths of 23–30 m which is overlain by a layer of much lower resistivity starting typically at a depth of 3–3.5 m for the lower to central portion of the river profile, to c. 6 m below the highest point. On top of this intermediate zone of low resistivities lies a layer of variable thickness and intermediate to high resistivity values (Fig. 4.2). Fig. 4.3 compares the resistivity profiles with depth for one of the boreholes: RS1b, located near the outlet of the catchment (see Fig. 4.1 and Fig. 4.4 for location and setting). The changes in soil nutrient concentrations in the top 50 cm and below 5–6 m (Fig. 4.3B) show the opposite pattern derived for resistivity (Fig. 4.3A). Conversely, no clear relationships are observed between gravimetric soil water content (Fig. 4.3C) and either soil chemistry (Fig. 4.3B) or resistivity (Fig. 4.3A). Similar findings were obtained for the other two boreholes [*Van Dijk et al.*, 1997]. On the basis of the 10 Schlumberger soundings distributed over the catchment (*cf.* Fig. 4.1) and the measurements made in the three boreholes a generalized subsurface profile was constructed for the Bisley II catchment (Fig. 4.4). The deepest zone of high resistivity is thought to represent the non-weathered bedrock which is generally found at depths exceeding 20 m. The intermediate zone of low resistivity values represents the saprolite (rotten rock) which grades into highly leached saprolite/sub-soil material of higher resistivity values and low nutrient contents, typically at a depth of 3–6 m (*cf.* Fig. 4.3B). Interestingly, the transitions between fresh and weathered bedrock, and between the latter and subsoil material closely follow the longitudinal profile of the streambed rather than that they run parallel to the surface topography (Fig. 4.4).

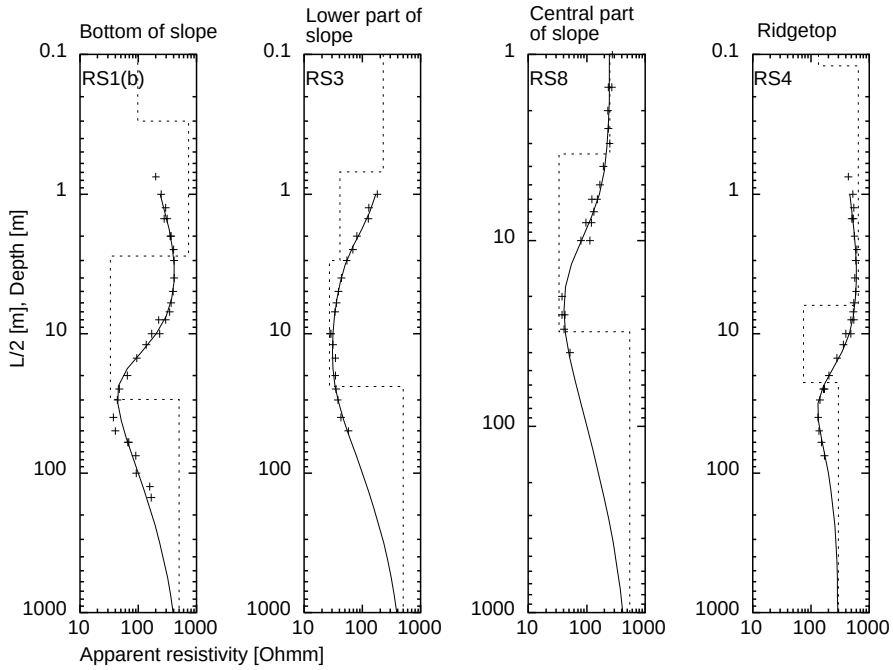

Figure 4.2: Schlumberger soundings of the substrate along four transects in the Bisley II catchment (see Fig. 4.1 and Fig. 4.4 for locations and topographic setting). Pluses (+) represent measured resistivity values (Ωm), the solid line the fitted curve, and the dotted line the resulting layered model representation of the substrate. The vertical axis shows L/2 (the length of the Schlumberger array) and the depth of the layered model, both in m.

4.4.2 SOIL PHYSICAL PARAMETERS

Soil hydraulic conductivity (K_{sat}) ranged from 0.01 $m\,d^{-1}$ to 7.33 $m\,d^{-1}$ depending on depth in the soil profile and the method used (Table 4.1). The range is especially large for the 0–20 cm and the 20–50 cm horizons, causing median values to be 25–70 times lower than arithmetic average values. This large scatter in K_{sat} values undoubtedly reflects the relative frequencies of macropores in the small core samples, as also evidenced by the much higher K_{sat} values obtained with the reverse auger hole method, despite the fact that the latter method tends to underestimate K_{sat} in clayey soils due to smearing of the holes [*Kessler and Oosterbaan*, 1973]. The strong decrease in K_{sat} with depth (auger hole values for the top 50 cm, small core samples for the subsoil) is paralleled by a decrease in porosity and an increase in bulk density below 50 cm (Table 4.1). Nevertheless, at 50 % the porosity of the soil below 50 cm depth is still quite high.

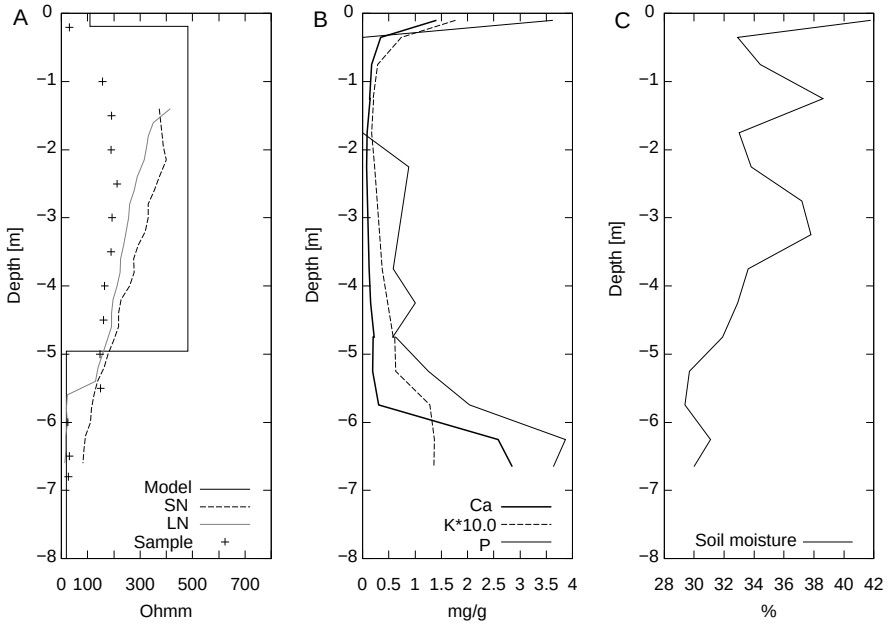

Figure 4.3: Variations with depth for various parameters as determined in borehole RS1b (bottom of slope; see Fig. 4.1 for location). (A) Interpreted layered model from the Schlumberger sounding (solid line) plus the results from the borehole logging (long- and short-normal, LN. SN) and measured sample resistivities (+). (B) Concentrations of Ca, K and P in soil samples taken at 50 cm intervals. (C) Gravimetric moisture content (%) of the samples.

Table 4.1: Saturated hydraulic conductivity [K_{sat}, $m\,d^{-1}$] as determined on small core samples and according to the reversed auger-hole method for three soil layers in the Bisley II catchment. Porosity and bulk density [BD, $g\ cm^{-3}$] were determined on small core samples.

Depth	K_{sat} (small cores)					K_{sat} (auger hole)				
[cm]	Min.	Max.	Mean	Median	n	Min.	Max.	Mean	Median	n
0–20	$3.0 \cdot 10^{-5}$	3.57	0.50	0.02	23	0.13	11.79	6.29	7.33	5
20–50	$9.0 \cdot 10^{-4}$	6.83	0.70	0.01	18	0.16	1.52	0.74	0.69	8
50–140	$1.7 \cdot 10^{-4}$	0.21	0.02	0.04	11	-	-	-	-	-

	BD				Porosity			
	Min.	Max.	Mean	n	Min.	Max.	Mean	n
0–20	0.62	1.32	0.87	10	0.53	0.74	0.68	10
20–50	0.81	1.13	0.90	10	0.56	0.68	0.66	10
50–140	0.98	1.32	1.18	7	0.53	0.65	0.58	7

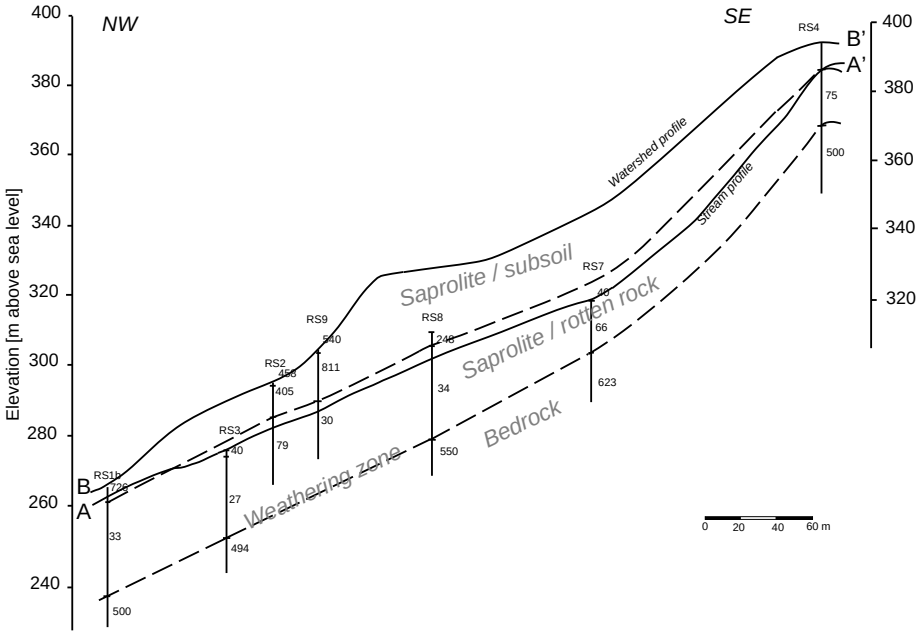

Figure 4.4: NW – SE profile of the subsurface of the Bisley II catchment showing the locations of the Schlumberger resistivity soundings (indicated by vertical bars with their location code; the numbers along the bars are resistivities in $Ohmm$) and the interpreted layered structure as indicated by the dashed lines. The lower dashed line separates unweathered bedrock (bottom layer of high resistivity values) from a zone with low resistivity values, the rotten rock part of the saprolite. The contact between these zones indicates the zone of active weathering. The upper dashed line separates the low resistivity zone from the highly leached upper part of the saprolite, the subsoil. Also indicated (by solid lines) are the watershed topographic profile as measured along the ridge, (B–B') and the streambed profile (A–A'). The locations of both profile lines are indicated in Fig. 4.1.

4.4.3 SOIL WATER TENSION

Using previously established 5-min rainfall interception and transpiration totals [*Schellekens et al.*, 1999, 2000, ; Chapter 2 and Chapter 3] the one-dimensional VAMPS site water balance model [*Schellekens*, 1997, ; Appendix A] was run to simulate soil water tensions at different depths at a near-level ridgetop site between 5 May and 15 July 1996. Five-min time steps and identical Van Genuchten curves were used in the model runs for each of the three soil layers. Macropore flow was not explicitly taken into account by the model. Instead, an approximate approach was used in which lateral drainage (both saturated and unsaturated) out of the modelled soil column was permitted at rates governed by the prevailing hydraulic conductivity (saturated or unsaturated, depending on the moisture conditions in each node) and the average slope angle of the

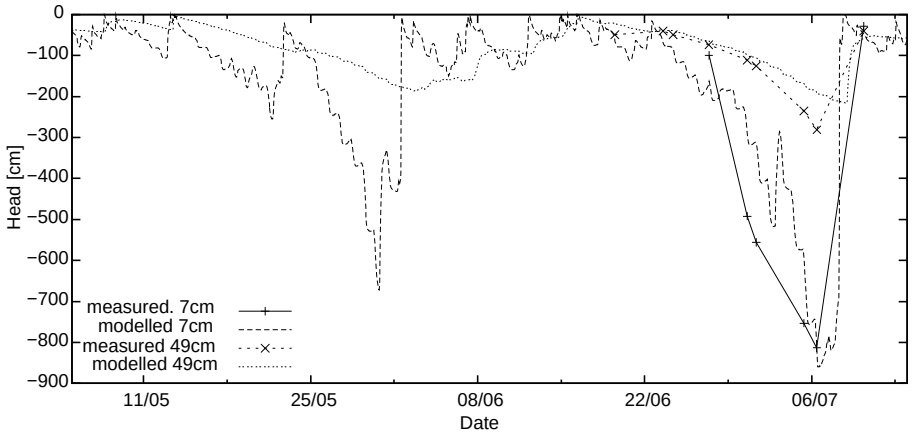

Figure 4.5: Measured and modelled soil water tension at two depths on a ridge top location between 5 May and 15 July 1996. The last part of the graph includes measured data that were used to calibrate the model.

site. Measured tension values at 7, 18, 36, 49, 67 and 84 cm depth were available from 17 June until 11 July against which model predictions were tested after averaging the results within each of the three soil layers (Fig. 4.5). During the virtually rainless period between 22 June and 6 July, soil water tensions at 7 cm depth increased to 813 cm *vs.* 281 cm at 49 cm depth and only 145 cm at 83 cm depth. The decline in K_{sat} (and rooting density) with depth, notably below 50 cm, caused soil water tension to remain relatively high throughout the simulation period (Fig. 4.5). Best fits between measured and modelled soil water tensions at the three depths (two of which are shown in Fig. 4.5) were obtained for optimized K_{sat} values of 3.6, 1.2 and 0.06 $m\,d^{-1}$ for the distinguished layers respectively. These values were within the range of actual fields measurements (Table 4.1). The simulated soil water tensions were used in the overall stormflow analysis (Section 4.5).

4.4.4 STRAIGHT-LINE FLOW SEPARATION

Using the simple straight-line separation method average quickflow amounts were determined for a total of 31 storms occurring in the period 19 April–9 July 1996 (Table 4.2). Maximum quickflow volume (63.8 cm) occurred in response to an exceptionally large (228 mm of gross precipitation) storm (no. 16 in Table 4.2) starting on 13 May for which quickflow lasted for 24hr38min. The corresponding quickflow/rainfall ratio was 0.28 (Table 4.2). The lowest quickflow volume (0.01 mm) was observed for a 7.8 mm storm (no. 45) falling on 25 May which produced a quickflow/rainfall ratio of only 0.02 (Table 4.2). The characteristics associated with the 31 storms listed in Table 4.2 are examined further in Table 4.3 in terms of their dependence on rainfall amount and in-

Table 4.2: Basic characteristics of 31 storms selected from the Bisley II record between 19 April and 9 July. Bold and underlined values indicate maximum and minimum values, respectively.

Date	Storm no.	P $[mm]$	Quickflow duration $[days]$	Peak flow $[mm/5m]$	Total flow $[mm]$	Quickflow $[mm]$	Delayed flow $[mm]$	QF/P [–]
23/04	2	–	0.61	0.48	27.67	8.11	19.56	–
26/04	5	–	0.29	0.02	2.38	0.58	1.80	–
30/04	9	–	0.28	0.09	2.59	1.11	1.48	–
06/05	11	8.84	0.21	0.02	1.37	0.34	1.03	0.04
07/05	12	31.24	0.38	0.38	18.95	4.82	14.14	0.15
08/05	13	14.81	0.29	0.17	4.57	2.52	2.05	0.17
09/05	14	5.76	0.21	0.02	1.95	0.35	1.60	0.06
13/05	16	**227.53**	**1.37**	**2.93**	**96.43**	**63.81**	**32.62**	**0.28**
21/05	19	5.71	0.13	0.02	1.80	0.09	1.70	0.02
22/05	20	3.23	0.10	0.02	1.53	0.08	1.45	0.03
22/05	21	16.34	0.23	0.10	5.01	1.39	3.62	0.09
23/05	22	4.07	0.15	0.03	1.15	0.32	0.82	0.08
24/05	23	3.36	0.10	0.01	0.95	0.07	0.87	0.02
01/06	25	24.41	0.26	0.19	5.21	2.38	2.83	0.10
02/06	26	15.95	0.27	0.09	3.06	1.34	1.72	0.08
06/06	28	9.74	0.20	0.03	2.75	0.59	2.15	0.06
07/06	29	38.54	0.53	0.18	13.56	4.59	8.97	0.12
08/06	30	4.36	0.16	0.03	1.02	0.31	0.72	0.07
11/06	32	40.14	0.61	0.28	13.34	4.55	8.79	0.11
14/06	37	20.46	0.30	0.13	5.86	2.38	3.48	0.12
15/06	38	10.83	0.22	0.07	2.63	1.21	1.42	0.11
15/06	39	12.74	0.24	0.15	3.49	1.84	1.65	0.14
16/06	40	54.76	0.58	0.49	24.60	12.56	12.04	0.23
18/06	41	8.00	0.13	0.05	1.26	0.48	0.78	0.06
18/06	42	11.82	0.24	0.08	2.73	1.00	1.72	0.08
18/06	43	5.06	0.13	0.03	1.38	0.25	1.13	0.05
21/06	44	5.82	0.15	0.03	2.03	0.28	1.75	0.05
22/06	45	7.83	0.16	0.02	3.96	0.10	3.86	0.01
22/06	46	12.77	0.24	0.12	3.21	1.20	2.01	0.09
08/07	49	17.80	0.20	0.08	3.22	1.20	2.02	0.07
08/07	50	61.41	0.50	0.48	15.83	12.65	3.18	0.21
mean	28.10	22.04	0.30	0.22	8.89	4.27	4.61	0.09
median	28.00	10.83	0.24	0.08	3.06	1.20	1.80	0.09
stdev	13.90	41.10	0.25	0.52	17.71	11.53	6.82	0.06

tensity, as well as antecedent soil water status as simulated using the VAMPS model (*cf.* . Fig. 4.5). Both quickflow volume (column 4 in Table 4.3) and peak discharge (column 2) turn out to be closely related to storm rainfall total (variable no. 7) but much less to average rainfall intensity (variable no. 8). A rather striking finding is the absence of strong (or even modest) correlations between key storm hydrograph parameters and a range of parameters describing antecedent conditions, such as soil moisture content or the precipitation for various periods preceding the storm (variables nos. 9–19).

4.4.5 PIEZOMETER AND GULLY RESPONSE

Compared to the water levels at the catchment outlet, stormflows emerging as return flow in a small tributary gully (see Fig. 4.1 for location) are seen to react faster to instantaneous changes in throughfall intensity (Fig. 4.6A). Generally, the delay between the peak in throughfall intensity and maximum discharge in the gully was less than 5 min (Fig. 4.6A). A comparison of the flow record for

Table 4.3: Correlation (r) matrix of storm parameters. For clarity all coefficients smaller than 0.15 have been replaced by a minus (-) sign. Columns headers are: **1:** Quickflow duration; **2:** Peak flow; **3:** Total flow; **4:** Quickflow amount; **5:** Baseflow amount; **6:** Quickflow/Total flow ratio; **7:** Total precipitation; **8:** Average precipitation intensity; **9:** Precipitation during the previous day; **10:** Precipitation in the previous week; **11:** Soil moisture at start (0–20 cm); **12:** Initial soil moisture (20–50 cm); **13:** Initial soil moisture (50–140 cm); **14:** Soil moisture on the previous day (0–20 cm); **15:** Soil moisture on the previous day (20–50 cm); **16:** Soil moisture on the previous day (50–140 cm); **17:** Average soil moisture in the previous week (0–20 cm); **18:** Average soil moisture in the previous week (20–50 cm); **19:** Average soil moisture previous in the week (50–140 cm); **20:** Initial discharge, **21:** Discharge at end of storm.

	1	**2**	**3**	**4**	**5**	**6**	**7**	**8**	**9**	**10**
1	1.00									
2	0.68	1.00								
3	0.75	0.99	1.00							
4	0.69	1.00	0.99	1.00						
5	0.80	0.92	0.96	0.91	1.00					
6	0.47	0.49	0.46	0.50	0.36	1.00				
7	0.76	0.99	0.99	0.99	0.93	0.54	1.00			
8	0.32	0.70	0.69	0.71	0.61	0.63	0.73	1.00		
9	-	-	-	-	-0.16	0.41	-	-	1.00	
10	-0.17	-	-	-	-	-	-	-	-	1.00
11	-	-	-	-	-	-	-	-0.16	0.48	0.61
12	-	-	-	-	-	-	-	-	0.24	0.67
13	-	-	-	-	-	-0.33	-	-0.17	-	0.28
14	-	-	-	-	-	-	-	-0.26	0.41	0.58
15	-	-	-	-	-	-	-	-	-	0.69
16	-	-	-	-	-	-0.37	-	-0.15	-0.18	0.26
17	-	-	-	-	-	-0.22	-	-	-	0.66
18	-	-	-	-	-	-0.28	-	-	-	0.46
19	-	-	-	-	-	-0.47	-	-0.28	-0.19	-0.23
20	-0.51	-0.22	-0.25	-0.21	-0.32	-	-0.28	-	-	0.66
21	-	0.56	0.54	0.57	0.46	0.26	0.51	0.61	-	0.56

	11	**12**	**13**	**14**	**15**	**16**	**17**	**18**	**19**	**20**	**21**
11	1.00										
12	0.85	1.00									
13	0.45	0.71	1.00								
14	0.94	0.88	0.51	1.00							
15	0.79	0.99	0.76	0.83	1.00						
16	0.38	0.64	0.99	0.43	0.70	1.00					
17	0.78	0.94	0.77	0.82	0.95	0.73	1.00				
18	0.55	0.82	0.91	0.58	0.86	0.89	0.89	1.00			
19	0.08	0.25	0.81	-	0.30	0.83	0.38	0.65	1.00		
20	0.49	0.57	0.38	0.40	0.56	0.38	0.49	0.50	-	1.00	
21	0.38	0.53	0.41	0.32	0.56	0.41	0.49	0.49	-	0.64	1.00

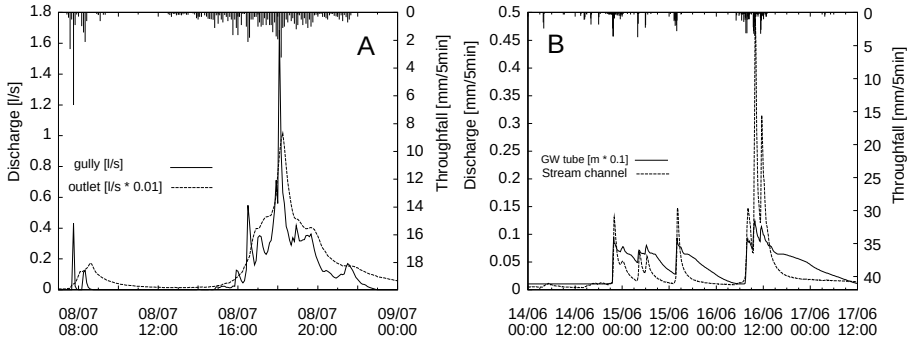

Figure 4.6: A: Discharge in the creek and in a small tributary gully for two throughfall events in July 1996 (note: creek discharge is divided by 100 for scaling purposes). B: Reaction of groundwater levels in piezometer G1 compared to the water level in the creek.

the gully with simulated soil water tensions in the top 10 cm of the soil (Fig. 4.7) shows that the soil is very wet (tensions < 50 cm) when the gully starts to carry water although it does not reach full saturation. Interestingly, the timing of the flow in the gully coincides closely with the occurrence of lateral drainage from the top 10 cm of the soil as inferred from the VAMPS model simulations (Fig. 4.7B).

The level of shallow groundwater as determined in piezometer G1 (see Fig. 4.1 for location) is seen to rise at the same time as the level of the creek and at times even earlier (Fig. 4.6B). The location of the piezometer tube and the magnitude of the fluctuations (the rise in the creek is about an order of magnitude smaller) rule out any direct influence by the water level in the creek. As will be discussed in more detail later, these rapid fluctuations in shallow groundwater levels relate to contributions by lateral macropore flow.

4.4.6 CHEMICAL COMPOSITION OF THE DIFFERENT WATER TYPES

In support of the hydrometrical observations, a total of 102 samples was taken of the various water types within the catchment. In particular, two storms were sampled in detail, including an extreme event occurring on 13 May (storm no. 16 in Table 4.2) and a smaller event occurring on 7 June (part of storm no. 29 in Table 4.2). The corresponding quickflow amounts (QF) were 63.8 and 4.6 mm and the quickflow ratios (QF/P) 0.28 and 0.12. In general the concentrations of the various constituents in the samples were low, with the lowest concentrations found in precipitation and the highest in streamflow during periods of baseflow (Table 4.4). Based on the average electrical conductivities (EC) of the water, the respective contributing water types ranked in the following sequence for their overall solute concentrations: Baseflow (BF) $>$ shallow groundwater (G) $>$ matrix soil water (SW) $>$ return flow (RF) $>$ rainfall (P), although different rankings were sometimes obtained for certain elements

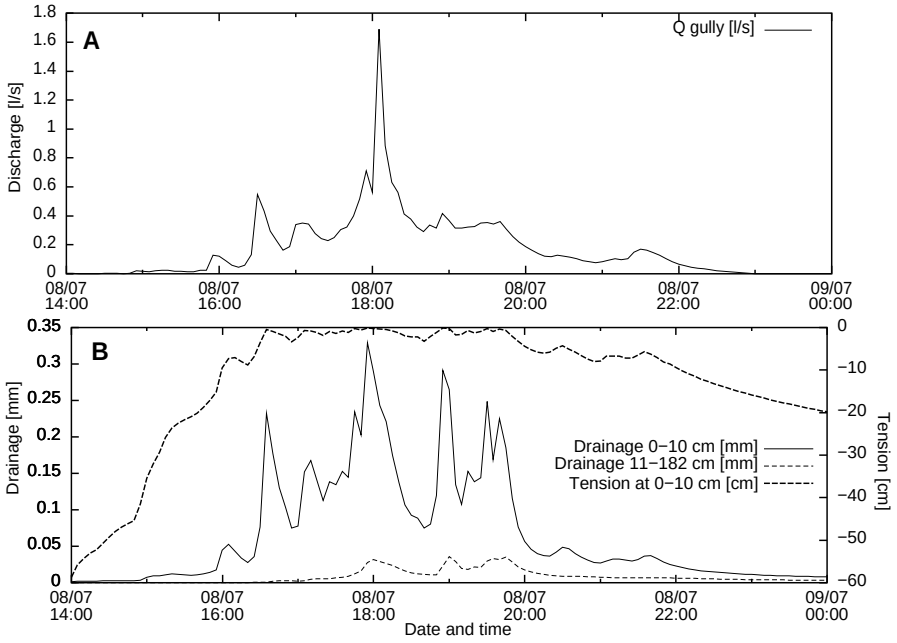

Figure 4.7: Discharge from a tributary gully (A) compared to VAMPS-simulated soil water tensions in the top 10 cm of the soil profile and lateral drainage from the 0–10 and 11–182 cm horizons (B).

Table 4.4: Mean concentrations (μeql^{-1}), pH and electrical conductivity (EC, μScm^{-1}) of chemical constituents sorted by water type. P: precipitation, SW: matrix soil water, RF: return flow (small gully), G: shallow groundwater from piezometer, BF: streamwater (baseflow), STF: streamwater (during storms).

Type	No. of samples	pH	EC	Si	Ca	Mg	K	Na	Cl
P	3	5.5	11	19.8	53	10	12	94	95
SW	37	5.3	503	54.9	44	46	23	252	297
RF	8	5.8	178	40.9	105	40	53	172	214
G	7	5.5	487	58.0	167	67	61	191	239
BF	9	6.8	1913	92.7	303	125	34	301	216
STF	36	6.8	774	56.8	170	65	33	194	178

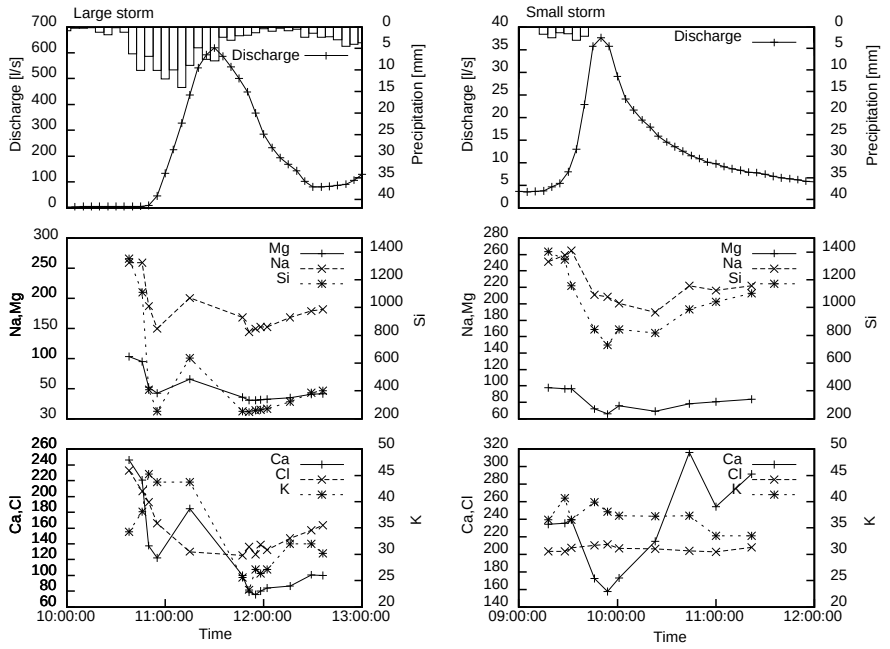

Figure 4.8: Dilution/enrichment patterns for streamwater concentrations of Ca, Mg, Si, K, Na and Cl [μeql^{-1}] during two storm events at Bisley. The large event occurred on 13 May 1996, the smaller event on 7 June 1996.

(*e.g.* K, for which flow types such as return flow and shallow groundwater had relatively high concentrations (Table 4.4)).

The concentrations of silica (Si) showed the widest range in the different water types, with very little Si in precipitation and by far the highest values during baseflow conditions. Intermediate values were found in SW and G whereas relatively low concentrations were also determined for return flow (gully water). Consequently, the clear dilution patterns observed for Si during the two storm events that were sampled in detail must reflect contributions by water types with low concentrations, especially during the largest event (Fig. 4.8).

The lowest Ca concentrations were found in precipitation and soil water, and to a lesser extent in return flow (Table 4.4). During both storm events Ca concentrations diminished rapidly during the first part of the storm, indicating an increase in contributions by one or more low Ca sources (soil water, precipitation or return flow), although concentrations increased again to exceed pre-storm levels at the end of the smaller event event (Fig. 4.8).

A similar behaviour was shown by concentrations of Mg and Na, although soil water was more enriched in this case compared to precipitation. Again, concentrations of Mg and Na decreased during both storm events indicating

increased contributions by rain, and return flow.

Potassium (K) concentrations showed a markedly different pattern with the highest concentrations occurring RF and G, indicating a near-surface source of K enrichment such as litter leaching [*Burghouts et al.*, 1998]. As such, the behaviour of K during the two storm events differed accordingly: concentrations in the stream initially increased as K was temporarily flushed from the litter layer before dropping below pre-storm levels (Fig. 4.8).

Chloride (Cl) concentrations were highest in soil water and lowest in precipitation. During the smaller storm event Cl concentrations rose slightly during the initial phase and than dropped to about half the pre-storm concentration during the remainder of the event. As Cl is not present in the soil material itself the increase is due to dry deposition and concentration due to evapotranspiration. Assuming a 50 % increase in concentration due to interception losses and a 15 % increase due to transpiration [*cf. Schellekens et al.*, 2000], one would expect the Cl concentration in BF to be 271 μeql^{-1} $(95/(1-0.5-0.15))$ and in STF to be 190 μeql^{-1} $(95/(1-0.5))$. However, these simple assumptions disregard any temporal variations in the Cl content of the precipitation between and during storms which may be high [*cf. Turvey*, 1974].

4.4.7 Mass balance-based flow separation

Mixing plots of hydrochemical constituent pairs in streamflow such as Fig. 4.9 can be used to identify those constituent pairs that provide the best contrast between potentially contributing water types, which can therefore be used successfully in a mass balance flow separation model [*Elsenbeer et al.*, 1995a]. The following points emerge from Fig. 4.9: *(i)* Stream water during baseflow is needed as the end member providing the highest concentrations of Ca, Si, Mg and Na. *(ii)* Other useful end members are soil water, precipitation, return (gully) flow and the shallow groundwater as sampled from the piezometers. The latter two water types, however, show very similar concentrations (except for Si; Table 4.4) and are mostly of the same origin (*cf.* Fig. 4.6B). *(iii)* Having the lowest concentrations, precipitation is also needed as an end member, representing an additional fast flow component next to return (gully) flow.

To successfully apply a mass balance flow separation model the water types used as end members must differ significantly for the constituent chosen. Based on the above-mentioned considerations, the three-component mass balance flow separation model (Eq. 4.1) was run for the two storms that were sampled in detail using all the constituent pairs displayed in Fig. 4.9, viz: Cl–K, Na–K, Mg–K, Si–K, Ca–K, Si–Cl, Cl–Mg and Cl–Ca, albeit not always with the same end members. For Cl–K, Na–K, Si–Cl, Cl–Mg Mg–K and Cl–Ca the end members used were: P, RF and BF. For the remaining constituent pairs, SW, RF and BF were used as end members.

The results of the application of the three-component mass balance streamflow separation model are presented in Fig. 4.10 and Fig. 4.11 and summarized in Table 4.5. The different scale of the two events (the large event delivered 228 mm of precipitation while the smaller event only had 14.3 mm of rain) is

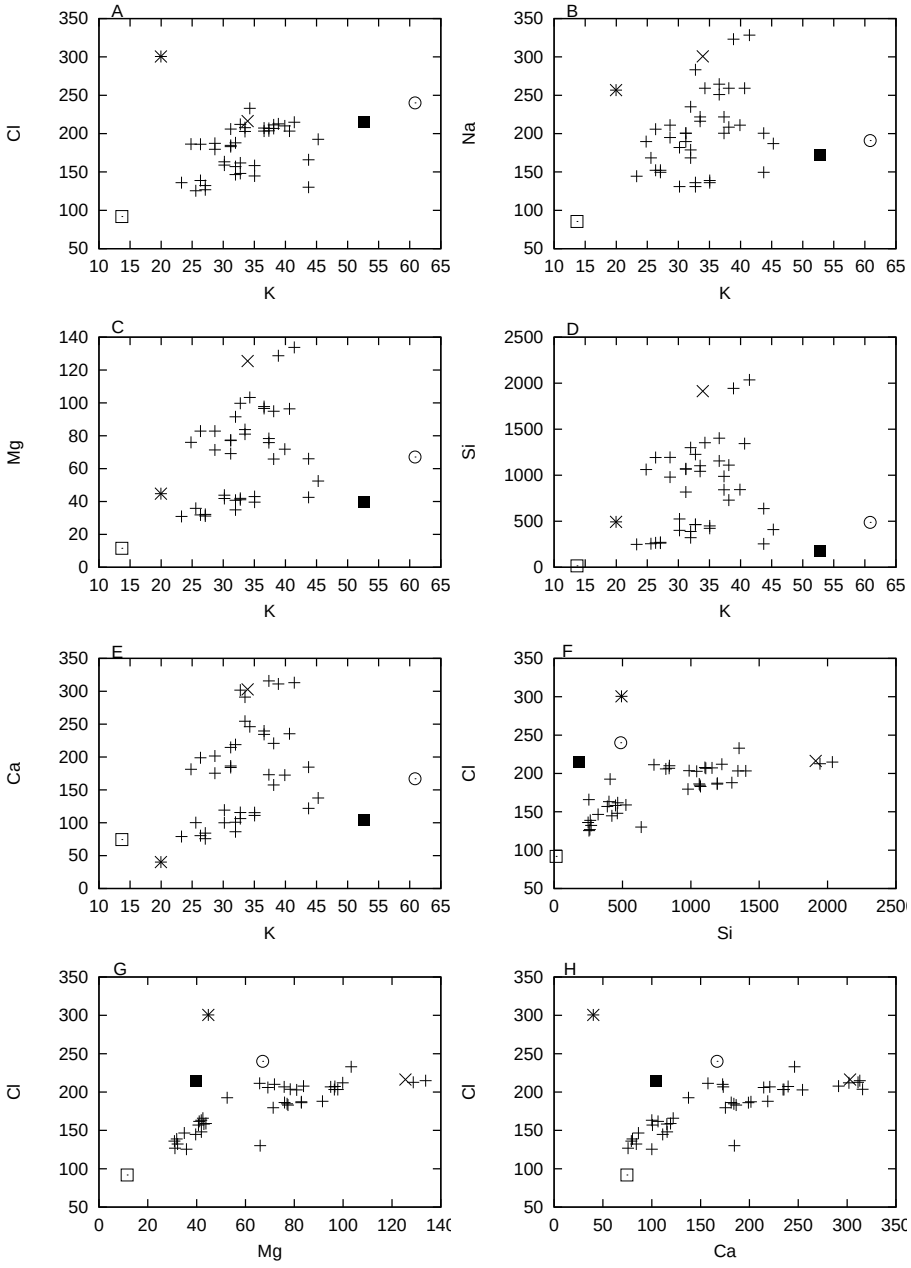

Figure 4.9: Selected mixing diagrams for hydrochemical constituent pairs in stream water at Bisley. Potential end members are indicated by: $*$ = mean soil moisture, ■ = mean returnflow (gully), ⊡ = mean precipitation ⊙ = mean shallow groundwater, $\times$ = mean of stream water at baseflow conditions, $+$ = stream water during stormflow conditions.

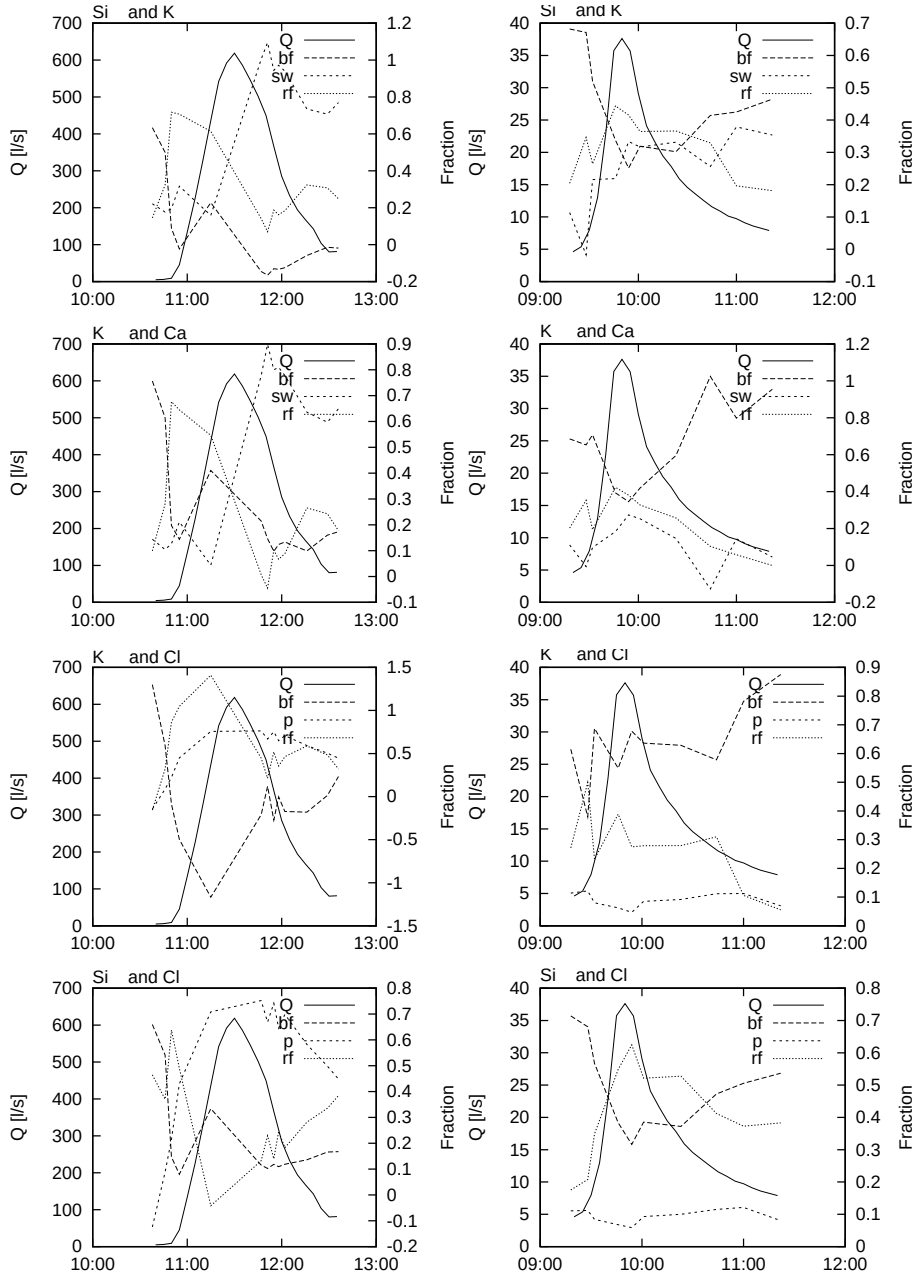

Figure 4.10: Discharge (Q, left-hand y-axes) and the fraction of total discharge (right-hand y-axes) contributed by the different flow components as established with a three-component mass balance model for different hydrochemical constituent pairs during two storm events of contrasting magnitude at Bisley. The results for the large event are shown in the left column while those for the small event are shown in the right column.

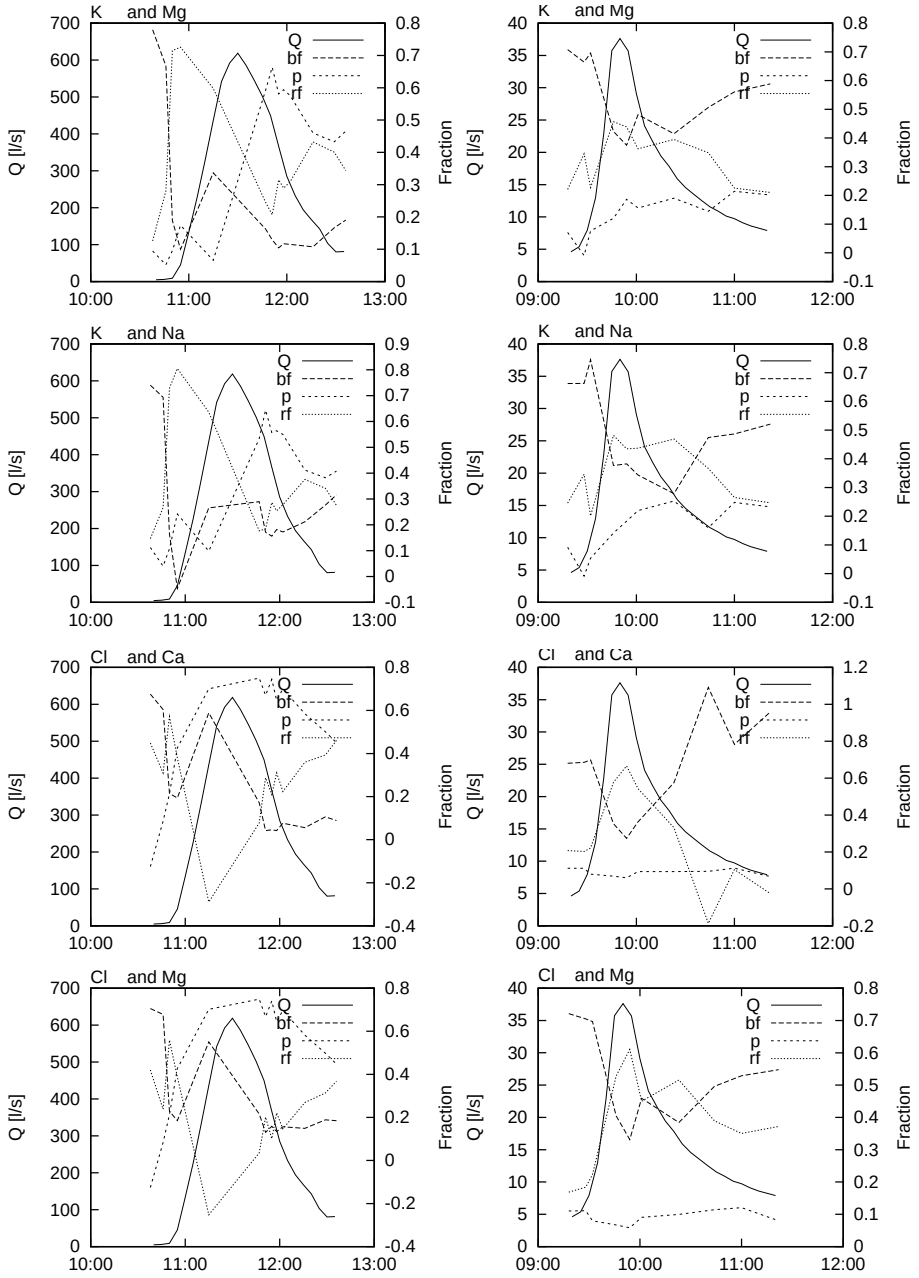

Figure 4.11: Discharge (Q, left-hand y-axes) and the fraction of total discharge (right-hand y-axes) contributed by the different flow components as established with a three-component mass balance model for different hydrochemical constituent pairs during two storm events of contrasting magnitude at Bisley. The results for the large event are shown in the left column while those for the small event are shown in the right column.

Table 4.5: Average runoff component fractions as determined with a three-component mass balance model for several constituent pairs for event I and event II.

	Large event(P = 228 mm)			Small event (P = 14.3 mm)		
Constituents	BF	SW	RF	BF	SW	RF
Si–K	0.049	0.633	0.318	0.439	0.250	0.311
K–Ca	0.252	0.506	0.243	0.658	0.112	0.230
	BF	P	RF	BF	P	RF
K–Cl	-0.026	0.496	0.529	0.641	0.090	0.270
Si–Cl	0.215	0.489	0.296	0.493	0.094	0.412
K–Mg	0.244	0.373	0.384	0.542	0.135	0.323
K–Na	0.276	0.358	0.366	0.493	0.157	0.349
Cl–Ca	0.224	0.489	0.288	0.646	0.089	0.264
Cl–Mg	0.282	0.487	0.231	0.528	0.093	0.379
Mean	0.206	0.449	0.349	0.557	0.110	0.332
Median	0.234	0.488	0.331	0.535	0.094	0.335

clearly shown in Fig. 4.10 and Fig. 4.11. As expected, fast flow paths like RF and P account for a much greater part of the total flow in the large event. Also, based on the Si–$K$and K–Ca pairs the soil water contribution for the large event was estimated at more than 50 % of total flow (with a maximum of about 100 % about midway on the falling limb of the hydrograph), *vs.* only about 20 % for the smaller event (Table 4.5 and Fig. 4.10). Similar values were obtained for the estimated baseflow contribution based on the same constituent pairs. For the other constituent pairs matrix soil water could not be used as an end member and precipitation (P) was used instead. As expected, for the smaller event the influence of P proved rather small at about 10 % while an average of about 40 % was calculated for the large event. Calculated contributions by the RF component (gully water) varied between 27 and 41 % for the smaller event and 24 to 54 % for the large event, depending on constituent pair (Fig. 4.10 and Fig. 4.11).

4.5 Discussion

4.5.1 Catchment structure and soil physical properties

The consistency between the results obtained with the Schlumberger measurements of resistivity with depth throughout the catchment (Fig. 4.2), the borehole logs, and the sample resistivity analysis (Fig. 4.3) suggests a four-layer subsurface structure for the Bisley II catchment: *(i)* a thin top layer of soil having low resistivity (10 to 50 cm thick); this is followed by *(ii)* a 5–40 m (depending on topographic position) thick layer of nutrient-poor highly weathered subsoil and saprolite material of medium to high resistivity values, on top

of *(iii)* a layer of low resistivity of 20–25 m thickness representing less weathered saprolite material that gradually changes to *(iv)* unweathered bedrock (see also Fig. 4.4). The zone of active weathering is located at the bottom part of layer *iii* at the contact with the bedrock. These results suggest that rock weathering at Bisley has proceeded for such a long time that the weathering front — which is 60 m deep in places (Fig. 4.4) — has reached the local base level of the stream channel. The heavily leached nature of the saprolite (Fig. 4.3B) and the available geologic evidence suggesting that the Bisley area has been above sea-level since Miocene times [*Scatena*, 1989] provide further support for this contention.

The results of the saturated hydraulic conductivity (K_{sat}) measurements on small sample cores show an apparent rapid decrease in K_{sat} with depth with the mean K_{sat} in the deepest layer (50–140 cm) being only 4 % of K_{sat} in the top 20 cm. However, median values showed no such strong decrease with depth, indicating the much larger differences in K_{sat} observed between topsoil samples compared to subsoil samples (Table 4.1). *Davis et al.* [1996] demonstrated the importance of core sample size to the ultimately estimated K_{sat} for soils with abundant macropores such as forest soils. Large core samples generally give much higher K_{sat} values. This is illustrated further by the large difference in topsoil K_{sat} values obtained with small core samples and the reversed auger hole method in the present study (Table 4.1). The auger hole method covers a much larger soil sample that will include many more macropores, thus yielding much higher estimates for K_{sat}. The fact that the K_{sat} estimates for the intermediate layer (20–50 cm) differed significantly less between methods suggests that macropores are becoming less important with depth (Table 4.1). Similarly contrasting results were obtained by *McDowell et al.* [1992] in another part of the Bisley area where a large difference was noted between topsoil K_{sat} derived by infiltrometry (1–20 $m\,d^{-1}$) and values estimated for the deeper layers using well recovery tests (0.009–0.09 $m\,d^{-1}$). Fig. 4.12 shows saturated conductivity profiles for the present study catchment and three other data-rich tropical forest sites. The La Cuenca catchment in western Amazonia experiences modest rainfall intensities but the K_{sat} profile shows a sharp decrease with depth [*Elsenbeer et al.*, 1992, 1994a]. As a result, widespread overland flow on hillslopes occurs frequently at this site. A similarly sharp decline in K_{sat} with depth has been reported for the soils in the Babinda catchment in northeast Queensland, Australia [*Bonell et al.*, 1981]. Although the high K_{sat} values in the topsoil at Babinda allow rapid subsurface stormflow the combination of very high rainfall intensities and the presence of the impeding layer also result in widespread saturation overland flow. The profile for the Bisley II catchment shows a significant decline in K_{sat} with depth although less extreme than in the La Cuenca and Babinda catchments. In addition, the higher K_{sat} values in the top part of the soil are a result of macropores and not a feature of the soil matrix. Combined with the steep topography this results in a flow regime where most of the water is transported laterally along the hillslopes. However, overland flow is not observed to occur frequently as at La Cuenca and Babinda, probably due to the lower rainfall intensities and the fact that the

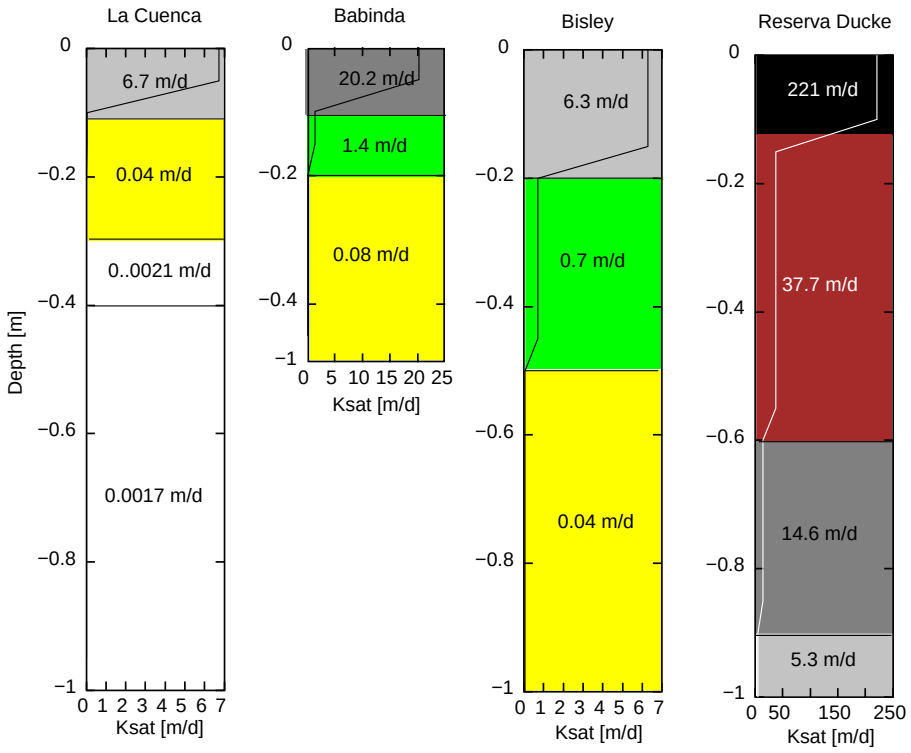

Figure 4.12: Schematic diagram comparing the changes in saturated hydraulic conductivity (K_{sat}) with depth for the present study and three other tropical forest sites: La Cuenca, western Amazonia [*Elsenbeer et al.*, 1992]; Bibinda, north east Queensland [*Bonell et al.*, 1981] and central Amazonia [*Nortcliff and Thornes*, 1981].

impeding layer is located deeper in the soil profile at Bisley. By contrast, the K_{sat} profile at Reserva Ducke in central Amazonia [*Nortcliff and Thornes*, 1981] permits a flow regime which is essentially vertical because of the high K_{sat} values throughout and the absence of an impeding layer. As such, stormflow at Ducke is generated almost exclusively by saturation overland flow in the wet sandy valley fills around the streams where groundwater is always close to the surface [*Nortcliff and Thornes*, 1984].

4.5.2 Response to precipitation

Streamflow response to precipitation at Bisley is rapid with less than 10 min delays on average between precipitation and discharge peaks (*cf.* Fig. 4.6A). The small size of the catchment, the steep topography and the highly permeable topsoil with its abundant macropores are the most likely factors generating this rapid response. The nearly instantaneous response of the piezometers to precipitation (Fig. 4.6B) must be regarded as anomalous, however, as

it can only be explained by short-circuit flow through macropores. Further support for this contention comes from the remarkably high concentrations on K in shallow groundwater samples (Table 4.4). Potassium is known to originate from near-surface sources, notably the litter layer [*Waterloo*, 1994; *Elsenbeer et al.*, 1995a; *Burghouts et al.*, 1998]. Thus, the combined hydrometric (Fig. 4.6B) and hydrochemical (Table 4.4) evidence suggests that the piezometers tapped water traveling through macropores in the upper part of the soil [*cf. McDowell et al.*, 1992]. *Larsen and Torres-Sanches* [1990] had piezometers installed at similar topographic positions in the nearby Bisley III catchment that showed a much slower response time which was more in line with measured K_{sat} values. In their case, short screens were used that were sealed with bentonite at the top. This probably prevented the short-circuit flow that was encountered in the present study. Although the current piezometers did therefore not function as intended, the results do provide additional evidence for the occurrence of fast flow through the top part of the soil down to the riparian zone.

As shown in Fig. 4.3C, the soil at Bisley becomes drier with depth below about 3.5 m and no groundwater was found in any of our boreholes down to a depth of 8 m. Similarly, *Larsen and Torres-Sanches* [1990] reported gravimetric soil moisture profiles in the Bisley area to range from 37 % at the top of the soil to 17 % in the deeper (> 1.6 m) layers. Further support for the contention that relatively small volumes of water are percolating vertically to the subsoil, with lateral pulses though the topsoil being both frequent and volumetrically more important, comes from the soil water modelling exercise. As shown in Fig. 4.5, modelled soil water tensions at the ridgetop site were more frequently close to saturation than those deeper in the soil profile. If no allowance would have been made for lateral drainage, the soil profile would have become saturated very rapidly and the soil water depletion curves (*e.g.* between 22 June and 7 July 1996) would have been much too slow (Fig. 4.5). At 123 mm, the total volume of this inferred lateral flux between 5 May and 9 July 1996 far exceeded the 4 mm of water draining beyond a depth of 185 cm. Figures 4.6 and 4.7 illustrate two important aspects in this respect: *(i)* the hydrograph of the tributary gully closely resembles the amount of lateral drainage that is modelled for the top 10 cm of the soil profile (Fig. 4.7AB) in particular, the timing of the peaks and the point at which the gully starts to hold water agree closely; *(ii)* the resemblance of the gully hydrograph to the stormflow hydrograph of the main stream channel can be taken as another indication of the importance of rapid subsurface stormflow in the study catchment (Fig. 4.6A).

The combined data of Table 4.2 and Table 4.3 provide a picture of a catchment whose response to rainfall is dominated by rapid flow paths. On average an equivalent of 9 % of the precipitation during storm events leaves the catchment as quickflow, with a maximum value of 28 % (Table 4.2). Taking the (very high) interception losses at Bisley [about 50 %, *Schellekens et al.*, 1999] into account, these value increase to 18 and 56 %, respectively. The correlation matrix linking stormflow parameters to potential causal variables in Table 4.3 shows that quickflow amounts (column 4) are highly correlated to rainfall parameters (notably amount, less so to intensity) but hardly to parameters describing an-

tecedent catchment conditions such as soil moisture and precipitation in the preceding days. These conclusions must be viewed with considerable caution, however, because the soil moisture data that were used in the analysis only represent a single element on a ridgetop, which can hardly be held representative for the entire catchment. We will come back to this finding in the chapter on streamflow modelling (Chapter 5). Nevertheless, the results of Table 4.3 suggest that rainfall characteristics outweigh antecedent influences in this particular catchment.

4.5.3 WATER AND SOIL CHEMISTRY

The results presented in Table 4.4 present a familiar picture: concentrations of hydrochemical constituents are lowest in precipitation and highest in stream water during baseflow [*Bruijnzeel*, 1983b; *Waterloo*, 1994; *Elsenbeer et al.*, 1995a]. However, some of the results deviate from the usual. For instance, calcium concentrations in soil moisture at Bisley were lower than in precipitation. This may be related due to the limited number of precipitation samples ($n = 3$), but could also be caused by preferential uptake of Ca by the vegetation [*Jordan*, 1985]. In addition, Ca concentrations in precipitation are likely to vary more in time than those in soil water. A positive relation was found by *McDowell* [1998] between storm size and Ca concentrations in throughfall in the nearby forest at El Verde. Adding this to the fact that soil water samples collected by vacuum tube lysimetry often 'integrate' the inputs of a number of storms due to the time lag between precipitation infiltration and redistribution of soil water into the soil matrix suggests that the apparently anomalous low concentrations of Ca in soil water may also be explained in terms of such temporal dynamics.

Because silica concentrations are strongly governed by the contact time of the water with the soil they can be used to indicate the relative residence times of the respective water types [*Bruijnzeel*, 1983a]. As such, baseflow can be expected to have the highest Si concentrations. However, as none of the runoff sources that were sampled had Si concentrations that resembled those of the baseflow (Table 4.4) it must be concluded that the actual source of the baseflow was not sampled. Working at nearby El Verde, *McDowell* [1998] also noted that concentrations during baseflow were considerably higher than any of the sources that were sampled. *Brouwer* [1996] reported enhanced elemental concentrations in matrix soil water flowing downslope along the contact between saprolite and fresh bedrock at a depth of 4 m in Guyana. A similar mechanism may be at work at Bisley. Based on the combination of geophysical and geochemical evidence it may be assumed that some of the soil water percolates through the saprolite zone of low resistivity (*cf.* Fig. 4.3). The zone around the saprolite-bedrock contact may well be the source of the water having such high concentrations of Si. On a related note, the stream base in the upper reaches of the catchment is closer to the zone of low resistivity (Fig. 4.4) enhancing the chances for water to come into contact with the less weathered parts of the substrate. This contention is strengthened by the results of an EC routing along the stream channel which showed a steady increase in EC when going

upstream [*Van Hogezand*, 1996].

4.5.4 CHEMICAL FLOW SEPARATION

Elsenbeer et al. [1995b] highlighted some of the problems that may be encountered when trying to apply mixing models to catchments whose runoff response is dominated by fast flow paths such as return flow and various forms of overland flow. The soil physical (Table 4.1) and hydrometrical parts (Table 4.4; Fig. 4.7) of the present study already suggest that the Bisley II catchment's response is also dominated by fast flow paths. Our mixing model application (Table 4.5) provides additional evidence for this. However, some ambiguities remain. Looking at the respective constituent pairs used in Table 4.5 to separate the contributions by baseflow, precipitation and return flow, the importance of the fast flow paths — especially during the large event — is evident (see also the bottom two rows of Fig. 4.10 and all of Fig. 4.11). On the other hand, when Si–K and K–Ca were used as constituent pairs, a very large contribution was calculated for soil water, especially at the end of the large event (Fig. 4.10). Because soil matrix water cannot be regarded as a fast flow component something else must cause this apparent anomaly. *McDonnell* [1990] described how rapid mixing of 'old' soil matrix water with fast-flowing 'new' water through macropores could explain a similar pattern in the Maimai steepland catchment in New Zealand. Also, the sampling of soil water via tension lysimetry, as practiced in the present study, makes the exact source of the water in the samplers (matrix or macropore water) uncertain [*DeWalle et al.*, 1988]. However, it is pertinent in this respect that the computed 'soil water' contribution starts to increase only at the end of the large event, *i.e.* after a considerable amount of rain has fallen. Saturation overland flow (SOF) was not sampled directly in this study although it was observed in the field (on a slope near the main stream channel) during the large storm and at other times. Combining this with the fact that the influence of the rainfall component (as shown in the top two rows of Fig. 4.11) increases in a similar fashion as the apparent soil water contribution, it seems likely that SOF is the actual source at that moment although only direct sampling can provide a more definite conclusion.

According to the mixing diagrams of Fig. 4.9 it is clear that for some constituent pairs there is more than one choice of possible end members. For example, the bottom part of Fig. 4.9 shows the Cl – Mg and Cl – Ca mixing plots for which BF, RF and P were chosen as end members. Instead of RF, SW could also have been chosen which would also have included the whole mixing region. Fig. 4.13 shows the result of doing so, using Cl – Ca as the constituent pair. Combining these results with those of Fig. 4.11 it appears that: *(i)* the large event (13 May 1996) is dominated by a different fast flow path than the smaller event; *(ii)* the 'real' soil water contribution to storm runoff (as apparent from Fig. 4.13) is much smaller than envisaged originally in Fig. 4.11 when using RF as an end member; *(iii)* two fast flow paths, flow through macropores and saturation overland flow (SOF), emerge as the principal contributors to storm runoff in Bisley. However, the exact contribution of this SOF could not be de-

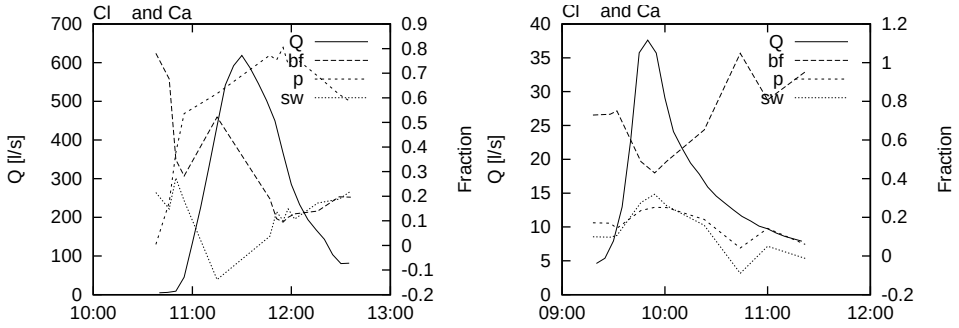

Figure 4.13: Discharge (left hand y-axes) and the fraction of total discharge (right hand y-axes) of the different flow components as established with a three-component mass balance model using Cl and Ca with P, SW and BF as end members during two storm events of contrasting magnitude at Bisley. The large event is shown in the figure on the left while the the small event is shown in the right figure.

termined as it was not sampled directly, although it is clear that the large event includes a considerably bigger contribution by SOF than the smaller event (Fig. 4.11).

The present analysis used constant concentrations for the different sources. As noted by *Hinton et al.* [1994] this might be the greatest single source of error in predicted flow volumes, as the assumption of constant concentration is often not valid for many sources. Flushing effects (notably for K and Ca) are an example, especially during large events (*cf.* Fig. 4.8).

4.5.5 A FLOW-GENERATION PICTURE OF THE BISLEY II CATCHMENT

The results of the various techniques presented in the previous sections suggest a picture of a catchment whose storm response is dominated by fast flow paths. The rapid decay of saturated hydraulic conductivity with depth (Table 4.1) clearly allows only small quantities of water to percolate to the deeper parts of the soil profile. The continuous decrease in soil moisture with depth below 3.5 m underlines this further [Fig. 4.3C; *cf. Larsen and Torres-Sanches*, 1990]. The combination of the above and the (very) steep topography in parts of the catchment favours rapid lateral flow through the uppermost soil horizon (sub-surface storm flow, $SSSF$). The discrepancy in results obtained with different methods for the measuring of saturated hydraulic conductivity in the topsoil in this and other studies in the Bisley area [*McDowell et al.*, 1992], suggests that abundant macropores and a pronounced soil structure are the primary reasons for the relatively high conductivity of the topsoil (Table 4.1). Another source of rapid flow in the area is saturation overland flow (SOF). This type of flow is favoured by a rapidly decreasing hydraulic conductivity with depth which allows a perched water table to develop easily, especially under high rainfall conditions [*Bonell and Gilmour*, 1978]. At places where $SSSF$, con-

verges such as in hillslope hollows, return flow (RF) may emerge which again causes SOF, showing that the two flow types can be closely linked [*Dunne*, 1978; *Elsenbeer et al.*, 1996]. The mixing model results presented in Fig. 4.10 and Fig. 4.11 point to return flow (as measured in a tributary gully) as the main contributor to quick runoff. Additional hydrometric evidence (Fig. 4.6) supports this contention. However, as discussed in Section 4.5.4, SOF, including precipitation onto already saturated areas, may also account for a significant portion of the quickflow at Bisley, especially during large events occurring during wet periods. Although the choice of end members and constituents used in the flow separation procedure influences the results considerably (*cf.* Fig. 4.10 and Fig. 4.11), it is clear that fast flow paths comprise an important part of the storm hydrograph at Bisley. Nevertheless, the baseflow percentage inferred for the smaller of the two sampled events is still considerable (56 % on average, *vs.* 20 % for the large event). As discussed earlier, a flaw in the present application of the mixing model is the fact that we have not been able to sample the deep source of the baseflow directly. Two sources remain possible candidates: *(i)* soil water that flows along the weathering front before entering the stream channel, and *(ii)* soil moisture (or even groundwater) from unsampled parts of the catchment where either less weathering has occurred or where the weathering zone is closer to the surface (*e.g.* due to tectonic activity).

Further work is necessary which could usefully employ isotope analytical techniques [*Brammer and McDonnell*, 1996; *Nimz*, 1998].

ACKNOWLEDGEMENT

The people at the hydrochemistry laboratory in Amsterdam, notably Mrs. Hetty Schäfer were able to process the water samples at great speed and accuracy: thanks. The assistance of the VUA workshop and fieldwork equipment store is gratefully acknowledged. We want to thank the electronics department of the Vrije Universiteit, notably J. de Lange and R. Lootens, for their help. The assistance of the IITF chemical laboratory with the soil chemical analyses and of F. Holwerda and A.J. Wickel in collecting core samples is gratefully acknowledged.

5

MODELLING WATER YIELD AND RUNOFF RESPONSE OF A SMALL TROPICAL RAIN FOREST CATCHMENT USING A PHYSICALLY-BASED DISTRIBUTED MODEL*

ABSTRACT

This paper marks the first application of the physically-based distributed TOPOG model to predict water yield and runoff response of rain forested steepland terrain under wet maritime tropical conditions. The study was conducted in the small (6.4 ha) and steep (average slope 0.54 $m\ m^{-1}$) Bisley II catchment which is situated at 265–456 m above sea level in the Luquillo Mountains of eastern Puerto Rico. Two versions of the TOPOG model were tested: *(i)* the TOPOG_SBM model that uses a simplified bucket model for soil water accounting and *(ii)* the more elaborate TOPOG_DYNAMIC model that solves the Richards equation for unsaturated flow. Both versions of the model were run to simulate streamflow patterns during a three-month period in 1996 using daily time steps and for 16 storm events of different magnitude (3 – 78 mm of net precipitation) occurring during this period using 5-min time steps. Both models simulated observed discharge patterns for the three-month period satisfactorily (model efficiencies were 0.94 and 0.96 for the TOPOG_SBM and TOPOG_DYNAMIC model respectively). However, to achieve this in the case of the TOPOG_SBM model the effective thickness of the soil had to be reduced from 100 cm to 25 cm. In general, both models also performed adequately upon modelling the 16 individual storm events although the response to small storms (< 5 mm of net precipitation) was systematically overestimated. Also, flows during the later part of the recession curve were significantly overestimated by the models. It is concluded that the absence of a separate macropore flow component in the models — rapid subsurface flow was previously shown to be an important flow path in this catchment — somewhat limits the predictive capability of the model under the circumstances prevailing in the study area.

*submitted to: *J. of Hydrol.*

5.1 INTRODUCTION

The use of physically-based distributed models in catchment hydrology has been rising steadily for the last decade. This increased use is mostly generated by the notion that catchments may react to rainfall and various types of disturbance in many different ways. Because practical catchment/forest management questions generally have a spatial dimension attached, and because most landscapes consist of a complex mosaic of different land uses and covers, physically-based models should preferably be of a distributed nature, *i.e.* capable of taking into account spatial variations in topography, soils, vegetation and climate [*Vertessy et al.*, 1993]. Traditionally, forest hydrologists have relied on catchment experiments to evaluate such effects [*Gilmour*, 1977; *Pearce and Griffiths*, 1980; *Swindel et al.*, 1983; *Hewlett et al.*, 1984; *Hsia*, 1987; *Malmer*, 1992; *Fritsch*, 1992]. However, apart from being time-consuming, the paired catchment approach is unable to evaluate the relative importance of various factors that might underly differences in results between sites and this severely limits the possibilities for extrapolation of such results to other areas or periods. The same applies to empirical models due to the fact that the parameter associations on which they are based are generally not transferable to sites where catchment characteristics or disturbances differ [*Bosch*, 1979; *Vertessy et al.*, 1993].

Despite their relative complexity, a certain amount of lumping and conceptualization still remains in physically-based distributed models, even in the most sophisticated ones, and they must still be regarded as an extreme simplification of reality [*Beven*, 1989]. Also, little consensus exists among modellers regarding the best way to evaluate the results of their modelling efforts. To avoid getting the 'right answers' for the 'wrong reasons' [*Beven*, 1989; *Grayson et al.*, 1992], and account for the empirical parts and generalizations of the models, a priori knowledge of the major processes operating within a catchment is needed; thus allowing for a better interpretation and validation of the model results [*Vertessy and Elsenbeer*, 1999; *Zhu et al.*, 1999]. This also suggests that the predictive value of a model is related to the amount of knowledge available about the underlying system. Consequently, any advances in process research should have an impact on model development and research as to improve on the representation of the catchment's physical processes within the models. At the same time it is becoming clear that the data requirements of today's physically-based models are enormous already [*Abbott et al.*, 1986b], notwithstanding the fact that often only a few parameters are needed to provide reasonable results [*Beven*, 1989]. As such, a priori knowledge about the principal processes operating within a catchment may also be used to single out the most important parameters.

A comprehensive process-based distributed model is the TOPOG modelling framework [*O'Loughlin*, 1986; *Vertessy et al.*, 1993; *Vertessy and Elsenbeer*, 1999]. TOPOG integrates the water, carbon, solute and sediment balances at the small catchment scale (typically $\ll 10\ km^2$) and is particularly suited to explore complex feedback mechanisms between system properties. Examples

of within-catchment applications of TOPOG include: the prediction of steady-state soil moisture distributions and saturated zones in the landscape during wet and dry periods [*O'Loughlin*, 1986; *Moore et al.*, 1988], the spatial distribution of surface erosion, gully initiation and landslide hazard [*Vertessy et al.*, 1990; *Constantini et al.*, 1993; *Dietrich et al.*, 1992], and the evaluation of the water balance and growth performance of different tree planting configurations under sub-humid conditions [*Silberstein et al.*, 1999]. Off-site applications of TOPOG included the successful simulation of changes in tree growth and water yield for a small catchment after clearfelling during 20 years of regeneration [*Vertessy et al.*, 1996].

The present paper marks the first application of the TOPOG model in a wet maritime tropical steepland setting: the Bisley II catchment in the Luquillo Experimental Forest (LEF), eastern Puerto Rico. The present simulations were carried out for the 81-day period between 24 April and 13 July 1996 using a 1-day time step, and for 16 selected individual storms occurring during this period using a 5-min time base. In addition, the effect of using two different soil water accounting schemes within TOPOG is investigated. These are: *(i)* a simple bucket model (similar to the TOPMODEL implementation of *Beven and Kirkby* [1979]; *Beven* [1997]; *cf. Vertessy and Elsenbeer* [1999]) and *(ii)* a full Richards equation-based scheme [*Vertessy et al.*, 1993].

The climate and ecology of the LEF have been extensively researched in the past [*Odum and Pidgeon*, 1970; *Brown et al.*, 1983; *Lugo and Scatena*, 1995]. Previous work by *Scatena* [1990b] and more recently by *Schellekens et al.* [1999, 2000] (Chapter 2 and Chapter 3) concerning rainfall interception and the catchment water budget, plus a runoff generation study [Chapter 4; *Schellekens et al.*, submitted] have contributed to a basic conceptual understanding of the hydrological processes operating in the Bisley area. As such, the comparison of the results obtained with these detailed process studies with the modelling results may be considered a first test of the robustness of the TOPOG package under the conditions prevailing in the study area.

5.2 SITE DESCRIPTION

The Bisley II catchment is part of a set of three experimental catchments situated at 18^o 18′ N, 65^o 50′ W at an elevation of 265–456 m above sea level (asl) The 6.4 ha catchment drains a dissected mountainous terrain with steep stream gradients [*Scatena*, 1989]. More than half of the area has slopes greater than 45 % (24^o). Shallow earth movement, soil creep [*Lewis*, 1974, 1976] and tree throw are important geomorphological processes. The clayey soils that have developed in the underlying thick-bedded tuffaceous sandstones and indurated siltstones are strongly leached Ultisols. *Silver et al.* [1994] reported bulk densities within the Bisley catchments of 0.6 (0–10 cm), 1.0 (10–35 cm) and 1.3 $g\ cm^{-3}$ (35–60 cm) while *Schellekens et al.* [submitted] obtained values between 0.9 and 1.2 $g\ cm^{-3}$. Using small core samples *Schellekens et al.* [submitted] (Chapter 4) found saturated hydraulic conductivity (K_{sat}) to range from

0.02 to 0.5 $m\,d^{-1}$, with the lowest values pertaining to the subsoil (< 50 cm). However, when using the inverses auger-hole method much higher values (up to 6.3 $m\,d^{-1}$) were obtained for the top 20 cm of the soil profile. Similarly, saturated conductivity in riparian zones was estimated by *McDowell et al.* [1992] to range from 1 to 20 $m\,d^{-1}$ based on infiltrometry and from 0.009 to 0.09 $m\,d^{-1}$ using groundwater recovery tests in piezometers. Both *McDowell et al.* [1992] and *Schellekens et al.* [submitted] considered macropores (and the blocky structure of the topsoil) responsible for the high K_{sat} values of the topsoil. *Schellekens et al.* [submitted] observed the presence of water-conducting macropores down to 60 cm depth although the bulk was concentrated in the top 20 cm. The saprolite extends down to 40 m below the surface at which the transition to unweathered bedrock is found. Based on the low K_{sat} value obtained for the subsoil ($1.7 \cdot 10^{-4}$ $m\,d^{-1}$) transport through the deep saprolite layer is believed to be negligibly small [*Van Dijk et al.*, 1997; *Schellekens et al.*, submitted].

The so-called Tabonuco forest of the study catchment has an irregular, 20–25 m high upper canopy, an understory of palms and woody vegetation, and ground level herbs and shrubs. The average leaf area index (LAI) of mature Tabonuco forest is between 6 and 7 but may range between 12 on ridges and 2 in dark ravines and riparian valleys [*Odum et al.*, 1970a]. In September 1989 the Bisley area was severely impacted and nearly completely defoliated by Hurricane Hugo [*Scatena et al.*, 1993]. However, by 1996 when the present study was initiated the LAI, canopy interception, and forest biomass were again similar to pre-hurricane conditions [*Scatena et al.*, 1996; *Holwerda*, 1997].

The climate is maritime tropical (type A2m according to the Köppen classification), with an annual rainfall of 3530 mm [as measured at the nearby long-term rainfall station at El Verde, 450 m asl, *Schellekens et al.*, 2000]. Rainfall is distributed fairly evenly throughout the year, with May and November being relatively wet (average precipitation 370 and 380 mm, respectively) and the period January to March being relatively 'dry' (average precipitation ranging between 177 and 238 mm). Rainfall at El Verde is delivered as numerous (267 rain days per year), relatively small (median daily rainfall 3.0 mm) storms of low intensity [$<$5 $mm\,hr^{-1}$; *Brown et al.*, 1983; *García-Martinó et al.*, 1996]. *Schellekens et al.* [1999] reported the rainfall intensity for the period between 5 May and 9 July 1996 to have a mean value of 3.0 $mm\,hr^{-1}$ and a median of 1.9 $mm\,hr^{-1}$.

Evapotranspiration totals (ET) at Bisley are very high (2420 $mm\,yr^{-1}$ for 1996) with the interception part (E_i) making up the bulk of the loss [1788 $mm\,yr^{-1}$ *Schellekens et al.*, 2000, Chapter 2]. Transpiration (E_t) by the Tabonuco forest is rather modest at 632 $mm\,yr^{-1}$ for 1996. For the present study period ET was established at 6.6 $mm\,d^{-1}$, E_t at 2.2 $mm\,d^{-1}$ and E_i at 4.9 $mm\,d^{-1}$, discharge (Q) amounted to 3.5 $mm\,d^{-1}$ [*Schellekens et al.*, 2000, Chapter 2].

5.3 MODEL DESCRIPTION

5.3.1 THE TOPOG MODELLING FRAMEWORK

TOPOG consists of a series of models capable of solving water, energy, solute,

carbon and sediment balances of a catchment in a fully distributed manner [*Vertessy et al.*, 1993, 1996; *Dawes et al.*, 1997]. A recent development [*Vertessy and Elsenbeer*, 1999] also allows the model to run on sub-daily time steps as opposed to earlier versions that were geared towards daily water budget calculations. The basis for all TOPOG versions is the same: a network of elements defined by intersections of elevation contours and slope lines which can be derived from a well-defined digital elevation model (DEM) of the catchment in a semi-automated way [*O'Loughlin*, 1986; *Dawes and Short*, 1994]. Different properties (soil physical, surface roughness, vegetation) can be attributed to each element. Two different soil moisture accounting schemes can be used in TOPOG: *(i)* a simple bucket model (referred to further as the TOPOG_SBM model) and *(ii)* a solution of the Richards equation for multi-layered soils (referred to further as the TOPOG_DYNAMIC model). The TOPOG_SBM scheme is similar in concept to the widely used TOPMODEL soil water accounting scheme of *Beven and Kirkby* [1979]. Overland flow in both models can occur in any element whenever rainfall intensity exceeds the element's infiltration capacity or when the rain falls onto an already saturated element. The contour-based element network allows subsurface and overland flow to be routed using a one-dimensional kinematic wave equation [see for example *Keulegan*, 1944; *Lighthill and Whitham*, 1955; *Henderson and Wooding*, 1964]. Re-infiltration of overland flow can occur when an unsaturated element is encountered. Overland flow velocity is calculated using the Manning equation [*Vertessy and Elsenbeer*, 1999].

The TOPOG_SBM *soil water accounting scheme*

A detailed description of the TOPOG_SBM model has been given by *Vertessy and Elsenbeer* [1999]. Briefly: the soil is considered as a bucket with a certain depth (z_t), divided into a saturated store (S) and an unsaturated store (U), the magnitudes of which are expressed in units of depth. The top of the S store forms a pseudo-water table at depth z_i such that the value of S at any time is given by:

$$S = (z_t - z_i)(\theta_s - \theta_r) \tag{5.1}$$

where θ_s and θ_r are the saturated and residual soil water contents, respectively. The unsaturated store (U) is subdivided into storage (U_s) and deficit (U_d) which are again expressed in units of depth:

$$U_d = (\theta_s - \theta_r)z_i - U \tag{5.2}$$

and:

$$U_s = U - U_d \tag{5.3}$$

The saturation deficit (S_d) for the soil profile as a whole is defined as:

$$S_d = (\theta_s - \theta_r)z_t - S \tag{5.4}$$

All infiltrating rainfall enters the U store first. The transfer of water from the U store to the S store (st) is controlled by the saturated hydraulic conductivity

K_{sat} at depth z_i and the ratio between U and S_d:

$$st = K_{sat}\frac{U_s}{S_d} \tag{5.5}$$

Hence, as the saturation deficit becomes smaller, the rate of the transfer between the U and S stores increases.

Saturated conductivity (K_{sat}) declines with soil depth (z) in the model according to:

$$K_{sat} = K_0 e^{(-fz)} \tag{5.6}$$

where:

K_0	saturated conductivity at the soil surface	$[m\,d^{-1}]$
f	scaling parameter	$[m^{-1}]$

The scaling parameter f is defined by:

$$f = \frac{\theta_s - \theta_r}{M} \tag{5.7}$$

with θ_s and θ_r as defined previously and M representing a model parameter (expressed in meters). The S store can be drained laterally via subsurface flow according to:

$$sf = K_0 tan(\beta) e^{-S_d/M} \tag{5.8}$$

where:

β	element slope angle	[deg.]
sf	calculated subsurface flow	$[m^2 d^{-1}]$
S_d	saturation deficit ($(\theta_s - \theta_r)z_t - S$)	$[m]$

with M and S_d as defined previously. A schematic representation of the various hydrological processes and pathways modelled by TOPOG_SBM (infiltration, exfiltration, Hortonian and saturation overland flow, subsurface flow) is provided by *Vertessy and Elsenbeer* [1999].

The TOPOG_DYNAMIC *soil water accounting scheme*

The TOPOG_DYNAMIC model solves the Richards equation for unsaturated flow one-dimensionally (in the vertical) for each element while allowing lateral flow out of saturated nodes according to Darcy's law and a kinematic wave equation. TOPOG uses the following formulation of the Richards equation:

$$\frac{\partial\theta}{\partial t} = \frac{\partial}{\partial z}\left(D\frac{\partial\theta}{\partial z}\right) - \frac{\partial K}{\partial z}\frac{\partial\theta}{\partial z} \tag{5.9}$$

where:

θ	volumetric water content	$[m^3 m^{-3}]$
z	depth below the soil surface	$[m]$
K	unsaturated hydraulic conductivity	$[m\,d^{-1}]$
t	time	$[days]$
D	diffusivity	$[m^2 d^{-1}]$

In addition, a Kirchoff transformation is applied in order to minimize non-linearity in space [*Ross and Bristow*, 1990]:

$$F = \int_{-\infty}^{\Psi} K d\Psi \equiv \int_{0}^{\theta} D d\theta \tag{5.10}$$

where:

Ψ	suction head	$[m]$
t	time	$[days]$
F	Kirchoff transform variable	$[m^2 d^{-1}]$

Combining these yields:

$$\frac{\partial \theta}{\partial t} = -\frac{\partial}{\partial z}\left(K - \frac{\partial F}{\partial z}\right) \tag{5.11}$$

Ross and Bristow [1990] showed how this formulation can be applied to include layered soils. It has also been shown that the solution of Eq. 5.11 allows for a very small mass balance error in addition to being relatively fast [see *Vertessy et al.*, 1993, for details].

5.3.2 METHODOLOGY

In the present application the TOPOG model is used in four modes of operation:

1. Solving the Richards equation using a daily time step (the TOPOG_DYNAMIC model) during a 81-day period in 1996.
2. Using the TOPOG_SBM model for the same period and time step.
3. Solving the Richards equation at a 5-min time step during 16 selected storms.
4. Using the TOPOG_SBM model at a 5-min time step for the same 16 selected storms.

The first two modes were used for the initial parameterization of the models and to assess the associated performance. The runs in the third and fourth modes were initially conducted with the same parameter sets as used in the first two modes, although some parameters were adjusted in the process.

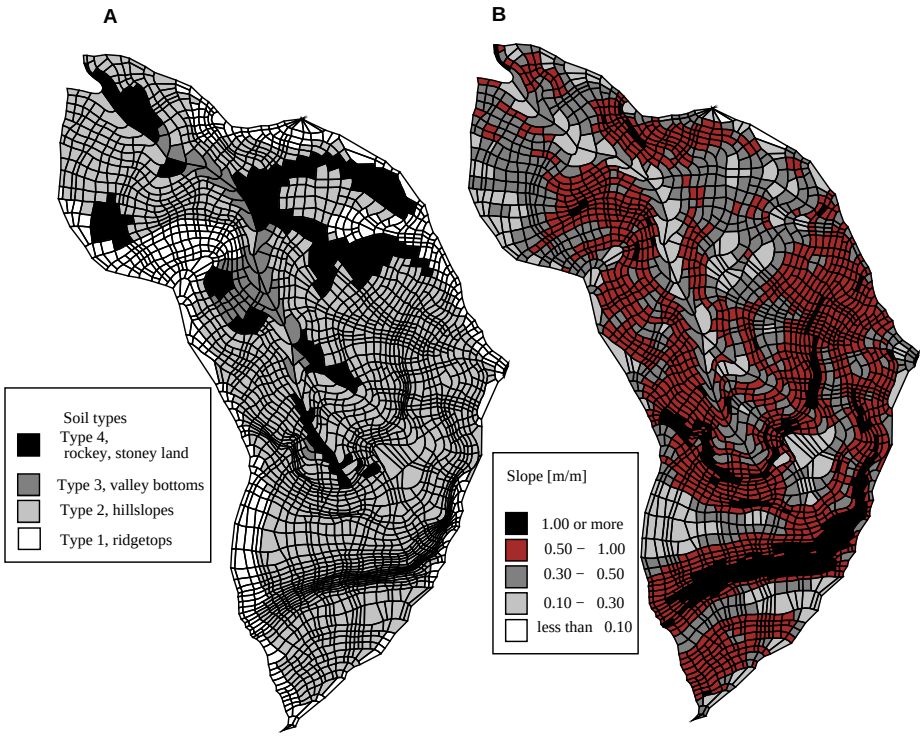

Figure 5.1: The element network for TOPOG. A: Soil types attributed to each element (*cf.* Table 5.1). B: Slope steepness [$m\ m^{-1}$] of each element.

DEM *and element network construction*

The rectangular grid-type DEM used to generate the TOPOG flow element network was derived from a hand-drawn 5 m contour map based, in turn, on a geodetic field survey. Construction of the DEM was performed using the spline-based interpolation procedure of *Hutchinson* [1989], as used in the TOPOG_SPLINE2H module. This procedure was developed specifically with hydrological applications in mind. It allows for the inclusion of drainage channels as well as depressions and topographic saddles that are used to prevent the occurrence of conflicting downslope drainage directions. In addition, the generation of spurious 'pits' is prevented, ensuring hydrologically realistic behaviour. The steep and dissected nature of the terrain required a considerable amount of smoothing (achieved by increasing the 'tension' to the spline function in the gridding program) before a usable DEM could be obtained. In the next step the basic DEM is used to generate the TOPOG element network in a semi-automated way using the TOPOG_DEMGEN program. During this step the program also calculates terrain attributes for each element, such as slope steepness, aspect and upslope contributing area. The final element network was constructed using a 2.5 m contour interval and consisted of 2876 elements

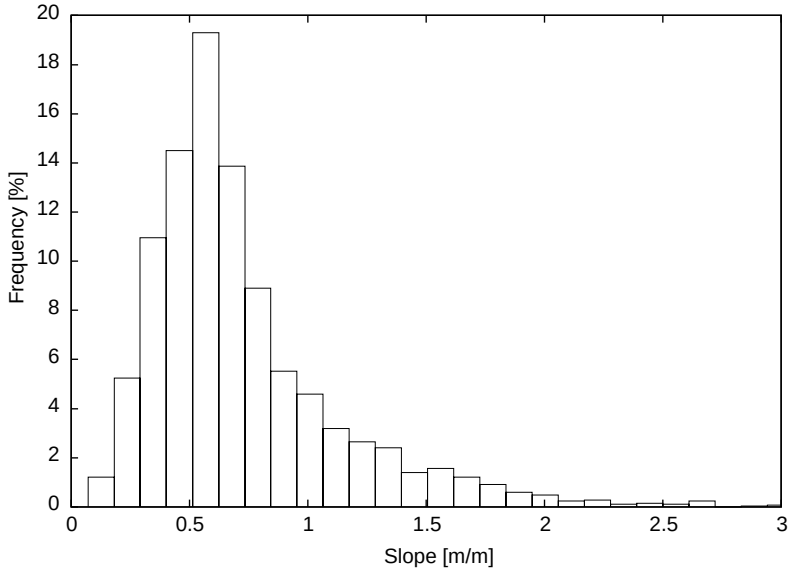

Figure 5.2: Frequency distribution of elements according to slope class (at 0.11 $m\ m^{-1}$ increments per bin) for the Bisley II catchment. Slopes greater than 3.0 $m\ m^{-1}$ not shown (0.2 % of the total).

(Fig. 5.1) with an average element size of 23.55 m^2. The total catchment area obtained in this way for use in the model is 67,722 m^2, *i.e.* slightly larger than the commonly used value of 6.4 ha [*Scatena*, 1989]. The largest element measured 169.78 m^2, and the smallest 1.53 m^2. The average slope of all the elements in the catchment is 0.75 $m\ m^{-1}$ (0.54 $m\ m^{-1}$ when weighted for element size). The steepest element had a slope of 5.59 $m\ m^{-1}$ (on a hillslope in the southern part of the catchment) while the smallest slope (0.07 $m\ m^{-1}$) was associated with an element located at a ridgetop. Most of the elements (84 %) had a slope of 1.0 $m\ m^{-1}$ and smaller. Only 0.2 % of the elements had a slope greater than 3.0 $m\ m^{-1}$ (Fig. 5.1 and Fig. 5.2).

Soil physical parameters

Four different soil units, closely related to topographic position and slope morphology, were used in the model (Table 5.1): *(1)* ridgetop soils, *(2)* hillslope soils, *(3)* valley bottom soils and *(4)* patches of rocky stony land [see *Scatena*, 1989, for a fuller description]. Fig. 5.1A shows the distribution of the respective soil types within the catchment.

Initially, Van Genuchten-type suction head *vs.* water content functions [*Mualem*, 1976; *Van Genuchten*, 1980] were used in the simulations after determining the associated parameters α and n via non-linear regression [*Marquardt*, 1963]. The same set of functions had been used previously in the one-dimensional

Table 5.1: Value of key soil physical parameters assigned to the four soil units used in the model runs with the TOPOG_SBM model. 1: ridgetop soils, 2: hillslope soils, 3: valley bottom soils, 4: rocky stony land (*cf.* Fig. 5.1A).

	Unit			
Soil characteristic	1	2	3	4
Initial thickness $[cm]$	100	100(25)	100	100
Optimized thickness $[cm]$	40	20	30	30
Decay parameter f (optimized) $[m^{-1}]$	2.0	2.0(0.01)	2.0	2.0
K_0 $[m\,d^{-1}]$	3.0	6.0	4.0	3.0
Porosity	0.61	0.61	0.61	0.61

Table 5.2: Generalized soil physical parameters [*sensu Broadbridge and White*, 1988] as used in the model runs with the TOPOG_DYNAMIC model.

	B & W-Type curve				
Soil characteristic	a	b	c	d	e
$K_{sat}[m\,d^{-1}]$	0.36	0.83	1.29	0.5	6.5
Porosity	0.68	0.60	0.66	0.50	0.68

modelling of the soil water status at Bisley using the VAMPS model [*Schellekens et al.*, submitted, , Chapter 4]. However, TOPOG_DYNAMIC experienced severe numerical instability (mostly in valley bottom elements) upon using these functions and the model runs could not be completed. In a comparison of different soil hydraulic models supported by TOPOG, *Beverly* [1994] showed that the *Broadbridge and White* [1988] model was the most suitable for the type of numerical solution used in the TOPOG model. After converting the present Van Genuchten-type curves to *Broadbridge and White*-type curves and slightly adjusting their shape, the model no longer encountered instability problems. Due to the relatively small number of core samples taken for the determination of soil-water retention relationships ($n = 52$) and the lack of any clear differences between the curves associated with the respective soil units, the *Broadbridge and White* parameters (apart from K_{sat}) were assumed to be applicable for all soil types. Five sets of *Broadbridge and White* type parameters were used (Table 5.2) and assigned to the various nodes of the respective soil types in the catchment according to the specification given in Table 5.3.

Table 5.3: Assignment of *Broadbridge and White*-type parameters a–e (see Table 5.2) to the four soil units as used in the TOPOG_DYNAMIC model.

Soil Unit	Depth range $[cm]$ with B & W type in brackets		
1	0–35(e)	35–50(a)	50–100(b)
2	0–40(e)	40–100(b)	
3	0–5(a)	5–50(c)	50–100(b)
4	0–5(a)	5–100(d)	

The initial values for K_{sat}, the decay parameter f and effective soil thickness used in the TOPOG_SBM model runs, are presented in Table 5.1. As will be discussed in Section 5.4.1, the depth of the hydrologically active layer of the soil had to be adjusted considerably to provide optimal results.

Interception and transpiration losses

Instead of using the built-in interception loss routine of TOPOG, the model was fed with actually measured net precipitation data. For the sub-daily (5-min time steps) runs the available 5-min throughfall records plus an additional average stemflow fraction of 2.3 % of gross precipitation [*Scatena*, 1990b] were used [see *Schellekens et al.*, 1999, Chapter 3] whereas the 5-min totals were summed to daily amounts for use in the runs with a daily time step. Transpiration (E_t) was only taken into account in the runs with a daily time step, but was neglected in the runs for individual storms using a 5-min time step because TOPOG is presently not capable of computing E_t over sub-daily intervals. The effect of omitting E_t in the simulations of stormflow response is believed to be small, however, because transpiration is known to cease when the canopy is wetted [*Rutter*, 1967]. Transpiration in TOPOG is calculated according to the Penman-Monteith equation [*Monteith*, 1965, equation 2.9 in Chapter 2]. Further information on losses via transpiration in Bisley has been given by *Schellekens et al.* [2000] (Chapter 2).

5.4 MODEL RESULTS

5.4.1 THREE-MONTH PERIOD USING DAILY TIME STEPS

An 81-day period (from 24 April until 13 July 1996) was modelled with the TOPOG_SBM and the TOPOG_DYNAMIC models using a daily time step. Initially, a total soil thickness of 100 cm was used for all soil types in the TOPOG_SBM model runs, combined with the soil properties listed in Table 5.1. However, the hydrograph generated by the model showed little resemblance to the observed hydrograph: predicted peak discharges were too low (about 1/10th of the observed values) and flow during dry periods was too high. This 'compression' of the hydrograph indicates that the TOPOG_SBM model overestimated the amounts of water stored in the soil. After decreasing the effective soil depth from 100 cm to 20–40 cm (depending on soil type; Table 5.1), a much closer fit to the measured hydrograph was obtained (Fig. 5.3). At the same time the decay parameter f for the hillslope soil (unit 2 in Table 5.1) was adjusted to generate a nearly uniform conductivity layer. The reduced values for the soil thickness in combination with the adjusted decay parameter effectively mirror the depth of the uppermost, highly conductive, soil horizon where the macropores are concentrated [*Schellekens et al.*, submitted]. The rationale for these optimizations is discussed in Section 5.5. The model efficiency according to the criteria of *Nash and Sutcliffe* [1970] was 0.943, whereas the mean absolute error between measured and modelled daily discharges was 1.39 mm. The per-

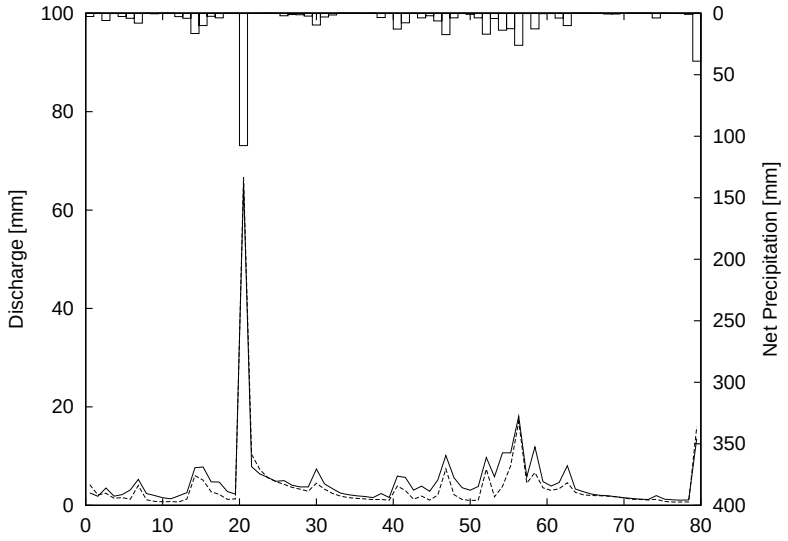

Figure 5.3: Discharge as predicted by the TOPOG_SBM model (solid line) compared to measured discharge (dashed line) for the 81-day period between 24 April and 13 July 1996. Scale for net precipitation (throughfall plus stemflow in $mm\,d^{-1}$), given on the right-hand y-axis. The x-axis shows days since the start of the model run.

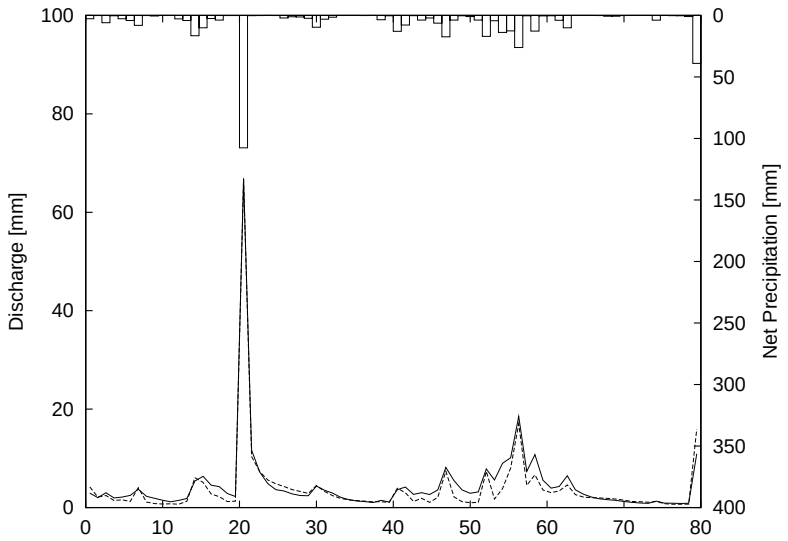

Figure 5.4: Discharge as predicted by the TOPOG_DYNAMIC model (solid line) compared to measured discharge (dashed line) for the 81-day period between 24 April and 13 July 1996. Scale for net precipitation (throughfall plus stemflow in $mm\,d^{-1}$), given on the right-hand y-axis. The x-axis shows days since the start of the model run.

centage of the catchment that was predicted to be saturated during this period varied from 9 % (valley bottoms only) to 76 % during the very large storm of day 20. On average 19 % of the catchment was predicted to be saturated, a very high value. Saturation overland flow was predicted to occur in all valley bottom elements during all days, a phenomenon that is to be expected as TOPOG has no notion of channel flow and discharge from the catchment can only occur if the element(s) at the catchment outlet are (partly) saturated. In addition, occurrence of overland flow was also predicted for some hillslope elements in the southern (steepest) part of the catchment.

The runs with the TOPOG_DYNAMIC model did not need the adjustments for soil profile thickness that had to be made with the TOPOG_SBM model, most probably because the TOPOG_DYNAMIC model allows the generation of a perched water table. The modelled hydrograph depicted in Fig. 5.4 was obtained using the *Broadbridge and White* parameters listed in Table 5.3 and Table 5.2. The modelling efficiency of the discharges predicted with TOPOG_DYNAMIC according to the method of *Nash and Sutcliffe* [1970] is 0.964, and the mean absolute error between measured and modelled daily discharges 1.03 mm. During the large storm on day 20 the model predicted that up to 52 % of the catchment was saturated while the minimum value during the overall period was 7 %. The predicted average catchment saturation percentage was 11 %. Predicted occurrence of saturation overland flow was again restricted to the valley bottom elements and a few elements in the steep southern part of the catchment. On the whole, the predicted occurrence of overland flow was less than in the TOPOG_SBM model runs. A perched water table was predicted to occur most of the time over a considerable part of the catchment.

5.4.2 HYDROGRAPH CHARACTERISTICS FOR 16 SELECTED STORM EVENTS

Amounts of net precipitation for 16 storms selected for use in the modelling exercise ranged from 3 to 78 mm whereas the associated streamflow totals ranged from 0.7 mm to 63.8 mm (Table 5.4). Average net precipitation intensity of all storms was 0.25 $mm/5\ min$ with an highest overall intensity of 5.4 $mm/5\ min$ (during storm no. 3). The average lag time (defined as the time between the center of gravity of the net precipitation input and the center of gravity of the discharge) for all storms was 114 min, with minimum and maximum values of 55 and 350 min respectively. Most storms were multi-peaked, with only storms 1, 2, 4 and 7 having a well-defined single peak. The parameters used for comparing modelled and measure discharge records were derived from points with an absolute slope greater than 0.05 $mm/5\ min$ to avoid biased results due to exceptionally long recession limbs. An estimated value for the Manning roughness coefficient (n) of 0.3 was used throughout the modelling. Initial moisture conditions were equal for all storms and derived from the runs with a daily time step.

Table 5.4: Basic characteristics of 16 storm events selected for modelling. P_{net} is the amount of net precipitation (TF + SF), Q the total discharge, I the average intensity of P_{net} for periods with rain, Q_{start} the discharge at the start of the storm, Q_{end} the discharge at the end of the storm, Q_{max} the maximum discharge during the storm, and Lag time the time between the centers of gravity of P_{net} and Q.

No.	P_{net}	Q	I	Q_{start}	Q_{end}	Q_{max}	Lag time
	mm	mm	$mm/5\ min$	mm	mm	$mm/5\ min$	min
1	14.1	5.8	0.15	0.0028	0.0026	0.385	55
2	8.0	4.6	0.09	0.0064	0.0061	0.170	100
3	77.9	63.8	0.83	0.0669	0.0536	2.927	60
4	7.4	2.6	0.19	0.0094	0.0091	0.095	70
5	12.6	3.1	0.28	0.0041	0.0043	0.193	55
6	6.4	2.2	0.13	0.0039	0.0036	0.089	100
7	5.2	1.2	0.37	0.0041	0.0094	0.034	120
8	20.1	6.6	0.47	0.0043	0.0043	0.178	150
9	2.9	1.0	0.29	0.0070	0.0067	0.025	95
10	24.5	6.7	0.29	0.0028	0.0034	0.285	60
11	25.5	10.5	0.13	0.0043	0.0043	0.148	350
12	27.2	15.0	0.33	0.0088	0.0107	0.489	70
13	9.0	4.3	0.21	0.0151	0.0151	0.080	80
14	5.0	2.7	0.06	0.0101	0.0104	0.029	155
15	7.0	2.7	0.12	0.0101	0.0097	0.119	75
16	4.2	0.7	0.13	0.0039	0.0056	0.009	235

Table 5.5: Basic hydrograph characteristics of 16 selected storm events predicted by the TOPOG_SBM model. Q is the modelled total discharge, Q_{max} is the maximum discharge during the storm, Q_{start} the discharge at the start of the storm, Q_{end} the discharge at the end of the storm and Lag time the time between the centers of gravity of P_{net} and Q. The last two columns show model efficiency [*sensu Nash and Sutcliffe*, 1970] and the mean absolute error between measured and modelled discharges.

No.	Q	Q_{max}	Q_{start}	Q_{end}	Lag time	modeff.	$\overline{abs.err.}$
	mm	$mm/5\ min$	$mm/5\ min$	$mm/5\ min$	min		$mm/5\ min$
1	4.3	0.1590	0.0067	0.0100	50	0.6136	0.0200
2	3.2	0.0728	0.0067	0.0070	165	0.5312	0.0095
3	44.9	1.6671	0.0067	0.0090	105	0.6929	0.1371
4	2.1	0.0647	0.0067	0.0068	70	0.8392	0.0057
5	3.4	0.1392	0.0067	0.0082	55	0.8048	0.0111
6	2.0	0.0543	0.0067	0.0077	130	0.8377	0.0040
7	1.6	0.0518	0.0067	0.0444	100	0.0629	0.0047
8	6.8	0.1769	0.0067	0.0069	225	0.8216	0.0085
9	1.1	0.0342	0.0067	0.0072	65	0.1320	0.0029
10	8.9	0.2837	0.0067	0.0201	60	0.9196	0.0117
11	11.7	0.1603	0.0067	0.0069	400	0.7677	0.0071
12	9.7	0.2364	0.0067	0.0122	105	0.5945	0.0357
13	3.0	0.0559	0.0067	0.0142	75	0.4701	0.0086
14	2.5	0.0280	0.0067	0.0114	125	0.7341	0.0018
15	2.1	0.0721	0.0067	0.0074	75	0.8113	0.0051
16	1.5	0.0337	0.0067	0.0333	225	-43.5367	0.0073

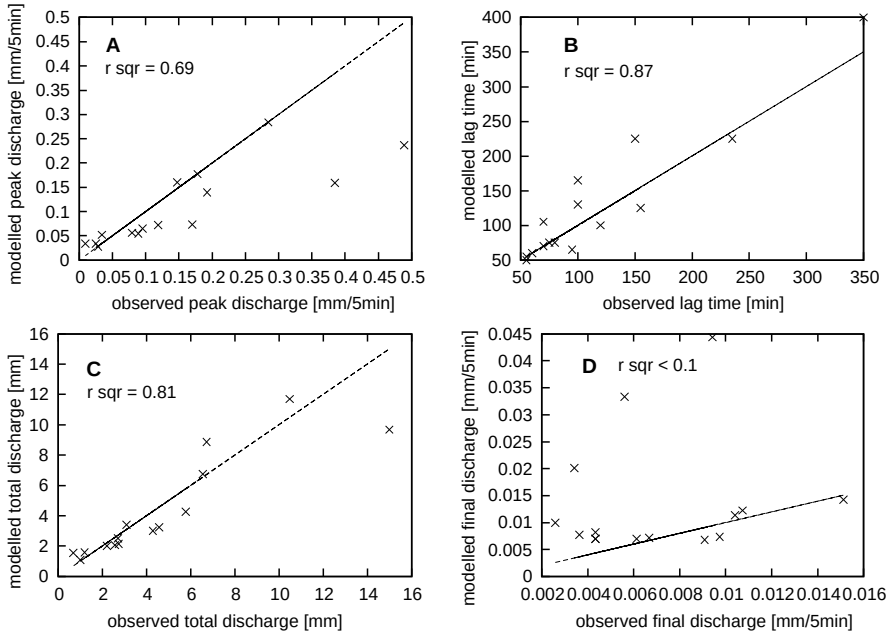

Figure 5.5: Measured and predicted hydrograph parameters for selected storms according to the TOPOG_SBM model runs. To facilitate comparison of the results with those obtained with TOPOG_DYNAMIC (Fig. 5.7) values for the (extreme) event no. 3 have been omitted from the graphs. The r^2 values shown were calculated without event no. 3 as well.

5.4.3 HYDROGRAPH PREDICTIONS BY THE TOPOG_SBM MODEL

The results of the hydrograph predictions obtained with the TOPOG_SBM model are presented in different ways: *(i)* The various hydrograph characteristics predicted for the 16 storms are summarized in Table 5.5 together with the associated efficiency values [sensu *Nash and Sutcliffe*, 1970] and the mean absolute error between measured and modelled discharge for each storm (see Fig. 5.5 for a graphical representation of the latter); *(ii)* Measured and modelled hydrographs with contrasting rainfall patterns for six storms are depicted in Fig. 5.6. Model efficiencies for individual storms ranged from 0.9 (a good fit) to values < 0.20 (poor fit) or even a negative value (*e.g.* storm no. 16). Interestingly, the mean absolute difference between measured and modelled runoff is not clearly related to the model efficiency parameter. Further inspection of Table 5.5 shows that the poorest results (in model efficiency terms) generally pertain to very small storms (*e.g.* storm nos. 7, 9 and 16), for which the mean absolute difference is inherently small. In Fig. 5.5 values of selected hydrograph characteristics as predicted by TOPOG_SBM are compared with observed values for all but the largest storm (no. 3). Although modelled and measured peak discharges

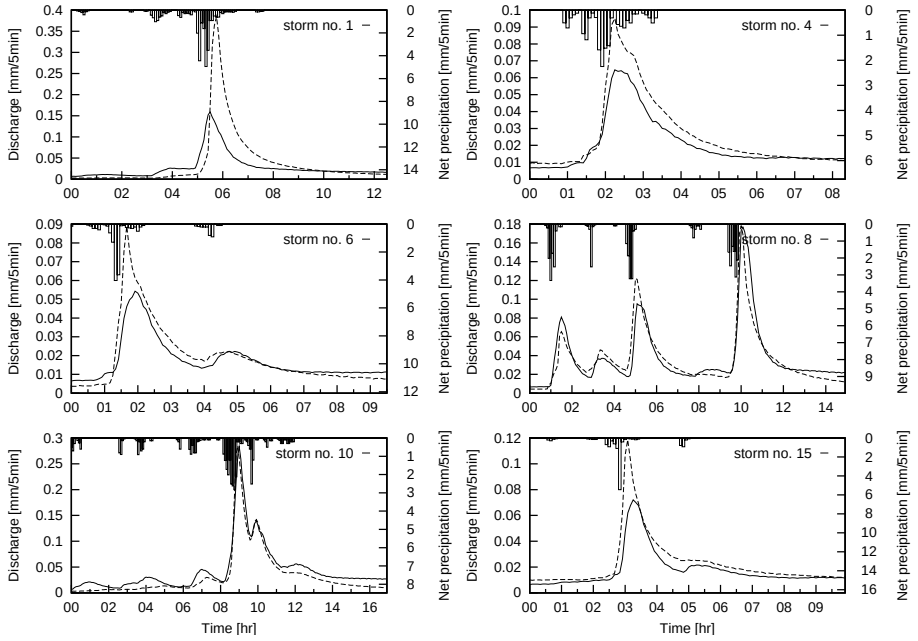

Figure 5.6: Measured and TOPOG_SBM modelled hydrographs for 6 selected storms of contrasting magnitude and rainfall patterns. Measured discharges are indicated by the dashed lines while modelled discharges are indicated by the solid lines. Storm numbers shown in the upper right-hand corner of each panel correspond to those in Table 5.4.

were correlated fairly well (r^2 = 0.69 for $n = 15$ storms and 0.98 for $n = 16$ when event no. 3 is included), modelled maximum discharges were generally underestimated whereas they were significantly overestimated for the smallest storms (Fig. 5.5A). Lag times were also predicted adequately with r^2 values of 0.874 and 0.886 with and without the large storm respectively (Fig. 5.5B). Total discharge is also predicted rather well, possibly because measured amounts of net precipitation were used as an input to the model. Values of r^2 ranged from 0.815 ($n = 15$, excluding extreme event no. 3) to 0.982 ($n = 16$, including no. 3). However, as shown in Fig. 5.5D, discharge at the end of the storm is often poorly predicted in the model, with observed values being grossly over-predicted for about 50 % of the storms ($r^2 < 0.1$). Furthermore, it is evident from Fig. 5.6 that the slope of the modelled streamflow recession during the last stages of a storm is generally too flat, yielding the observed over-prediction of the discharge at the end of the storm. This phenomenon will be investigated further in the discussion section.

Table 5.6: Basic hydrograph characteristics of 16 selected storm events predicted by the TOPOG_DYNAMIC model. Q is the modelled total discharge, Q_{max} is the maximum discharge during the storm, Q_{start} the discharge at the start of the storm, Q_{end} the discharge at the end of the storm and Lag time the time between the centers of gravity of P_{net} and Q. The last two columns show model efficiency [*sensu Nash and Sutcliffe*, 1970] and the mean absolute error between measured and modelled discharges. Storm no. 3 not included (see text for explanation).

no.	Q	Q_{max}	Q_{start}	Q_{end}	Lag time	modeff.	$\overline{abs.err.}$
	mm	$mm/5\ min$	$mm/5\ min$	$mm/5\ min$	min		$mm/5\ min$
1	5.1	0.1930	0.0095	0.0128	50	0.7486	0.0182
2	4.1	0.0838	0.0094	0.0100	170	0.6340	0.0097
3	–	–	–	–	–	–	–
4	2.6	0.0745	0.0094	0.0096	80	0.9284	0.0033
5	4.1	0.1702	0.0092	0.0110	55	0.8694	0.0119
6	2.6	0.0594	0.0092	0.0107	145	0.8015	0.0053
7	2.0	0.0560	0.0094	0.0513	120	-0.7375	0.0089
8	7.7	0.1971	0.0094	0.0099	185	0.8385	0.0080
9	1.4	0.0373	0.0094	0.0101	75	-0.4389	0.0045
10	9.7	0.3059	0.0094	0.0217	50	0.8411	0.0159
11	12.2	0.1376	0.0094	0.0099	320	0.8492	0.0069
12	10.6	0.2723	0.0094	0.0148	85	0.6792	0.0303
13	3.7	0.0630	0.0094	0.0168	80	0.8405	0.0042
14	3.3	0.0321	0.0094	0.0141	150	0.3276	0.0028
15	2.7	0.0802	0.0092	0.0104	85	0.8788	0.0027
16	2.0	0.0372	0.0094	0.0353	235	-84.0150	0.0114

5.4.4 HYDROGRAPH PREDICTIONS OF THE TOPOG_DYNAMIC MODEL

Generally, the results obtained with the TOPOG_DYNAMIC model were very similar to those for the much simpler TOPOG_SBM model, with one major exception, however: event no. 3 caused TOPOG_DYNAMIC to crash. The severe numerical instability that was caused by the combination of the high net precipitation intensities (up to 65 $mm\ hr^{-1}$) that occurred during this major storm and a clayey soil that rapidly became saturated during the process resulting in very high mass balance errors while solving the Richards equation. Predicted discharges even became zero during the peak of the storm and remained that low until the end of the simulation. Consequently, the results shown below do not include the results obtained for event no. 3. The similarity in results obtained with the TOPOG_DYNAMIC (Table 5.6) and the TOPOG_SBM (Table 5.5) models becomes particularly evident when comparing Figures 5.7 and 5.5. Once again, model efficiencies for predictions of discharge totals during the 15 (16 minus no. 3) storms varied considerably, with generally slightly better efficiencies in the case of TOPOG_DYNAMIC for all but the smallest storms, for which the TOPOG_DYNAMIC model performed even worse than the TOPOG_SBM model (*cf.* Table 5.6 *vs.* Table 5.5). Q_{max} was again underestimated, except for the smallest storms (again overestimated). The overall correlations between predicted and observed peak discharge ($n = 15$) was better for TOPOG_DYNAMIC than for TOPOG_SBM ($r^2 = 0.769$ *vs.* $r^2 = 0.689$, respectively) whereas performance by the two models was virtually identical with respect to

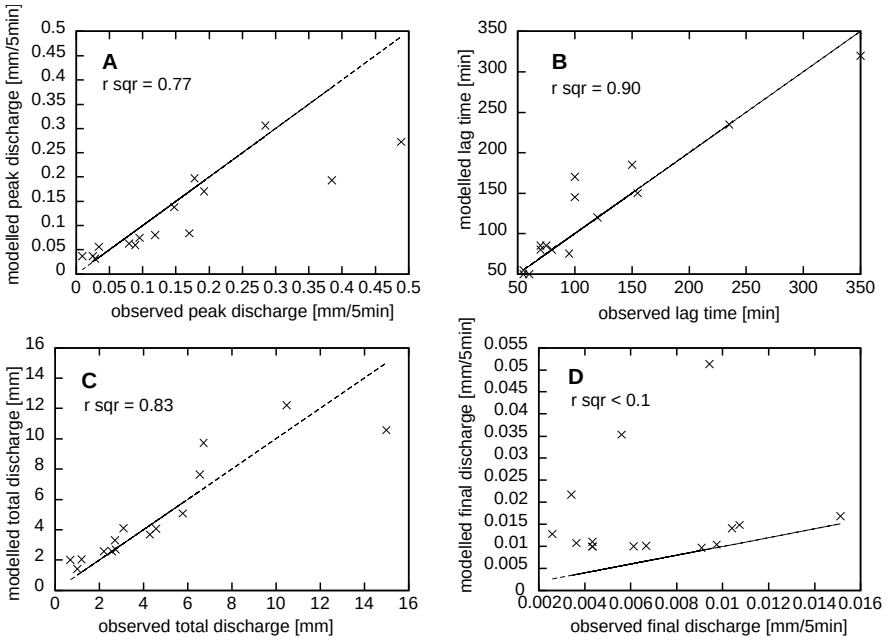

Figure 5.7: Measured and predicted hydrograph parameters for selected storms according to the TOPOG_DYNAMIC model runs. The run for storm event no. 3 has been omitted (see text for explanation)

the estimate of lag time ($r^2 = 0.899$ *vs.* $r^2 = 0.886$, respectively). Total discharge was again predicted rather well by TOPOG_DYNAMIC ($r^2 = 0.827$ *vs.* $r^2 = 0.815$ for TOPOG_SBM) and Q_{end} equally poorly ($r^2 < 0.10$ in both cases). The slightly higher r^2 values obtained with the TOPOG_DYNAMIC model may in part be related to the use of the marginally different initial conditions as these could not be made completely identical for the two models due to the intrinsic differences in their design. Despite the slightly better overall performance of TOPOG_DYNAMIC the predicted hydrograph recessions were again, too flat (Fig. 5.8).

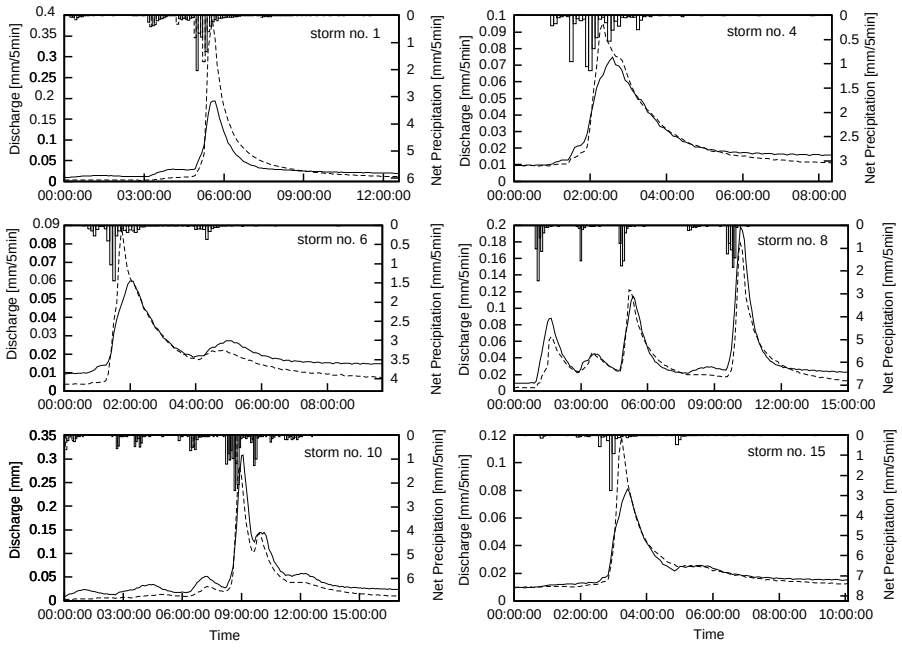

Figure 5.8: Measured and TOPOG_DYNAMIC modelled hydrographs for 6 selected storms of contrasting magnitude and rainfall patterns. Measured discharges are indicated by the dashed lines while modelled discharges are indicated by the solid lines. Storm numbers shown in the upper right-hand corner of each panel correspond to those in Table 5.4.

5.5 DISCUSSION AND CONCLUSIONS

The two versions of the TOPOG model described and applied here each use a different approach to model the behaviour of a catchment. While the TOPOG_SBM model is relatively easily parameterized (for a distributed model) the TOPOG_DYNAMIC model allows for the inclusion of a wider variety of flow types, although this is achieved at the cost of a big appetite for data as well as high computational requirements. Considering that the present application marks the first published attempt to use the TOPOG model in a maritime humid tropical steepland setting, the present results are encouraging.

The steep topography necessitated a considerable amount of smoothing of the basic topographic information that was used to build the digital elevation model before the latter could be converted to the contour-based element network used by TOPOG. The difference in size of the modelled catchment (6.7 ha) compared to that used in previous studies (6.4 ha) at Bisley may be attributable to a combination of this smoothing and the discrepancy between the manual estimation of a catchment boundary and the algorithm used in TOPOG_DEMGEN to define the water divide [*Dawes and Short*, 1994]. The largest elements in a TOPOG network are found in the flattest parts of the catchment (*e.g.* valley bottoms and ridgetops, *cf.* Fig. 5.1). As the valley zones are often very active hydrologically [*Dunne*, 1978; *Ward*, 1984] this particular feature of TOPOG tends to cause an overestimation of the extend of saturation within a catchment.

Schellekens et al. [submitted] (Chapter 4) demonstrated that a considerable part of the stormflow in the Bisley II catchment is conveyed by macro-pores in the top 20 cm of the soil profile (*cf.* Table 4.1). Their contention was based on hydrometrical and hydrochemical evidence, complemented by one-dimensional soil water calculations. At present there is no concept of macropore flow in TOPOG and some of the problems that have been encountered in this paper and other applications of the model [*e.g. Vertessy and Elsenbeer*, 1999] to predict catchment rainfall response can be attributed to this shortcoming. *Vertessy and Elsenbeer* [1999] suggested that 'macropore flow' algorithms similar to those described by *Bronstert and Plate* [1997] could be incorporated in the TOPOG modelling framework fairly easily and this might improve the model's currently rather poor predictions of the hydrograph recessions.

When parameterizing the TOPOG_SBM model it became clear that the initially imposed soil thickness (1 m) gave entirely unrealistic results and that only the use of a much reduced effective soil depth (down to 25 cm on the hillslopes) produced a more faithful simulation of the observed hydrographs (Fig. 5.6). As the TOPOG_SBM model only allows lateral flow out of the saturated part of elements and as these elements can only be saturated from the bottom upwards (*i.e.* there is no concept of a perched water table), lateral flow in the early stages of a storm will only occur from those elements that are already saturated. For elements situated midway on a hillslope flow can only occur after the water has percolated down to the bottom of the element. Naturally, given the low values of K_{sat} below 50 cm at Bisley (Table 4.1), this would

take a long time, with severe underestimation of peak discharges and overestimation of low flows as a result. As shown in Fig. 5.6 the present remedy of imposing a thin soil on the sideslopes better mimics the inferred combination of fast lateral flow through macropores and slower matrix flow for the Bisley catchment although this does not necessarily imply an exact representation of the actual processes taking place on the hillslope. Similarly, after encountering similar problems of underestimation of peak flows and poor prediction of hydrograph recessions when applying the TOPOG_SBM model to a microcatchment in the western Amazon, *Vertessy and Elsenbeer* [1999] suggested that model performance could not only be enhanced by adding a 'fast' subsurface flow pathway (pipe flow) to the model but also by modifying the hydraulic conductivity *vs.* depth function.

Although the TOPOG_DYNAMIC model presently also lacks the notion of macropore flow it does have certain properties that help to produce better results under the conditions prevailing in the study area. Its soil moisture accounting scheme allows saturation at the base of the thin, highly conductive, top layer without the need to first saturate the rest of the profile from the bottom up. This development of a perched water table at shallow depth introduces the potential for a fast lateral path similar to macropore flow. At the same time, the use of the highly non-linear Richards equation in TOPOG_DYNAMIC to represent soil water dynamics generates its own problems, notably in terms of numerical stability. Numerical stability comes at a price: in this case the Van Genuchten type moisture retention curves had to be abandoned to allow TOPOG_DYNAMIC to function at all. Even the use of approximate *Broadbridge and White* curves — which are smoother and should thus afford better numerical stability [*Beverly*, 1994] — posed many problems when fitted to the measured soil water retention curves and they had to be adjusted to represent more 'general' curves for clayey soils. It is evident that this must have an effect on the outcome of the model calculations. However, it is not possible to oversee the exact extent due to the various complex interactions within the model itself. At least, the problems with numerical stability encountered in the present application defy the purpose of obtaining reliable runoff predictions using a complex model that can be fed with field measurements. In addition, it is clear that the lack of a macropore flow routine in TOPOG leads to an overestimation of saturation overland flow (*SOF*) either by complete saturation of the entire soil profile (in the TOPOG_SBM model) or by the generation of a perched water table (in the TOPOG_DYNAMIC model).

Both models were able to predict the measured hydrographs for certain storms rather well while the performance for other storms was poor (see Tables 5.5 and 5.6). In addition, the occurrence of numerical instability prevented the TOPOG_DYNAMIC model from completing the run for storm no. 3 which delivered large amounts of high intensity precipitation. Overall, the present application highlights two clear shortcomings in the predictions of both models: *(i)* the serious overestimation of baseflow recession; and *(ii)* the overestimation of runoff for small events. As to the first problem, when run at subdaily time steps, the TOPOG model does not take transpiration losses into ac-

count. Considering that the average E_t rate at Bisley of 2.2 $mm\,d^{-1}$ [*Schellekens et al.*, 2000, Chapter 2] would account for a steepening of the recession curve by 0.008 $mm/5\ min$ it becomes clear that the neglect of soil water uptake shortly after rainfall has ceased may well go some way towards explaining a large part of the discrepancy between predicted and measured recessions in the later parts of the hydrograph. As such, the addition of a transpiration component to the sub-daily model might significantly improve the performance of the model for a large part of the recession curve, especially under tropical conditions [with their relatively high transpiration rates, *Bruijnzeel*, 1990]. As to the second problem, a number of reasons can be given for the overestimation of runoff associated with small events. For one, the TOPOG concept does not include channel flow. For storm runoff to occur the valley bottom elements must be saturated. Due to their shallow slope the valley bottom elements tend to be rather large in a TOPOG element network. This can easily lead to an overestimation of the extent of local saturation which, in turn, will cause an overestimation of storm runoff volumes due to the amounts of SOF predicted for these valley bottom elements. The effect is most notable during small events when overall stormflow volumes are low. Initial soil moisture conditions in the model runs were kept identical for all storms. Inspecting the actual pre-storm runoff rates (Q_{start}) listed in Table 5.4 it is evident that initial moisture conditions were not the same for all storms. As pointed out by *Grayson et al.* [1992], the initial moisture status of a catchment can be one of the most important parameters determining its runoff response.

Although only weak correlations were found to exist at Bisley between various hydrograph parameters and antecedent moisture conditions [*Schellekens et al.*, submitted, Chapter 4], the latter deserve some further consideration in the present context. If it is accepted that pre-storm runoff rate is a good integrator of overall moisture conditions at the beginning of a storm, the importance of having the model runs start with the actually observed pre-storm discharge becomes self-evident. However, the estimation of Q_{start} using TOPOG_DYNAMIC presents problems in that discharges often vary during the day whereas longer-term applications of TOPOG normally use a daily time step. Ideally the incorporation of flexible time steps (*e.g.* from daily to subdaily steps and back) in the model would greatly facilitate the representation of initial conditions, even making continuous runs possible, thereby rendering the laborious and subjective generation of initial conditions unnecessary [*Vertessy and Elsenbeer*, 1999; *Zhu et al.*, 1999]. The following approach was followed in the present study: the soil moisture conditions of day no. 76 of the long-term series using daily time steps was used as a starting point from which the catchment was allowed to drain while imposing an average daily transpiration loss of 2.2 $mm\,d^{-1}$ [*Schellekens et al.*, 2000]. Next, the values of observed pre-storm discharges listed in Table 5.4 (except storm no. 3 for reasons given previously) were matched to computed daily values and the corresponding moisture distributions used as a starting point for the simulations using the 5-min time step. Re-running the TOPOG_DYNAMIC simulation for all 15 events with the adjusted initial conditions gave a significant improvement for the small storms

Table 5.7: Basic hydrograph characteristics of 16 selected storm events as predicted by the TOPOG_DYNAMIC model. In these runs initial conditions were adjusted to fit measured discharge at the beginning of the storms. Q is the modelled discharge, Q_{max} the maximum discharge in the storm, Q_{start} the discharge at the start of the storm, Q_{end} the discharge at the end of the storm and Lag time the time between the centers of gravity of P_{net} and Q. The last two columns show model efficiency [*sensu Nash and Sutcliffe*, 1970] and the mean absolute error between measured and modelled discharges.

no.	Q	Q_{max}	Q_{start}	Q_{end}	lag time	modeff.	$abs.err.$
	mm	$mm/5\ min$	$mm/5\ min$	$mm/5\ min$	min		$mm/5\ min$
1	3.3	0.1090	0.0044	0.0065	65	0.4635	0.0204
2	4.1	0.0751	0.0082	0.0087	210	0.5849	0.0101
3	–	–	–	–	–	–	–
4	2.5	0.0679	0.0082	0.0085	90	0.8814	0.0046
5	3.2	0.1139	0.0053	0.0067	65	0.8198	0.0103
6	1.8	0.0400	0.0053	0.0064	160	0.6287	0.0055
7	1.4	0.0405	0.0055	0.0339	125	0.6653	0.0035
8	6.5	0.1777	0.0055	0.0058	255	0.8708	0.0079
9	0.9	0.0244	0.0055	0.0060	75	0.6588	0.0022
10	8.6	0.2681	0.0055	0.0138	70	0.8753	0.0120
11	10.8	0.1314	0.0055	0.0058	395	0.8396	0.0060
12	12.3	0.3294	0.0082	0.0129	105	0.7949	0.0211
13	4.7	0.0832	0.0127	0.0211	75	0.8758	0.0040
14	3.2	0.0304	0.0082	0.0124	175	0.5213	0.0024
15	2.6	0.0713	0.0080	0.0091	105	0.8300	0.0038
16	0.9	0.0177	0.0035	0.0163	235	-4.6176	0.0022

(*e.g.*. nos. 7, 9 and 16), but no improvement for the larger storms (Table 5.7). Given the limited storage capacity of the catchment, the limited influence of initial soil water conditions on the runoff response of large events does not come as a surprise. Moreover, antecedent moisture conditions do not vary too much under the rainfall regime prevailing in the study area [*cf. Schellekens et al.*, 2000].

The present results underline the importance of a good conceptual understanding of a catchment's behaviour before undertaking a hydrological modelling exercise [*cf. Vertessy and Elsenbeer*, 1999]. When using a physically-based model to predict the effects of disturbance to a catchment this becomes even more important. It is sobering to realize that the availability of a substantial amount of data alone is not necessarily enough. Recently, *Vertessy and Elsenbeer* [1999] applied the TOPOG_SBM model to a very small (0.75 ha) fast-responding lowland rain forest catchment in the Amazonian part of Peru for which an extensive dataset was available on spatial variability of K_{sat} [*Elsenbeer et al.*, 1992] and overland flow occurrence [*Elsenbeer and Lack*, 1996], as well as on runoff chemistry [*Elsenbeer et al.*, 1995a]. The model generally predicted the right amount of storm runoff but usually underpredicted peak discharges and overpredicted the lag time. Moreover, the 'best' parameterization could only predict credible hydrographs for about half of the 34 studied events whereas 'significant, and sometimes gross errors' were encountered for about one fourth of the modelled events [*Vertessy and Elsenbeer*, 1999]. It was concluded that model

performance could be enhanced by adding a 'fast' subsurface flow pathway (pipe flow) to the model or by modifying the hydraulic conductivity *vs.* depth function. The ability of the TOPOG modelling system to adequately predict the runoff behaviour for the Peruvian micro-catchment is thus seen to be limited despite the availability of a comprehensive dataset on the spatial variability of soil hydraulic conductivity and a good conceptual understanding of the workings of the catchment based on extensive hydrochemical evidence [*Elsenbeer et al.*, 1995b; *Elsenbeer and Lack*, 1996].

Although the present study can not boast such a comprehensive dataset as the Peruvian study, it essentially encountered similar problems (underestimation of peak discharges, overestimation of hydrograph recession) Moreover, serious numerical instability occurred in the present application of TOPOG_DYNAMIC when using Van Genuchten-type curves to represent soil water retention and $K(\theta)$ relationships. Future work at Bisley will focus on the quantification of rapid subsurface flow through macropores and its return to the surface in tributary gullies [*cf. Schellekens et al.*, submitted, Chapter 4] and the use of isotopes to characterize the different flow components [*McDonnell*, 1990].

5.6 ACKNOWLEDGEMENT

The effort taken by L. A. (Sampurno) Bruijnzeel to improve the quality and readability of this paper is gratefully acknowledged. In addition, I wish to thank Rob Vertessy and Richard Silberstein and Maarten Waterloo for answering my TOPOG questions and the VUA IT department, notably Gerard Kok, for keeping up with my appetite for CPU cycles.

6

SUMMARY OF RESEARCH RESULTS AND IMPLICATIONS FOR FUTURE WORK

6.1 BACKGROUND

Continued and indiscriminate clearing of the world's tropical forests and the associated deterioration of soil and water quality due to erosion and pollution threaten the supply of high quality drinking water in many areas in the face of often explosively growing populations and increasing per capita demands for water. The possibility of gradually less dependable precipitation inputs in some areas and an increasing frequency of devastating hurricanes and floods due to 'global change' in others may well aggravate the problem. To evaluate the hydrological effects of tropical forest disturbance and conversion to other land uses, first a sound understanding of the hydrological functioning of tropical forests is required [*cf. Bruijnzeel*, 1990, 2000a; *Bonell and Balek*, 1993; *Gash et al.*, 1996]. Traditionally, paired catchment experiments have been used to evaluate the effects of disturbances. However, apart from being time-consuming, this approach is unable to evaluate the relative importance of various factors that might underly differences in results between sites, severely limiting the possibilities for extrapolation of such results to other areas or periods. Practical catchment/forest management questions generally have a spatial dimension attached and most landscapes consist of a complex mosaic of different land uses and covers. Physically-based distributed hydrological models are capable of taking into account spatial variations in topography, soils, vegetation and climate. As such, they are being increasingly used instead of the paired catchment approach to study the effects of disturbances to a catchment [*Vertessy and Elsenbeer*, 1999; *Zhu et al.*, 1999] notwithstanding the large data demand of these models [*Abbott et al.*, 1986b].

Starting in January 1995, the present study was funded by the International Institute for Tropical Forestry (IITF), Rio Piedras, Puerto Rico and the Faculty of Earth Sciences, Vrije Universiteit Amsterdam, The Netherlands. The objectives of the study were: *(i)* to describe and quantify the chief hydrological processes (rainfall interception, transpiration and runoff generation) operating in the rain forested Bisley II catchment under the wet maritime tropical con-

ditions prevailing in eastern Puerto Rico; and *(ii)* to test the performance of the TOPOG modelling system in this area of frequent, low intensity rainfall and steep topography.

The 6.4 ha Bisley II catchment is located at an elevation of 265–456 m in the Luquillo Experimental Forest (LEF), eastern Puerto Rico. The area is steep and dissected. It is located in so-called Tabonuco forest which is a rain forest with an irregularly shaped, 20–25 m high upper canopy. The climate is maritime tropical (type A2m according to the Köppen classification), with an annual rainfall — that is distributed fairly evenly throughout the year — of about 3500 mm. Soils are clayey and have developed in thick-bedded tuffaceous sandstones and indurated siltstones.

6.2 SUMMARY OF RESEARCH RESULTS

6.2.1 RAINFALL INTERCEPTION, TRANSPIRATION AND TOTAL EVAPORATION

As a first step, evaporation losses were determined using complementary hydrological and micrometeorological techniques during 1996 and 1997 (Chapter 2). Evapotranspiration (ET) of the forest as determined with the catchment water balance technique was found to be exceptionally high at 2420 $mm\,yr^{-1}$ (6.6 $mm\,d^{-1}$) for 1996 and 2179 $mm\,yr^{-1}$ (6.0 $mm\,d^{-1}$) for 1997. A break-down into the chief components that make up ET shows that rainfall interception (E_i) accounted for much (62–74 %) of the ET at 1788 $mm\,yr^{-1}$ (4.9 $mm\,d^{-1}$) in 1996 and 1364 $mm\,yr^{-1}$ (3.7 $mm\,d^{-1}$) in 1997. This interception loss was computed as the difference between incident rainfall as measured above the canopy and net rainfall (throughfall plus stemflow) using an average stemflow fraction of 2.3 % [*Scatena*, 1990b]. On the other hand, transpiration (E_t), as determined with the Penman-Monteith equation, was modest at 817 $mm\,yr^{-1}$ (2.3 $mm\,d^{-1}$) and 858 $mm\,yr^{-1}$ (2.4 $mm\,d^{-1}$) in 1996 and 1997, respectively. Both estimates compared reasonably well with the water-budget based estimates (ET – E_i) of 632 $mm\,yr^{-1}$ (1.7 $mm\,d^{-1}$) and 815 $mm\,yr^{-1}$ (2.2 $mm\,d^{-1}$). Interestingly, inferred rates of wet canopy evaporation were roughly four to five times those predicted by the Penman-Monteith equation, with night-time rates being very similar to day-time rates, suggesting radiant energy is not the dominant controlling factor. Rainfall interception at Bisley is thus seen to be exceptionally high at 49 and 39 % of incident precipitation for 1996 and 1997, respectively. Several factors are believed to be responsible for these observations, including: *(i)* the frequent occurrence of rainstorms of low intensity associated with frontal activity; *(ii)* a highly effective net upward transport of evaporated moisture from the wetted canopy driven by the release of heat upon condensation; probably aided by: *(iii)* the proximity of the site to the warm waters of the Atlantic Ocean which may act as a source of advected energy brought in by the tradewinds; and *(iv)* a comparatively low aerodynamic resistance due to the broken-up character of the forest as a result of previous hurricane damage and (possibly) its location in highly dissected terrain. One consequence of the above is the fact that the Penman-Monteith evaporation model failed to predict

the observed high values for E_i unless the value of r_a was reduced to 2.1 $s\,m^{-1}$, a very low value.

Having found that rainfall interception by the canopy is the main cause of the very high ET losses from the Bisley catchment, the underlying processes were investigated further in an interception modelling study (Chapter 3). A total of 66 days of detailed throughfall and above-canopy climatic data were collected in May–July 1996 and analyzed using the Rutter and Gash models of rainfall interception. Measured interception loss during this period was 50 % of gross precipitation. When Penman-Monteith based estimates of wet canopy evaporation rates (0.11 $mm\,hr^{-1}$ on average) and a canopy storage of 1.15 mm were used, both models severely underestimated measured interception loss. A detailed analysis of four storms of contrasting magnitude using the Rutter model showed that optimizing the model for the wet canopy evaporation component yielded much better results than increasing the canopy storage capacity (as has been proposed by some). Thus, these findings support the idea that it is primarily a high rate of evaporation from a wet canopy that is responsible for the high interception losses observed under these wet maritime tropical conditions. Combining this with the 'low to normal' values for transpiration results in very high values for total evapotranspiration (ET). Comparison of the present results with those obtained for other tropical island and continental edge locations leads to the interesting conclusion that such high ET losses may well be a distinct feature of near-coastal locations, both in the tropics and in the temperate zone (Fig. 2.10).

The results also underline the contention of *Shuttleworth* [1989] that, compared to mid-continental sites, tropical deforestation is likely to have the greatest effect on river flow at continental edge and island locations. Assuming that deforested land is converted to agriculture or grassland, transpiration from these lands will remain in the same order of magnitude [*Bruijnzeel*, 1990; *Calder*, 1998]. Consequently, the change in interception loss will determine the bulk of the changes in water yield after deforestation. Accepting this, high interception sites (such as the maritime tropical forest studied here) can be expected to show the largest changes in water yield upon deforestation.

6.2.2 RUNOFF GENERATION

Various complementary techniques were used to investigate the stormflow generation process at Bisley (Chapter 4). A total of 102 samples was taken of soil matrix water, macropore flow, streamflow and precipitation during two storms of contrasting magnitude for the analysis of Ca, Mg, Si, K, Na and Cl. These were combined with hydrometric information on streamflow, return flow, precipitation, throughfall and soil moisture to distinguish water following different flow paths. Geoelectric sounding was used to survey the subsurface structure of the catchment revealing a weathering front that coincided with the elevation of the stream channel rather than run parallel to surface topography. The hydrometric data were used in combination with soil physical data (notably hydraulic conductivity and soil water retention curves), a

one-dimensional hydrological model (VAMPS) and a three-component chemical mass balance mixing model to describe the stormflow response of the catchment. It was found that most stormflow traveled through macropores in the top 20 cm of the soil profile. During large events saturation overland flow in the riparian zone also accounted for a considerable portion of the stormflow although it was not possible to fully quantify the associated volumes. No evidence was found for Hortonian overland flow. The mixing model results point to return flow from macropores (as measured in a tributary gully) as the main contributor to quick runoff. Additional hydrometric evidence (such as the very similar response to rainfall of runoff discharging from the tributary gully and the main stream) supported this contention. The rapid decay of saturated hydraulic conductivity with depth clearly allows only small quantities of water to percolate to the deeper parts of the soil profile. The combination of the above and the (very) steep topography in parts of the catchment favours rapid lateral flow through the uppermost soil horizon (sub-surface stormflow, $SSSF$). However, saturation overland flow (SOF) including precipitation onto already saturated areas, may also account for a significant portion of the quickflow at Bisley, especially during large events occurring in wet periods.

Although the runoff generation picture at Bisley is not entirely complete yet, the present description does allow a brief analysis of the effect of catchment disturbance on the flow regime. As described previously, the effect of tropical deforestation on river flow at continental edge and island locations is thought to be relatively large and mirror the observed high interception losses. As such, any disturbance that decreases the forest's potential for rainfall interception will increase the amount of precipitation reaching the forest floor and thus the amount of quickflow. At the same time, as the catchment will probably become wetter as well, the amount of SOF (both relative and absolute) may increase as a result. The picture becomes more complicated when also taking into account disturbances of the soil. The present results show that the high conductivity of the topsoil is a result of the presence of abundant macropores in this part of the soil. The underlying subsoil and saprolite, however, have a very low conductivity. If the conductivity of the topsoil would be reduced due to compaction or if increased erosion (as a result of a larger SOF contribution to quickflow for example) would expose the lower parts of the soil to the surface, than a considerable increase in surface runoff may be expected, as a result of which the effect will be strengthened further due to the positive feedback. In addition, as soil material with significantly lower hydraulic conductivities becomes exposed, the introduction of infiltration-excess overland flow during high intensity storms seems plausible as well.

6.2.3 RUNOFF MODELLING

In an attempt to model the stormflow and water yield of the catchment, the performance of two versions of the TOPOG model was tested: *(i)* the TOPOG_SBM model that uses a simplified bucket model for soil water accounting and *(ii)* the more elaborate TOPOG_DYNAMIC model that solves the Richards equation for

unsaturated flow (Chapter 5). Both versions of the model were run to simulate streamflow patterns during the three-month period in 1996 for which detailed throughfall and above-canopy weather data were available, using daily time steps and for 16 storm events of different magnitude (3 – 78 mm of net precipitation) occurring during this period using 5-min time steps. Both models simulated observed discharge patterns for the three-month period satisfactorily (model efficiencies [*sensu Nash and Sutcliffe*, 1970] were 0.94 and 0.96 for the TOPOG_SBM and TOPOG_DYNAMIC model, respectively). However, to achieve this in the case of the TOPOG_SBM model the effective thickness of the soil had to be reduced considerably (from 100 to 25 cm). In general, both models also performed adequately upon modelling the 16 individual storm events although the response to small storms (< 5 mm of net precipitation) was systematically overestimated. Also, flows during the later part of the recession curve were significantly overestimated by both models.

The lack of a macropore flow routine – and in the the case of the TOPOG_SBM model also the representation of the soil as a single layer – were shown to be the main shortcomings of the TOPOG model in the present application. As these points could only be addressed because of the insight gained by previous process studies, the present results underline the importance of a good conceptual understanding of a catchment's rainfall-runoff response before undertaking a modelling exercise using a physically-based distributed hydrological model [*cf. Vertessy and Elsenbeer*, 1999]. Indeed, it is sobering to realize that the availability of a substantial amount of data alone may not be enough to properly assess the performance of such a model. On the other hand, the combination of conceptual knowledge and a state-of-the-art modelling framework allows the propagation of process knowledge at the (small) catchment scale and as such represents a tool for further improving our current models. In particular, the TOPOG modelling results supported the contention that rapid flow through macropores is the main contributor to quickflow in the Bisley catchment. In addition, the increased importance of SOF during large events was clearly illustrated by the derived degree of catchment saturation. Better results for the Bisley catchment can probably be obtained if: *(i)* the TOPOG model is equipped with a variable time step allowing it to run continuously for both intra-storm and inter-storm periods, in this way solving the problems encountered with generating initial moisture conditions for each storm, *(ii)* the soil moisture accounting scheme would be adjusted to include the possibility of lateral flow through macropores; and *(iii)* when a multi layered version is used for the TOPOG_SBM model.

Physically-based distributed parameter models such as TOPOG are often seen as suitable tools to evaluate the results of disturbances to a catchment and are beginning to be used more extensively for this purpose [*Vertessy et al.*, 1993, 1996]. The present results, however, suggest that such models should preferably be used when a good conceptual picture of the primary processes that determine catchment runoff response is available. In the case of the Bisley catchment it has been demonstrated that the catchment water yield can be simulated satisfactorily using daily time steps with interception losses deter-

mined using the analytical model [*Gash*, 1979; *Gash et al.*, 1995] and transpiration using the Penman-Monteith formula. As such, one may be confident that the effects of a subsequently imposed scenario of change (*e.g.* forest disturbance by hurricane or clearing for pasture) on water yield will be properly represented in the model's predictions. On a sub-daily basis, however, this is much less certain. Although the lack of the macropore flow component did not prevent a satisfactory representation of measured storm hydrographs for the present conditions, the lack of this flow type might well have a major impact on the simulation results for future disturbance scenarios.

6.3 IMPLICATIONS FOR FUTURE RESEARCH (AT BISLEY)

Future research in the area should and will focus on the nature of the actual mechanism(s) responsible for maintaining the high rates of rainfall interception at Bisley. To resolve this issue, insight needs to be gained in the forest energy budget along the entire elevational gradient in the Luquillo Experimental Forest (*i.e.* including lateral transfer of heat and moisture) in combination with the use of a meso-scale meteorological model [*e.g.* RAMS; *Pielke et al.*, 1992]. Knowledge of the latter would also allow an evaluation of the elevational dynamics of cloud condensation along the mountain as a function of the hydrological processes lower down on the mountain. This would also help to better understand the hydrological functioning of the cloud forest zone higher up the mountain and evaluate to what extent the magnitude of cloud water stripping by this forest will be affected by changes in the level of the cloud base. A study combining the water budget of the forest along the elevational gradient with meso-scale meteorological modelling is scheduled to start later in the year 2000 [*Vugts and Bruijnzeel*, 1999]. Particular attention should also be paid to attempts at direct determination of wet canopy evaporation rates; for example, by direct measurement of the amount of water stored on the canopy during and shortly after storms by weighing (parts of) trees [*cf. Tsukamoto and Ishigaki*, 1989] or using micro-wave radiation [*cf. Bouten et al.*, 1991].

The quantification of rapid subsurface flow through macropores and its return to the surface in tributary gullies should be the focus of future work on stormflow generation at Bisley. In addition, the spatial and temporal extent of saturation overland flow needs to be investigated further. As such, the use of isotopes to characterize the different flow components [*McDonnell*, 1990; *Brammer and McDonnell*, 1996] is recommended, preferably in combination with chemical tracers (*cf.* Chapter 4) and a thorough hydrometrical study. This should include tensiometry and time domain reflectometry (TDR) to study soil water content and the use of throughflow troughs [*Dunne*, 1978] and overland flow detectors [*Elsenbeer and Cassel*, 1990] to capture and quantify subsurface stormflow and overland flow, respectively.

Using the improved (quantitative) insight in the runoff processes in Bisley, an adjusted version of the TOPOG model that includes macropore flow should be tested in both the TOPOG_DYNAMIC and TOPOG_SBM (including an extended

two-layer version) incarnations. Quantitative data on $SSSF$ through macropores and SOF as well as soil moisture (via TDR) may be used to examine the performance of the model in detail. In addition, a flexible time step version of the model can be used to run the entire period in one continuous run, thereby removing the need for the (subjective) process of generating initial soil moisture conditions for each storm. Given Moore's law (first formulated in 1965 by G. Moore and adjusted later) stating that the amount of storage that a microchip can hold doubles every year or at least every 18 months, and applying it to CPU speed, TOPOG_DYNAMIC will probably run fast enough for such a version to be viable by the time the model will be adjusted.

7

SAMENVATTING

7.1 ACHTERGROND

Als gevolg van voortdurend en ondoordacht kappen van het regenwoud in grote delen van de tropen is de kwaliteit van de bodem en het water in die gebieden sterk achteruitgegaan. Met name de achteruitgang van de waterkwaliteit door erosie en vervuiling vormt een bedreiging voor de toevoer van schoon drinkwater in deze gebieden, terwijl de vraag groeit door een groter gebruik per hoofd van de bevolking in combinatie met een explosieve bevolkingsgroei. Bovendien bestaat er de mogelijkheid dat de hoeveelheid neerslag vermindert en de frequentie van tropische stormen toeneemt door wereldwijde klimaat veranderingen, wat de geschetste problemen danig zou kunnen verergeren. Om de hydrologische effecten van verstoring van het regenwoud en omzetten naar een ander landgebruik te voorspellen zullen allereerst de belangrijkste hydrologische processen in het tropisch regenwoud goed begrepen moeten worden [*cf. Bruijnzeel*, 1990, 2000a; *Bonell and Balek*, 1993; *Gash et al.*, 1996]. Lange tijd was het gebruik van twee stroomgebieden — waarbij het ene ongestoord bleef en het andere een bepaalde verstoring onderging — de enige manier om het effect van verstoringen op een stroomgebied te evalueren (de zgn. 'paired catchment' benadering). Deze methode kost niet alleen veel tijd, maar bovendien is het zo ook niet mogelijk een goed inzicht te krijgen in de factoren die de afwijkende resultaten van verschillende studies bepalen. Hierdoor is extrapolatie van resultaten van één situatie naar een andere niet goed mogelijk.

Vraagstukken rond het beheer van stroomgebieden zijn vaak van ruimtelijke aard. Bovendien bestaan de gebieden vaak uit een scala van verschillende landgebruiken en bedekkingen. De nieuwste generatie stroomgebiedsmodellen kan ruimtelijke variatie in bodem, vegetatie en klimaat in aanmerking nemen. Deze modellen worden daarom steeds vaker gebruikt, als vervanger van de 'paired catchment' benadering, bij onderzoek naar de effecten van verstoringen in een stroomgebied [*Vertessy and Elsenbeer*, 1999; *Zhu et al.*, 1999]. Dergelijke modellen vergen echter veel invoergegevens om waardevolle resultaten te kunnen leveren [*Abbott et al.*, 1986b].

Het in dit proefschrift gepresenteerde onderzoek startte in Januari 1995, met financiële ondersteuning van het International Institute for Tropical Forestry (IITF), in Rio Piedras, Puerto Rico en de Faculteit der Aardwetenschappen van de Vrije Universiteit, in Amsterdam. Als belangrijkste onderzoeksdoelen werden geformuleerd:

1. het beschrijven en quantificeren van de belangrijkste hydrologische processen (zoals de interceptie van neerslag, transpiratie en het afvoergedrag van het stroomgebied), zoals die zich voordoen in het tropisch regenwoud van het Bisley II stroomgebied;

2. het testen van het TOPOG modelleersysteem in dit gebied met, dat gekenmerkt wordt door frequente neerslag en zeer steile topografie.

Het Bisley II stroomgebied (6,4 ha) bevind zich tussen 265 en 456 m boven zeenivo in het Luquillo Experimental Forest (LEF) in het noordoosten van Puerto Rico. Het is een steil gebied met sterk ingesneden dalen. Het gebied is bedekt met Tabonuco bos (genoemd naar de dominante boomsoort), een type tropisch regenwoud dat 20 to 25 m hoog is met een grillig gevormd bladerdak. Het klimaat is maritiem tropisch (type A2m volgens de Köppen classificatie), met een jaarlijkse neerslag van ongeveer 3500 mm. Er is geen duidelijk droog seizoen. De bodems zijn zeer kleirijk en gevormd in onderliggende vulkanische zand- en siltstenen.

7.2 SAMENVATTING VAN DE ONDERZOEKSRESULTATEN

7.2.1 NEERSLAGINTERCEPTIE, TRANSPIRATIE EN TOTALE VERDAMPING

Een combinatie van hydrologische en micrometeorologische technieken werd gebruikt om de evapotranspiratieverliezen van het stroomgebied te bepalen voor de jaren 1996 en 1997 (Hoofdstuk 2). De hoeveelheid evapotranspiratie (ET), bepaald d.m.v. een water balans voor het stroomgebied, was erg hoog, te weten 2420 $mm\,jr^{-1}$ (6,6 $mm\,d^{-1}$) in 1996 en 2179 $mm\,jr^{-1}$ (6,0 $mm\,d^{-1}$) in 1997. De bijdrage van belangrijkste componenten va ET in ogenschouw nemende blijkt dat interceptie van neerslag (E_i) het grootste aandeel (62–74 %) in het totaal heeft, met 1788 $mm\,jr^{-1}$ (4,9 $mm\,d^{-1}$) in 1996 en 1364 $mm\,jr^{-1}$ (3,7 $mm\,d^{-1}$) in 1997. In dit geval werd het interceptieverlies berekend als het verschil tussen de hoeveelheid neerslag gemeten boven het bladerdak en de hoeveelheid doorval en stamafvoer die de bosbodem bereikte (ook wel netto neerslag genoemd), waarbij de hoeveelheid stamafvoer werd bepaald via een fractie van de totale neerslag [2,3 % *Scatena*, 1990b]. De hoeveelheid transpiratie (E_t), bepaald met behulp van de Penman-Monteith vergelijking, was bescheiden in vergelijking tot de hoeveelheid interceptie met 817 $mm\,jr^{-1}$ (2,3 $mm\,d^{-1}$) in 1996 en 858 $mm\,jr^{-1}$ (2,4 $mm\,d^{-1}$) in 1997. Beide bepalingen kwamen goed overeen met de op de waterbalans gebaseerde schatting van E_t (ET minus E_i). Deze bedroegen 632 $mm\,jr^{-1}$ (1.7 $mm\,d^{-1}$) in 1996 en 815 $mm\,jr^{-1}$ (2,2 $mm\,d^{-1}$) in 1997. Het bleek dat de verdamping van het natte bladerdak, wanneer deze bepaald werd uit het gemeten interceptieverlies, vier to vijf maal hoger uitviel dan wanneer deze via de Penman-Montieth vergelijking werd bepaald. Tevens bleek dat de interceptieverliezen gedurende de nacht niet significant lager waren dan overdag, hetgeen suggereert dat stralingsenergie niet de meest bepalende factor voor de hoeveelheid interceptie

is. De interceptie van neerslag in het gebied was zeer hoog (49 en 39 % van de totale neerslag) tijdens 1996 en 1997. Verschillende oorzaken kunnen hieraan ten grondslag liggen, zoals: *(i)* de lage intensiteit van de (zeer frequente) neerslag; *(ii)* een zeer effectief verticaal transport van vocht, afkomstig van het natte bladerdak en gevoed door het vrijkomen van warmte bij condensatie; waarschijnlijk geholpen door *(iii)* de nabijheid van de (warme) Atlantische oceaan, die als een bron van door de passaatwinden aangevoerde advectieve energie kan fungeren en *(iv)* een relatief lage aërodynamische weerstand van het bos, door haar ligging op een steile topografie en de grillige vorm van het bladerdak als gevolg van schade door vroegere orkanen. Een belangrijk gevolg was de onderschatting van de hoge interceptieverliezen door de Penman-Monteith vergelijking, tenzij de waarde van de aërodynamische weerstand (r_a) gereduceerd werd tot 2,1 $s\,m^{-1}$, hetgeen een zeer lage waarde is.

Na de conclusie dat de hoge ET-verliezen in het Bisley stroomgebied het gevolg zijn van een zeer grote neerslaginterceptie-component, werden de processen die hieraan ten grondslag liggen verder onderzocht in een studie waarbij het neerslaginterceptie-proces modelmatig werd nagebootst (Hoofdstuk 3). Gedetailleerde metingen van doorval door het bladerdak en klimaatsgegevens boven het bladerdak werden verzameld gedurende een periode van 66 dagen (Mei – Juli 1996). Vervolgens werden deze gegevens verwerkt in de modellen van neerslaginterceptie zoals geformuleerd door [*Rutter et al.*, 1971] en [*Gash*, 1979]. Het gemeten interceptieverlies tijdens deze periode bedroeg 50 % van de neerslag. Beide modellen onderschatte het gemeten interceptieverlies aanzienlijk wanneer de volgens de Penman-Monteith formule berekende verdampingssnelheid van het natte bladerdak werd gebruikt (0,11 $mm\,u^{-1}$) in combinatie met een bergingscapaciteit van het bladerdak van 1,15 mm. En gedetailleerde analyse van vier buien van verschillende grootte met behulp van het Rutter model onthulde dat een optimalisatie van de verdampingssnelheid van het natte bladerdak betere resultaten opleverde dan het vergroten van de bergingscapaciteit van het bladerdak. Deze resultaten ondersteunen de hypothese dat de hoge interceptieverliezen in de natte maritieme tropen voornamelijk worden veroorzaakt door een hoge verdampingssnelheid van het natte bladerdak. In combinatie met de 'normale' hoeveelheid transpiratie verklaart dit de hoge waarde voor totale evapotranspiratie (ET). Een vergelijking van de huidige resultaten met die van andere studies op tropische eilanden of kustnabije locaties leidt tot de interessante conclusie dat zulke hoge ET verliezen waarschijnlijk een karakteristiek zijn van dergelijke locaties, zowel in de tropen als in de gematigde zone (Fig. 2.10).

De resultaten bevestigen ook de door *Shuttleworth* [1989] geopperde suggestie dat kappen van het tropisch regenwoud, in vergelijking to continentale locaties, een groter effect heeft op rivierafvoeren heeft op eiland- en kustnabije locaties. Als we aannemen dat het vrijgekomen land wordt gebruikt als landbouwgrond of grasland, dan kunnen we stellen dat de transpiratie component van deze stukken land in de zelfde orde van grootte blijft. Dientengevolge is de verandering in de hoeveelheid neerslaginterceptie de belangrijkste oorzaak van de verandering in totale rivierafvoer na ontbossing. Locaties met hoge in-

terceptieverliezen (zoals het hier bestudeerde maritieme tropisch regenwoud) zullen daardoor de grootste veranderingen in rivierafvoer vertonen na ontbossing.

7.2.2 HET AFVOERPROCES IN HET BISLEY II STROOMGEBIED

Een combinatie van verschillende technieken werd gebruikt om het afvoerproces in het Bisley-stroomgebied tijdens buien te bestuderen (Hoofdstuk 4). Monsters (102 in totaal) van bodemvocht, water in macroporiën in de bodem, beekafvoer en neerslag werden genomen om de concentraties van de elementen Ca, Mg, Si, K, Na en Cl te bepalen. Voor twee buien van verschillende grootte werden deze gegevens gecombineerd met hydrometrische metingen aan beekafvoer, exfiltrerend grondwater, neerslag, doorval en bodemvocht om de verschillende paden waarlangs het water zich een weg naar de bedding van de beek baant te bepalen. Geo-electrische metingen werden uitgevoerd om de ondergrondse structuur van het stroomgebied in kaart te brengen. Hieruit bleek dat het verweringsfront parallel met de bedding van de beek loopt en in mindere mate de topografie volgt. De hydrometrische gegevens werden gecombineerd met bodemgegevens, een één dimensionaal hydrologisch model (VAMPS) en een (drie-componenten tellende) chemisch massabalans mengmodel om afvoer tijdens buien te beschrijven. Het blijkt dat het grootste deel van het water dat tot snelle afvoer komt, door de bovenste 20 cm van het bodemprofiel stroomt via zgn. macroporiën. Tijdens erg grote buien maakt oppervlakkige afvoer over verzadigde delen van de bodem een groot deel van de snelle afvoer uit. Deze hoeveelheden konden echter niet gekwantificeerd worden. Voor oppervlakkige afvoer als gevolg van een overschrijding van de infiltratiecapaciteit van de bodem is geen bewijs gevonden. De resultaten van het mengmodel laten zien dat exfiltrerend water uit macroporiën de belangrijkste component van de snelle afvoer is. Verder hydrometrisch bewijs ondersteunt deze conclusie. De verzadigde hydraulische doorlatendheid van de bodem neemt snel af met de diepte, waardoor slechts kleine hoeveelheden water verticaal naar de diepere delen van het bodemprofiel kunnen percoleren. In combinatie met de steile topografie van het gebied, heeft dit tot gevolg dat laterale stroming in de bovenste delen van het bodemprofiel overheerst in dit gebied. Niettemin blijft de exacte grootte van snelle afvoer als gevolg van neerslag op reeds verzadigde bodems onbekend, terwijl deze tijdens grote buien een belangrijk deel van de snelle afvoer uit kan maken.

Hoewel de beschrijving het proces van snelle afvoer in het Bisley stroomgebied nog niet geheel compleet was, is het wel mogelijk een korte analyse te geven van de gevolgen van verstoringen in het stroomgebied op het afvoerregime. Zoals eerder beschreven, is het waarschijnlijk dat ontbossing op tropische eilanden en kustnabije locaties, als gevolg van de hoge interceptieverliezen, grotere gevolgen heeft voor het afvoerregime van rivieren dan in continentale gebieden. Elke verstoring die de neerslaginterceptie van het bos vermindert (zoals de beschadiging van het bladerdak door orkanen) zal tot gevolg hebben dat meer neerslag de bosbodem kan bereiken. Daardoor zal de ho-

eveelheid (snelle) afvoer toenemen. Doordat meer water de bosbodem bereikt zal deze natter worden, hetgeen tot gevolg heeft dat de hoeveelheid snelle afvoer over verzadigde bodems toe zal nemen, zowel in absolute als relatieve zin. Wanneer ook verstoringen aan de bodem in aanmerking worden genomen wordt één en ander gecompliceerder. De grote hydraulische doorlatendheid van de bovenste bodemlaag is het gevolg van macroporiën in die laag. De onderliggende bodem en verweerde zone bevatten deze macroporiën niet en hebben een zeer lage doorlatendheid. Als nu de doorlatendheid van de bovenste bodemlaag gereduceerd zou worden door compactie, of door erosie weg zou spoelen of dunner word, dan kan een sterke toename van oppervlakkige afvoer over verzadigde bodems worden verwacht. Omdat door een toegenomen hoeveelheid oppervlakkige afvoer de erosie ook toe zal nemen, zal het effect steeds sterker worden (positieve terugkoppeling). Tevens is het denkbaar dat oppervlakkige afvoer doordat de neerslag intensiteit de infiltratiecapaciteit overschrijdt, nu ook op zal treden doordat de verweerde zone (met een lage doorlatendheid) aan het oppervlakte komt.

7.2.3 HET MODELLEREN VAN DE RIVIERAFVOER

Twee verschillende versies van het TOPOG-model zijn getest in een poging het afvoerregime van het Bisley-II-stroomgebied te modelleren voor zowel afzonderlijke buien (tot enkele dagen in lengte) als langere perioden (tot drie maanden). Het TOPOG_SBM-model gebruikt een simpel 'leeglopend reservoir'-model om het bodemvocht te simuleren terwijl het TOPOG_DYNAMIC-model de Richards vergelijking voor onverzadigde stroming oplost (Hoofdstuk 5). Beide modellen werden eerst gebruikt om het afvoerpatroon tijdens een periode van drie maanden in 1996 te simuleren. Voor deze periode waren gedetailleerde metingen van klimaat, doorval en afvoer beschikbaar. Tevens werden de modellen getest met 16 buien van verschillende grootte in deze periode, waarbij gebruik gemaakt werd van tijdstappen van 5-min. Beide modellen waren in staat om de gemeten afvoerpatronen voor de periode van drie maanden goed te voorspellen: de model-efficiëntie [volgens *Nash and Sutcliffe*, 1970] was 0.94 voor het TOPOG_SBM model en 0.96 voor het TOPOG_DYNAMIC model). In het geval van het TOPOG_SBM model was het echter nodig om de effectieve dikte van het bodemprofiel terug te brengen van 100 naar 25 cm. Over het algemeen waren beide modellen ook in staat de afvoercurves voor de 16 buien met redelijke nauwkeurigheid te voorspellen, hoewel de hoeveelheid afvoer voor kleine buien (< 5 mm netto-neerslag) systematisch werd overschat. Tevens werd de hoeveelheid afvoer tijdens het laatste deel van de buien (de recessie) overschat door beide modellen.

Geen van beide modellen gebruikt een routine die de stroming door zgn. macroporiën in de bodem beschrijft en dit blijkt voor de huidige toepassing één van de belangrijkste tekortkomingen. In het geval ven het TOPOG_SBM model komt daar nog bij dat bodem als een enkele laag wordt voorgesteld, waardoor het optreden van oppervlakkige afstroming over verzadigde bodems niet goed wordt gesimuleerd. Het feit dat deze tekortkomingen alleen konden

worden gesignaleerd aan de hand van de resultaten van het voorafgaande procesonderzoek in het stroomgebied, laat zien dat het van groot belang is een goed conceptueel begrip te hebben van de belangrijkste processen in een stroomgebied alvorens dergelijke modellen toe te passen [*cf. Vertessy and Elsenbeer*, 1999]. Enerzijds is het ontnuchterend te moeten concluderen dat een grote hoeveelheid data alléén niet genoeg is om het functioneren van een model te evalueren. Anderzijds is het juist de combinatie van nieuw ontwikkelde modellen en goede conceptuele kennis op stroomgebiedsschaal dé manier om de huidige modellen te verbeteren. Als voorbeeld kan worden genoemd dat juist de huidige resultaten met het TOPOG model (waarin macroporiën niet voorkomen) de veronderstelling dat snelle stroming door macroporiën een zeer belangrijk deel van de snelle afvoer veroorzaakt, hebben onderbouwd. Ook is het belang van snelle afvoer over verzadigde bodems tijdens grote buien duidelijk aangetoond. De volgende mogelijkheden worden gesuggereerd om het gebruikte TOPOG-model beter te laten functioneren wanneer toegepast op het Bisley-II-stroomgebied:

- het gebruik van variabele tijdstappen, zodat het model een doorlopende tijdreeks kan simuleren en daarmee de problemen met het genereren van initiële vochtcondities voor de afzonderlijke buien kan voorkomen;

- een aanpassing van het bodemvocht-model zodat stroming door macroporiën ook kan worden gesimuleerd;

- het ontwikkelen van een versie van het TOPOG_SBM model dat meerdere bodemlagen beschrijft.

Modellen zoals TOPOG worden vaak gezien als goede hulpmiddelen om de gevolgen van verstoringen in stroomgebieden te evalueren, en worden steeds vaker gebruikt voor dit doel [*Vertessy et al.*, 1993, 1996]. De resultaten van het huidige onderzoek laten echter zien dat het gebruik van dit soort modellen onderbouwd moet worden met een grondige kennis van de belangrijkste processen die de afvoergedrag in het te modelleren stroomgebied bepalen. Het is aangetoond dat de hoeveelheid afvoer uit het Bisley-stroomgebied op dagbasis goed kan worden voorspeld, indien voor de bepaling van neerslagintercepte het analytische model [*Gash*, 1979; *Gash et al.*, 1995] wordt gebruikt in combinatie met de Penman-Monteith vergelijking voor de bepaling van transpiratieverliezen. In dat geval kan er op vertrouwd worden dat de effecten van een verstoringsscenario (b.v. verstoring van het bos door een orkaan of kappen voor omzetting naar landbouwgrond) worden beschreven door het model. Echter, dit vertrouwen is er niet op een kleinere tijdschaal. Hoewel het model ook zonder de gesimuleerde stroming van water door macroporiën de gemeten afvoer goed kan voorspellen, is het mogelijk dat het weglaten van deze vorm van snelle afvoer in het model een groot effect heeft op de resultaten van verstoringsscenarios.

7.2.4 IMPLICATIES VOOR TOEKOMSTIG ONDERZOEK IN HET GEBIED

Het mechanisme dat de de hoge neerslaginterceptie in Bisley mogelijk maakt zal één van de speerpunten van toekomstig onderzoek in het gebied (moeten) worden. Om dit vraagstuk op te kunnen lossen dient de energiebalans van het bos over het gehele hoogtebereik van het Luquillo Experimental Forest te worden bestudeerd, inclusief het laterale transport van warmte en vocht. Een koppeling met een meso-schaal meteorologisch model [b.v. RAMS; *Pielke et al.*, 1992] maakt het misschien mogelijk om de hoogte van de wolkenbasis in relatie tot de hydrologische processen lager op de berg te bestuderen. Op deze wijze kan een beter inzicht worden verkregen in het hydrologisch functioneren van de mistbos-zone boven op de berg, alsmede een evaluatie van de afhankelijkheid tussen de hoeveelheid mistinvang en veranderingen van de hoogte van de wolkenbasis. Een onderzoek dat de waterbalans van het bos langs het gehele hoogtebereik van het LEF bestudeerd in combinatie met een meso-schaal meteorologisch model is onlangs opgestart [*Vugts and Bruijnzeel*, 1999]. Verder dient ook aandacht te worden besteed aan de bepaling van de verdampingsflux van het natte bladerdak (tijdens en vlak na buien), bijvoorbeeld door het direct meten van de hoeveelheid water opgeslagen op het bladerdak gedurende die periodes door middel van het wegen van (delen van) bomen [*cf. Tsukamoto and Ishigaki*, 1989] of met behulp van straling in het microgolf-bereik [*cf. Bouten et al.*, 1991].

Toekomstig werk betreffende de snelle afvoer van water uit het stroomgebied dient zich te richten op de snelle laterale stroming van water door macroporiën in het bovenste gedeelte van het bodemprofiel en de vraag hoe dit water via geulen (na geëxfiltreerd te zijn) naar het afvoerkanaal stroomt. Tevens dient het voorkomen (in plaats en tijd) van oppervlakkige afstroming over verzadigde bodems verder onderzocht te worden. Daarbij zou het gebruik van isotopen om de verschillende componenten te karakteriseren [*McDonnell*, 1990; *Brammer and McDonnell*, 1996] een belangrijke rol kunnen spelen, vooral in combinatie met chemische tracers (zoals beschreven in Hoofdstuk 4) en een grondige hydrometrische studie. Het gebruik van tensiometers en 'time domain reflectometry' (TDR) om bodemvocht te monitoren, in combinatie met detectoren van oppervlakkige afstroming [*Elsenbeer and Cassel*, 1990] en laterale stroming door de bodem [*Dunne*, 1978] is daarbij noodzakelijk.

Gebruik makende van de verworven kennis van het afvoerproces in het Bisley-stroomgebied, zou een verbeterde versie van het TOPOG-model kunnen worden toegepast. Een dergelijke versie, die dan eveneens de stroming door macroporiën in de bodem dient te beschrijven, zou zowel in de TOPOG_SBM als de TOPOG_DYNAMIC versie moeten worden getest. Gegevens over laterale snelle afvoer door macroporiën en over verzadigde bodems, alsmede bodemvochtmetingen zouden gebruikt kunnen worden om het functioneren van het model in detail te testen. Een versie van het TOPOG-model met flexibele tijdstappen zou het toelaten de gehele periode als een continue reeks te modelleren, hiermee het (subjectieve) genereren van de initiële vochtcondities voor ieder bui overbodig makend. Als we de wet van Moore (geformuleerd door

G. Moore in 1965 en later aangepast) in acht nemen — die stelt dat de hoeveelheid schakelingen op een microchip elke 18 maanden verdubbelt — en deze betrekken op de rekensnelheid van de computers waarop het model kan worden gedraait, dan zal het TOPOG_DYNAMIC-model tegen de tijd dat de voorgestelde aanpassing zijn gemaakt, snel genoeg werken om dit ook echt mogelijk te maken.

REFERENCES

Abbott, M. B., J. C. Bathurst, J. A. Cunge, P. E. O'Connell, and J. Rasmussen, An introduction to the European Hydrological System — Système Hydrologique Européen, "SHE", 1: History and philosophy of a physically-based, distributed modelling system, *J. Hydrol.*, *87*, 45–59, 1986a.

Abbott, M. B., J. C. Bathurst, J. A. Cunge, P. E. O'Connell, and J. Rasmussen, An introduction to the European Hydrological System — Système Hydrologique Européen, "SHE", 2: Structure of a physically-based, distributed modelling system, *J. Hydrol.*, *87*, 61–77, 1986b.

Abdul Rahim, N., and K. Baharuddin, Hydrologic regime of dipterocarp forest catchments in Peninsular Malaysia, paper presented at the Universiti Kebangsaan Malaysia Hydrology Workshop, Kota Kinabalu, Sabah, Malaysia, 1986.

Abdul Rahim, N., S. Saifiddin, and Y. Zulkifli, Water balance and hydrological characteristics of forested watersheds in Peninsular Malaysia, in *2nd International Study Conference on GEWEX in Asia and GAME*, pp. 6–10, Pattaya, Thailand, 1995.

Anderson, J. M., and T. Spencer, Carbon, nutrient and water balances of tropical rain forest ecosystems subject to disturbance: management implications and pesearch proposals, *MAB Digest 7*, UNESCO, Paris, 1991.

Asdak, C., P. G. Jarvis, and P. van Gardingen, Evaporation of intercepted precipitation based on an energy balance in unlogged and logged forest areas of Central Kalimantan, Indonesia, *Agric. For. Meteo.*, *92*, 173–180, 1998.

Ataroff, M. S., Importance of cloud-water in Venezuelan Andean cloud forest water dynamics, in *First International Conference on Fog and Fog Collection*, edited by R. S. Schemenauer and H. A. Bridgman, pp. 25–38, IDRC, Ottawa, Canada, 1998.

Bell, T. I. W., Erosion in the Trinidad teak plantations, *Commonwealth Forestry Review*, *52*, 223–233, 1973.

Belmans, C., J. G. Wesseling, and R. A. Feddes, Simulation model of the water balance of a cropped soil: SWATRE, *J. Hydrol.*, *63*, 271–286, 1983.

Beven, K., Spatially distributed modeling: Conceptual approach to runoff prediction, in *Recent Advances in the Modeling of Hydrologic Systems*, edited by D. S. Bowles and P. E. O'Connell, chap. 17, pp. 373–387, Kluwer Academic Publishers, 1991.

Beven, K., and P. Germann, Macropores and water flow in soils, *Water Resour. Res.*, *18*, 1311–1325, 1982.

Beven, K. J., Changing ideas in hydrology – The case of physically-based models, *J. Hydrol.*, *105*, 157–172, 1989.

Beven, K. J., TOPMODEL: a critique, *Hydrol. Proc.*, *11*, 1069–1085, 1997.

Beven, K. J., and M. J. Kirkby, A physically based variable contributing area model of basin hydrology, *Hydrol. Sci. Bull.*, *24*, 43–69, 1979.

Beverly, C. R., Background notes on the CSIRO Topog model. 2. Details of the soil hydraulic models supported in Topog-Soil, *Tech. rep.*, CSIRO Division of Water Resources, Black Mountain, Canberra, Australia, 1994.

Bonell, M., Progress in the understanding of runoff generation dynamics in forests, *J. Hydrol.*, *150*, 217–275, 1993.

Bonell, M., and J. Balek, Recent scientific developments and research needs in hydrological processes of the humid tropics, in *Hydrology and Water Management in the Humid Tropics*, edited by M. Bonell, M. M. Hufschmidt, and J. S. Gladwell, chap. 11, pp. 167–260, UNESCO, Paris, and Cambridge University Press, Cambridge, 1993.

Bonell, M., and J. M. Fritsch, Combining hydrometric-hydrochemistry methods: a challenge for advancing runoff generation process research, in *Proceedings of the Rabat Symposium*, pp. 165–184, IAHS Publ. no 244, 1997.

Bonell, M., and D. A. Gilmour, The development of overland flow in a tropical rainforest catchment, *J. Hydrol.*, *39*, 365–382, 1978.

Bonell, M., D. A. Gilmour, and D. F. Sinclair, Soil hydraulic properties and their effect on surface and subsurface water transfer in a tropical rainforest catchment, *Hydrol. Sci. Bull.*, *26*, 1–18, 1981.

Bonell, M., M. M. Hufschmidt., and J. S. Gladwell, eds., *Hydrology and Water Management in the Humid Tropics*, 1993.

Bosch, J. M., Treatment effects on annual and dry period streamflow at Cathedral Peak, *South African Forestry Journal*, *108*, 29–38, 1979.

Bouten, W., P. J. F. Swarts, and E. De Water, Microwave transmission, a new tool in forest hydrological research, *J. Hydrol.*, *124*, 119–130, 1991.

Brammer, D. D., and J. J. McDonnell, An evolving perceptual model of jillslope flow at the Maimai catchment, in *Advances in Hillslope Processes*, edited by M. G. Anderson and S. M. Brooks, pp. 35–60, J. Wiley, Chichester, 1996.

Broadbridge, P., and I. White, Constant rate rainfall infiltration: a versatile nonlinear model 1. Analytic solution, *Water Resour. Res.*, *23*, 145–154, 1988.

Bronstert, A., and E. J. Plate, Modeling of runoff generation and soil moisture dynamics for hillslopes and micro-catchments, *J. Hydrol.*, *198*, 177–195, 1997.

Brouwer, L. C., Nutrient cycling in pristine and logged tropical rain forest, *Tropenbos Guyana Series 1*, Georgetown, Guyana, 1996.

Brown, A. G., E. K. S. Nambiar, and C. Cossalter, Plantations for the tropics their role, extent and nature., in *Management of Soil, Nutrients and Water in Tropical Plantation Forests*, edited by E. K. S. Nambiar and A. G. Brown, pp. 1–23, ACIAR/CSIRO/CIFOR, Canberra/Bogor, 1997.

Brown, S., A. E. Lugo, S. Silander, and L. Liegel, Research history and opportunities in the Luquillo Experimental Forest, *Gen. Tech. Rep. SO-44*, USDA Forest Service, Southern Forest Experiment Station, New Orleans, Louisiana, USA, 1983.

Bruijnzeel, L. A., evaluation of runoff sources in a forested basin in a wet monsoonal environment: a combines hydrological and hydrochemical approach, pp. 165–174, IAHS Publ. no. 140, 1983a.

Bruijnzeel, L. A., Hydrological and biochemical aspects of man-made forests in South-Central Java, Indonesia, Ph.D. thesis, Faculty of Earth Sciences, Vrije Universiteit, Amsterdam, 1983b.

Bruijnzeel, L. A., Estimates of evaporation in plantations of *Agathis dammara* Warb. in South-Central Java, Indonesia, *J. Trop. For. Sci.*, *1*, 145–161, 1988.

Bruijnzeel, L. A., (de)forestation and dry season flow in the tropics: A closer look, *J. Trop. For. Sci.*, *1*, 229–243, 1989a.

Bruijnzeel, L. A., Nutrient content of bulk precipitation in South-central Java, Indonesia, *J. Trop. Ecol.*, *5*, 000–000, 1989b.

Bruijnzeel, L. A., *Hydrology of Moist Tropical Forests and Effects of Conversion: A State-of Knowledge Review*, Unesco International Hydrological Programme, Paris, 1990.

Bruijnzeel, L. A., Managing tropical forest watersheds for production: Where contradictory theory and practice co-exist, in *Wise Management of Tropical Forests*, edited by F. R. Miller and K. L. Adam, pp. 37–75, Oxford Forestry Institute, Oxford, 1992.

Bruijnzeel, L. A., Land-use and hydrology in warm humid regions: where do we stand?, in *Hydrology of Warm Humid Regions*, edited by J. S. Gladwell, pp. 1–34, IAHS Publ. no. 216, 1993.

Bruijnzeel, L. A., Forest hydrology, in *The Forestry Handbook*, edited by J. Evans, vol. 1, chap. 11, Blackwell Scientific Press, Oxford, 2000a, (in press).

Bruijnzeel, L. A., Tropical forests and water yield, *Iufro task force on forests and water*, IUFRO, Vienna, 2000b, (in press).

Bruijnzeel, L. A., and N. Abdul Rahim, Ecological and environmental services provided by tropical trees and forests, in *Centre for International Forestry Research (CIFOR). Strategic Planning Thematic Papers*, pp. 23–26, ACIAR, Canberra, 1992.

Bruijnzeel, L. A., and F. N. Scatena, Hydrological modeling in a humid tropical island setting: with special reference to the Luquillo Experimental Forest, Puerto Rico, Research proposal, Vrije Universiteit Amsterdam, International Institute for Tropical Forestry, Rio Piedras, 1994.

Bruijnzeel, L. A., and K. F. Wiersum, Rainfall interception by a young *Acacia auriculiformis* (A. Cunn) plantation forest in West Java, Indonesia: Application of Gash's analytical model, *Hydrol. Proc.*, *1*, 309–319, 1987.

Brutsaert, W. H., *Evaporation into the Atmosphere*, D. Reidel Publishing Company, Dordrecht, The Netherlands, 1982.

Burghouts, T. B. A., N. M. van Straalen, and L. A. Bruijnzeel, Spatial heterogeneity of element and litter turnover in a Bornean rain forest, *J. Trop. Ecol.*, *14*, 477–506, 1998.

Calder, I. R., A model of transpiration and interception loss from a spruce forest in Plynlimon, Central Wales, *J. Hydrol.*, *33*, 247–265, 1977.

Calder, I. R., A stochastic model of rainfall interception, *J. Hydrol.*, *89*, 65–71, 1986.

Calder, I. R., *Evaporation in the Uplands*, John Wiley & Sons Ltd., Chichester, UK, 1990.

Calder, I. R., Water use by forests, limits and controls, *Tree Phys.*, *18*, 625–631, 1998.

Calder, I. R., I. R. Wright, and D. Murdiyarso, A study of evaporation from tropical rain forest – West Java, *J. Hydrol.*, *89*, 13–31, 1986.

Cavelier, J., M. Jaramillo, D. Solis, and D. de León, Water balance and nutrient inputs in bulk precipitation in tropical montane cloud forest in Panama, *J. Hydrol.*, *193*, 83–96, 1997.

Chappell, N., Upscaling water and sediment flows in disturbed rainforest mosiacs to the lumped catchment unit, *Final report on nerc project gr3/9439*, Institute of Env. & Natural Sciences, Univ. Lancaster, Lancaster, U.K., 1998.

Clapp, R. B., and G. M. Hornberger, Empirical equations for some soil hydraulic properties, *Water Resour. Res.*, *14*, 601–604, 1978.

Clark, K. L., N. M. Nadkarni, D. Schaeffer, and H. L. Gholz, Atmospheric deposition and net retention of ions by the canopy in a tropical montane forest, Monteverde, Costa Rica, *J. Trop. Ecol.*, *14*, 27–45, 1998.

Clegg, A. G., Rainfall interception in a tropical forest, *Caribbean Forester*, *24*, 1963.

Clements, R. G., and J. A. Colon, The rainfall interception process and mineral cycling in a montane rain forest in eastern Puerto Rico, in *Mineral Cycling in Southeastern Ecosystems*, edited by F. Howell, J. Gentry, and M. Smith, pp. 812–823, US Energy Research and Development Administration, Washington D.C., 1975.

Collinet, J., B. Montény, and B. Pouyaud, Le milieu physique, in *Recherche et Aménagement en Milieu Forestier Tropical Humide: le Projet Taï de Côte d'Ivoire*, Notes Techniques du MAB no. 15, pp. 35–58, UNESCO, Paris, 1984.

Commissie Voor Hydrologisch Onderzoek TNO, Van Penman naar Makkink. Een nieuwe berekeninswijze voor klimatologisch verdampingsgetallen, *Rapporten en Nota's/Commissie voor hydrologisch onderzoek TNO 19*, TNO, 'S-Gravenhage, 1988.

Constantini, A., W. Dawes, E. O'Loughlin, and R. A. Vertessy, Hoop pine plantation management in Queensland. i. gully erosion hazard prediction and watercourse classification, *Australian Journal of Soil and Water Conservation*, *6*, 35–39, 1993.

Davis, J. E., *S-Lang C Programmer's guide*, 1995a.

Davis, J. E., *S-Lang Programmer's guide*, 1995b, version 0.1.

Davis, S. H., R. A. Vertessy, D. L. Dunkerley, and R. G. Main, The influence of scale on the measurement of saturated conductivity in a forest soil, in *23rd Hydrology and Water Resources Symposium*, pp. 103–108, Hobart Australia, 1996.

Dawes, W. R., and D. L. Short, The significance of topology for modelling the surface hydrology of fluvial landscapes, *Water Resour. Res.*, *30*, 1045–1055, 1994.

Dawes, W. R., L. Zhang, T. J. Hatton, P. H. Reece, and G. T. H. Beale, Evaluation of a distributed parameter ecohydrological model (Topog_IRM) on a small cropping rotation catchment, *J. Hydrol.*, *191*, 64–86, 1997.

De Bruin, H. A. R., The energy balance of the earth's surface: a practical approach, Ph.D. thesis, Wageningen Agricultural University, Wageningen, The Netherlands, 1982.

De Bruin, H. A. R., W. Kohsiek, and B. J. J. M. van den Hurk, A verification of some methods to determine the fluxes of momentum, sensible heat, and water vapour using standard deviation and structure parameter of scalar meteorological quantities, *Boundary-Layer Meteo.*, *63*, 231–257, 1993.

DeWalle, D. R., B. R. Swistock, and W. E. Sharpe, Three-component tracer model for stormflow on a small Appalachian forested catchment, *J. Hydrol.*, *104*, 301–310, 1988.

Dietrich, W. E., C. J. Wilson, D. R. Montgomery, J. McKean, and R. Bauer, Erosion tresholds and land surface morphology, *Geology*, *20*, 675–679, 1992.

Douglas, I., and T. Spencer, Prsent-day processes as a key to the effect of environmental change, in *Environmental Change and Tropical Geomorphology*, edited by I. Douglas and T. Spencer, pp. 39–73, Allen and Unwin, London, 1985.

Dunin, F. X., E. M. O'Loughlin, and W. Reyenga, Interception loss from eucalypt forest: lysimeter determination of hourly rates for long term evaluation, *Hydrol. Proc.*, *2*, 315–329, 1988.

Dunne, T., Field studies of hillslope flow processes, in *Hillslope Hydrology*, edited by M. J. Kirkby, pp. 227–293, J. Wiley, 1978.

Dykes, A. P., Rainfall interception from a lowland tropical rainforest in Brunei, *J. Hydrol.*, *200*, 260–279, 1997.

Eaton, J. W., *GNU Octave – A high-level interactive language for numerical computations*, 3rd ed., 1997.

Edmisten, J., Soil studies in the El Verde rain forest, in *A tropical rain forest*, edited by H. T. Odum and R. F. Pidgeon, chap. H-3, pp. H–79–H–86, U.S. Atomic Energy Commission, 1970.

Elsenbeer, H., and D. K. Cassel, Surficial processes in the rainforest of western Amazonia, *IAHS Publication*, *192*, 289–297, 1990.

Elsenbeer, H., and A. Lack, Hydrometric and hydrochemical evidence for fast flowpaths at La Cuenca, western Amazonia, *J. Hydrol.*, *180*, 237–250, 1996.

Elsenbeer, H., K. Cassel, and J. Castro, Spatial analysis of soil hydraulic conductivity in a tropical rain forest catchent, *Water Resour. Res.*, *28*, 3201–3214, 1992.

Elsenbeer, H., D. K. Cassell, and L. Zuñiga, Throughfall in the Terra Firme forest of western Amazonia, *J. Hydrol. (N.Z.)*, *32*, 30–44, 1994a.

Elsenbeer, H., A. West, and M. Bonell, Hydrological pathways and stormflow hydrochemistry at South Creek, notheast Queensland, *J. Hydrol.*, *162*, 1–21, 1994b.

Elsenbeer, H., A. Lack, and K. Cassel, Chemical fingerprints of hydrological compartments and flowpaths at La Cuenca, western Amazonia, *Water Resour. Res.*, pp. 3051–3058, 1995a.

Elsenbeer, H., D. Lorieri, and M. Bonell, Mixing model approaches to estimate storm flow sources in an overland flow-dominated tropical rain forest catchment, *Water Resour. Res.*, *31*, 2267–2278, 1995b.

Elsenbeer, H., A. Lack, and K. Cassel, The stormflow chemistry at La Quenca, western Amazonia, *Interciencia*, *21*, 133–139, 1996.

Evans, J., *Plantation Forestry in the Tropics*, Clarendon Press, Oxford, 1992.

Feddes, R. A., P. J. Kowalik, and H. Zarasny, *Simulation of Field Water Use and Crop Yield*, John Wiley & Sons, 1978.

Fritsch, J. M., Les effets du Défrichement de la forêt Amazonienne et de la mise en culture sur L'hydrologie de petits bassins versants, *Tech. rep.*, Institute Francais de Recherche Scientifique pour le Développement en Coopération, 1992, editions de l'ORSTOM, Collection ÉTUDES et THÈSES.

García-Martinó, A. R., F. N. Scatena, G. S. Warner, and D. L. Civo, Statistical low flow estimations using GIS analysis in humid montane regions in Puerto Rico, *Wat. Resour. Bull.*, *32*, 1259–1271, 1996.

García-Martinó, A. R., G. S. Warner, F. N. Scatena, and D. L. Civco, Rainfall, runoff and elevation relationships in the Luquillo Mountains of Puerto Rico, *Caribbean J. Sci.*, *32*, 413–424, 1996.

Gash, J. H. C., An analytical model of rainfall interception by forests, *Quart. J. Roy. Meteo. Soc.*, *105*, 43–55, 1979.

Gash, J. H. C., and A. J. Morton, An application of the Rutter model to the estimation of the interception loss from Thetford Forest, *J. Hydrol.*, *38*, 49–58, 1978.

Gash, J. H. C., and J. B. Stewart, The evaporation from Thetford Forest during 1975, *J. Hydrol.*, *35*, 385–396, 1977.

Gash, J. H. C., I. R. Wright, and C. R. Lloyd, Comparative estimates of interception loss from three coniferous forests in Great Britain, *J. Hydrol.*, *48*, 89–105, 1980.

Gash, J. H. C., C. R. Lloyd, and G. Lachaud, Estimating sparse forest rainfall interception with an analytical model, *J. Hydrol.*, *170*, 79–86, 1995.

Gash, J. H. C., C. A. Nobre, J. M. Roberts, and R. L. Victoria, *Amazonian Deforestation and Climate*, John Wiley & Sons, Chichester, 1996.

Genereux, D. P., H. F. Hemond, and P. J. Mulholland, Use of radon-222 and calcium as tracers in a three-and-member mixing model for streamflow generation on the West Fork of Walker Branch Watershed, *J. Hydrol.*, *142*, 167–211, 1993.

Giambelluca, T. W., and D. Nullet, Evaporation at high elevations in Hawaii, *J. Hydrol.*, *136*, 219–235, 1992.

Gilmour, D. A., Catchment water balance studies on the wet tropical coast of North Queensland, Ph.D. thesis, James Cook University, Townsville, Australia, 1975.

Gilmour, D. A., Effects of rainforest logging and clearing on water yield and quality in a high rainfall zone of north-east queensland, in *Proceedings of the Brisbane Hydrology Symposium*, pp. 156–160, Institution of Engineers Australia, Canberra, Australia, 1977.

Gosh, D. P., The aplication of linear filter theory to the direct interpretation of geoelectrical resistivity sounding measurements, *Geophys. Prospect.*, *19*, 192–217, 1971.

Grayson, R. B., I. D. Moore, and T. A. McMahon, Physically based hydrologic modeling. 2. Is the concept realistic, *Water Resour. Res.*, *28*, 2659–2666, 1992.

Hafkenscheid, R. L. L. J., L. A. Bruijnzeel, and R. A. M. de Jeu, Estimates of fog interception by montane rain forest in the Blue Mountains of Jamaica, in *First International Conference on Fog and Fog Collection*, edited by R. Schemenauer and H. Bridgman, pp. 33–36, IDRC, Ottowa, Canada, 1998.

Hall, F. R., Base-flow recessions – A review, *Water Resour. Res.*, *4*, 973–982, 1968.

Hatton, T. J., J. Walker, W. Dawes, and F. X. Dunin, Simulations of hydroecological responses to elevated co_2 at the catchment scale, *Aus. J. Bot.*, *40*, 679–696, 1992.

Henderson, F. M., and R. A. Wooding, Overland flow and groundwater flow from a steady rainfall of finite duration, *J. Geophys. Res.*, *69*, 1531–1540, 1964.

Herwitz, R. S., Interception storage capacities of tropical rainforest canopy trees, *J. Hydrol.*, *77*, 237–252, 1985.

Herwitz, S. R., Episodic stemflow inputs of magnesium and potassium to a tropical forest floor during heavy rainfall events, *Oecologia*, *70*, 423–425, 1986.

Hewlett, J. D., and A. R. Hibbert, Factors affecting the response of small watersheds to precipitation in humid areas., in *Forest Hydrology*, edited by W. E. Sopper and H. W. Lull, pp. 275–290, Pergamon Press, 1967.

Hewlett, J. D., H. E. Post, and R. Doss, Effect of clear-cut silviculture on dissolved ion export and water yield in the Piedmont, *Water Resour. Res.*, *20*, 1030–1038, 1984.

Hinton, M. J., S. L. Schiff, and M. C. English, Examining the contributions of glacial till water to storm runoff using two- and three-component hydrograph separations, *Water Resour. Res.*, *30*, 983–993, 1994.

Hölscher, D., T. D. de A. Sá, T. X. Bastos, M. Denich, and H. Fölster, Evaporation from young secondary vegetation in eastern Amazonia, *J. Hydrol.*, *193*, 293–305, 1997.

Holwerda, F., A study of evaporation from lowland and montane tropical rain forests in the Luquillo Mountains, Puerto Rico, *Working Paper 3*, Faculty of Earth Sciences, Vrije Universiteit, Amsterdam, The Netherlands, 1997.

Horton, R. E., The role of infiltration in the hydrological cycle, *Trans. Am. Geophys. Union*, *14*, 446–460, 1933.

Hsia, Y. J., Changes in storm hydrographs after clearcutting a small hardwood forested watershed in central Taiwan, *For. Ecol. Man.*, *20*, 117–134, 1987.

Hunter, A. H., International soil fertility and improvement procedures, *Laboratory procedures*, Department of Soil Science, Carolina State University, Raleigh, North Carolina, 1982.

Hutchinson, M. F., A new procedure for gridding elevation and stream line data with automatic removal of spurious pits, *J. Hydrol.*, *106*, 211–232, 1989.

Hutjes, R. W. A., A. Wierda, and A. W. L. Veen, Rainfall interception in the Taï forest, Ivory Coast: application of two simulation models to a humid tropical system, *J. Hydrol.*, *114*, 259–275, 1990.

Jackson, I. J., Problems of throughfall and interception assessment under tropical forest, *J. Hydrol.*, *12*, 234–254, 1971.

Jackson, I. J., Relationships between rainfall parameters and interception by tropical rainforest, *J. Hydrol.*, *24*, 215–238, 1975.

Jepma, C. J., *Tropical Deforestation A Socio-Economic Approach*, Earthscan Publications, London, 1995.

Jetten, V., Modelling the lffects of logging on the water balance of a tropical rain forest, Ph.D. thesis, University of Utrecht, Utrecht, The Netherlands, 1994.

Jetten, V. G., Interception of tropical rain forest: performance of a canopy water balance model, *Hydrol. Proc.*, *10*, 671–685, 1996.

Jones, J. A. A., Soil piping and stream channel initiation, *Water Resour. Res.*, *7*, 602–610, 1971.

Jordan, C. F., *Nutrient Cycling in Tropical Forest Ecosystems*, J. Wiley, New York, 1985.

Kendall, C., and J. J. McDonnell, Effect of intrastorm isotopic heterogeneities of rainfall, soil water and groundwater on runoff modeling, in *Tracers in Hydrology, Proceedings of the Yokohama Symposium*, pp. 41–48, IAHS Publ. no. 215, 1993.

Kernighan, B. W., and D. M. Ritchie, *The C programming language*, 2nd ed., Prentice Hall, 1988.

Kessler, J., and R. J. Oosterbaan, Determining hydraulic conductivity of soils, in *I.L.R.I. Publication no. 16. Volume III.*, pp. 253–296, International Institute for Land Reclamation and Improvement, Wageningen, The Netherlands, 1973.

Keulegan, G. H., Spatially variable discharge over a sloping plane, *Trans. Am. Geophys. Union*, *25*, 956–959, 1944.

Koefoed, O., *Geosounding Principles, 1: Resistivity Sounding Measurements*, vol. 14a of *Methods in Geochemistry and Geophysics*, Elsevier, Amsterdam, 1979.

Kuraji, K., and L. L. Paul, Effects of rainfall interception on water balance in two tropical rainforest catchments, Sabah, Malaysia, in *Proceedings of the International Symposium on Forest Hydrology*, pp. 291–298, Tokyo, Japan, 1994.

Lal, R., *Tropical Ecology and Physical Edaphology*, John Wiley & Sons Ltd., UK, 1987.

Larsen, M. C., and I. M. Concepción, Water budgets of forested and agriculturally-developed watersheds in Puerto Rico, in *Third International Symposium on Water Resources, Fifth Caribbean Islands Water Resources Congress*, pp. 199–204, American Water Resources Association, 1998.

Larsen, M. C., and A. Simon, A rainfall intensity-duration treshold for landslides in a humid-tropical environment, Puerto Rico, *Geografiska Annaler*, *75A*, 13–23, 1993.

Larsen, M. C., and A. J. Torres-Sanches, Rainfall soil moisture relations in landslide-prone areas of a tropical rain forest, Puerto Rico, *Tropical Hydrology and Caribbean Water Resources*, pp. 121–129, 1990.

Lee, R., Theoretical estimates versus forest water yield, *Water Resour. Res.*, *6*, 1327–1334, 1970.

Leopoldo, P. R., W. Franken, and E. Salati, Water balance of a small catchment in 'Terra Firme' Amazonian forest, *Acta Amaz.*, *12*, 333–337, 1982, in Portuguese with english summary.

Lesack, L. F. W., Water balance and hydrologic characteristics of a rain forest catchment in the Central Amazonian Basin, *Water Resour. Res.*, *29*, 759–773, 1993.

Lewis, L. A., Slow movement of earth under tropical rain forest conditions, *Geology*, *2*, 9–10, 1974.

Lewis, L. A., Slow soil movement in the tropics – a general model, *Zeitschrift für Geomorphologie, Neue Folge, Suppl. Bd*, *25*, 125–144, 1976.

Lighthill, M. J., and G. B. Whitham, On kinematic waves, I. flood movement in long rivers, *Proc. Roy. Soc. London*, *229A*, 281–316, 1955.

Lloyd, C. R., and A. Marques-Filho, Spatial variability of throughfall and stemflow measurements in Amazonian rain forest, *Agric. For. Meteo.*, *42*, 63–73, 1988.

Lloyd, C. R., J. H. C. Gash, W. J. Shuttleworth, and A. Marques-Filho, The measurement and modelling of rainfall interception by Amazonian rain forests, *Agric. For. Meteo.*, *43*, 277–294, 1988.

Loague, K., and P. C. Kyriakidis, Spatial and temporal variability in the R-5 infiltration data set: Deja vu and rainfall-runoff simulations, *Water Resour. Res.*, *33*, 2883–2895, 1997.

Low, K. S., and G. C. Goh, The water balance of five catchments in Selangor, West Malaysia., *J. Trop. Geogr.*, *35*, 60–66, 1972.

Lugo, A. E., Water and the ecosystems of the Luquillo Experimental Forest, *General Techical Teport SO-63*, United States Department of Agriculture, Forest Service, Southern Forest Experiment Station, New Orleans, Louisiana, USA, 1986.

Lugo, A. E., and F. N. Scatena, Ecosystem-level properties of the Luquillo Experimental Forest with emphasis on the Tabonuco forest, in *Tropical Forests: Management and Ecology*, edited by A. E. Lugo and C. Lowe, vol. 112 of *Ecological Studies*, chap. 4, pp. 59–108, Springer-Verlag, New York, 1995.

Lundgren, B., Soil conditions and nutrient cycling under natural and plantation forests in Tanzanian highlands, Reports in Forest Ecology and Forest Soils *31*, Dept. of Forest Soils, Swedish Univ. of Agric. Sci., Uppsala, 1978.

Makkink, G. F., Testing the Penman formula by means of lysismeters, *Int. of Water Eng.*, *11*, 277–288, 1957.

Makkink, G. F., De verdamping uit vegetaties in verband met de formule van Penman, Proceedings and Informations *4*, Commision for Hydrological Research TNO, The Hague, 1961.

Malkus, J. S., The effects of a large island upon the trade-wind air stream, *Quart. J. Roy. Meteo. Soc.*, *81*, 538–550, 1955.

Malmer, A., Water-yield changes after clear-felling troppical rainforest and establishment of forest plantation in Sabah, Malaysia, *J. Hydrol.*, *134*, 77–94, 1992.

Malmer, A., Dynamics of hydrology and nutrient losses as response to establishment of forest plantation: A case study on tropical rainforest land in Sabah, Malaysia, Ph.D. thesis, Swedish University of Agricultural Sciences, Umeå, Sweden, 1993.

Marquardt, D. W., An algorithm for least-square estimates of nonlinear parameters, *J. Soc. Ind. Appl. Math.*, *11*, 431–441, 1963.

Marsalek, J., Calibration of the tipping bucket rain gauge, *J. Hydrol.*, *53*, 343–354, 1981.

McDonnell, J. J., A rationale for old water discharge through macropores in a steep, humid catchment, *Water Resour. Res.*, *26*, 2821–2832, 1990.

McDonnell, J. J., J. Freer, R. Hooper, C. Kendall, D. Burns, K. Beven, and J. Peters, A new approach to characterizing hillslope hydrology, 1996.

McDowell, W. H., Internal nutrient fluxes in a Puerto Rican rain forest, *J. Trop. Ecol.*, *14*, 521–536, 1998.

McDowell, W. H., W. H. Bowden, and C. E. Asbury, Riparian nitrogen dynamics in two geomorphologically distinct tropical rain forest watersheds: subsurface solute patterns, *Biochemistry*, *18*, 53–75, 1992.

McNaughton, K. G., and J. Laubach, Unsteadiness as a cause of non-equality of eddy diffusivities for heat and vapour at the base of an advective inversion, *Boundary-Layer Meteo.*, *88*, 479–504, 1998.

Meesters, A. G. C. A., and H. F. Vugts, Calculation of heat storage in stems, *Agric. For. Meteo.*, *78*, 181–202, 1996.

Merz, B., and E. J. Plate, An analysis of the effects of spatial variability of soil and soil moisture on runoff, *Water Resour. Res.*, *33*, 2909–2922, 1997.

Molicova, H., M. Grimaldi, M. Bonell, and P. Hubert, Using TOPMODEL towards identifying and modelling the hydrological patterns within a headwater, humid tropical catchment, *Hydrol. Proc.*, *11*, 1169–1196, 1997.

Monteith, J. L., Evaporation and the environment, in *Symposium of the Society of Experimental Biology no. 19*, pp. 245–269, 1965.

Moore, C. J., Frequency response correction for eddy correlation systems, *Boundary-Layer Meteo.*, *37*, 17–35, 1986.

Moore, I. D., E. M. O'Loughlin, and G. J. Burch, A contour-based topgraphic model for hydrological and ecological applications, *Earth Surf. Proc. Landforms*, *13*, 305–320, 1988.

Mosley, M. P., Streamflow generation in a forested watershed, New Zealand, *Water Resour. Res.*, *15*, 795–806, 1979.

Mosley, M. P., Subsurface flow velocities through selected forest soils, South Island, New Zealand, *J. Hydrol.*, *55*, 65–92, 1982.

Mualem, Y., A new model for predicting the hydraulic conductivity of unsaturated porous media, *Water Resour. Res.*, *12*, 513–522, 1976.

Murdiyarso, D., Forest transpiration and evaporation, Ph.D. thesis, University of Reading, Reading, U.K., 1985.

Nash, J. E., and J. V. Sutcliffe, River flow forecasting through conceptual models part I – A discussion of principles, *J. Hydrol.*, *10*, 282–290, 1970.

Nepstad, D., A. Verissimo, A. Alencar, C. Nobre, E. Lima, P. Lefebvre, P. Schlesinger, C. Potter, P. Moutinho, E. Mendoza, M. Cochrane, and V. Brooks, Large-scale impoverishment of amazonian forests by logging and fire, *Nature*, *398*, 505–508, 1999.

Nimz, G. J., Lithogenic and cosmogenic tracers in catchment hydrology, in *Isotope Tracers in Catchment Hydrology*, edited by C. Kendall and J. J. McDonnell, pp. 247–289, Elsevier, Amsterdam, 1998.

Noguchi, S., A. Rahim Nik, T. Sammori, M. Tani, and Y. Tsuboyama, Rainfall characteristics of tropical rain forest and temperate forest: comparison between Bukit Tarek in Peninsular Malaysia and Hitachi Ohta in Japan, *J. Trop. For. Sci.*, *9*, 206–220, 1996.

Nortcliff, S., and J. B. Thornes, Seasonal variations in the hydrology of a small forested catchment near Manaus, Amazonas, and the implications for its management, in *Tropical Agricultural Hydrology*, edited by R. Lal and E. W. Russel, pp. 37–57, Wiley, Chichester, 1981.

Nortcliff, S., and J. B. Thornes, Floodplain response of a small tropical stream, in *Catchment Experiments in Fluvial Hydrology*, edited by T. P. Burt and D. E. Walling, pp. 73–85, Geo-Books, Norwich, 1984.

Nullet, D., Energy sources for evaporation on tropical islands, *Phys. Geogr.*, *8*, 36–45, 1987.

Odum, H. T., and R. F. Pidgeon, *A tropical rain forest. A study of irradiation and ecology at El Verde, Puerto Rico.*, U.S. Atomic Energy Commission, Washington DC, 1970.

Odum, H. T., W. Abbot, R. K. Selander, F. B. Golley, and R. F. Wilson, Estimates of chlorophyll and biomass of the Tabonuco forest of Puerto Rico, in *A Tropical Rain Forest*, edited by H. T. Odum and R. F. Pidgeon, pp. I3–I19, U.S. Atomic Energy Commission, Washington DC, 1970a.

Odum, H. T., G. Drewry, and J. R. Kline, Climate at El Verde, 1963–1966, in *A tropical rain forest*, edited by H. T. Odum and R. F. Pidgeon, pp. B–347–B–418, U.S. Atomic Energy Commission, Washington DC, 1970b.

Oldeman, L. R., The global extent of soil degradation, in *Soil Resilience and Sustainable Land Use*, edited by D. J. Greenland and I. Szabolcs, pp. 99–118, CAB International, Wallingford, U.K, 1994.

O'Loughlin, E. M., Prediction of surface saturation zones in natural catchments by topographic analysis, *Water Resour. Res.*, *22*, 794–804, 1986.

Pearce, A. J., and A. D. Griffiths, Effects of selective logging on physical water quality in small streams, Okarito forest, *J. Hydrol. (N.Z.)*, *19*, 60–67, 1980.

Pearce, A. J., and K. Rowe, Forest management effect on interception, evaporation and water yield, *J. Hydrol. (N.Z.)*, *18*, 73–87, 1979.

Pearce, A. J., and L. K. Rowe, Rainfall interception in a multi-storied, evergreen mixed forest: estimates using Gash's analytical model, *J. Hydrol.*, *49*, 341–353, 1981.

Pearce, A. J., C. L. O'Louglin, and L. K. Rowe, Hydrologic regime of small, undisturbed beech forest catchments, North Westland, *Soil and Plant Water Symposium 1976*, pp. 150–158, 1976.

Pearce, A. J., L. K. Rowe, and J. B. Stewart, Nighttime, wet canopy evaporation rates and the water balance of an evergreen mixed forest, *Water Resour. Res.*, *16*, 955–959, 1980.

Penman, H. L., Evaporation: An introductory survey, *Neth. J. Agric. Sci.*, *4*, 9–29, 1956.

Pielke, R. A., W. Cotton, R. Walko, C. Tr back, W. Lyons, L. Grasso, M. Nicholls, M. Moran, D. Wesley, T. Lee, and J. Copeland, A comprehensive meteorological modeling system – RAMS, *Meteor. Atmos. Phys.*, *49*, 69–91, 1992.

Pinder, G. F., and J. F. Jones, Determination of the groundwater component of peak discharge of total runoff, *Water Resour. Res.*, *5*, 438–445, 1969.

Quinn, P. F., K. J., P. Chevallier, and O. Planchon, The prediction of hillslope flow paths for distributed hydrological modelling using digital terrain models, *Hydrol. Proc.*, *5*, 59–79, 1991.

Read, R. G., Microclimate as background environment for ecological studies of insects in a tropical forest, *J. Appl. Meteo.*, *16*, 1282–1291, 1977.

Richardson, J. H., Some implications of tropical forest replacement in Jamaica, *Z. Geomorph. N.F.*, *44*, 107–118, 1982.

Roche, M. A., Evapotranspiration réelle de la forêt amazonienne en Guyane, *Cah. ORSTOM, Sér. Hydrol.*, *19*, 37–44, 1982.

Rose, C. W., and B. F. Yu, Dynamic process modelling of hydrology and erosion, in *Soil erosion at multiple scales*, edited by F. W. T. Penning de Vries, F. Agus, and J. Kerr, pp. 269–286, CABI, Wallingford, U.K., 1998.

Ross, P. J., and K. L. Bristow, Simulating water movement in layerd and gradational soils using the Kirchoff transform, *Soil Sci. Soc. Am. J.*, *54*, 1519–1524, 1990.

Rowe, L. K., Rainfall interception by a beech-podocarp-hardwood forest near Reefton, North, Westland, New Zealand, *J. Hydrol. (N.Z.)*, *18*, 63–72, 1979.

Rowe, L. K., Rainfall interception by an evergreen beech forest, Nelson, New Zealand, *J. Hydrol.*, *66*, 143–158, 1983.

Running, S. W., and J. C. Coughlan, A general model of forest ecosystem processes for regional applications. I. Hydrologic balance, canopy gas exchange and primary production processes, *Ecol. Mono.*, *42*, 125–154, 1988.

Rutter, A. J., An analysis of evaporation from a stand of Scots pine, in *International Symposium on Forest Hydrology*, edited by W. E. Sopper and H. W. Lull, pp. 403–417, Pergamon Press, Oxford, UK, 1967.

Rutter, A. J., and A. J. Morton, A predictive model of rainfall interception in forests: III. Sensitivity of the model to stand parameters and meteorological variables, *J. Appl. Ecol.*, *14*, 567–588, 1977.

Rutter, A. J., K. A. Kershaw, P. C. Robins, and A. J. Morton, A predictive model of rainfall interception in forests. I. A derivation of the model from observations in a plantation of Corsican pine, *Agric. Meteo.*, *9*, 367–384, 1971.

Rutter, A. J., A. J. Morton, and P. C. Robins, A predictive model of rainfall interception in forests. II. Generalization of the model and comparison with observations in some coniferous and hardwood stands, *J. Appl. Ecol.*, *12*, 367–380, 1975.

Scatena, F. N., An introduction to the physiography and history of the Bisley Experimental Watersheds in the Luquillo Mountains of Puerto Rico, *Gen. Tech. Rep. SO-72*, USDA, Forest Service, Southern Forest Experiment Station, New Orleans, USA, 1989.

Scatena, F. N., Culvert flow in small drainages in montane tropical forests: observations from the Luquillo Experimental Forest of Puerto Rico, *Tropical Hydrology and Caribbean Water Resources*, pp. 237–245, 1990a.

Scatena, F. N., Watershed scale rainfall interception on two forested watersheds in the Luquillo mountains of Puerto Rico, *J. Hydrol.*, *113*, 89–102, 1990b.

Scatena, F. N., and M. C. Larsen, Physical aspects of hurricane Hugo in Puerto Rico, *Biotropica*, *23*, 317–323, 1991.

Scatena, F. N., and A. E. Lugo, Geomorphology, disturbance and the soil and vegetation of two subtropical wet steepland watersheds in Puerto Rico, *Geomorphology*, *13*, 199–213, 1995.

Scatena, F. N., W. Silver, T. Siccama, A. Johnson, and M. J. Sanchez, Biomass and nutrient content of the Bisley Experimental Watersheds, Luquillo Experimental Forests, Puerto Rico, before and after hurricane Hugo, *Biotropica*, *25*, 15–27, 1993.

Scatena, F. N., S. Moya, C. Estrada, and J. D. Chinea, The first five years in the reorganization of above-ground biomass and nutrient use following hurricane Hugo in the Bisley Experimental Watersheds, Luquillo Experimental Forest, Puerto Rico, *Biotropica*, *28*, 424–440, 1996.

Schellekens, J., *Vamps, a Vegetation-AtMosPhere-Soil water model*, Faculty of Earth Sciences, Vrije Universiteit, 0th ed., 1997.

Schellekens, J., Hydrological processes in a humid tropical rain forest: a combined experimental and modelling approach, Ph.D. thesis, Faculty of Earth Sciences, Vrije Universiteit, Amsterdam, The Netherlands, 2000a.

Schellekens, J., Modelling water yield and runoff response of a small tropical rain forest catchment using a physically-based distributed model, *J. Hydrol.*, 2000b, submitted.

Schellekens, J., L. A. Bruijnzeel, A. J. Wickel, F. N. Scatena, and W. L. Silver, Interception of horizontal precipitation by elfin cloud forest in the Luquillo Mountains, Eastern Puerto Rico, in *First International Conference on Fog and Fog Collection*, edited by R. S. Schemenauer and H. A. Bridgman, pp. 29–32, IDRC, Ottawa, Canada, 1998.

Schellekens, J., F. N. Scatena, L. A. Bruijnzeel, and A. J. Wickel, Modelling rainfall interception by a lowland maritime tropical rain forest in northeastern Puerto Rico, *J. Hydrol.*, *225*, 168–184, 1999.

Schellekens, J., L. A. Bruijnzeel, F. N. Scatena, N. J. Bink, and F. Holwerda, Evaporation from a tropical rain forest, Luquillo Experimental Forest, Puerto Rico, *Water Resour. Res.*, 2000, in press.

Schellekens, J., F. N. Scatena, L. A. Bruijnzeel, and R. J. P. van Hogezand, Stormflow generation in a small catchment in the Luquillo Experimental Forest, Puerto Rico, *J. Hydrol.*, submitted.

Shuttleworth, W. J., Evaporation from Amazonian rainforest, *Phil. Trans. Roy. Soc.*, *B323*, 321–346, 1988.

Shuttleworth, W. J., Micrometeorology of temperate and tropical forest, *Phil. Trans. Roy. Soc.*, *B324*, 299–334, 1989.

Shuttleworth, W. J., J. H. C. Gash, C. R. Lloyd, C. J. Moore, A. de O. Marques-Filho, G. Fisch, V. de Paula Silva Filho, M. de Nazaré Góes Ribeiro, L. B. Molion, L. D. de Abreu Sá, J. C. A. Nobre, O. M. R. Cabral, S. R. Patel, and J. C. de Moraes, Eddy correlation measurements of energy partition for Amazonian forest, *Quart. J. Roy. Meteo. Soc.*, *110*, 1143–1162, 1984.

Shuttleworth, W. L., and I. R. Calder, Has the Priestley-Taylor equation any relevance to forest evaporation?, *J. Appl. Meteo.*, *18*, 639–646, 1979.

Silberstein, R. P., R. A. Vertessy, and J. Morris, Modelling the effects of soil moisture and solute conditions on tree growth, *Agric. Water Man.*, *39*, 283–315, 1999.

Silver, W. L., F. N. Scatena, A. H. Johnson, T. G. Siccama, and M. J. Sanchez, Nutrient availability in a montane wet tropical forest: Spatial patterns and mothodological considerations, *Plant and Soil*, *164*, 129–145, 1994.

Silver, W. L., A. E. Lugo, and M. Keller, Soil oxygen availability and biogeochemistry along rainfall and topographic gradients in upland wet tropical forest soils, *Biogeochem.*, *44*, 301–328, 1999.

Simon, A., M. C. Larsen, and C. R. Hupp, The role of soil processes in determining mechanisms of slope failure and hillslope development in a humid-tropical forest, eastern Puerto Rico, *Geomorphology*, *3*, 263–286, 1990.

Sivapalan, M., N. R. Viney, and C. G. Jeerjav, Water and salt balance modelling to predict the effects of land use changes in forested catchments. 3. the large catchment model, *Hydrol. Proc.*, *10*, 429–446, 1996.

Smith, R. E., and R. H. B. Hebbert, A Monte Carlo analysis of the hydrologic effects of spatial variability of infiltration, *Water Resour. Res.*, *15*, 419–429, 1979.

Stakman, W. P., Measuring soil moisture, in *I.L.R.I. Publication no. 16. Volume III.*, pp. 221–251, International Institute for Land Reclamation and Improvement, Wageningen, The Netherlands, 1973.

Swindel, B. F., C. J. Lassiter, and H. Riekerk, Effects of clearcutting and site preparation operations on water yields from Slash pine forests, *Forest Ecology and Management*, *5*, 101–113, 1983.

Tabón Marin, C., Monitoring and modelling hydrological fluxes in support of nutient cycling studies in Amazonian rain forest ecosystems, Ph.D. thesis, Universiteit van Amsterdam, Amsterdam, The Netherlands, 1999.

Telford, W. M., L. P. Geldart, R. E. Sheriff, and D. A. Keys, *Applied Geophysics*, Cambridge University Press, 1976.

Thom, A. S., Momentum, mass and heat exchange of plant communities, in *Vegetation and the Atmosphere. Volume 1. Principles*, edited by J. L. Monteith, pp. 57–109, Academic Press, London, 1975.

Tillman, J. E., The indirect determination of stability, heat and momentum fluxes in the atmosphere boundary layer from simple scalar variables during dry unstable conditions, *J. Appl. Meteo.*, *11*, 783–792, 1972.

Tsukamoto, Y., and I. Ishigaki, Evaporation rates from a forest canopy during storm in a humid region, in *Regional seminar on tropical forest hydrology*, p. 10, IHP, Unesco, FRIM, Kuala Lumpur, Malaysia, 1989.

Turvey, N. D., Nutrient cycling under tropical rain forest in Central Papua, *Occasional Paper 10*, Department of Geography, University of Papua New Guinea, Port Moresby, 1974.

Ubarana, V. N., Observation and modelling of rainfall interception loss in two experimental sites in Amazonian forest, in *Amazonian Deforestation and Climate*, edited by J. H. C. Gash, C. A. Nobre, J. M. Roberts, and R. L. Victoria, pp. 151–162, John Wiley & Sons, Chichester, 1996.

Van Asselt, C. J., E. F. G. Jacobs, J. H. Van Boxel, and A. E. Jansen, A ridgid fast-response thermometer for atmospheric research, *Meas. Sci. Technol.*, *2*, 26–31, 1991.

Van Beers, W. F. J., The auger hole method, *Tech. rep.*, International Institute for land reclamation and improvement/ILRI, Wageningen, The Netherlands, 1979.

Van Dijk, A. I. J. M., J. Schellekens, and M. M. A. Groen, Geophysical survey of the Bisley I and II catchments, Luquillo Experimental Forest, Puerto Rico, *Working Paper 4*, Faculty of Earth Sciences, Vrije Universiteit, 1997.

Van Genuchten, M. T., A closed-form equation for predicting the hydraulic conductivity of unsaturated soils, *Soil Sci. Soc. Am. J.*, *44*, 892–898, 1980.

Van Hogezand, R. J. P., The use of chemical tracers in identifying stormflow generating processes in a small catchment in the Luquillo Mountains, Puerto Rico, *Hydrological modelling in a humid tropical island setting: with special reference to the Luquillo Experimental Forest, Puerto Rico, Working Paper 1*, Faculty of Earth Sciences, Vrije Universiteit, Amsterdam, The Netherlands, 1996.

Veneklaas, E. J., and R. Van Ek, Rainfall interception in two tropical montane rain forests, Columbia, *Hydrol. Proc.*, *4*, 311–326, 1990.

Vertessy, R. A., and H. Elsenbeer, Distributed modelling of storm flow generation in an Amazonian rainforest catchment: effects of model parameterization, *Water Resour. Res.*, *35*, 2173–2187, 1999.

Vertessy, R. A., C. J. Wilson, D. M. Silburn, R. D. Conolly, and C. A. Ciesiolka, Predicting erosion hazzard areas using digital terrain analysis, in *Proc. IHAS INt. Symp. on Research Needs and Applications to Reduce Erosion and Sedimentation in Tropical Steeplands, Suva, Fiji*, pp. 298–308, IAHS, Wallinford, 1990.

Vertessy, R. A., T. J. Hatton, P. J. O'Shaughnessy, and M. D. A. Jayasuriya, Predicting water yield from a mountain ash forest catchment using a terrain analysis based catchment model, *J. Hydrol.*, *150*, 665–700, 1993.

Vertessy, R. A., T. J. Hatton, R. G. Benyon, and W. R. Dawes, Long-term growth and water balance predictions for a mountain ash (*e. regnans*) forest catchment subject to clear-felling and regeneration, *Tree Phys.*, *16*, 221–232, 1996.

Vugts, H. F., and L. A. Bruijnzeel, Water and energy budgets of rain forest along an elevational gradient under maritime tropical conditions: a combined experimental and modelling approach, *Project description*, WOTRO W79-201, 1999.

Vugts, H. F., M. J. Waterloo, F. J. Beekman, K. F. A. Frumau, and L. A. Bruijnzeel, The temperature variance method: a powerful tool in the estimation of actual evaporation rates., in *Hydrology of Warm Humid Regions, Proc. of the Yokohama Symp.*, edited by J. S. Gladwell, IAHS Publication no. 216, pp. 251–260, 1993.

Wadsworth, F. H., The development of the forest land resources of the Luquillo Mountains, Puerto Rico, Ph.D. thesis, Univ. of Michigan, Ann Arbor, Michigan, 1949.

Wadsworth, F. H., and J. A. Bonnet, Soil as a fector in occurrence of two types of montane forest in Puerto Rico, *Caribbean Forester*, *12*, 67–70, 1951.

Walker, L. R., N. V. L. Brokaw, D. J. Lodge, and R. B. W. (eds.), Ecosystem, plant, and animal responses to hurricanes in the Caribbean, *Biotropica*, *Special issue Volume 23*, 1991.

Ward, R. C., On the response to precipitation of headwater streams in humid areas, *J. Hydrol.*, *74*, 171–189, 1984.

Ward, R. C., and M. Robinson, *Principles of Hydrology*, 2nd ed., McGraw-Hill, Maidenhead, UK, 1990.

Wasser, H. J., and J. R. E. Harger, Several environmental factors affecting the rainfall in indonesia, *Report*, ROSTSEA/UNESCO, Jakarta, Indonesia, 1992.

Waterloo, M. J., Water and nutrient dynamics of *Pinus caribaea* plantation forest on former grassland soils in southwest Viti Levu, Fiji, Ph.D. thesis, Faculty of Earth Sciences, Vrije Universiteit, Amsterdam, The Netherlands, 1994.

Waterloo, M. J., L. A. Bruijnzeel, H. F. Vugts, and T. T. Rawaqa, Evaporation from *Pinus caribaea* plantations on former grassland soils under maritime tropical conditions, *Water Resour. Res.*, *35*, 2133–2144, 1999.

Watson, F. G. R., R. A. Vertessy, and R. B. Grayson, Large-scale modelling of forest hydro-ecological processes and their long term effect on water yield, *Hydrol. Proc.*, *13*, in press, 1999.

Weaver, P. L., Cloud moisture interception in the Luquillo Mountains of Puerto Rico, *Caribbean Journal of Sciences*, *12*, 129–144, 1972.

Whipkey, R. Z., Sub-surface stormflow from forested slopes, *Buletin of the International Association of Scientific Hydrology*, *10*, 74–85, 1965.

Wit, K. E., Meting van de doorlatendheid in ongeroerde monsters, *Rapport 17*, ICW, Wageningen, 1962.

Zhu, T. X., L. E. Band, and R. A. Vertessy, Continuous modeling of intermittent stromflows on a semi-arid agricultural catchment, *J. Hydrol.*, *226*, 11–29, 1999.

A

Vamps, A VEGETATION-ATMOSPHERE-SOIL WATER MODEL

A.1 INTRODUCTION

Vamps is a one-dimensional water balance model for soils covered by forest, agricultural crop or bare land particularly suited for use in tropical environments. Vamps can be used as a complete forest hydrological model or as a tool to determine just one or more parameters (e.g. calculate interception using Gash' model). Vamps was designed to be extensible. At the same time the model should be simple to operate. The model is therefore build in a modular fashion and is equipped with a simple C-like scripting language. Features such as variable time steps and the ability to select modules allow the model to be used in both data-rich and data-poor environments. Interactive graphics functions (on selected operating systems) allow quick visualization of variables for evaluation of model runs.

The model has been developed as part of a collaborative project 'Hydrological modeling in a humid tropical island setting: with special reference to The Luquillo experimental Forest, Puerto Rico' between the International Institute of Tropical Forestry and the Vrije Universiteit Amsterdam [*Bruijnzeel and Scatena*, 1994]. The model is free and distributed with complete source code. It runs on a variety of operating systems.

The soil part of Vamps was developed after SWATR* [*Feddes et al.*, 1978]. The large number of models that have been developed is an indication that models need to be tailored or adapted for each specific application. In order to make Vamps easily extensible a C-like interpreted language [*Davis*, 1995a, b] allows the user to redefine built-in functions with functions tailored to the site in question. These features in combination with testing on several tropical sites make the model of particular importance to those interested in the tropics as a whole and tropical forests in particular.

The main development goals of Vamps are: *(i)* make a parameterized model

*Currently the swap/swatr program is maintained and documented in by: Dept. of Agrohydrology, Winand Staring Centre and Dept. of Water Resources, Wageningen Agricultural University

- The program is written in ANSI C [*Kernighan and Ritchie*, 1988]
- Documentation for both model principles and model operation
- Both binaries and source code available via the World Wide Web
- Most parts of the model can be used separately
- Variable time-steps (e.g. 0.5 seconds to two weeks)
- No limit to the number of soil layers
- Run with Sun-OS, Linux, AIX, Net-BSD, MS-DOS and OS/2
- Includes pre- and postprocessors
- Simple ASCII input and output file format
- Easy extension by the users through built-in (high level) library
- Screen and hardcopy graphics on several platforms
- Simple to adjust to specific needs at source code level

Table A.1: Selected features of the Vamps model

which can adequately describe the flow of water in a forested environment (on a plot base) and *(ii)* be flexible enough to be applied to the variety of forested environments that exist. Due to its flexibility it is also possible to apply Vamps to plots covered with agricultural crops or bare soils. Furthermore the software is distributed with complete source code and documentation to allow the user to adapt the program to new situations and examine the program's internal operation.

A.2 MODEL PRINCIPLES

The flow of water through a forested ecosystem is shown in Figure A.1. Three pathways are generally distinguished by which precipitation reaches the forest floor. A small fraction of the precipitation reaches the forest floor without touching leaves or stems. This is known as direct throughfall. Another small fraction flows down the tree trunks as stemflow. The remaining fraction hits the forest canopy and will leave the canopy as crown drip or evaporate from the wet canopy depending on canopy storage capacity and shape, the kinetic energy of the droplets and the atmosphere's evaporative demand. Water infiltrating the soil profile can runoff laterally as saturated or unsaturated flow, percolate to deep groundwater or is extracted by the roots of plants or trees. If the throughfall intensity exceeds the infiltration capacity of the topsoil, Hor-

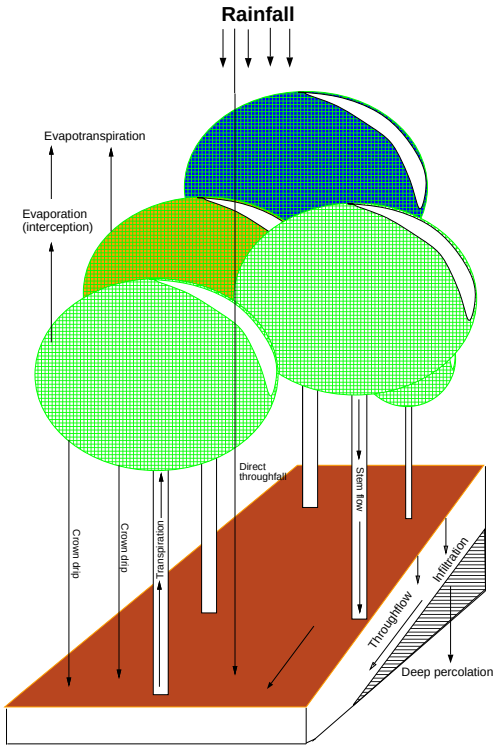

Figure A.1: Simplified diagram of the flow of water through a forested ecosystem (after *Bruijnzeel* [1983b])

tonian overland flow can occur. The top layer of the soil profile can become saturated resulting in saturation overland flow. Vamps simulates most of these fluxes which is illustrated in Figure A.2. The model is mainly driven by input from the atmosphere*.

Most of the fluxes in the model can either be calculated or given by the user. The atmosphere, canopy and soil part of the model can be combined or used separately. However, the strength of the model is the ability to combine these parts into an integrated model for the forest hydrological cycle.

The following briefly summarizes the methods used to calculate the water fluxes:

Throughfall can be determined in several ways. *(1)* using a complete canopy water balance model based on the model developed by *Rutter et al.* [1971]. *(2)* using the simpler analytical approache of *Gash* [1979]. *(3)* the Leaf Area Index based solution also used by the TOPOG model [*Vertessy et al.*, 1993].

*As the bottom boundary conditions can also change in time one could probably regard this as a driving force as well

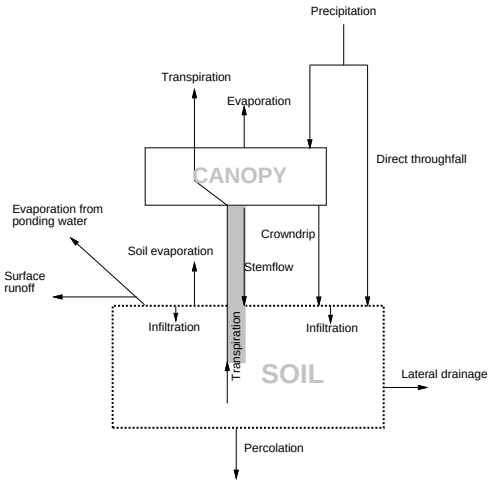

Figure A.2: Simplified flow diagram of the Vamps model

Transpiration is commonly determined using the Penman-Monteith equation [*Monteith*, 1965]. Several alternative methods can be used as well [*Penman*, 1956; *Makkink*, 1957, 1961; *Commissie Voor Hydrologisch Onderzoek TNO*, 1988].

Soil water fluxes in the unsaturated zone are determined using Richard's equation. An adapted form of the numerical solution described by *Feddes et al.* [1978] and *Belmans et al.* [1983] is used. The relation between water content and pressure head can be described in several ways [*Mualem*, 1976; *Clapp and Hornberger*, 1978; *Van Genuchten*, 1980].

These fluxes can also be calculated by a user supplied method.

A.3 OTHER INFORMATION

The latest version and other information is available on the Word Wide Web (http://flow.geo.vu.nl or http://www.xs4all.nl/ schj).

PUBLICATIONS AND REPORTS

Hafkenscheid, R. L. L. J., F. Holwerda, L. A. Bruijnzeel, R. A. M. De Jeu, J. Schellekens, and F. N. Scatena, Transpiration from tropical montane cloud forests in the Blue Mountains, Jamaica and the Luquillo Mountains, Puerto Rico, in *Second International Colloquim on Hydrology and Water Management in the Humid Tropics*, Panama City, Panama, 1999.

Plassche, O., S. Heteren, R. K. Lubberts, J. V. der Molen, S. de Rijk, and J. Schellekens, Sea-level change and coastal evolution in areas of submergence, *progress report*, Faculty of Earth Sciences, Vrije Universiteit, 1993.

Schellekens, J., Water and nutrient balance of the Oleologa catchment, Viti Levu, Fiji, in the undisturbed state and its rainfall-runoff response, Master's thesis, Faculty of Earth Sciences, Vrije Universiteit, Amsterdam, 1992, working Paper no. 2, Project on water and nutrient dynamics of *Pinus caribaea* plantation forest on degraded grassland soils in western Viti Levu, Fiji.

Schellekens, J., Hydrology of the Great Marshes, Barnstable, Mass. USA, *Core pionier project (pgs 75-305)*, Faculty of Earth Sciences, Vrije Universiteit, 1994.

Schellekens, J., *Vamps, a Vegetation-AtMosPhere-Soil water model*, Faculty of Earth Sciences, Vrije Universiteit, 0th ed., 1997.

Schellekens, J., The interception and runoff generating processes in the Bisley catchment, Luquillo Experimental Forest, Puerto Rico, *Phys. Chem. Earth*, 2000, in press.

Schellekens, J., L. A. Bruijnzeel, A. J. Wickel, F. N. Scatena, and W. L. Silver, Interception of horizontal precipitation by elfin cloud forest in the Luquillo Mountains, Eastern Puerto Rico, in *First International Conference on Fog and Fog Collection*, edited by R. S. Schemenauer and H. A. Bridgman, pp. 29–32, IDRC, Ottawa, Canada, 1998.

Schellekens, J., F. N. Scatena, L. A. Bruijnzeel, and A. J. Wickel, Modelling rainfall interception by a lowland maritime tropical rain forest in northeastern Puerto Rico, *J. Hydrol.*, *225*, 168–184, 1999.

Schellekens, J., L. A. Bruijnzeel, F. N. Scatena, N. J. Bink, and F. Holwerda, Evaporation from a tropical rain forest, Luquillo Experimental Forest, Puerto Rico, *Water Resour. Res.*, 2000, in press.

Venneker, R. G. W., and J. Schellekens, A framework for development of hydrological models, *Technical Report CRMI-TR-001*, IHE Delft, FdA/VU Amsterdam, 1997.

Waterloo, M. J., F. J. Beekman, L. A. Bruijnzeel, K. F. A. Frumau, E. Harkema, H. Opdam, J. Schellekens, H. F. Vugts, and T. T. Rawaqa, The impact of converting grassland to pine forest on water yield in Viti Levu, Fiji, in *Hydrology of Warm Humid Regions*, edited by J. S. Gladwell, pp. 149–156, IAHS Publication No. 216, 1993.

Waterloo, M. J., J. Schellekens, L. A. Bruijnzeel, H. F. Vugts, P. N. Assenberg, and T. T. Rawaqa, Chemistry of bulk precipitation in southwestern Viti Levu, Fiji, *J. Trop. Ecol.*, *13*, 427–447, 1997.